Global and targeted proteomics in *Arabidopsis thaliana*: A study of secondary metabolism and phytohormone signaling

William Orrin Slade

Dissertation submitted to the faculty of the Virginia Polytechnic Institute and State University in partial fulfillment of the requirements for the degree of

Doctor of Philosophy
In
Biological Sciences

Brenda S.J. Winkel, Chair
Richard F. Helm
Dorothea Tholl
Florian D. Schubot

August 19th, 2013
Blacksburg, VA

Keywords: Proteomics, mass spectrometry, *Arabidopsis*, auxin, ethylene, flavonoids.

Copyright 2013 William O. Slade

Global and targeted proteomics in *Arabidopsis thaliana:* A study of secondary metabolism and phytohormone signaling

William Orrin Slade

ABSTRACT

Proteomics is defined as a tool to explore how proteins control and regulate important molecular and physiological processes. Further, peptide-centric approaches, or bottom-up methods, provide more comprehensive coverage of a proteome compared to whole-protein approaches. This body of work assesses the technical feasibility of several bottom-up proteomics technologies applied to *Arabidopsis thaliana*, including gel-based methods, those that require peptide derivitization, and those that do not. Selected-reaction monitoring (SRM) for targeted proteomics, and data-independent acquisition (MS^E) was also evaluated. In addition to assessing the capabilities of these technologies, we then applied them to the context of uncovering new insights into the flavonoid biosynthetic pathway and the auxin and ethylene signaling pathways.

Chapter one provides background information related to secondary metabolism, phytohormone signaling, and the status of proteomics in plants. In Chapter 2 and Appendix A, we establish the methodology to apply traditional and DiGE-based 2D-GE strategies to global proteomics in *Arabidopsis*. Our results suggest that while 2D-GE is applicable to *Arabidopsis*, there are practical and conceptual limitations that must be understood. Further, our results suggest that pertubations in the flavonoid pathway do not affect the abundance of proteins in *Arabidopsis* seedlings, roots, or flowers that can be studied using 2D-GE and DiGE. Additionally, we demonstrated the first parallel comparison of the effects of auxin and ethylene on the *Arabidopsis* root proteome and observed no overlap among the proteins regulated by the two phytohormones, at least for the most abundant proteins observed by 2D-GE.

Chapter 3 explores the efficacy of selected reaction monitoring for relative peptide quantification in *Arabidopsis* roots. Our results suggest that while the technology parallels application in yeast and humans, there are substantial analytical challenges that much be addressed. In Chapter 4 we explore the MS^E data acquisition scheme for global proteomics in *Arabidopsis.* We observe that treatment with exogenous auxin affects the abundance of many proteins representing diverse biological processes. Interestingly, we observe minimal overlap among genes and proteins regulated by exogenous auxin. Appendix B explores the efficacy of iTRAQ labeling for relative peptide quantification in *Arabidopsis* roots.

Acknowledgements

Without the love and support of my wife, Amanda G. Slade, I would not have completed this degree. Thanks for all the years of emotional, mental, and physical support, and for carrying me when I could no longer continue myself.

Thanks to Dr. Brenda S.J. Winkel and Dr. Richard F. Helm, for taking a chance on me when no one else wanted to and showing me light when my world was filled with darkness. I can only hope to emulate half of Dr. Winkel's kindness and understanding. Without Dr. Helm's patience and guidance none of this work would have been possible. I cannot state how much I appreciate his good advice, even if I only realize how good it is retroactively. Thanks for putting up with my nonsense for all these years.

Thanks to my committee members, Dr. Florian Schubot and Dr. Dorothea Tholl, for being active voices yet extremely reasonable and helpful.

To those that provided friendship, emotional support, and superb scientific advice: Dr. Dennis Dean, Dr. Callie Raulfs, Dr. Ina Puleri O'Carroll, Dr. Patricia Dos Santos, Valerie Cash, Dr. Pablo Sobrado, Janet Donahue, Dr. Elitsa Ananieva, Dr. Shannon Alford, Dr. Sherry Hildreth, Dr. Peter Bowerman, Dr. Ryan Anderson, Dr. Piyum Khatibi, Dr. Payam Mershashi, Jody Jervis, Dr. Kenneth Webb, and Patricia Williams.

ATTRIBUTION

Several colleagues aided in the writing and research behind the chapters of this dissertation. A brief description of their contributions is included here.

Brenda S.J. Winkel, Ph.D. is currently the head of the department of biological sciences at Virginia Tech. Dr. Winkel was a co-principal investigator for the grant supporting this research. Additionally, Dr. Winkel contributed editorial comments to all chapters.

Richard F. Helm, Ph.D. is currently an Associate Professor in the department of biochemistry and Director of the Mass Spectrometry Incubator at Virginia Tech. Dr. Helm was a co-principal investigator for the grant supporting this research. Dr. Helm provided analytical guidance and contributed editorial comments to all chapters.

W. Keith Ray, Ph.D. is a senior research associate in the department of biochemistry at Virginia Tech. Dr. Ray provided technical support.

Patricia M. Williams is a lab manager in the department of animal and poultry sciences at Virginia Tech. Mrs. Williams provided analytical guidance.

Sherry B. Hildreth, Ph.D. is a postdoctoral research associate in the department of biological sciences at Virginia Tech. Dr. Hildreth assisted with mass spectrometry experiments.

Table of Contents

Abstract ii

Acknowledgements iii

Attribution iv

List of figures viii

List of tables ix

List of abbreviations x

Chapter 1: Introduction and Background 2
- **I. Introduction** 2
- **II. Background** 2
  - ***i. Secondary Metabolism*** 3
  - *ii. The Shikimate Pathway* 5
  - *iii. Flavonoids: General* 5
  - *iv. Flavonoids: Biological Function* 6
  - *v. Auxin and Ethylene: General* 8
  - *vi. Auxin and Ethylene: Proteomics* 9
  - vii. Proteomics in Plants 10
  - viii. DiGE Technology 10
  - ix. iTRAQ 12
  - x. Selected-Reaction Monitoring (SRM) of Peptides 12
  - xi. Ultra-high performance liquid chromatography (UPLC) coupled to high mass-accuracy mass spectrometry 14
  - xii. Data Analysis 14
- **III. References** 17

Chapter 2: Effects of exogenous auxin and ethylene on the *Arabidopsis* root proteome 26
- **I. Abstract** 27
- **II. Introduction** 28
- **III. Results** 29
- **IV. Discussion** 30
- **V. Experimental** 34
  - *i. Plant Material* 34
  - *ii. IAA and ACC treatments* 34
  - *iii. Protein extraction* 34
  - *iv. 2D-gel electrophoresis* 35
  - *v. Image analysis and spot excision* 35

vi. In-gel tryptic digest 35
vii. Matrix assisted laser desorption ionization mass spectrometry (MALDI) 36
viii. Protein identification 36
VI. Supplemental 37
VII. References 45

Chapter 3: Evaluation of selected-reaction monitoring 50
for peptide quantification in the model plant, *Arabidopsis thaliana*
I. Abstract 50
II. Introduction 51
III. Results 52
IV. Discussion 56
V. Experimental 57
i. Plant Material 57
ii. Protein Extraction 57
iii. SDS-Page 57
iv. In-gel tryptic digest 58
v. Protein Selection 58
vi. Peptide selection and synthesis 58
vii. Mass spectrometry and nanoLC set-up 58
viii. Spectral library 58
x. Design of SRM assays 59
xi. Validation of SRM assays 59
VI. Supplemental 60
VII. References 100

Chapter 4: Effects of exogenous auxin on the *Arabidopsis* 106
root proteome as observed using UPLC-Data Independent
Acquisition mass spectrometry
I. Abstract 104
II. Introduction 105
III. Results 106
IV. Discussion 107
V. Experimental 111
i. Plant material 111
ii. Hormone treatment 112
iii. Protein extraction 112
iv. In-solution digestion 112
v. C18-RP SPE and ion-exchange chromatography 112
vi. LC-MS configuration 113
vii. Data analysis 113
VI. Supplemental 115
VII. References 125

Chapter 5: Conclusions 128
I. Context 129
II. Summary 129
III. Outlook 129

IV. Future Directions 130
V. References 132

Appendix A: Effects of perturbing the flavonoid biosynthetic pathway on the *Arabidopsis* seedling, root, and flower proteomes 133
I. Abstract 134
II. Introduction 134
III. Results 135
IV. Discussion 136
V. Experimental 139
i. Plant Material 139
ii. Protein Extraction 139
iii. DiGE Labeling 139
iv. Isoelectric focusing 139
v. SDS-Page electrophoresis 140
vi. Image analysis 140
vii. Selected-Reaction Monitoring 140
viii. In-gel tryptic digest 140
VI. Supplementary Material 142
VII. References 144

Appendix B: Evaluation of isobaric tagged for relative and absolute quantification (iTRAQ) using hydrophilic interaction chromatography (HILIC) on a MALDI TOF/TOF platform for relative quantification of peptides in *Arabidopsis thaliana* 146
I. Abstract 146
II. Introduction 147
III. Results 148
IV. Discussion 148
V. Experimental 150
i. Plant material 150
ii. Protein extraction 150
iii. In-solution digestion 150
iv. Peptide labeling using iTRAQ reagents 150
v. Solid-phase extraction 151
vi. Hydrophilic-interaction chromatography 151
vii. Nano liquid chromatography 151
viii. MALDI TOF/TOF 151
x. Data processing 150
VI. References 153

Appendix C: Supplementary Information 155
I. Table of contents 156

List of Figures

Figure 1-1. Schematic of the shikimate pathway in plants. 4

Figure 1-2. Schematic of flavonoid metabolism. 7

Figure 1-3 Overview of different mass analyzers 11

Figure 2-1. Master gel representing all gels of *Arabidopsis* roots treated with 1 μM IAA or 1 μM ACC. 30

Figure 2-S1: Experimental schematic 37

Figure 2-S2: PDQuest images of IAA-responsive spots 38

Figure 2-S3: PDQuest Images of ACC-responsive spots 39

Figure 3-1: Distribution of physiochemical properties of the screened proteins. 53

Figure 3-2: Distribution of physiochemical properties of the screened peptides. 53

Figure 3-3: Spectral library success and ESP score distribution 54

Figure 3-4: Collision energy and declustering potential optimization using Skyline. 54

Figure 3-5: Protein and peptide response to SRM assays in *Arabidopsis* Roots. 55

Figure 3-6: Increased fractionation improves resolution and sensitivity of SRM assays. 55

Figure 3-S1: Scheme for fractionation of protein lysates by SDS-page. 60

Figure 3-S2: Overlap between IAA- and ACC-regulated genes. 60

Figure 4-1: Three-way Venn diagram. 110

Figure 4-S1: Experimental schematic. 116

Figure 4-S2: Comparison of the reproducibility of unfractionated technical replicates at the level of protein identifications. 117

Figure 4-S3: Venn diagram comparing proteins identified at each time point And the overlap between combined Control (no IAA) and Treatment (+IAA) biological replicates. 118

Figure 4-S4: Venn diagram comparing peptides identified at each time point and the overlap between combined Control (no IAA) and Treatment (+IAA) biological replicates. 119

Figure 4-S5: Comparison of RuBiSCo protein levels across the time-course. 120

Figure 4-S6: Three-way Venn diagram demonstrating the overlap among our dataset, a comparable microarray dataset, and our previously published protein dataset. 121

Figure 4-S7: *pme18* mediates lateral root formation 122

Figure 4-S8: Comparison of identified proteins in an unfractionated lysate using UPLC-HDMS^{E} in intensity or resolution mode. 123

Figure 4-S9: Comparison of identified proteins using different collision energy ramps in HDMS^{E} mode. 124

Figure A-1: SRM analysis of CHS in WT and *tt4-13*. 135

Figure A-2: 2D-GE analysis of WT and *tt4-13* in seedlings. 136

Figure A-3: DiGE analysis of WT and *tt4-13* in roots. 137

Figure A-4: 2D-GE analysis in WT and *tt4-13* in flowers. 138

Figure A-S1: Experimental scheme. 142

Figure A-S2: The primary amino acid sequence of CHS (top) with the unique peptides (proteotypic) highlighted in yellow. 143

List of tables

Table 1-1: Characteristics and performance of commonly used mass spectrometers. 16

Table 2-S1: Peptides used for protein identification 40

Table 2-S2: Additional protein information with links to TAIR and UNIPROT 44

Table 3-S1: List of all peptides and transitions tested in unfractionated lysates 61

Table 3-S2: List of all peptides and transitions tested 62

Table 4-1: Identities of spots that change in abundance after treatment with IAA for 8 h. 108

Table 4-2: Identities of spots that change in abundance after treatment with IAA for 12 h. 109

Table 4-3: Identities of spots that change in abundance after treatment with IAA for 24 h. 109

Table 4-S1: Analysis of MSE versus HDMSE using intensity mode at a constant loading level, different gradient lengths, and different flow rates 115

Table 4-S2: Number of proteins and peptides identified and corresponding false discovery (FDR) rates 115

Table 4-S3: Evaluation of the effect of MS/MS tolerance (Da) parameters on data quality for the merged control samples at the 8 h time point 115

Table B-1: *Arabidopsis* proteins identified with high confidence using iTRAQ HILIC on a MALDI TOF/TOF. 149

List of abbreviations

2D-GE: Two-dimensional gel electrophoresis

4CL: *p*-coumarate:CoA ligase

ACC: 1-aminocycopropoane carboxylic acid

ADK2: Adenosine kinase 2

ANR: Anthocyanidin reductase

ARF2: Auxin-response factor

C4H: Cinnamate 4-hydroxylase

CE: Collision energy

CHI: Chalcone isomerase

CHS: Chalcone synthase

Da: Dalton

DAHP: 3-dexoy-D-arabino-heptulosonate-7-phosphate

DDA: Data-dependent acquisition

DFR: Dihydroflavonol reductase

DIA: Data-independent acquisition

DiGE: Difference gel eletrophoresis

DP: Declustering potential

DTT: Dithiothreitol

ESI-MS: Electrospray mass spectrometry

ESP: Enhanced signature peptide

F3H: Flavonoid 3'hydroxylase

FDR: False discovery rate

GAPC: Glyceraldehyde-3-phosphate dehydrogenase

GPM: Global proteome machine database

HILIC: Hydrophilic interaction chromatography

HPLC: High performance liquid chromatography

IAA: Indole-3-acetic acid

IEF: Isoeletric focusing

IPG: Immobilized pH-gradient

iTRAQ: Isobaric tags for relative and absolute quantification

LAR: Leucoanthocyanidin reductase

MALDI TOF/TOF: Matrix-assisted laser desorption ionization time-of-flight time-of-flight mass spectrometry

MCA: Metabolic control analyses

MI: Monoisotopic

MS/MS: Tandem mass spectrometry

NHS: N-hydroxysuccinimide

PAL: Phenylalanine ammonia-lyase

PGK1: Phosphoglycerate kinase 1

PMF: Peptide mass fingerprint

QQQ: Triple-quad mass spectrometer

RHD1: Root hair defective 1

RHM1: Rhamnose biosynthesis 1

SCX: Strong-cation exchange

SCX-RP: Strong-cation exchange reverse phase

SDS: Sodium dodecyl sulfate

SDS-PAGE: Sodium dodecyl sulfate polyacrylamide gel electrophoresis

SILAC: Stable isotope labeling of amino acids in cell culture

SNX1: Sorting nexin 1

SPIRE: Systematic protein investigative research environment

SRM: Selected-reaction monitoring

T-DNA: Transfer DNA

TMT: Tandem-mass tags

TOF: Time-of-flight

UIS: Unique ion signature

UPLC: Ultra-performance liquid chromatography

UPLC-HDMS^{E}: Ultra-performance liquid chromatography high-definition ion-mobility mass spectrometry

UV: Ultraviolet

Chapter 1

Introduction and Background

I. Introduction

Never has there been a time in biology when systems-level approaches were more warranted or viable. Systems biology represents the natural evolution of molecular biology: a change from a reductionist single-gene to single-phenotype viewpoint, to the realization that most interesting processes, whether medical or agricultural, are controlled by multiple genes and pathways (Benfey and Mitchell-Olds, 2008; Westerhoff and Palsson, 2004). In fact, it is the consensus that most major challenges facing plant biology over the next 20 years will require an integrated, systems approach (Raikhel, 2008). Interestingly, systems biology is not a new commodity. In the 1950s, researchers began to appreciate the integrated nature of cellular processes with the elucidation of lac operon function and feedback inhibition of amino acid biosynthetic pathways (Beckwith, 1967; Umbarger and Brown, 1957; Yates and Pardee, 1957). During the 1970s and 1980s, much effort was invested into metabolic control analyses (MCA), a precursor to the modern field of metabolomics (Westerhoff and Palsson, 2004). Finally, in the early 2000s it was realized that integrated approaches were critical and that more methodical approaches were needed (Ge et al., 2003; Palsson, 2002). Integrated approaches are now generating more data than researchers can comprehend. A substantial shortcoming in the field of systems biology at the present time is proof-of-principle analysis, where a well-studied pathway or physiological process is analyzed at as many levels as possible, such as the transcriptome, metabolome, proteome, and/or interactome, and the resulting data used to develop rigorous mathematical and computational models to model and predict the relationship among genes, proteins, and metabolites. Such a pathway or process would ideally be well characterized using traditional molecular biology and biochemistry, supported by a strong community of researchers, and implicated in a multitude of essential biological processes. A striking candidate for such an analysis is the flavonoid biosynthetic pathway.

The plant flavonoid pathway is one of the best-characterized metabolic systems in any organism, the focus of chemical analyses dating back to the 1800's and the basis of fundamental discoveries that include Mendelian genetics, mobile DNA elements, and microRNAs. Over the past three decades, traditional molecular biology and biochemical experiments in a variety of model plant species have yielded a detailed understanding of the regulation and biochemistry of the pathway. For example, structural analyses of type III polyketide synthases such as CHS evolved from a β-ketoacyl ACP synthase involved in fatty acid biosynthesis (Winkel, 2006; Winkel-Shirley, 2001a). Additionally, the products of the pathway have been observed to affect several general physiological processes in animals and plants (Dixon, 2004; Korkina, 2007). As there is a strong community of interdisciplinary researchers interested in the flavonoid pathway, a collaborative team of biologists, bioinformaticists and biochemists can utilize the flavonoid pathway as an exemplary model for systems biology.

The flavonoid biosynthetic pathway regulates numerous physiological processes, and is in turn modulated by several abiotic and biotic factors (Winkel-Shirley, 2002). Wounding, attack by pathogens, or exposure to elevated light levels all stimulate flavonoid production. Additionally, several processes have been shown to be regulated by

flavonoids, including auxin transport, root development, nodulation, and pollen germination (Winkel-Shirley, 2001a). Reorientation of plants relative to gravity leads to induction of flavonoid synthesis in the epidermal tissues of Arabidopsis root tips, which may regulate gravitropic curvature (Blancaflor and Masson, 2003; Buer and Muday, 2005). Interestingly, recent research has revealed that the effects of auxin and ethylene on root gravitropism and root architecture may be mediated by a specific class of flavonoids (Muday et al. 2012).

II. Background

i. Secondary Metabolism

Although there has been substantial research in the field of secondary metabolites over the past century, the definition of secondary metabolism remains controversial. In his 1873 textbook, Julius Sachs, one of the founding fathers of plant physiology, gave a traditional viewpoint of secondary metabolism as producing compounds that were not as important as primary metabolites, specifically, that they were by-products of metabolism no longer used in the formation of new cells (Sachs, 1873). This definition was expanded further by Albrecht Kossel in 1891 to include a clear distinction between primary metabolism, essential for growth and development, and secondary metabolism, not required for survival. A modern appreciation of secondary metabolism began in 1959 with Fraenkel's classic *Science* article, "Raison d'Etre of Secondary Plant Substances" (Fraenkel, 1959). Since this seminal work, the debate on the importance and function of secondary metabolism has continued. Several authors still contend that secondary metabolites are small molecular weight compounds that do not play essential roles in growth and development (D'Auria and Gershenzon, 2005). However, it has been noted that due to numerous recent observations that secondary metabolites do indeed play pivotal roles in plant responses to the environment, as well as in reproduction and survival, distinguishing between secondary metabolism and primary metabolism is difficult at best and may not even be necessary (Firn and Jones, 2009; Pichersky and Gang, 2000). Thus, the best distinction between primary and secondary metabolism is probably the following: primary metabolism covers the majority of processes essential for growth and development whereas secondary metabolism is indispensable for the survival of the individual in its environment (Hartmann, 2007).

Over the past 50 years, research into secondary metabolism has evolved from simple chemical analysis of secondary compounds to the detailed molecular characterization of pathway organization and regulation (Hartmann, 2007). At first, many researchers were discouraged by the challenge of studying the biochemistry of enzymes involved in the pathways of secondary metabolism (Hartmann, 2007). A major breakthrough for the field came during the 1960s when Eric Conn's group described the purification and characterization of phenylalanine deaminase from *Horeum vulgare* (Koukol and Conn, 1961). After two decades of biochemical exploration of the enzymes of secondary metabolism, another major breakthrough occurred in the mid 1980s when the first genes encoding enzymes of plant secondary metabolism were cloned and functionally expressed (Edwards et al., 1985; Kuhn et al., 1984; Ryder et al., 1984; Winkel-Shirley,

2001b). Since that time there has been a great deal of research into diverse aspects of secondary metabolism, with particular focus on the development of new drugs, the biochemical and functional elucidation of each pathway, and the investigation of secondary metabolism using systems biology techniques (Hartmann, 2007; Verpoorte, 1998).

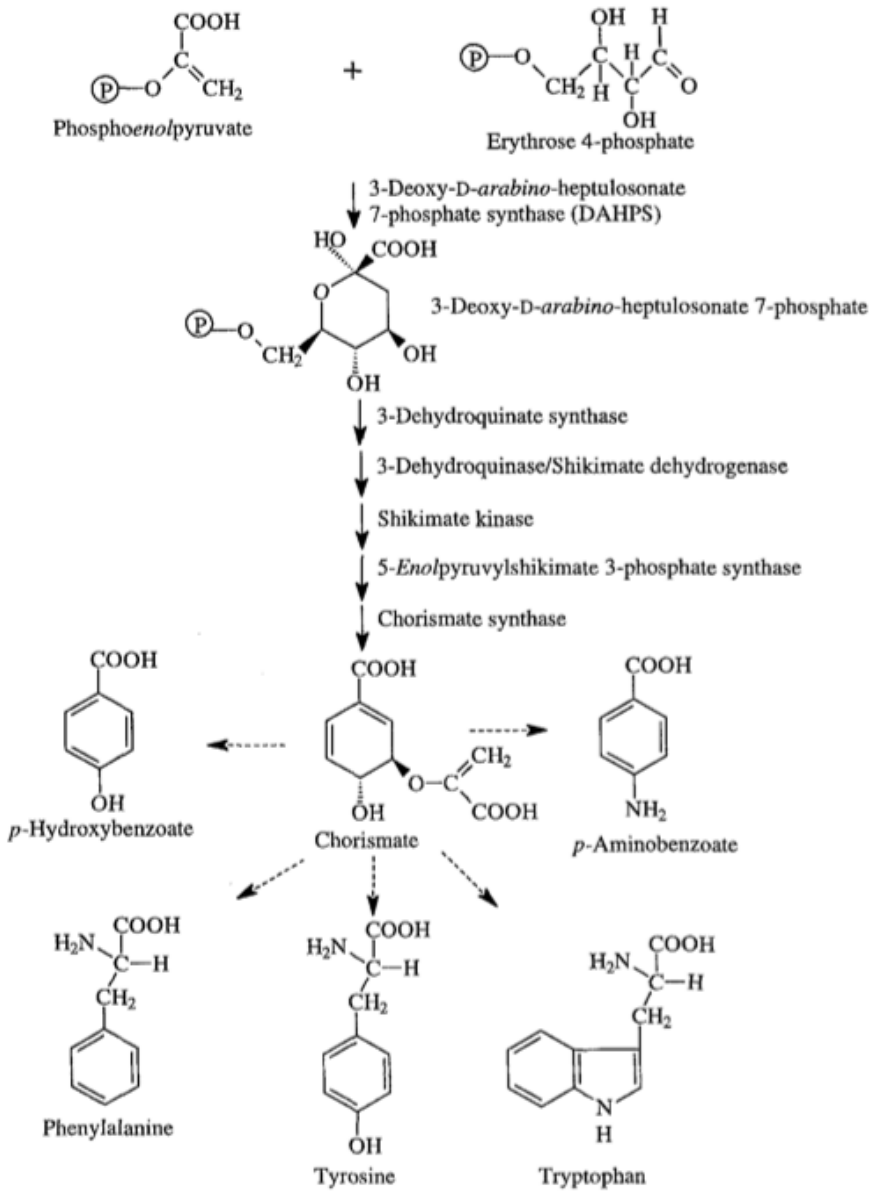

Figure 1-1. Schematic of the shikimate pathway in plants. Erythrose-4-phosphate and phosphoenolpyruvate are condensed into 3-deoxy-D-arabino-heptulosonate-7-phosphate (DAHP). After several more steps, DAHP is turned into chorismate, which serves as a precursor for several important compounds, such as the aromatic amino acids and quinones. Reproduced with permission from Herrmann and Weaver (1999).

In the first committed step of the pathway, phosphoenolpyruvate from aerobic respiration and erythrose-4-phosphate from the pentose phosphate pathway are condensed into 3-deoxy-D-arabino-heptulosonate-7-phosphate (DAHP) by the enzyme DAHP synthase (Herrmann and Weaver, 1999). From DAHP, several more steps are needed to synthesize shikimate and then chorismate. Chorismate serves as the precursor for several important compounds, such as the aromatic amino acids, the quinones, and the folates (Herrmann, 1995). These compounds serve a variety of important roles in growth and development and response to the environment.

ii. The Shikimate Pathway

The shikimate pathway is the essential starting point for a large number of secondary metabolites in plants and microorganisms (Figure 1-1). First discovered by Bernhard Davis and David Sprinson in the 1950s (Davis et al., 1956a, b; Srinivasan et al., 1956) the shikimate pathway serves as the biosynthetic route to the aromatic amino acids phenylalanine, tyrosine, and tryptophan (Herrmann, 1995). Since the shikimate pathway serves as the beginning for many branch points of secondary metabolism, an understanding of its regulation provides insight into the control of a large variety of downstream pathways considered. Work in plants and microorganisms has revealed both highly conserved and divergent modes of regulation for this pathway (Herrmann and Weaver, 1999). Traditional metabolic analyses in bacteria and plants determined that both feedback inhibition of gene expression and enzyme activity play important roles in regulating shikimate metabolism. In bacteria, the first enzyme of the pathway, DAHP synthase, is regulated at the levels of transcription and enzyme activity by downstream products, such as the aromatic amino acids (Herrmann, 1983). In contrast, no classical feedback regulator has yet been discovered for the plant enzyme (Herrmann and Weaver, 1999). Surprisingly, tryptophan activates the plant DAHP synthase (Suzich et al., 1985) This is in contrast to *E. coli* where tryptophan functions in a classical sense by inhibiting DAHP synthase in a mechanism of feedback regulation. Several bacterial enzymes clearly require divalent cations for catalysis; in contrast, several plant enzymes are allosterically inactivated by divalent cations (Frost et al., 1984; Herrmann and Weaver, 1999). Thus, although the general regulatory themes are similar in different organisms, the modes of action are quite different. Despite significant differences in regulation, several plant cDNAs, which display moderate homology at the DNA level to their bacterial counterparts, have been found to complement mutations in their bacterial counterparts (Keith et al., 1991), indicating that the important functional regions of the pathway enzymes has been conserved.

iii. Flavonoids: General

The flavonoid biosynthetic pathway uses relatively simple precursors to produce myriad metabolites with extremely disparate, but biologically-important, functions. Flavonoid biosynthesis represents a mode of specialized metabolism that is ubiquitous in plants and has now also been suggested to occur in some algae (Blanc et al., 2010; Bowler et al., 2008; Cock et al., 2010; May et al., 2008).

The simple chemical core structure of flavonoids allows for a diverse combination of substituents to be added and modified, resulting in a large array of chemical diversity. In the first step of the flavonoid pathway, the condensation of *p*-coumaryl-CoA with three molecules of malonyl-CoA generates a core C-15 compound, tetrahydroxychalcone. From this core structure a multitude of compounds are generated via numerous chemical reactions, including isomerization, dehydration, reduction, as well as the addition of functional groups by alkylation, glycosylation, and hydroxylation. More than 6000 flavonoid compounds have been described to date (Aszalos, 2008), a number indicative of their diversity.

iv. Flavonoids: Biological Function

Flavonoids contribute to many important and diverse cellular processes. It has long been proposed that flavonoids function to protect plants from UV-B damage given their absorptive capacity in the 280-320 nm range (Stafford, 1991). Evidence from the 1980s demonstrated flavonoids accumulate in leaf epidermal tissue in response to UV-B irradiation (Beggs, 1986; Caldwell et al., 1983). Additionally, conditions that induce flavonoid synthesis were shown to yield UV-B tolerant plants. Li et al. (1993) showed that plants containing mutations in the genes for the first two steps of the flavonoid pathway are hypersensitive to UV-B irradiation. Although other research has been used to suggest that sinapate esters, which are related to flavonoids, are likely the most important compounds in UV-B protection (Jin et al., 2000; Landry et al., 1995), flavonoids themselves clearly contribute to the UV-B response and influence sinapate ester levels (Li et al., 1993). Flavonoids are also known to play an important role in plant protection from herbivory. Recent evidence has shown that that flavones and flavonols, in addition to the bittersweet proanthocyanidins, can act as deterrents towards herbivory against species such as *Niloparvata lugens* (Harborne and Williams, 2000). Additionally, flavones and isoflavones have been shown to function against herbivory of legumes by Rhizobia (Harborne, 1999).

In addition to the established roles of flavonoids as protectants, new evidence is emerging that implicates flavonoids as essential compounds in mediating the action of the phytohormones, auxin and ethylene. The idea that flavonoids mediate the effects of auxin and/or ethylene was originally proposed by Jacobs and Bubery (1988) but was perceived as controversial until recently. Current research indicates that primary and secondary metabolism converge when flavonoids mediate the effects of auxin and ethylene on root gravitropism. Auxin influences root gravitropism and architecture (Casimiro et al., 2001; Marchant et al., 1999). Additionally, the polar transport of auxin is required for the root gravitropic response (Muday and DeLong, 2001). Recent work demonstrates that not only do flavonoids accumulate in a spatial and temporal manner similar to auxin (Peer et al., 2001), but root gravitropism is impaired in a chalcone synthase (*tt4*) mutant that is completely lacking in flavonoids (see Figure 1-2) (Buer and Muday, 2005). Additionally, the asymmetric accumulation of flavonoids is required for auxin transport (Kuhn et al., 2011). Interestingly, using naringenin to feed around the

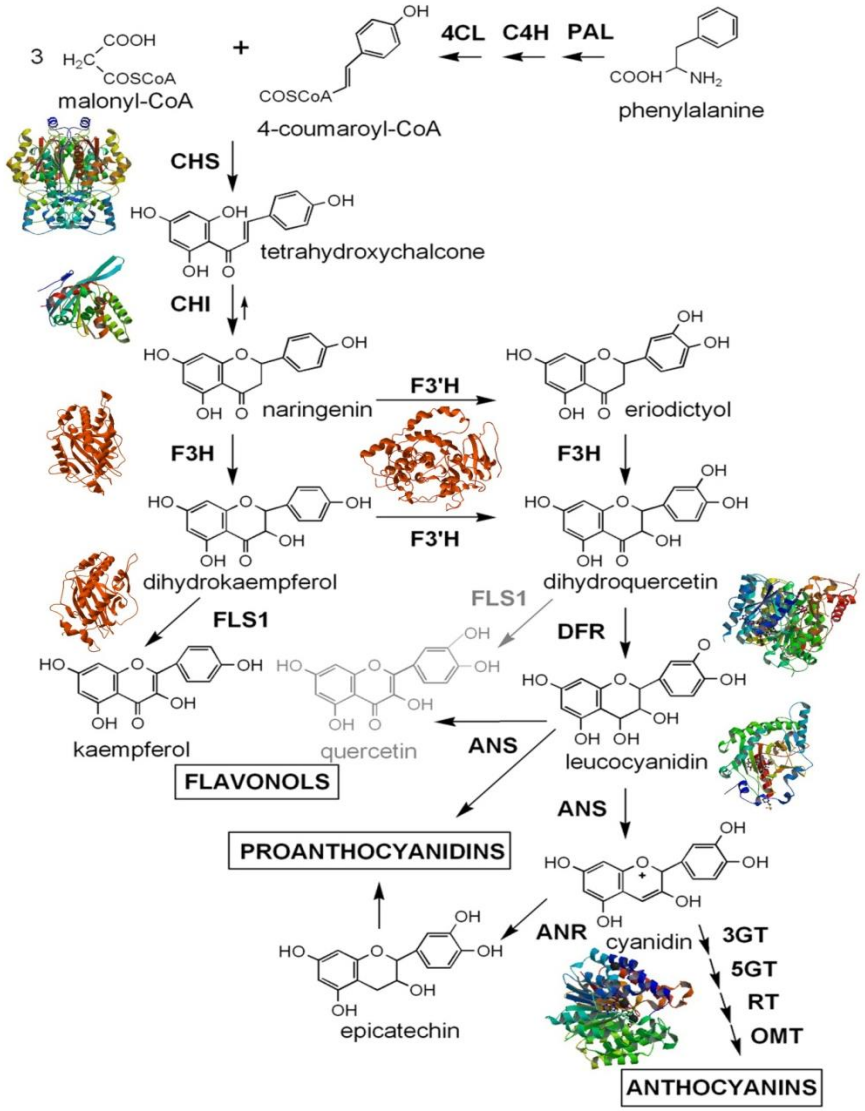

Figure 1-2. Schematic of Flavonoid Metabolism. Protein structures in multicolor represent the four enzymes in the pathway for which crystal structures have been solved: chalcone synthase and chalcone isomerase (CHS and CHI; from *Medicago sativa*, pdb ids 1CGK and 1EYP), dihydroflavonol reductase (DFR; from grape, 3C1T) and anthocyanidin synthase (ANS; from Arabidopsis, 1GP6). Structures in orange are homology models for, flavanone 3-hydroxylase (F3H) and flavonol synthase (FLS) (Winkel lab, unpublished) and flavonoid 3' hydroxylase (F3'H) (Schuler lab, Rupasinghe et al., 2003) Other abbreviations: anthocyanidin reductase (ANR), cinnamate 4-hydroxylase (C4H), *p*-coumarate:CoA ligase (4CL), leucoanthocyanidin reductase (LAR), and phenylalanine ammonia-lyase (PAL). The step shown in gray is not favored by the *Arabidopsis* enzyme *in vitro.* Reproduced from Winkel (Unpublished).

blockage caused by the absence of CHS restores root gravitropism to normal levels (Buer and Muday, 2005).

Recent evidence suggests a surprising link between flavonoid glycosides and the auxin response in *Arabidopsis thaliana*. *In planta*, flavonoids occur overwhelmingly as glycosides (Kachlicki et al., 2008; Kerhoas et al., 2006; Stobiecki et al., 2006; Vallabhaneni et al., 2012). The *rol1-2* mutant, which is defective in accumulation of flavonoid glycosides, displays hyponastic cotyledons, suggesting a link between flavonoid glycosides and this phenotype typically linked to auxin (Ringli et al., 2008). Additionally, Buer et al. (2013) observed that mutants accumulating abnormally high levels of the flavonol, quercetin, or its glycosides were most affected relative to the most abundant metabolites observed in regards to auxin transport and root gravitropism.

Evidence is also emerging that flavonoids and ethylene regulate the same genes in a similar fashion to affect root gravitropism. Treatment of wild-type plants with the ethylene precursor, 1-aminocyclopropane carboxylic acid (ACC), reduces root elongation and gravitropic curvature (Buer et al., 2006a). Interestingly, treatment with ethylene also induces flavonoid accumulation in root tips except in two ethylene-insensitive mutants, *ein2*-5 and *etr1*-3. Buer et al. (2006b) observed that a *tt4* mutant, which makes no flavonoids, displays a delayed gravitropic response. In addition, the gravity response of *tt4* plants is also much less inhibited by ACC. This work suggests that ethylene regulates flavonoid levels using EIN2- and ETR1-dependent pathways, which in turn regulate root gravitropism.

In addition to the established *in planta* roles of flavonoids, the human health benefits of these compounds have been a major area of research interest in recent years. Flavonoids have long been thought to have antioxidant properties; flavonoids such as quercetin and kamperfol are excellent scavengers of free-radicals due in part to their hydrogen- or electron-donating capacity (Rice-Evans et al., 1997; Rice-Evans et al., 1995). Interestingly, experiments assessing radical-scavenging in an *in vitro* assay indicates the 3'4' dihydroxy subsituents in the B ring and conjugation between the A and B ring is needed for maximum antioxidant activity (Rice-Evans et al., 1995). The ability of flavonoids to scavenge free radicals is important since free radicals are believed to contribute to cancer, DNA damage, and cell proliferation. Additionally, numerous correlative and *in vivo* studies indicate that flavonoids can help prevent cancer (Androutsopoulos et al., 2010; Chen and Chen, 2013; Ren et al., 2003). Because flavonoids are so abundant in fruits and vegetables, their application as human-health agents could have far-reaching effects on social and medical policies.

v. Auxin and Ethylene: General

Auxin and ethylene interact in plants to control a wide range of cellular and physiological processes, at least in part by controlling the expression of genes essential for cell wall reorganization, and specialized metabolism, including flavonoid synthesis (Lewis et al., 2011; Stepanova et al., 2007). The auxin and ethylene signaling and response pathways appear to be interdependent, such that the response of one is often dependent on the other

(Muday et al., 2012; Stepanova et al., 2007; Strader et al., 2010). For example, Strader et al. (2010) observed that increased ethylene levels sensitize roots for auxin-responsive lateral root formation, suggesting that functioning through auxin, which is highly localized, may allow the highly volatile ethylene to still have highly precise and controlled effects. Recent research has not only confirmed that certain physiological responses regulated by auxin and ethylene rely upon each other (Grana et al., 2013; Tatsuki et al., 2013), but also that the auxin and ethylene biosynthetic pathways are linked by the enzymatic regulation of a single enzyme (Zheng et al., 2013b).

vi. Auxin and Ethylene: Proteomics

Auxin and ethylene biology is just recently becoming elucidated at the protein level. In contrast to studies using physiological and genomics tools, proteomics has not yet observed much interaction between auxin and ethylene to coordinately regulate a subset of proteins. For example, we observed that after treating *Arabidopsis* seedlings with 1 μM auxin or 1 μM ethylene for 24 h, a condition where auxin and ethylene interact to control gene expression and plant physiology, there was no overlap among auxin- and ethylene-responsive proteins (Slade et al., 2012). Additionally, more in-depth proteomics studies evaluating the auxin (Zhang et al., 2013) or ethylene (Zheng et al., 2013a) response in *Arabidopsis* revealed significant changes in protein abundance, but little overlap between the specific proteins affected by the two hormones. Thus, while there is good evidence that auxin and ethylene coordinately regulate gene expression and physiological responses, how this is manifested at the protein level remains to be determined.

The AUX/IAA gene family produces proteins that play pivotal roles in the auxin-signaling pathway. The AUX/IAA genes were originally observed as a gene family that was rapidly induced upon indole-3-acetic acid exposure (Reed, 2001). Since that original discovery, the AUX/IAA proteins have been observed to regulate many aspects of plant development. Yeast-2-Hybrid analysis shows that AUX/IAA proteins physically interact with auxin-responsive factors (ARFs) to control gene expression, and ultimately, plant biology (Kim et al., 1997; Ulmasov et al., 1997). Additionally, most auxin responses require Aux/IAA protein turnover, which is regulated by a physical interaction with SCF^{TIR1}(Gray et al., 2001). Interestingly, indole-3-acetic acid promotes the interaction between Aux/IAA proteins and SCF^{TIR1} in a soluble extract, indicating the Aux/IAA proteins are a major target of regulation.

Interrogation of the auxin-signaling pathway using global proteomics permits insight into the pathway not available to targeted and traditional methodologies. For example, Zhang et al. (2013) used a stable-isotope labeling strategy to identify over 3000 phosphopeptides, including PIN2, Auxin Response Factor (ARF2), and Sorting Nexin1 (SNX1). Interestingly, phosphorylation of a motif-specific serine recruits PIN2 into shootward recycling (Dhonukshe et al., 2010), while Zhang et al. (2013) observed down-regulation of PIN2 phosphorylation upon auxin treatment, suggesting discovery of a novel phosphorylation site. Additionally Chen et al. (Chen et al., 2010b) observed the dynamic regulation of PIN-formed auxin transport proteins in response to exogenous

IAA, suggesting a rapid response to the hormone and subsequent adaption to the stimulus.

vii. Proteomics in Plants

Mass spectrometry is the study and manipulation of charged molecules in the gas phase (Aebersold et al. 2003). A source of energy, perhaps in the form of a chemical, a laser, or a current, is applied to a molecule, which induces volatilization and ionization. Once a molecule is in the gas phase and is charged it can be persuaded to separate from other ions via manipulation using different properties in the region of a mass spectrometer called a mass analyzer. For example, quadrupole mass analyzer (Figure 1-3, A) separates ions using electricity. In addition to using electricity, a time-of-flight (TOF) analyzer separates ions by considering their drift time in a vacuum (Figure 1-3, B). Even more complex, hybrid mass analyzers separate ions using combinations of quadrupole and TOF mass analyzers (Figure 1-3, C). These analyzers, in many analytical workflows, have been used to study proteins in plants.

The field of plant proteomics is still in its infancy. While model systems like yeast and human cell lines have proven quite amenable to systems-level analyses, proteomic analyses in plants have been constrained by a number of technical hurdles (Barkla et al., 2013; Rose et al., 2004; Uhrig and Moorhead, 2013). Plant cells are surrounded by a sturdy cell wall that makes protein extraction difficult and at times inconsistent. Fortunately, technical developments in gel-based and gel-free proteomics methods are now making global proteomic analyses in plants a possibility. Until now plant proteomic research has largely focused on global profiling (Baerenfaller et al., 2008) and comparative analyses, including successful studies examining the response to salt (Jiang et al., 2007), cadmium (Alvarez, 2009), and cold stress (Amme et al., 2006).

Despite the technical improvements and the growing examples of successful global profiling, the field of plant proteomics is still struggling with how to integrate information about the proteome with physiological processes. Attempts have likely been most successful in yeast, where, for example, the comparison of haploid versus diploid yeast revealed that key members of the pheromone pathway are expressed only in the haploid, resulting in an efficient control of the mating response (de Godoy et al., 2008). The most successful attempts to date in plants have involved elucidating signal pathways. For example, Deng et al. (2007) used Difference-Gel Electrophoresis (DiGE) technology to uncover novel proteins involved in the brassinosteroid signaling pathway in *Arabidopsis.* Additionally, Shi et al. (2011) used DiGE to discover a novel effector of salt stress resistance, Receptor for activated C kinase 1C (RACK1C). However, the plant research community is in need of a proof-of-principle approach, where a well-studied physiological process is related to global proteomic changes.

viii. DiGE Technology

DiGE technology is an improvement upon two dimensional gel electrophoresis (2D-GE) that chemically links fluorophores to proteins in order to assess their abundance based on fluorescence. 2D-GE has been used for decades as the methodology of choice for

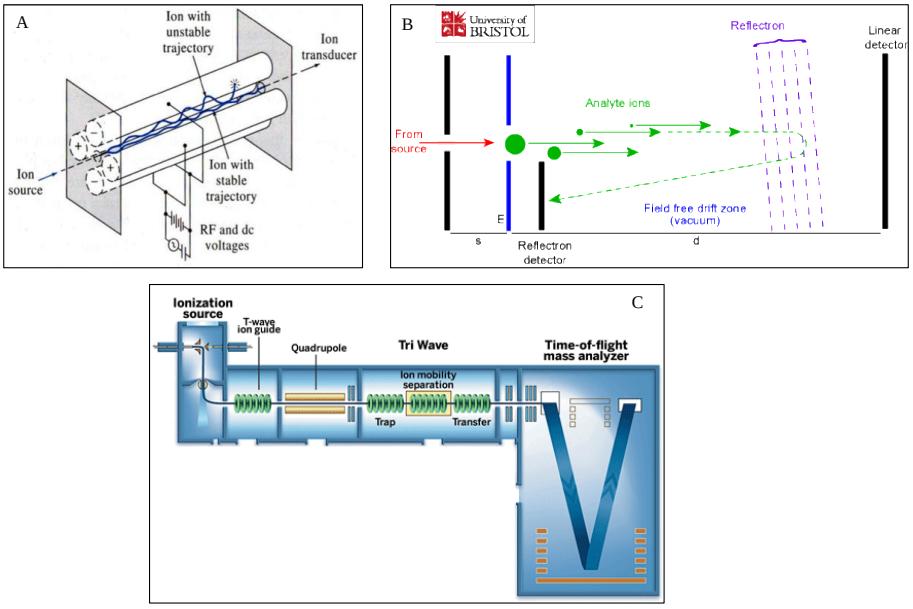

Figure 1-3 Overview of different mass analyzers. Shown are quadrupole (A), TOF (B), and hybrid (C).

proteomics. Thousands of proteins can be screened relatively quickly and target proteins identified via Matrix-assisted laser desorption ionization time of flight mass spectrometry (MALDI TOF/TOF). Unfortunately, 2D-GE has been plagued by the technical difficulty of the method and inter-lab variation. A major improvement came in 1997 when Unlu et al. (1997) established the DiGE methodology. Proteins from the conditions to be examined are labeled with spectrally-different fluorophores and processed on the same 2D gel. In this manner, proteins differentially expressed will be observed due to their differing fluorescence. Additionally, an internal control, representative of all proteins from every condition, is labeled with a control dye and processed in parallel with samples to be compared. The internal control reduces the number of gels needed for a 2D-GE analysis and reduces inter-gel variation (Marouga et al., 2005).

DiGE analysis has been used successfully in several model systems. In yeast, DiGE analysis has been used to begin the construction of a map for how meiosis functions at the proteomic level (Grassl et al., 2010). Studies of nutrition depletion in yeast have revealed upregulation of Cpc2p, the yeast ortholog of mammalian RACK1, a highly conserved and important translational regulator (Valerius et al., 2007). Further analysis showed that a *CPC2* deletion caused sensitivity to cell-wall-disrupting drugs, suggesting Cpc2 functions for general cell wall integrity. In humans, a great deal of research is focused on applying DiGE to studying human disease. Swatton et al. (2004) utilized DiGE in order to characterize the proteome profile of post-mortem brains, hopefully as a means to better understand disease. In conjunction with other high-throughput techniques, including transcriptomics and metabolomics, proteome profiling using DiGE could offer great insight into human disease. Additionally, DiGE combined with

bioinformatics is currently being explored as an exciting tool for biomarker discovery for cancer (Ludwig and Weinstein, 2005). In plants, several groups have utilized DiGE technology successfully. In *Brassica juncea*, DiGE was used to build a proteome map of the response of root tissues to cadmium stress (Alvarez, 2009). Such maps will be useful for understanding how changes at the proteome level direct responses to environmental stimuli.

ix. iTRAQ

Gel-free proteomics methods have garnered significant interest in recent years due to technical advances and increased accessibility of mass spectrometry. Several gel-free methods exist including Stable Isotope labeling by Amino Acids in Cell Culture (SILAC) (Ong et al., 2002), Tandem-Mass Tags (TMT) (Thompson et al., 2003), and Isobaric-Tagged Relative and Absolute quantification (iTRAQ). Advantages of the iTRAQ methodology include the ability to multiplex parallel samples (up to eight), the ability to rapidly identify components of a proteome (as compared to DiGE) and the possibility for relative quantification of several peptides for each protein.

Much like DiGE technology, iTRAQ has been used successfully for proteome studies in several model systems. In humans, iTRAQ was used successfully as part of a comprehensive approach to discover nine potential biomarkers for endometrial cancer (DeSouza et al., 2005). Additionally, iTRAQ followed by 2D-LC-MS/MS was used to discover several proteins that are up- or down-regulated during prostate cancer cell progression in humans (Glen et al., 2008). In plants, iTRAQ analyses have led to several discoveries. iTRAQ analysis of fungal-elicited proteome changes in Norway spruce revealed an unknown theme of calcium-mediated signaling (Lippert et al., 2009). In *Arabidopsis*, iTRAQ has been successfully used to study how innate-immune responses are reflected at the phosphoproteome level in both the cytosol (Nuhse et al., 2007) and plasma membrane (Jones et al., 2006).

x. Selected-Reaction Monitoring (SRM) of Peptides

Protein quantitation is an important and challenging concern for basic and biomedical scientists. This concern represents an understanding that organisms control many important processes by regulating the abundance of its proteins. Traditionally, protein abundance has been quantified using analytical techniques based on affinity reagents. While these affinity reagents offer excellent sensitivity (Pawlak et al., 2002), these assays are notoriously difficult and laborious. Additionally, protein quantitation using affinity reagents is expensive and difficult to multiplex. An alternative to affinity assays is Selected-Reaction Monitoring (SRM), which not only offers attomole sensitivity (Stahl-Zeng et al., 2007), but also allows multiplexing of hundreds of proteins in a single run (Picotti and Aebersold, 2012). To quantify proteins via SRM a triple-quadropule (QQQ) mass spectrometer acts as a mass filter and selectively analyses a specific molecular ion and one or more fragment ions. The analysis of these ions, typically online with chromatography, produces an elution profile displaying the time and intensity of the ions. This elution profile can then be extracted and analyzed for quantification of individual

peptides that can then be correlated with specific protein targets. In addition to quantifying target peptides, advances in SRM technology make screening peptides for their amenability to mass spectrometry easy and affordable. Thus, researchers can screen many target peptides to find those that work best for their instrumental configuration.

SRM technology has been successfully used for the relative and absolute quantification of proteins from many different organisms. In yeast, SRM was used to quantitate 45 proteins from glycolysis and the tricarboxylic acid and glyoxylate cycles under different nutrient conditions, providing insights into how yeast adapts to changing environmental conditions at the metabolic level (Picotti et al., 2009). In plants, SRM technology was used to assess how 13 members of the terpenoid pathway facilitate the plant response to insect attack (Zulak et al., 2009). In colon cancer cell lines, SRM was used to quantify 17 proteins in the Wnt/B-catenin signaling pathway (Chen et al., 2010a). Additionally, SRM was used to establish that the amount of tissue obtained in core biopsies could also be used for protein quantification (Chen et al., 2010a).

The analysis of SRM data poses unique challenges. Currently, the biggest challenge is the validation of SRM assays, or ensuring an assay monitors only one peptide. SRM validation is based on the selectivity of the SRM methodology and the observation of co-eluting product ions (Lange et al., 2008). Additionally, many groups acquire product-ion spectra triggered by the SRM assay to support their validation (Mortstedt et al., 2013). Although these guidelines have served the community well, there are additional considerations that must still be addressed. Complex proteomes result in many precursor/product pairs of similar masses. These similar masses are often not discriminated concretely by the liberal mass transmission window of most triple-quad instruments. Additionally, SRM assays are typically more sensitive than traditional data-dependent acquisition (DDA)-based fragmentation schemes (Picotti and Aebersold, 2012). Thus, peptides observed using SRM assays are not always available to a DDA method, meaning SRM-triggered acquisition of product-ion spectra for validation is not always feasible.

The proteomics community has developed several computational and analytical methods to overcome these limitations of the SRM methodology. One computational method is SRM Collider (Rost et al., 2012), which calculates a unique ion signature (UIS) based on the frequency of precursor-to-product ion masses in a given proteome. Thus, researchers can assess how effectively their SRM assay targets a single peptide. Another method, mProphet (Reiter et al., 2011), automates SRM validation by using decoy transitions and false discovery rates, which can be integrated with Skyline (MacLean et al., 2010), a computational environment that facilitates visualization and organization of SRM data. To address the issue of quadrupole selectivity and specificity, some researchers are spiking peptides labeled with heavy isotopes as internal standards (Abbatiello et al., 2010). Additionally, any measures of biological verification, such as the analysis of mutants that do not express a targeted protein, confirm validation of an SRM assay. Finally, in order to over the overcome the limitations of SRM-triggered acquisition of fragment ions, product-ion spectra can be obtained on an instrument better suited for

DDA methods by using a retention time scale that is normalized using standards (Escher et al., 2012).

xi. Ultra-high performance liquid chromatography (UPLC) coupled to high mass-accuracy mass spectrometry

New technologies are continuing to change proteomics research. Traditionally, proteomics relied on high-throughput, low-resolution technologies, such as 2D-GE, Surfance-enhanced laser desorption/ionization (Seldi), and protein arrays (Mann and Kelleher, 2008). Although these assays are affordable and accessible, they lack the sensitivity and resolution needed for an in-depth proteome analysis. However, in-depth analysis is now becoming a reality through the use of ultra-high performance liquid chromatography (UPLC) coupled to high mass-accuracy mass spectrometry. This technology represents a paradigm shift in discovery proteomics, which had suffered from limitations of traditional HPLC that struggles to balance the need for smaller particle sizes of column material (Welsch and Michalke, 2003) and the instrumentation to handle the subsequent back pressure (de Villiers et al., 2006). The groups of Jorgenson (MacNair et al., 1997; MacNair et al., 1999) and Lee (Wu et al., 2001) solved these issues by developing instrumentation capable of nanoscale flow rates under pressures as high as 7100bar. Commercial instruments, such as the Waters Acquity, have been developed that achieve a balance between high pressure and instrument reliability.

Advances in the capabilities of mass spectrometers are also changing proteomics. Traditionally, scientists relied on 3D-Ion Traps or TOF instruments capable of low to medium resolving power (10,000) (Mann and Kelleher, 2008). Additionally, these instruments exhibit a tradeoff among dynamic range, scan speed, and sensitivity (Table 1-1). Current machines, such as the Orbitraps and Ion-mobility instruments, offer an excellent balance among dynamic range (10^3-10^4 in complex samples), resolving power (50-100,000), and scan speed (0.1-1 scan/sec) (Mann and Kelleher, 2008). For example, Grauman et al. (2008) quantified over 5000 proteins from embryonic stem cells at 300 ppb accuracy using an LTQ-Orbitrap.

xii. Data Analysis

Following in the footsteps of the genomics revolution, proteomics is emerging as a data-driven field. Even the simplest of experiments can generate 1 TB of data. This quantity of data requires unprecedented computational resources and power. Currently, the life sciences community is not equipped to handle such data, and its analysis represents a huge bottleneck. Additionally, the proteomics field is plagued by non-standardized processing and analysis workflows. Reproducibility in science is a problem (Begley and Ellis, 2012), and application of different algorithms and statistical methods to the same dataset yields different results (Domon and Aebersold, 2006). Thus, to ensure that both the quality and analysis of proteomics data is valid for future researchers, there is an urgent need to develop both computational resources and standardized workflows.

Recent computational developments have improved the quality and reliability of data analysis for proteomics. Cloud computing offers scalable data storage and computing abilities. Recently, Kolker et al. (2011b) used the Microsoft Azure Cloud system using over 475 8-core virtual machines to align over 10 million protein sequences in the UniRef100 (Suzek et al., 2007) database in only six days. This type of computational power will be increasingly important as multi-site efforts for proteomics experiments continues (Hermjakob, 2006). In addition to advances in the utilization of computational resources, much effort has been invested in establishing standardized workflows for data analysis. The development of SPIRE (Systematic Protein Investigative Research Environment) represents a step towards high-quality, standardized data analysis (Kolker et al., 2011a). Additionally, MOPED represents a community resource for the standardized visualization of proteomics data (Kolker et al., 2012).

The current research aims to use a systems approach to study how phytohormone signaling affects a diverse array of cellular processes, including those mediated by flavonoid metabolism. The work presented here specifically addresses the question of whether exposure to auxin or ethylene results in changes in the Arabidopsis root proteome. These experiments are complemented with genetic analyses that probe connections between auxin and ethylene signaling and gravitropism. Not only can this research stand alone by identifying specific proteins of interest for future study, but it can also be integrated with transcriptomics and metabolomics data in order to provide a broad view of how the response to auxin and ethylene is mediated. This research will impact the plant biology community by providing a systems-level analysis of three processes that have already been extensively studied using traditional molecular and biochemical approaches: auxin/ethylene signaling, root gravitropism, and flavonoid metabolism. On a broader scale, this research will benefit scientists outside of the plant biology community by providing a proof-of-principle analysis and by developing new proteomics and computational tools essential for rigorous systems biology approaches to complex problems.

This body of work focuses on evaluating global and targeted proteomics methods in *Arabidopsis thaliana.* In Chapter 2, Chapter 3 and Appendix 1, we establish the methodology to apply traditional and DiGE-based 2D-GE strategies to global proteomics in *Arabidopsis*. Our results suggest that while 2D-GE is applicable to *Arabidopsis*, there are practical and conceptual limitations that must be understood. Additionally, we demonstrated the first parallel comparison of the effects of auxin and ethylene on the *Arabidopsis* root proteome and observed no overlap among the proteins regulated by the two phytohormones, at least for the most abundant proteins observed by 2D-GE.

Chapter 4 explores the efficacy of selected reaction monitoring for relative peptide quantification in *Arabidopsis* roots. Our results suggest that while the technology parallels application in yeast and humans, there are substantial analytical challenges that much be addressed. In Chapter 5 we explore the MS^E data acquisition scheme for global proteomics in *Arabidopsis.* Appendix 2 explores the efficacy of iTRAQ labeling for relative peptide quantification in *Arabidopsis* roots.

Table 1-1. Characteristics and performance of commonly-used mass spectrometers. Adapted from Domon et al. (2006).

	IT-LIT	**Q-Q-ToF**	**ToF-ToF**	**FT-ICR**	**Q-Q-Q**	**QQ-LIT**
Mass accuracy	Low	Good	Good	Excellent	Medium	Medium
Resolving power	Low	Good	High	Very high	Low	Low
Sensitivity (LOD)	Good		High	Medium	High	High
Dynamic range	Low	Medium	Medium	Medium	High	High
ESI	✓	✓		✓	✓	✓
MALDI	(✓)	(✓)	✓			
MS/MS capabilities	✓	✓	✓	✓	✓	✓
Additional capabilities	Seq. MS/MS			Precursor, Neutral loss, MRM		
Identification	++	++	++	+++	+	+
Quantification	+	+++	++	++	+++	+++
Throughput	+++	++	+++	++	++	++
Detection of modifications	+	+	+	+		+++

III. References

Abbatiello, S. E., Mani, D. R., Keshishian, H., Carr, S. A., 2010. Automated detection of inaccurate and imprecise transitions in peptide quantification by multiple reaction monitoring mass spectrometry. *Clinical Chemistry* 56, 291-305.

Aebersold, R. and Mann, M., 2003. Mass spectrometry-based proteomics. *Nature*. 422, 198-207.

Alvarez, S., 2009. Comprehensive analysis of the *Brassica juncea* root proteome in response to cadmium exposure by complementary proteomic approaches (p NA) (vol 9, pg 2419, 2009). *Proteomics* 9, 3220-3220.

Amme, S., Matros, A., Schlesier, B., Mock, H. P., 2006. Proteome analysis of cold stress response in *Arabidopsis thaliana* using DIGE-technology. *Journal of Experimental Botany* 57, 1537-1546.

Androutsopoulos, V. P., Papakyriakou, A., Vourloumis, D., Tsatsakis, A. M., Spandidos, D. A., 2010. Dietary flavonoids in cancer therapy and prevention: Substrates and inhibitors of cytochrome P450 CYP1 enzymes. *Pharmacology and Therapeutics* 126, 9-20.

Aszalos, A., 2008. Role of ATP-Binding Cassette (ABC) transporters in interactions between natural products and drugs. *Current Drug Metabolism* 9, 1010-1018.

Baerenfaller, K., Grossmann, J., Grobei, M. A., Hull, R., Hirsch-Hoffmann, M., Yalovsky, S., Zimmermann, P., Grossniklaus, U., Gruissem, W., Baginsky, S., 2008. Genome-scale proteomics reveals *Arabidopsis thaliana* gene models and proteome dynamics. *Science* 320, 938-941.

Barkla, B. J., Vera-Estrella, R., Pantoja, O., 2013. Progress and challenges for abiotic stress proteomics of crop plants. *Proteomics* 13, 1801-1815.

Beckwith, J. R., 1967. Regulation of the lac operon: Recent studies on the regulation of lactose metabolism in *Escherichia coli* support the operon model. *Science* 156, 597-604.

Beggs, C. J., Schneider-Ziebert, U., and Wellmann, E. 1986. UV-B radiation and adaptive mechanisms in plants. Springer-Verlag, New York.

Begley, C. G., Ellis, L. M., 2012. Drug development: Raise standards for preclinical cancer research. *Nature* 483, 531-533.

Benfey, P. N., Mitchell-Olds, T., 2008. From genotype to phenotype: systems biology meets natural variation. *Science* 320, 495-497.

Blanc, G., Duncan, G., Agarkova, I., Borodovsky, M., Gurnon, J., Kuo, A., Lindquist, E., Lucas, S., Pangilinan, J., Polle, J., Salamov, A., Terry, A., Yamada, T., Dunigan, D. D., Grigoriev, I. V., Claverie, J. M., Van Etten, J. L., 2010. The *Chlorella variabilis* NC64A genome reveals adaptation to photosymbiosis, coevolution with viruses, and cryptic sex. *Plant Cell* 22, 2943-2955.

Blancaflor, E. B., Masson, P. H., 2003. Plant gravitropism: Unraveling the ups and downs of a complex process. *Plant Physiology* 133, 1677-1690.

Bowler, C., Allen, A. E., Badger, J. H., Grimwood, J., Jabbari, K., Kuo, A., Maheswari, U., Martens, C., Maumus, F., Otillar, R. P., *et al*, 2008. The *Phaeodactylum* genome reveals the evolutionary history of diatom genomes. *Nature* 456, 239-244.

Buer, C. S., Kordbacheh, F., Truong, T. T., Hocart, C. H., Djordjevic, M. A., 2013. Alteration of flavonoid accumulation patterns in *transparent testa* mutants disturbs auxin transport, gravity responses, and imparts long-term effects on root and shoot architecture. *Planta* 231, 171-189.

Buer, C. S., Muday, G. K., 2005. The *transparent testa4* mutation prevents flavonoid synthesis and alters auxin transport and the response of *Arabidopsis* roots to gravity and light (vol 16, pg 1191, 2004). *Plant Cell* 17, 2614-2614.

Buer, C. S., Sukumar, P., Muday, G. K., 2006a. Ethylene modulates flavonoid accumulation and gravitropic responses in roots of *Arabidopsis*. *Plant Physiol*ogy 140, 1384-1396.

Caldwell, M. M., Robberecht, R., Flint, S. D., 1983. Internal filters - prospects for UV-acclimation in higher-plants. *Physiology Plantarum* 58, 445-450.

Casimiro, I., Marchant, A., Bhalerao, R. P., Beeckman, T., Dhooge, S., Swarup, R., Graham, N., Inze, D., Sandberg, G., Casero, P. J., Bennett, M., 2001. Auxin transport promotes *Arabidopsis* lateral root initiation. *Plant Cell* 13, 843-852.

Chen, A. Y., Chen, Y. C., 2013. A review of the dietary flavonoid, kaempferol on human health and cancer chemoprevention. *Food Chemistry* 138, 2099-2107.

Chen, Y., Gruidl, M., Remily-Wood, E., Liu, R. Z., Eschrich, S., Lloyd, M., Nasir, A., Bui, M. M., Huang, E., Shibata, D., Yeatman, T., Koomen, J. M., 2010a. Quantification of beta-catenin signaling components in colon cancer cell lines, tissue sections, and microdissected tumor cells using reaction monitoring mass spectrometry. *Journal of Proteome Research* 9, 4215-4227.

Chen, Y., Hoehenwarter, W., Weckwerth, W., 2010b. Comparative analysis of phytohormone-responsive phosphoproteins in *Arabidopsis thaliana* using TiO2-phosphopeptide enrichment and mass accuracy precursor alignment. *Plant Journal* 63, 1-17.

Cock, J. M., Sterck, L., Rouze, P., Scornet, D., Allen, A. E., Amoutzias, G., Anthouard, V., Artiguenave, F., Aury, J. M., et al. 2010. The *Ectocarpus* genome and the independent evolution of multicellularity in brown algae. *Nature* 465, 617-621.

D'Auria, J. C., Gershenzon, J., 2005. The secondary metabolism of *Arabidopsis thaliana*: growing like a weed. *Current Opinion in Plant Biology* 8, 308-316.

Davis, B. D., Kalan, E. B., Sprinson, D. B., Srinivasan, P. R., 1956a. The conversion of various carbohydrates to 5-dehydroskikimic acid by bacterial extracts. *Journal of Biological Chemistry* 223, 907-912.

Davis, B. D., Kalan, E. B., Sprinson, D. B., Srinivasan, P. R., 1956b. The enzymatic conversion of sedoheptulose-1, 7-diphosphate to shikimic acid. *Journal of Biological Chemistry* 223, 913-920.

de Godoy, L. M. F., Olsen, J. V., Cox, J., Nielsen, M. L., Hubner, N. C., Frohlich, F., Walther, T. C., Mann, M., 2008. Comprehensive mass-spectrometry-based proteome quantification of haploid versus diploid yeast. *Nature* 455, 1251-1254.

de Villiers, A., Lestremau, F., Szucs, R., Gelebart, S., David, F., Sandra, P., 2006. Evaluation of ultra performance liquid chromatography. Part I. Possibilities and limitations. *Journal of Chromatography A* 1127, 60-69.

Deng, Z. P., Zhang, X., Tang, W. Q., Oses-Prieto, J. A., Suzuki, N., Gendron, J. M., Chen, H. J., Guan, S. H., Chalkley, R. J., Peterman, T. K., Burlingame, A. L., Wang, Z. Y., 2007. A proteomics study of brassinosteroid response in *Arabidopsis*. *Molecular and Cellular Proteomic*s 6, 2058-2071.

DeSouza, L., Diehl, G., Rodrigues, M. J., Guo, J., Romaschin, A. D., Colgan, T. J., Siu, K. W. M., 2005. Search for cancer markers from endometrial tissues using differentially labeled tags iTRAQ and cICAT with multidimensional liquid chromatography and tandem mass spectrometry. *Journal of Proteome Research* 4, 377-386.

Dhonukshe, P., Huang, F., Galvan-Ampudia, C. S., Mahonen, A. P., Kleine-Vehn, J., Xu, J. A., Quint, A., Prasad, K., Friml, J., Scheres, B., Offringa, R., 2010. Plasma membrane-bound AGC3 kinases phosphorylate PIN auxin carriers at TPRXS(N/S) motifs to direct apical PIN recycling. *Development* 137, 3245-3255.

Dixon, R. A., 2004. Phytoestrogens. *Annual Review of Plant Biology* 55, 225-261.

Domon, B., and Aebersold, R., 2006. Challenges and opportunities in proteomics data analysis. *Molecular and Cellular Proteomics* 5, 1921-1926.

Domon, B., and Aebersold, R. 2006. Mass spectrometry and protein analysis. *Science* 14, 212-217

Edwards, K., Cramer, C. L., Bolwell, G. P., Dixon, R. A., Schuch, W., Lamb, C. J., 1985. Rapid transient induction of phenylalanine ammonia-lyase mRNA in elicitor-treated bean cells. *Proceedings of the National Academy of Sciences* U S A 82, 6731-6735.

Escher, C., Reiter, L., MacLean, B., Ossola, R., Herzog, F., Chilton, J., MacCoss, M. J., Rinner, O., 2012. Using iRT, a normalized retention time for more targeted measurement of peptides. *Proteomics* 12, 1111-1121.

Firn, R. D., Jones, C. G., 2009. A Darwinian view of metabolism: molecular properties determine fitness. *Journal of Experimental Botany* 60, 719-726.

Fraenkel, G. S., 1959. The Raison d'Etre of secondary plant substances: These odd chemicals arose as a means of protecting plants from insects and now guide insects to food. *Science* 129, 1466-1470.

Frost, J. W., Bender, J. L., Kadonaga, J. T., Knowles, J. R., 1984. Dehydroquinate synthase from *Escherichia coli*: purification, cloning, and construction of overproducers of the enzyme. *Biochemistry* 23, 4470-4475.

Ge, H., Walhout, A. J., Vidal, M., 2003. Integrating 'omic' information: a bridge between genomics and systems biology. *Trends in Genetics* 19, 551-560.

Glen, A., Gan, C. S., Hamdy, F. C., Eaton, C. L., Cross, S. S., Catto, J. W. F., Wright, P. C., Rehman, I., 2008. iTRAQ-facilitated proteomic analysis of human prostate cancer cells identifies proteins associated with progression. *Journal of Proteome Research* 7, 897-907.

Grana, E., Sotelo, T., Diaz-Tielas, C., Araniti, F., Krasuska, U., Bogatek, R., Reigosa, M. J., Sanchez-Moreiras, A. M., 2013. Citral induces auxin and ethylene-mediated malformations and arrests cell division in *Arabidopsis thaliana* roots. *Journal of Chemical Ecology* 39, 271-282.

Grassl, J., Scaife, C., Polden, J., Daly, C. N., Iacovella, M. G., Dunn, M. J., Clyne, R. K., 2010. Analysis of the budding yeast pH 4-7 proteome in meiosis. *Proteomics* 10, 506-519.

Graumann, J., Hubner, N. C., Kim, J. B., Ko, K., Moser, M., Kumar, C., Cox, J., Scholer, H., Mann, M., 2008. Stable isotope labeling by amino acids in cell culture (SILAC) and proteome quantitation of mouse embryonic stem cells to a depth of 5,111 proteins. *Molecular and Cellular Proteomics* 7, 672-683.

Gray, W. M., Kepinski, S., Rouse, D., Leyser, O., Estelle, M., 2001. Auxin regulates SCFTIR1-dependent degradation of AUX/IAA proteins. *Nature* 414, 271-276.

Harborne, J. B., 1999. Recent advances in chemical ecology. *Natural Product Reports* 16, 509-523.

Harborne, J. B., Williams, C. A., 2000. Advances in flavonoid research since 1992. *Phytochemistry* 55, 481-504.

Hartmann, T., 2007. From waste products to ecochemicals: fifty years research of plant secondary metabolism. *Phytochemistry* 68, 2831-2846.

Hermjakob, H., 2006. The HUPO proteomics standards initiative--overcoming the fragmentation of proteomics data. *Proteomics* 6 Suppl 2, 34-38.

Herrmann, K. M. (Ed.), 1983. The common aromatic biosynthetic pathway. Addison-Wesley, London.

Herrmann, K. M., 1995. The shikimate pathway: early steps in the biosynthesis of aromatic compounds. *Plant Cell* 7, 907-919.

Herrmann, K. M., Weaver, L. M., 1999. The shikimate pathway. *Annual Review of Plant Physiology* 50, 473-503.

Jacobs, M., Rubery, P. H., 1988. Naturally-occurring auxin transport regulators. *Science* 241, 346-349.

Jiang, Y., Yang, B., Harris, N. S., Deyholos, M. K., 2007. Comparative proteomic analysis of NaCl stress-responsive proteins in *Arabidopsis* roots. *Journal of Experimental Botany* 58, 3591-3607.

Jin, H. L., Cominelli, E., Bailey, P., Parr, A., Mehrtens, F., Jones, J., Tonelli, C., Weisshaar, B., Martin, C., 2000. Transcriptional repression by AtMYB4 controls production of UV-protecting sunscreens in *Arabidopsis*. *Embo Journal* 19, 6150-6161.

Jones, A. M. E., Bennett, M. H., Mansfield, J. W., Grant, M., 2006. Analysis of the defense phosphoproteome of *Arabidopsis thaliana* using differential mass tagging. *Proteomics* 6, 4155-4165.

Kachlicki, P., Einhorn, J., Muth, D., Kerhoas, L., Stobiecki, M., 2008. Evaluation of glycosylation and malonylation patterns in flavonoid glycosides during LC/MS/MS metabolite profiling. *Journal of Mass Spectrometry* 43, 572-586.

Keith, B., Dong, X. N., Ausubel, F. M., Fink, G. R., 1991. Differential induction of 3-deoxy-D-arabino-heptulosonate 7-phosphate synthase genes in *Arabidopsis thaliana* by wounding and pathogenic attack. *Proceedings of the National Academy of Sciences* 88, 8821-8825.

Kerhoas, L., Aouak, D., Cingoz, A., Routaboul, J. M., Lepiniec, L., Einhorn, J., Birlirakis, N., 2006. Structural characterization of the major flavonoid glycosides from *Arabidopsis thaliana* seeds. *Journal of Agricultural and Food Chemistry* 54, 6603-6612.

Kim, J., Harter, K., Theologis, A., 1997. Protein-protein interactions among the Aux/IAA proteins. *Proceedings of the National Academy of Sciences* 94, 11786-11791.

Kolker, E., Higdon, R., Haynes, W., Welch, D., Broomall, W., Lancet, D., Stanberry, L., Kolker, N., 2012. MOPED: Model organism protein expression database. *Nucleic Acids Research* 40, D1093-D1099.

Kolker, E., Higdon, R., Welch, D., Bauman, A., Stewart, E., Haynes, W., Broomall, W., Kolker, N., 2011a. SPIRE: Systematic protein investigative research environment. *Journal of Proteomics* 75, 122-126.

Kolker, N., Higdon, R., Broomall, W., Stanberry, L., Welch, D., Lu, W., Haynes, W., Barga, R., Kolker, E., 2011b. Classifying proteins into functional groups based on all-versus-all BLAST of 10 million proteins. *Omics* 15, 513-521.

Korkina, L. G., 2007. Phenylpropanoids as naturally occurring antioxidants: from plant defense to human health. *Cellular and Molecular Biology* (Noisy-le-grand) 53, 15-25.

Koukol, J., Conn, E. E., 1961. The metabolism of aromatic compounds in higher plants. IV. Purification and properties of the phenylalanine deaminase of *Hordeum vulgare*. *Journal of Biological Chemistry* 236, 2692-2698.

Kuhn, B. M., Geisler, M., Bigler, L., Ringli, C., 2011. Flavonols accumulate asymmetrically and affect auxin transport in *Arabidopsis*. *Plant Physiology* 156, 585-595.

Kuhn, D. N., Chappell, J., Boudet, A., Hahlbrock, K., 1984. Induction of phenylalanine ammonia-lyase and 4-coumarate:CoA ligase mRNAs in cultured plant cells by UV light or fungal elicitor. *Proceeings of the National Academy of Science U S A* 81, 1102-1106.

Landry, L. G., Chapple, C. C. S., Last, R. L., 1995. *Arabidopsis* mutants lacking phenolic sunscreens exhibit enhanced ultraviolet injury and oxidative damage. *Plant Physiology* 109, 1159-1166.

Lange, V., Picotti, P., Domon, B., Aebersold, R., 2008. Selected reaction monitoring for quantitative proteomics: a tutorial. *Molecular Systems Biology* 4, 222.

Lewis, D. R., Ramirez, M. V., Miller, N. D., Vallabhaneni, P., Ray, W. K., Helm, R. F., Winkel, B. S. J., Muday, G. K., 2011. Auxin and ethylene induce flavonol accumulation through distinct transcriptional networks. *Plant Physiology* 156, 144-164.

Li, J. Y., Oulee, T. M., Raba, R., Amundson, R. G., Last, R. L., 1993. *Arabidopsis* flavonoid mutants are hypersensitive to UV-B Irradiation. *Plant Cell* 5, 171-179.

Lippert, D. N., Ralph, S. G., Phillips, M., White, R., Smith, D., Hardie, D., Gershenzon, J., Ritland, K., Borchers, C. H., Bohlmann, J., 2009. Quantitative iTRAQ proteome and comparative transcriptome analysis of elicitor-induced Norway spruce (*Picea abies*) cells reveals elements of calcium signaling in the early conifer defense response. *Proteomics* 9, 350-367.

Ludwig, J. A., Weinstein, J. N., 2005. Biomarkers in cancer staging, prognosis and treatment selection. *Nature Reviews Cancer* 5, 845-856.

MacLean, B., Tomazela, D. M., Shulman, N., Chambers, M., Finney, G. L., Frewen, B., Kern, R., Tabb, D. L., Liebler, D. C., MacCoss, M. J., 2010. Skyline: an open source document editor for creating and analyzing targeted proteomics experiments. *Bioinformatics* 26, 966-968.

MacNair, J. E., Lewis, K. C., Jorgenson, J. W., 1997. Ultrahigh-pressure reversed-phase liquid chromatography in packed capillary columns. *Analytical Chemistry* 69, 983-989.

MacNair, J. E., Patel, K. D., Jorgenson, J. W., 1999. Ultrahigh-pressure reversed-phase capillary liquid chromatography: isocratic and gradient elution using columns packed with 1.0-micron particles. *Analytical Chemistry* 71, 700-708.

Mann, M., Kelleher, N. L., 2008. Precision proteomics: the case for high resolution and high mass accuracy. *Proceedings of the National Academy of Sciences* 105, 18132-18138.

Marchant, A., Kargul, J., May, S. T., Muller, P., Delbarre, A., Perrot-Rechenmann, C., Bennett, M. J., 1999. AUX1 regulates root gravitropism in *Arabidopsis* by facilitating auxin uptake within root apical tissues. *Embo Journal* 18, 2066-2073.

Marouga, R., David, S., Hawkins, E., 2005. The development of the DIGE system: 2D fluorescence difference gel analysis technology. *Analytical and Bioanalytical Chemistry* 382, 669-678.

May, P., Wienkoop, S., Kempa, S., Usadel, B., Christian, N., Rupprecht, J., Weiss, J., Recuenco-Munoz, L., Ebenhoh, O., Weckwerth, W., Walther, D., 2008. Metabolomics- and proteomics-assisted genome annotation and analysis of the draft metabolic network of *Chlamydomonas reinhardtii*. *Genetics* 179, 157-166.

Mortstedt, H., Karedal, M. H., Jonsson, B. A. G., Lindh, C. H., 2013. Screening method using selected reaction monitoring for targeted proteomics studies of nasal lavage fluid. *Journal of Proteome Research* 12, 234-247.

Muday, G. K., DeLong, A., 2001. Polar auxin transport: controlling where and how much. *Trends in Plant Science* 6, 535-542.

Muday, G. K., Rahman, A., Binder, B. M., 2012. Auxin and ethylene: collaborators or competitors? *Trends in Plant Science.* 17, 181-195.

Nuhse, T. S., Bottrill, A. R., Jones, A. M. E., Peck, S. C., 2007. Quantitative phosphoproteomic analysis of plasma membrane proteins reveals regulatorymechanisms of plant innate immune responses. *Plant Journal* 51, 931-940.

Ong, S. E., Blagoev, B., Kratchmarova, I., Kristensen, D. B., Steen, H., Pandey, A., Mann, M., 2002. Stable isotope labeling by amino acids in cell culture, SILAC, as a simple and accurate approach to expression proteomics. *Molecular and Cellular Proteomics* 1, 376-386.

Palsson, B., 2002. In silico biology through "omics". *Nature Biotechnology* 20, 649-650.

Pawlak, M., Schick, E., Bopp, M. A., Schneider, M. J., Oroszlan, P., Ehrat, M., 2002. Zeptosens' protein microarrays: a novel high performance microarray platform for low abundance protein analysis. *Proteomics* 2, 383-393.

Peer, W. A., Brown, D. E., Tague, B. W., Muday, G. K., Taiz, L., Murphy, A. S., 2001. Flavonoid accumulation patterns of *transparent testa* mutants of *Arabidopsis*. *Plant Physiology* 126, 536-548.

Pichersky, E., Gang, D. R., 2000. Genetics and biochemistry of secondary metabolites in plants: an evolutionary perspective. *Trends in Plant Science* 5, 439-445.

Picotti, P., Aebersold, R., 2012. Selected reaction monitoring-based proteomics: workflows, potential, pitfalls and future directions. *Nature Methods* 9, 555-566.

Picotti, P., Bodenmiller, B., Mueller, L. N., Domon, B., Aebersold, R., 2009. Full dynamic range proteome analysis of *S. cerevisiae* by targeted proteomics. *Cell* 138, 795-806.

Raikhel, N., 2008. 2020 Vision for biology: The role of plants in addressing grand challenges in biology. *Molecular Plant* 1, 561-563.

Reed, J. W., 2001. Roles and activities of Aux/IAA proteins in *Arabidopsis*. *Trends in Plant Science* 6, 420-425.

Reiter, L., Rinner, O., Picotti, P., Huttenhain, R., Beck, M., Brusniak, M. Y., Hengartner, M. O., Aebersold, R., 2011. mProphet: automated data processing and statistical validation for large-scale SRM experiments. *Nature Methods* 8, 430-435.

Ren, W. Y., Qiao, Z. H., Wang, H. W., Zhu, L., Zhang, L., 2003. Flavonoids: Promising anticancer agents. *Medical Research Review* 23, 519-534.

Rice-Evans, C. A., Miller, J., Paganga, G., 1997. Antioxidant properties of phenolic compounds. *Trends in Plant Science* 2, 152-159.

Rice-Evans, C. A., Miller, N. J., Bolwell, G. P., Bramley, P. M., Pridham, J. B., 1995. The relative antioxidant activities of plant-derived polyphenolic flavonoids. *Free Radical Research* 22, 375-383.

Ringli, C., Bigler, L., Kuhn, B. M., Leiber, R. M., Diet, A., Santelia, D., Frey, B., Pollmann, S., Klein, M., 2008. The modified flavonol glycosylation profile in the *Arabidopsis* rol1 mutants results in alterations in plant growth and cell shape formation. *Plant Cell* 20, 1470-1481.

Rose, J. K. C., Bashir, S., Giovannoni, J. J., Jahn, M. M., Saravanan, R. S., 2004. Tackling the plant proteome: practical approaches, hurdles and experimental tools. *Plant Journal* 39, 715-733.

Rost, H., Malmstrom, L., Aebersold, R., 2012. A computational tool to detect and avoid redundancy in selected reaction monitoring. *Molecular and Cellular Proteomics* 11, 540-549.

Ryder, T. B., Cramer, C. L., Bell, J. N., Robbins, M. P., Dixon, R. A., Lamb, C. J., 1984. Elicitor rapidly induces chalcone synthase mRNA in *Phaseolus vulgaris* cells at the onset of the phytoalexin defense response. *Proceedings of the National Academy of Sciences* 81, 5724-5728.

Sachs, J. (Ed.), 1873. Lehrbuch der Botanik. Leipzig.

Shi, S. S., Chen, W., Sun, W. N., 2011. Comparative proteomic analysis of the *Arabidopsis* cbl1 mutant in response to salt stress. *Proteomics* 11, 4712-4725.

Slade, W. O., Ray, W. K., Williams, P. M., Winkel, B. S. J., Helm, R. F., 2012. Effects of exogenous auxin and ethylene on the *Arabidopsis* root proteome. *Phytochemistry* 84, 18-23.

Srinivasan, P. R., Shigeura, H. T., Sprecher, M., Sprinson, D. B., Davis, B. D., 1956. The biosynthesis of shikimic acid from D-glucose. *J Biol Chem* 220, 477-497.

Stafford, H. A., 1991. Flavonoid evolution - an enzymatic approach. *Plant Physiology* 96, 680-685.

Stahl-Zeng, J., Lange, V., Ossola, R., Eckhardt, K., Krek, W., Aebersold, R., Domon, B., 2007. High sensitivity detection of plasma proteins by multiple reaction monitoring of N-glycosites. *Molecular and Cellular Proteomics* 6, 1809-1817.

Stepanova, A. N., Yun, J., Likhacheva, A. V., Alonso, J. M., 2007. Multilevel interactions between ethylene and auxin in *Arabidopsis* roots. *Plant Cell* 19, 2169-2185.

Stobiecki, M., Skirycz, A., Kerhoas, L., Kachlicki, P., Muth, D., Einhorn, J., Mueller-Roeber, B., 2006. Profiling of phenolic glycosidic conjugates in leaves of *Arabidopsis thaliana* using LC/MS. *Metabolomics* 2, 197-219.

Strader, L. C., Chen, G. L., Bartel, B., 2010. Ethylene directs auxin to control root cell expansion. *Plant Journal* 64, 874-884.

Suzek, B. E., Huang, H. Z., McGarvey, P., Mazumder, R., Wu, C. H., 2007. UniRef: comprehensive and non-redundant UniProt reference clusters. *Bioinformatics* 23, 1282-1288.

Suzich, J. A., Dean, J. F., Herrmann, K. M., 1985. 3-deoxy-d-arabino-heptulosonate 7-phosphate synthase from carrot root (*Daucus carota*) is a hysteretic enzyme. *Plant Physiol* 79, 765-770.

Swatton, J. E., Prabakaran, S., Karp, N. A., Lilley, K. S., Bahn, S., 2004. Protein profiling of human postmortem brain using 2-dimensional fluorescence difference gel electrophoresis (2-D DIGE). *Molecular Psychiatry* 9, 128-143.

Tatsuki, M., Nakajima, N., Fujii, H., Shimada, T., Nakano, M., Hayashi, K., Hayama, H., Yoshioka, H., Nakamura, Y., 2013. Increased levels of IAA are required for system 2 ethylene synthesis causing fruit softening in peach (*Prunus persica* L. Batsch). *Journal of Experimental Botany* 64, 1049-1059.

Thompson, A., Schafer, J., Kuhn, K., Kienle, S., Schwarz, J., Schmidt, G., Neumann, T., Hamon, C., 2003. Tandem mass tags: A novel quantification strategy for comparative analysis of complex protein mixtures by MS/MS (vol 15, pg 1895, 2003). *Analytical Chemistry* 75, 4942-4942.

Ulmasov, T., Murfett, J., Hagen, G., Guilfoyle, T. J., 1997. Aux/IAA proteins repress expression of reporter genes containing natural and highly active synthetic auxin response elements. *Plant Cell* 9, 1963-1971.

Umbarger, H. E., Brown, B., 1957. Threonine deamination in *Escherichia coli*. II. Evidence for two L-threonine deaminases. *Journal of Bacteriology* 73, 105-112.

Unlu, M., Morgan, M. E., Minden, J. S., 1997. Difference gel electrophoresis: A single gel method for detecting changes in protein extracts. *Electrophoresis* 18, 2071-2077.

Valerius, O., Kleinschmidt, M., Rachfall, N., Schulze, F., López Marín, S., Hoppert, M., Streckfuss-Bömeke, K., Fischer, C., Braus, G. H., 2007. The *Saccharomyces* homolog of mammalian RACK1, Cpc2/Asc1p, is required for FLO11-dependent adhesive growth and dimorphism. *Molecular and Cellular Proteomics* 6, 1968-1979.

Vallabhaneni, P., Keith Ray, W., Winkel, B. S., Helm, R. F., 2012. Characterization of flavonol glycosides in individual *Arabidopsis* root tips by flow injection electrospray mass spectrometry. *Phytochemistry* 73, 114-118.

Verpoorte, R., 1998. Exploration of nature's chemodiversity: the role of secondary metabolites as leads in drug development. *Drug Discovery Today* 3, 232-238.

Welsch, T., Michalke, D., 2003. (Micellar) electrokinetic chromatography: an interesting solution for the liquid phase separation dilemma. *Journal of Chromatography A* 1000, 935-951.

Westerhoff, H. V., Palsson, B. O., 2004. The evolution of molecular biology into systems biology. *Nature Biotechnology* 22, 1249-1252.

Winkel, B. S. J., 2006. The biosynthesis of flavonoids. Springer Science & Business Media, New York.

Winkel-Shirley, B., 2001a. Flavonoid biosynthesis. A colorful model for genetics, biochemistry, cell biology, and biotechnology. *Plant Physiology* 126, 485-493.

Winkel-Shirley, B., 2001b. It takes a garden. How work on diverse plant species has contributed to an understanding of flavonoid metabolism. *Plant Physiology* 127, 1399-1404.

Winkel-Shirley, B., 2002. Biosynthesis of flavonoids and effects of stress. *Current Opinion in Plant Biology* 5, 218-223.

Wu, N., Lippert, J. A., Lee, M. L., 2001. Practical aspects of ultrahigh pressure capillary liquid chromatography. *Journal of Chromatography A* 911, 1-12.

Yates, R. A., Pardee, A. B., 1957. Control by uracil of formation of enzymes required for orotate synthesis. *Journal of Biological Chemistry* 227, 677-692.

Zhang, H., Zhou, H., Berke, L., Heck, A. J., Mohammed, S., Scheres, B., Menke, F. L., 2013. Quantitative phosphoproteomics after auxin-stimulated lateral root induction identifies a SNX1 phosphorylation site required for growth. *Molecular and Cellular Proteomics* 12, 1158-1169.

Zheng, Q., Song, J., Campbell-Palmer, L., Thompson, K., Li, L., Walker, B., Cui, Y., Li, X., 2013a. A proteomic investigation of apple fruit during ripening and in response to ethylene treatment. *Journal of Proteomics.*

Zheng, Z., Guo, Y., Novak, O., Dai, X., Zhao, Y., Ljung, K., Noel, J. P., Chory, J., 2013b. Coordination of auxin and ethylene biosynthesis by the aminotransferase VAS1. *Nature Chemical Biology* 9, 244-246.

Zulak, K. G., Lippert, D. N., Kuzyk, M. A., Domanski, D., Chou, T., Borchers, C. H., Bohlmann, J., 2009. Targeted proteomics using selected reaction monitoring reveals the induction of specific terpene synthases in a multi-level study of methyl jasmonate-treated Norway spruce (*Picea abies*). *Plant Journal* 60, 1015-1030.

Chapter 2

Effects of exogenous auxin and ethylene on the *Arabidopsis* root proteome

William O. Slade[A], W. Keith Ray[B], Williams P.M[C], Richard F. Helm[B], Brenda S.J. Winkel[A]

Departments of Biological Sciences[A], Biochemistry[B], and Animal and Poultry Sciences[C]. Virginia Tech, Blacksburg, VA 24061-0406, United States

Reprinted from *Phytochemistry*, 2012, 84, William O. Slade, W. Keith Ray, Patricia M. Williams, Richard F. Helm, and Brenda S.J. Winkel, Effects of exogenous auxin on the *Arabidopsis* root proteome, 18-23, Copyright (2012), with permission from Elsevier.

Contributions

William O. Slade
Designed the experiments, performed the experiments, analyzed the data, and wrote the manuscript.

Patricia M. Williams
Provided analytical support.

W. Keith Ray
Provided technical support.

Richard F. Helm
Conceived the experimental idea, designed the experiments, analyzed the data, and wrote the manuscript.

Brenda S.J. Winkel
Conceived the experimental idea, designed the experiments, analyzed the data, and wrote the manuscript.

I. Abstract

The phytohormones, auxin and ethylene, together control a wide range of physiological and developmental processes in plants. The lack of knowledge regarding how the underlying signaling processes are reflected at the protein level represents a major gap in understanding phytohormone signaling, including that mediated by crosstalk between auxin and ethylene. Herein is a parallel comparison of the effects of these two hormones on the *Arabidopsis* root proteome. *Arabidopsis* seedlings were exposed to 1 μm indole-3-acetic acid (IAA, auxin) or 1 μm 1-amino-cyclopropane carboxylic acid (ACC) for 24h. Root protein extracts were fractionated using two-dimensional gel electrophoresis and the proteins that changed the most were analyzed by MALDI TOF/TOF mass spectrometry. Of the 500 total spots that were matched across all gels, 24 were significantly different after IAA exposure, while seven others were different after ACC exposure. Using rigorous criteria, identities of eight proteins regulated by IAA and five regulated by ACC were assigned. Interestingly, although both hormones affected proteins associated with fundamental cellular processes, no overlap was observed among the proteins affected by auxin or ethylene treatment. This report provides a comparison of the effects of these two hormones relative to a control utilizing equivalent treatment regimes and suggests that, while these hormones communicate to control similar physiological and transcriptional processes, they have different effects on the most abundant proteins in *Arabidopsis* roots.

II. Introduction

Auxin and ethylene interact to control a variety of important physiological processes in plant roots, including root morphogenesis and the response to gravity and light (Lewis et al., 2011; Pitts et al., 1998; Rahman et al., 2002). The auxin and ethylene signaling and response pathways appear to be highly interdependent, so that the response to one hormone requires, in many situations, responsiveness to the other (Muday et al., 2012; Stepanova et al., 2007; Strader et al., 2010). For example, work by Strader et al. (2010) demonstrated that increased ethylene levels can prime the root for auxin-responsive lateral root formation, suggesting that functioning through auxin, which is highly localized, may allow the highly volatile ethylene to still have highly precise and controlled effects. At the molecular level, this crosstalk between auxin and ethylene regulates the expression of many important genes, including those involved in flavonoid metabolism (Lewis et al., 2011; Stepanova et al., 2007).

Proteomic technologies permit interrogation of these processes at the protein level, and efforts to characterize the effects of auxin and ethylene on the plant proteome presently focus on global analyses or changes in the phosphoprotein pool upon exposure to one of the two phytohormones. Altered phosphorylation states of five proteins associated with glycolytic and calcium signaling processes were found in rice leaf sheaths following treatment with the synthetic auxin, 2,4-D (Khan et al., 2005). More recent studies in *Arabidopsis* suspension cell cultures and dark-grown seedlings uncovered changes in the phosphorylation states, and in a few cases also the abundance, of several key proteins in response to ethylene and auxin treatment, including EIN2 and PIN proteins, respectively (Chen et al., 2011; Chen et al., 2010). Utilizing a proteomics platform specific for *Aradidopsis* root cell types, Petricka et al (2012) reported identification of several proteins associated with the auxin response. Several studies have also examined the whole proteome to link auxin to specific physiological responses, including its role in the early stages of *Medicago truncatula* root nodulation by *Sinorhizobium meliloti* (van Noorden et al., 2007) and its role in the gravitrophic response of Arabidopsis root tips (Tan et al., 2011). Given that transcriptome and proteome data are only modestly correlated in plant roots (Petricka et al., 2012), and proteins are often the ultimate effectors of biological function, proteomic efforts parallel testing of the effects of auxin and ethylene on the root proteome can help further delineate the physiological roles of these phytohormones.

Herein is the first comparison of the effects of auxin and ethylene on the root proteome. *Arabidopsis thaliana* seedlings were exposed to indole-3-acetic acid (IAA) or 1-amino-cyclopropane carboxylic acid (ACC) for 24h. Roots were harvested and proteome profiles analyzed using two-dimensional gel electrophoresis (2D-GE) and matrix assisted laser desorption ionization time-of-flight (MALDI TOF/TOF) mass spectrometry. Although several hundred-protein spots were observed in these experiments, less than 5% exhibited detectable changes in abundance. Although proteins with diverse functions in fundamental cellular processes could be identified, no overlap was observed among the proteins whose levels were affected by auxin and ethylene. This is in contrast to the results of gene expression analyses, which have indicated that crosstalk between these

two hormones in roots involves independent action on many of the same target genes (Stepanova et al., 2007). At least for the most abundant proteins present in roots, this does not appear to be the case.

III. Results

To characterize the response of the *Arabidopsis* root proteome to auxin or ethylene, *Arabidopsis* Columbia seedlings were grown for 5d following germination on agar plates (1X Murashige and Skoog medium supplemented with 1% sucrose) and transferred to medium containing auxin [1 μm indole-3-acetic acid (IAA)], ethylene [1 μm 1-amino-cyclopropane carboxylic acid (ACC)], or no added hormone, for 24h. Roots were then excised into liquid nitrogen and protein lysates prepared by a modified phenol-methanol method were fractionated by 2D-GE. To account for intrinsic biological variation, three biological replicates were analyzed.

Rigorous criteria were applied to identify proteins exhibiting changes in spot intensity across all three samples and for identification by MALDI TOF/TOF MS. Gel images were first analyzed by automated matching and then by manual validation of spots (Figure 2-S1 and Figure 2-S2). IAA treatment resulted in the change in intensity of 24 spots, with 13 increased and 11 decreased (Figure 2-1, normal font). ACC treatment affected seven spots, with four increased and three decreased in intensity (Fig. 2-1, bold). Surprisingly, no overlap was observed between the proteins affected by IAA or ACC. This suggests that, although both phytohormones modulate *Arabidopsis* root physiology, the resultant changes in the proteome for the abundant proteins that can be examined by 2D-GE are not the same.

The spots of interest were excised, digested with trypsin, analyzed by MALDI TOF/TOF MS, and queried against the Arabidopsis proteome appended with its reverse decoy database using the Mascot search algorithm. Identities could be assigned with high confidence (Mascot score >57 for peptide-mass fingerprint analysis, six or more peptide matches, and fragmentation data) for eight proteins whose levels were influenced by IAA and five influenced by ACC (Table 2-1 and Table 2-S1). While 2D-GE spots often contain more than one protein, identifications for spots were reported where only one protein was observed, using the outlined criteria. As suggested by the 2D-GE results, the proteins identified were unique for each phytohormone treatment. While IAA and ACC both affected the accumulation of proteins involved in transcription, translation, and protein folding, only IAA affected the accumulation of proteins involved in cytoskeleton function, cell-wall maintenance, and carbon metabolism. Conversely, only ACC affected proteins involved in sulfur metabolism. These observations indicate that, although auxin and ethylene may target similar cellular processes, likely through overlapping molecular mechanisms, the ultimate outcomes are distinct with regard to the most abundant proteins in *Arabidopsis* roots.

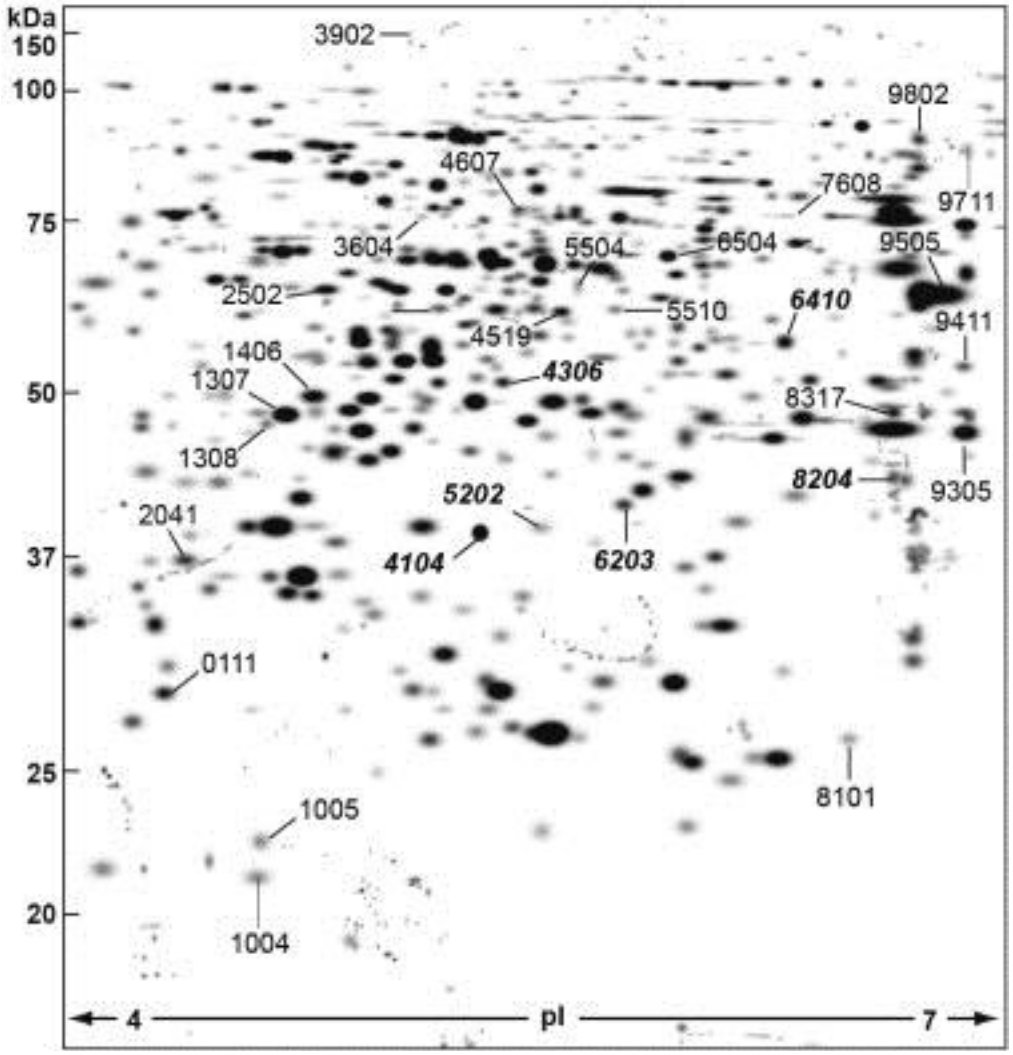

Figure 2-1. Master gel representing all gels of *Arabidopsis* roots treated with 1 μM IAA or 1μM ACC. Spots selected for MS analysis are labeled in black (IAA) or *bold italics* (ACC).

IV. Discussion

Auxin and ethylene appear to modulate many similar processes in roots. Treatment with auxin or ethylene inhibits root elongation (Ishikawa and Evans, 1997; Roman et al., 1995), perturbs root gravitropism (Buer et al., 2006; Maher and Martindale, 1980), and upregulates flavonoid biosynthesis (Buer and Muday, 2004; Buer et al., 2006). Additionally, both hormones affect lateral root development, as auxin acts to promote lateral root growth (Reed et al., 1998) while ethylene inhibits the formation of lateral roots (Negi et al., 2008). At the molecular level, auxin and ethylene regulate the transcription of many genes, often in an interdependent manner (Stepanova et al., 2007). In order to better understand the auxin and ethylene responses at the protein level, *Arabidopsis* seedlings were exposed to auxin and ethylene in parallel fashion, and subsequently the root proteomes were analyzed using 2D-GE and MALDI TOF/TOF.

Our study suggests that auxin and ethylene signaling occurs in *Arabidopsis* roots through the regulation of proteins that function in a variety of different cellular processes. Surprisingly, no overlap was observed between the proteins whose levels were affected by treatment with IAA or ACC. Thus, while auxin and ethylene affect similar physiological and molecular processes, the changes in the proteome that can be quantified by 2D-GE are different.

Two of the proteins whose abundances were increased by IAA treatment are plastidic phosphoglycerate kinase (PGK1) and cytosolic glyceraldehyde-3-phosphate dehydrogenase (GAPC), key enzymes of glycolysis and the Calvin cycle. Interestingly, there is growing evidence for the interaction of glucose with the auxin signaling and transport machinery in plant growth development, physiology, and metabolism (Benjamins and Scheres, 2008; Rolland et al., 2006; Rolland and Sheen, 2005). Indeed, root growth and development in *Arabidopsis* is controlled in part by the interaction between sugar and auxin (Mishra et al., 2009). Furthermore, both the glucose insensitive mutant line, *gin2*, which carries a defect in the glucose sensor *HXK1*, and a mutant allele of *hls1* (*N*-acetyltransferase), are affected not only in sugar- and IAA-mediated transcriptional responses, but also in how sugar and auxin interact to control gene expression and protein levels (Moore et al., 2003; Ohto et al., 2006). The finding that the levels of PGK1 and GAPC were elevated by IAA treatment suggests that auxin directly modulates glucose metabolism. This finding is consistent with evidence that 2,4-D (a synthetic auxin) increases GAPC levels in rice leaves (Khan et al., 2005). In contrast to these findings, the steady-state transcript levels of PGK1 and GAPC have not been observed as significantly regulated by auxin (Nemhauser et al., 2004). This discrepancy is likely a result in the differences in tissue source (whole seedlings versus roots) and methodologies used.

Control of RuBisCO regulates carbon metabolism in photosynthetic tissues such as leaves, where the large and small subunits (LSU and SSU) constitute a large proportion of the total protein (Whitney et al., 2011). An IAA-mediated increase in RuBisCO LSU protein levels was observed, suggesting a carbon fixing function not directly linked to photosynthesis. Indeed, RuBisCO LSU has been previously observed as a relatively abundant protein in roots (Mooney et al., 2006). Additionally, a study in *Brassica napus* observed a non-Calvin cycle, CO_2-scavenging role for the RuBisCO LSU (Schwender et al., 2004). Perhaps an IAA-induced upregulation of glycolysis and the Calvin cycle results in increased mitochondrial activity and hence an increased production of CO_2, with RuBisCO scavenging the CO_2. Previously, the transcription of RuBisCO LSU has not been shown to be IAA-responsive (Nemhauser et al., 2004; Stepanova et al., 2007). These studies were performed in light-grown seedlings and etiolated seedling roots, respectively, which most likely causes the plant to regulate RuBisCO differently upon exposure to IAA.

These results also provide further evidence for the connection between auxin and pectin metabolism, as IAA treatment affected the abundance of adenosine kinase 2 (ADK2) and rhamnose biosynthesis 1 (RHM1), both of which have previously been associated with pectin development (Moffatt et al., 2002; Reiter and Vanzin, 2001; Ringli et al., 2008).

A well-established role of auxin is to stimulate cell elongation during plant growth and responses to light and gravity (Chory et al., 1996; De Grauwe et al., 2005; Guo et al., 2009; Stephenson and Hawes, 1994). For this to occur, the tightly-linked mesh of cell wall polysaccharides must be relaxed and modified in a controlled and dynamic fashion (Cosgrove, 2005). Pectin is the most abundant macromolecule within the cell wall matrix (Willats et al., 2001) and contributes to a myriad of important functions, including cell-to-cell adhesion (Moffatt et al., 2002; Stephenson and Hawes, 1994), cell-wall porosity (Baron-Epel et al., 1988), and cell-wall strength (O'Neill et al., 2001). Several transcriptome analyses have established that auxin regulates the expression of several pectin-related genes, including At5g6230 (pectin methylesterase inhibitor family protein), At5g62350 (pectin lyase-like family protein) and At1g11580 (AtPMEPCRA, pectinesterase) (Laskowski et al., 2006).

In this study, ADK2 decreased in abundance after 24 h exposure to IAA. This enzyme was previously shown to be important for plant growth and development (Moffatt et al., 2002), cytokinin interconversion (Schoor et al., 2011), and the response of plant roots to gravity (Young et al., 2006). Lower ADK2 protein levels might lead to lower ADK2 activity, which is associated with a decrease in pectin methylesterification (Moffatt et al., 2002). This could, in turn, lead to calcium-dependent polysaccharide cross-linking and thus modulation of supramolecular assemblies and gels associated with cell-wall architecture (Willats et al., 2001). Interestingly, the *Medicago truncatula sunn* mutant, which exhibits increased endogenous auxin levels, also has decreased ADK2 levels (van Noorden et al., 2007), suggesting the IAA-responsiveness of ADK2 is conserved between the *Brassicaceae* and *Fabaceae*. In contrast, Stepanova et al. (2007) did not observe the expression of ADK2 to be regulated by IAA in the roots of etiolated *Arabidopsis* seedlings. Given the interaction between light and auxin (Tian and Reed, 2001), this discrepancy may indicate that the regulation of ADK2 by IAA is dependent upon light.

The cell wall matrix is also influenced by the regulation of UDP-L-rhamnose biosynthesis, an essential pectin precursor (Ridley et al., 2001). The *rol1* locus encodes for the RHM1, a putative synthase that converts UDP-D-glucose to UDP-L-rhamnose (Diet et al., 2006; Oka et al., 2007). The *rol1* mutants produce a catalytically inactive RHM1 protein and display defects in pectin architecture (Diet et al., 2006). In the current work, IAA decreased the abundance of RHM1, suggesting that regulation of UDP-L-rhamnose biosynthesis by IAA is mediated through control of RHM1. Interestingly, RHM1 physically interacts with UER1 (also called NRS/ER) (Braun et al., 2011), a bifunctional enzyme involved in UDP-L-rhamnose biosynthesis (Watt et al., 2004). Thus, regulation of RHM1 protein levels could affect both UDP-L-rhamnose synthesis as well as the RHM1/UER1 interaction.

Several proteomic studies have identified translation initiation factors and transcription elongation factors as being part of the auxin or ethylene response network (Chen et al., 2010; Yang et al., 2005). IAA decreased the abundance of TCP-1, a chaperonin previously identified as important for cell-to-cell KNOX1 trafficking (Xu et al., 2011), and the transcriptional elongation factor eEF-1B. In contrast, analysis of IAA-induced proteome changes in *Medicago truncatula* indicates an increased abundance of the

transcription elongation factor EF-2, suggesting complex regulation of different elongation factors is needed to mediate the IAA response (van Noorden et al., 2007). The work herein confirms the results of Chen et al. (2011), and further suggests that changes in the levels of PBP1 and translation initiation factor 4A-1 (EIF4A1) may help mediate the ethylene response.

In plants, the cytoskeleton is a dynamic structure that determines cell shape and facilitates a cohesive cellular response to many stimuli (Wasteneys and Galway, 2003). Given auxin's effect on growth and development, a plausible hypothesis is that the cytoskeleton is regulated by auxin. Indeed, an actin gene (*ACT7*) required for callous formation was shown to be regulated by auxin (Kandasamy et al., 2001). Herein, it was shown that IAA decreased the abundance of TUA2/TUA4 (identical proteins encoded by different genes) (Kopczak et al., 1992), a structural constituent of the cytoskeleton, supporting the concept that auxin and cytoskeleton dynamics are linked. Chen et al. (Tan et al., 2011) previously observed that several members of the TUA family are regulated at the level of protein abundance by ethylene. Through mutant analyses, it was shown that TUA3 is involved in ethylene-mediated nutation. Although we did not observe effects of ACC on the levels of TUA proteins, this is likely due to differences in growth conditions (light versus dark) and the methodologies used.

Since ethylene signaling and sulfur metabolism are essential components of root development (López-Bucio et al., 2003; Tanimoto et al., 1995) it is not surprising the two are linked. Sulfur is a vital cellular component imported via sulfate into plant roots by a plasma-membrane localized transporter (Saito, 2004). Once sulfate is reduced and incorporated into cysteine, it serves as a building block for ethylene, SAM, polyamines, and glucosinolates (Saito, 2004). ACC treatment decreased the abundance of two cysteine synthases, one cytoplasmic and one plastid-based, both of which catalyze the incorporation of inorganic sulfide into *O*-acetylserine to yield cysteine. Exposure to exogenous ethylene may be an intracellular cue to downregulate cysteine biosynthesis, which could serve as a point of feedback regulation for sulfur-containing compounds.

Although no overlap was observed between the proteins affected by IAA and ACC, proteome profiles are highly protocol- and technology-dependent (Alvarez et al., 2009). Proteins observed by 2D-GE are likely the most abundant proteins representing constitutive or highly-expressed genes rather than low abundance transcription factors or transient signaling pathway components (Gygi et al., 2000). Despite these limitations, 2D-GE has proven to be a useful assessment of proteome status across multiple fields and organisms (Chevalier, 2010; Rabilloud et al., 2010). For example, Tang et al. (2008) discovered integral components of the brassinosteroid signaling pathway in *Arabidopsis* using a 2D-GE approach.

The present study provides the first insights into how exogenous auxin and ethylene modulate the levels of the most abundant proteins in *Arabidopsis* roots. IAA affected the abundance of proteins involved in carbon metabolism, cell-wall maintenance, and glycolysis, while ACC altered the abundance of proteins involved in sulfur metabolism. While both hormones affected proteins involved in gene expression, protein translation,

and protein folding, the identified proteins were distinct for the two hormones, at least at the level of the most abundant members of the root proteome. Current efforts are aimed at exploring the connections between the protein changes observed in this study and the specific cellular processes that are mediated by the larger auxin and ethylene response networks. Because proteins are most often the effectors of biological function, proteomic approaches provide new insights into how complex regulatory networks, such as the auxin and ethylene signaling pathways, are manifested into a coherent biological response.

V. Experimental

i. Plant material

Seeds of the Columbia (Col-0) ecotype of *Arabidopsis* were obtained from Lehle Seeds (Round Rock, Texas). Plants were grown on 1X Murashige and Skoog medium from Caisson labs (North Logan, Utah) pH 5.7, 0.8% (w/v) agar, and supplemented with 1% (w/v) sucrose. After cold treatment for 48 h at 4°C, plates were moved to a growth chamber and grown under 100 µmol m^{-2} s^{-2} cool-white light (24 h lighting). The growth chamber was maintained at 22°C and 60% relative humidity. All assays were conducted 5 d after germination, which was typically 6-7 d after the cold treatment.

ii. IAA and ACC treatments

Hormone-transfer assays were conducted as described in by Lewis et al., 2011. Briefly, plants were germinated on a nylon screen (03-100/32; Sefar Filtration, Depew, New York) pressed tightly against control medium, with approximately 100 seedlings per plate, then after 5 d post-germination growth, the filter was transferred to a control plate or medium supplemented with 1 µM IAA or 1 µM ACC. After 24 h treatment, seedlings were collected and immediately frozen in liq. N_2. A razor blade was then used to carefully excise roots at the root-shoot junction. Harvesting of each plate always took less than 10 sec. Samples were stored at -80°C until protein extraction. Three biological replicates were used for each hormone treatment.

iii. Protein extraction

Proteins were extracted according to the phenol-methanol method (Hurkman and Tanaka, 1986) with modifications. For each biological replicate, plant tissue, (0.3 g), were mixed with 3 volume of SDS extraction buffer (100 mM Tris-HCl, pH 8.0, 2% SDS (v/v), 1% β-mercaptoethanol (v/v), 5 mM EGTA, 10 mM EDTA), heated for 10 min at 65°C, and then centrifuged at 6,710 g for 20 min. The supernatant was mixed with 1 volume of ice-cold Tris-buffered phenol, pH 7.5, and centrifuged at 6,710 g for 5 min to separate aqueous and phenol phases. The aqueous phase was removed leaving the interface intact, and the phenol phase was extracted twice with ice-cold 50 mM Tris HCl, pH 8.0 then mixed with 5 volumes of ice-cold 0.1 M ammonium acetate in methanol and left at -20°C. After centrifugation at 6,710 g for 10 min, the protein pellet was washed three times with ice-cold 0.1 M $(NH_4)OAc$ in MeOH, once with EtOH and then resuspended in

rehydration buffer (7 M urea, 2 M thiourea, 4% CHAPS (w/v), 0.5% IPG buffer (v/v). After centrifugation, protein concentration was determined with the 2D-Quant Kit (GE Healthcare; Piscatawy, NJ) using BSA as a standard. This extraction method yielded protein (0.4 to 0.6 g) per biological replicate.

iv. 2D-gel electrophoresis

Samples were applied to wells in isoelectric focusing (IEF) trays (17 cm; Bio-Rad, Hercules, CA) in Protean IEF cell units (Bio-Rad, Hercules, CA). The pH 4-7 nonlinear immobilized pH gradient (IPG) strips were applied to the wells followed by an overlay of mineral oil (Bio-Rad; Hercules, CA). IEF was carried out at 20°C with a maximum 50 µA/strip and the following setting: active rehydration for 12 h at 50 V, then 500 V and 1000V each for 1 h, gradient increase to 8000 V in 3 h, and remaining at 8000 V until reaching 80,000 V-h. After IEF, the strips were equilibrated in three successive steps on an orbital shaker: (1) 30 min (buffer 1; 4% SDS (w/v), 0.37 M, Tris-Cl, pH 8.8, 20% glycerol (v/v), (2) 30 min (2% DTT (w/v) in buffer 1, (3) 30 min (2.5% iodoacetamide (w/v) in buffer 1). Strips were then transferred on top of pre-cast 12% gels containing 0.375M Tris-Cl, pH 8.8 and 0.1% SDS (w/v) (Jule; Milford, CT, USA) and coated with a heated 0.5% agarose (w/v) gel solution containing bromophenol blue. Plates were then transferred to a Protean plus Dodeca Cell (Bio-Rad; Hercules, CA) tank chilled to 20°C containing 0.0125 M Tris, 0.096 M glycine, and 0.05% SDS (w/v). Electrophoresis was carried out approximately 16 h or until the dye front had migrated within 1 cm of the gel's edge. Gels were then fixed in MeOH-HOAc-H_20 (10:7:83 v/v) for 4 h and then stained with Sypro Ruby (Bio-Rad; Hercules, CA) overnight. After a brief destaining with ultrapure H_20, images were acquired using the Typhoon Trio (GE Healthcare; Piscataway, NJ, USA) with Sypro Ruby default settings.

v. Image analysis and spot excision

Images were analyzed using PDQuest v7.3.1 (Bio-Rad; Hercules, CA). After automated spot detection and matching, replicate groups were manually assigned. The group consensus tool was then used to manually examine each spot considered in the analysis. Only spots that could be reliably detected on all gels were considered further. A student's- t-test was then performed to evaluate which spots showed a difference in accumulation ($p < 0.001$). The integrated excision tool was then used to control a Proteome Works Spot Cutter (Bio-Rad, Hercules, CA) and excise spots of interest.

vi. In-gel tryptic digestion

Gel cores were washed twice with ultrapure H_20 followed by two washes with CH_3CN-H_20 (1:1, v/v) 50 mM NH_4HCO_3, pH 8.0. After dehydration with CH_3CN, cores were rehydrated in 10 ng/µl trypsin (Promega, Madison, WI) for 30 min at 4°C, followed by incubation at 37°C for 3 h. Peptides were extracted once with CH_3CN-H_20 containing 0.1% CF3CO2H (1:1, v/v) by sonication for 15 min.

vii. Matrix assisted laser desorption/ionization tandem time-of-flight (MALDI-TOF/TOF)

Aliquots of each digest (1 □l) were transferred to a freshly-polished MALDI plate and overlayed with freshly-prepared matrix containing 4 mg/ml α-cyano-4-hydroxycinnamic acid, 50% CH_3CN 0.1% formic acid (v/v), 0.1% TFA (v/v), and 5 mM $(NH_4)Cl$. Data were acquired utilizing an Applied Biosystems 4800 MALDI TOF/TOF (Framingham, MA) mass spectrometer. An MS scan for the *m/z* range of 800-4000, averaging data from 1200 laser shots, was acquired in reflector positive ion mode. The 4000 Series explorer was then used to generate a list of at most 10 peaks above a minimum signal-to-noise ratio for subsequent MS/MS analysis. MS/MS scans were the average of 2000 laser shots acquired (1kV, positive ion mode).

viii. Protein Identification

Protein identifications were obtained utilizing Mascot Daemon v. 2.2.2 (Matrix Science, Inc., Boston, MA) to automatically submit peak lists to a local Mascot Server v. 2.2.2 (Matrix Science, Inc., Boston, MA) search engine utilizing the Arabidopsis protein database (NCBInr 20100131) appended with its reverse decoy. A mascot score of 57 and six matched peaks were set as the minimum for protein identification using peptide-mass fingerprint (PMF) analysis. The most abundant ions per spectrum were then subjected to MS/MS analysis. Searches of MS/MS data used a trypsin protease specificity with the possibility of two missed cleavages, a peptide mass tolerance of ± 300 ppm, a peptide fragment mass tolerance of ± 0.2 Da, and the possibility of carbamidomethylation at cysteine and oxidation at methionine. The tandem MS spectra were validated manually by ensuring the spectra contained at least four consecutive -y or -b ions matching the predicted amino acid sequence.

VI. Supplemental

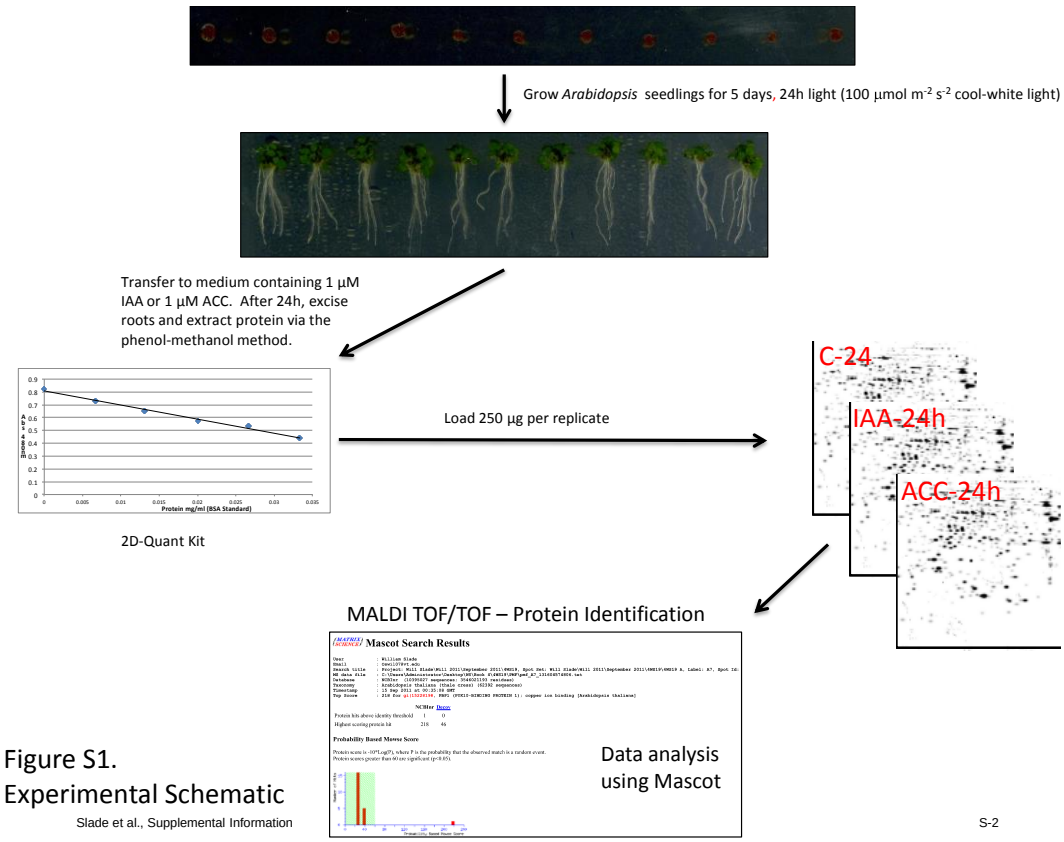

Figure S1.
Experimental Schematic

Slade et al., Supplemental Information

Figure 2-S1. Experimental Schematic

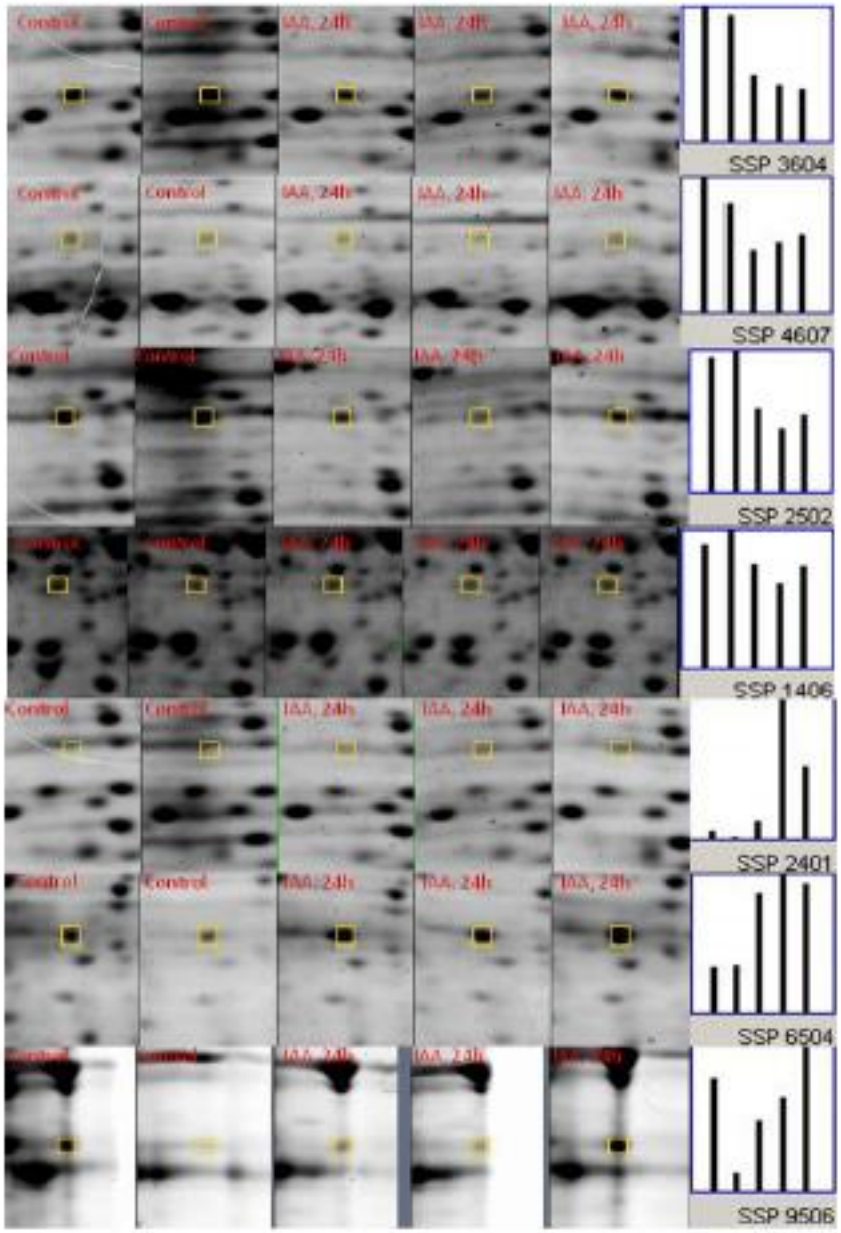

Figure 2-S2. PDQuest images of IAA-responsive spots. Spot image and normalized intensity across two control and three treatment (1μM IAA) samples. Yellow box indicates the matched spot among gels.

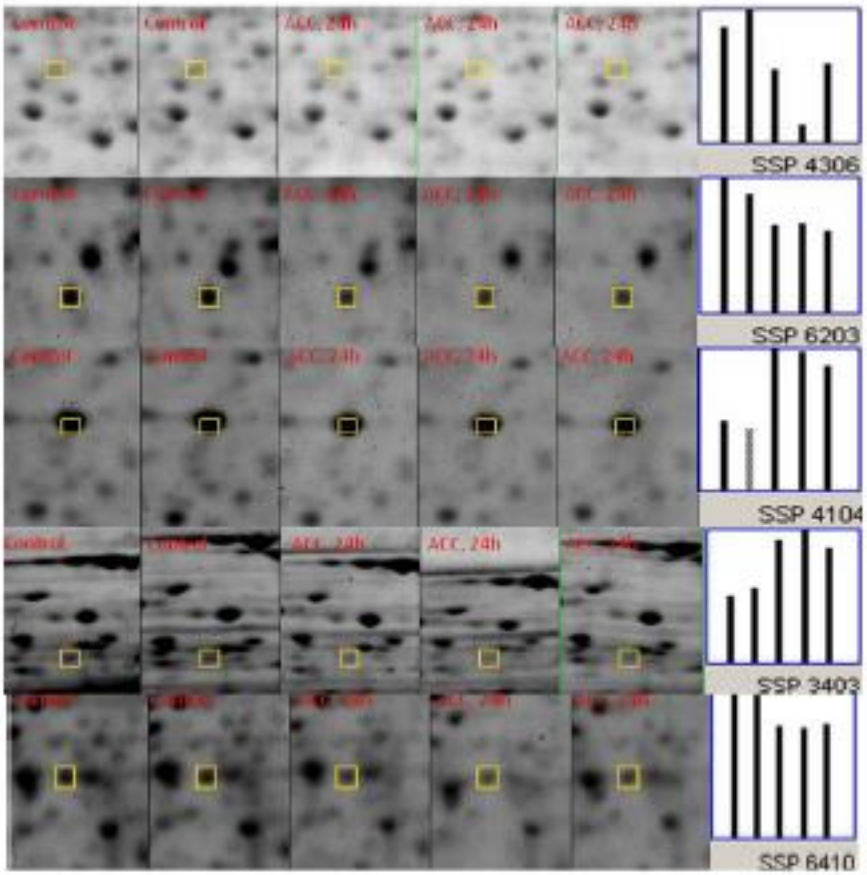

Figure 2-S3. PDQuest images of ACC-responsive spots. Spot image and normalized intensity across two control and three treatment (1μM ACC) samples. Yellow box indicates the matched spot among gels.

Table 2-S1. Peptides used for protein identification

Mr Calc (Da)	Mr Obsd (Da)	ppm	MC	Start Seq.	End Seq.	Peptide Sequence	MS2 Mascot Score
Spot ID: 4306; Gene: At2G43750; Protein: Cysteine Synthase; UniProt: P47999							
2477.35	2478.32	-16	0	61	85	K.AVSIKPEAGVEGLNIADNAAQLIGK.T	
2121.13	2122.08	-30	0	138	159	K.SVLVESTSGNTGIGLAFIAASK.G	
1493.73	1493.73	-24	0	163	175	K.LILTMPASMSLER.R	
1344.73	1345.72	-17	0	181	193	R.AFGAELVLTEPAK.G	
1980.9	1980.87	-23	0	209	225	K.TPNSYMLQQFDNPANPK.I	**17**
1954.12	1955.03	-52	1	241	261	R.GKIDILVAGIGTGGTITGVGR.F	
2076.12	2077.04	-44	1	272	292	K.VIGVEPTESAILSGGKTGPHK.I	
1333.74	1334.72	-21	0	360	371	K.LIAVVFPSFGER.Y	**31**
Spot ID: 4104; Gene: At3G16420; Protein: PBP1 (PYK10-Binding Protein 1); UniProt: O04314							
2141.12	2141.21	39	0	28	46	K.IQLAAGIDGIQYVQFDYVK.N	**150**
3231.77	3230.67	27	1	28	56	K.IQLAAGIDGIQYVAFDYVKNGQPEQAPLR.G	
1108.56	1109.62	43	0	47	56	K.NGQPEQAPLR.G	**63**
1394.73	1395.79	43	1	47	59	K.NGQPEQAPLRGTK.G	**52**
2061.04	2062.13	39	1	100	118	K.KTSDVIGSDEGTHFTLQFK.D	
1932.94	1934.02	38	0	101	118	K.TSDVIGSDEGTHFTLQVK.D	
3186.67	3187.78	33	0	122	153	K.IIGFHGSAGGNLNSLGAYFAPLTTTTPLTPAK.Q	
1561.85	1562.92	42	1	176	190	K.KVYVGQAQDGISAVK.F	
1434.82	1433.75	41	0	177	190	K.VYVGQAQDGISAVK.F	
1950.99	1949.9	41	1	191	207	K.FVYDKSPEEVTGEEHGK.S	**120**
3072.53	3071.45	23	0	208	234	K.STLLGFEEFVLDYPSEYITAVDGTYDK.I	
1410.72	1411.78	42	0	235	247	K.IFGSDGSVITMLR.F	
1819.94	1821.02	40	0	253	269	K.QTSPPFGLEAGTVFELK.E	
2400.2	2401.29	38	1	253	274	K.QTSPPFGLEAGTVFELKEEGHK.I	
1364.69	1365.79	42	1	270	281	K.EEGHKIVGFHGR.A	
1090.62	1091.68	42	0	289	298	K.IGVHVRPLSN.-	
Spot ID: 3403; Gene: At3G13920; Protein: Translation initiation factor 4A-1; UniProt: 4JEL4							
1826.93	1827.98	21	0	10	25	R.GIYAYGFEKPSAIQQR.G	**150**
1400.73	1401.77	27	0	33	46	K.GLDVIQQAQSGSTGK.T	
957.51	958.55	29	0	75	82	R.ELAQQIEK.V	
935.5124	934.51	25	0	86	94	R.ALGDYLFVK.V	**25**
1502.8729	1502.92	25	0	110	124	R.ILQAGVHVVVGTPGR.V	**16**
1586.7	1587.74	25	0	141	153	K.MFVLDEADEMLSR.G	**21**
2074.08	2075.13	21	0	170	188	K.IQVGVFSATMPPEALEITR.K	**35**
1172.64	1173.68	29	1	201	210	K.RDELTLEGIK.Q	
1025.52	1026.55	28	0	211	218	K.QFYVNVEK.E	
1799.75	1800.8	22	0	259	274	R.DHTVSATHGDMDQNTR.D	
1113.68	1114.72	29	0	288	297	R.VLITTDLLAR.G	**59**
1103.65	1104.69	34	1	332	341	R.KGVAINFVTR.D	
975.55	976.59	34	0	333	341	K.GVAINFVTR.D	**28**
1919.99	1921.06	36	0	353	369	K.FYNVVVEELPSNVADL.-	
Spot ID: 6203; Gene: At4G14880; Protein: Cysteine Synthase; UniProt ID: P47998							
2915.63	2915.63	35	1	5	31	R.IAKDVTELIGNTPLVYLNNVAEGCVGR.V	
2602.31	2603.42	43	0	8	31	K.DVTELIGNTPLVYLNNVAEGCVGR.V	
1963.91	1965.02	50	0	139	155	K.TPNGYMLQQFENPANPK.I	**85**
2107.09	2108.19	43	1	168	191	K.GTGGKIDGFVSGIGTGGTITGAGK.Y	
1706.88	1707.99	57	0	173	191	K.IDGFVSGIGTGGTITGAGK.Y	
2134.14	2135.25	48	0	202	222	K.LYGVEPVESAILSGGKPGPHK.I	
2720.48	2721.29	-75	1	262	289	K.EGLLVGISSGAEAAAAIKLAQRPENAGK.I	
1082.58	1083.65	52	0	280	289	K.LAQRPENAGK.L	
1381.74	1382.35	50	0	290	301	K.LFVAIFPSFGER.Y	**54**
1284.67	1285.75	53	0	302	312	R.YLSTVLFDATR.K	**28**
1412.77	1413.84	50	1	302	312	R.YLSTVLFDATRK.E	**15**

Spot ID: 6410; Gene: At4G38220; Protein: Peptidase M20/M25/M40 protein; UniProt ID: F4JTK8							
854.43	855.43	-7	0	28	33	R.FQEYLR.I	**21**
1464.72	1465.72	-6	0	34	45	R.INTVQPNPEYYK.A	
2562.39	2563.33	-27	0	46	68	K.AVDFIISQAKPLSLESQTEIFVK.G	
1115.65	1116.65	-3	0	140	149	K.LQASGFKPLR.S	
2147	2174	-4	0	150	169	R.SVYLSFVPDEEIGGHDGAEK.F	
2173.13	2174.12	-7	0	178	197	K.SLNIAIVLDEGLPSPTESYR.V	
1425.68	1426.68	-6	0	222	233	K.LYDNSAMENLLK.S	
920.5	921.49	-12	0	243	250	R.ASQFDLLK.A	
1792.9	1793.9	-8	0	251	268	K.AGGIAEGDVVSVNMAFLK.A	
2607.23	2608.22	-7	0	269	293	K.AGTPSPTGFVMNLQPSEAEAGFDIR.V	**25**
1281.66	1282.66	-1	0	294	305	R.VPPSVDAEALER.R	
1437.76	1438.76	-4	0	294	306	R.VPPSVDAEALERR.L	
1518.77	1519.77	-6	0	356	369	R.TSKPEIFPASTDAR.Y	**38**
2867.42	2868.73	-1	0	374	400	K.AGVPAFGFSPISNTPSLLHDHNEYLGK.A	
Spot ID: 3604; Gene: At3G03960; Protein: TCP-1/cpn60 chaperonin family protein; UniProt ID: Q94K05							
1717.79	1717.93	80	0	2	16	M.VGMSMQPYGIQSMLK.E	
2223.02	2223.21	83	1	2	20	M.VGMSMQPYGIQSMLKEGYR.H	
2135.05	2135.23	84	0	139	157	K.AVEILEQLVETGSETMDVR.N	
1289.62	1289.72	76	0	196	206	K.NPTNFNVDNVR.V	**1**
1709.94	1710.07	72	1	207	222	R.VSKLLGGGLHNSCIVR.G	
1940.05	1940.17	60	1	210	227	K.LLGGGLHNSCIVRGMVLK.S	
1538.85	1538.97	75	0	411	425	R.IVPGAAATEIELAQR.L	**41**
1780.03	1780.16	69	1	411	427	R.IVPGAAATEIELAQRLK.E	
2719.33	2719.59	97	0	454	480	K.TLADNAGLNAMEIIAALYTGHGSGNTK.L	
Spot ID: 4607; Gene: At1G57720; Protein: Transcription elongation factor EF1b; UniProt ID: 4JEL4							
2695.41	2695.37	-15	1	48	72	K.MNPIGKVPVLETPEGPIFESNAIAR.Y	
2039.07	2039.03	-21	0	54	72	K.VPVLETPEGPIFESNAIAR.Y	
2096.04	2096.01	-18	1	117	136	R.MGYAPFSAPAEEAAISALKR.G	
1318.68	1318.66	-20	1	178	188	K.KFTSAFPHVER.Y	
1190.59	1190.57	-23	0	179	188	K.FTSAFPHVER.Y	
2187.16	2187.11	-25	1	232	252	K.KAAPVAEAPKPAEEEEAPKPK.A	
2059.06	2059.02	-23	0	233	252	K.AAPVAEAPKPAEEEEAPKPK.A	
1689.77	1689.83	33	0	307	320	K.YNDENMVSFVTLNK.V	
1378.72	1378.69	-29	1	321	332	K.VGGFLQRMDLAR.K	
2111.93	2111.99	29	0	342	357	K.FIMDEVYDMELYEWTK.V	
2208.03	2208	-15	0	369	388	R.VSQMIEDAEPFEGEALLDAK.C	
Spot ID: 2502; Gene: At1G04820; Protein: TUA4, structural constituent of cytoskeleton; UniProt ID: P29510							
1977.88	1977.49	-195	0	41	60	K.TVGGGDDAFNTFFSETGAGK.H	
2467.16	2466.68	-195	1	41	64	K.TVGGGDDAFNTFFSETGAGKHVPR.A	**59**
1702.89	1701.57	-195	0	65	79	R.AVFVDLEPTVIDEVR.T	**86**
2280.18	2279.75	-192	1	65	84	R.AVFVDLEPTVIDEVRTGTYR.Q	**55**
2385.19	2384.73	-194	1	85	105	R.QLFHPEQLISGKEDAANNFAR.G	**144**
1888.95	1888.59	-194	1	106	121	R.GHYTIGKEIVDLCLDR.I	
3321.72	3321.09	-191	1	124	156	R.KLADNCTGLQGFLVFNAVGGGTGSGLGSLLLER.L	
3193.62	3194.01	118	0	125	156	K.LADNCTGLQGFLVFNAVGGGTGSGLGSLLLER.L	
1663.87	1663.55	-196	0	216	229	R.SLSIERPTYTNLNR.L	
1473.86	1473.57	-198	0	230	243	R.LVSQVISSLTASLR.F	
2395.19	2394.72	-196	0	244	264	R.FDGALNVDVTEFQTNLVPYPR.I	
1808.92	1808.57	-197	0	265	280	R.IHGMLSSYAPVISAEK.A	
2641.22	2640.72	-191	0	281	304	K.AFHEQLSVAEITNSAFEPASMMAK.C	
1396.69	1396.45	-175	1	391	401	R.IDHKFDLMYAK.R	
Spot ID: 9711; Gene: At1G78750; Protein: ROL1, Rhamnose Biosynthesis 1; UniProt ID: Q9SYM5							
1825	1824.94	-38	0	8	25	K.NILITGAAGFIASHVANR.L	
2207.27	2207.2	-34	1	8	28	K.NILITGAAGFIASHVANRLIR.S	
1300.6	1300.57	-34	0	164	175	K.AGAEMLVMAYGR.S	
1106.61	1106.58	-37	0	176	185	R.SYGLPVITTR.G	
1915	1914.9	-35	1	186	202	R.GNNVYGPNQFPEKLIPK.F	

2309.25	2309.18	-33	1	203	223	K.FILLAMRGQVLPIHGDGSNVR.S	
1448.75	1448.72	-30	0	210	223	R.GQVLPIHGDGSNVR.S	
1407.67	1407.63	-33	0	279	289	K.FVDNRPFNDQR.Y	**19**
3183.49	3184.4	-31	0	347	375	R.HFDGSEDNSLAATLSEKPSQTHMVVPSQR.S	
3832.78	3832.95	43	1	461	494	R.ANVAGTLTLADVCREHGLLMMNFATGCIFEYDDK.H	
2099	2098.94	-34	1	521	537	K.AMVEELLKEYDNVCTLR.V	
1514.77	1514.72	-34	1	538	550	R.VRMPISSDLNNPR.N	
2557.34	1558.17	-67	0	562	584	K.VVNIPNSMTVLDELLPISIEMAK.R	
2713.44	2714.3	-55	1	562	585	K.VVNIPNSMTVLDELLPISIEMAKR.N	
Spot ID: 1406; Gene: At5G03300; Protein: Adenosine Kinase 2; UniProt ID: Q9LZG0							
3254.61	3253.92	-212	0	2	32	M.ASSSNYDGILLGMGNPLLDISAVVDDEFLTK.Y	
2451.15	2451.75	244	1	37	57	K.LNNAILAEDKHLPMYDEMSSK.F	
1337.58	1337.39	-148	0	47	57	K.HLPMYDEMSSK.F	**16**
3062.42	3062.11	-104	1	47	73	K.HLPMYDEMSSKFNVEYIAGGATQNSIK.V	
1711.86	1711.51	-210	0	58	73	K.FNVEYIAGGATQNSIK.V	
842.41	842.32	-100	1	95	102	K.YGEAMKK.D	
3241.41	3240.74	-209	0	103	133	K.DATAAGVNVHYYEDESAPTGTCGVCVVGGER.S	
1967.94	1967.47	267	0	192	207	K.VFTMNLSAPFICEFFK.D	
1951.88	1951.47	-214	0	213	228	K.FLPYMDFVFGNETEAR.T	**47**
2027.09	2026.66	-216	1	261	280	R.TTVITQGADPVVVAEDGKVK.K	
2142.05	2141.61	-210	0	292	312	K.LVDTNGAGDAFVGGFMSQLVK.E	
2399.18	2398.69	-210	1	292	314	K.LVDTNGAGDAFVGGFMSQLVKEK.S	
2183.05	2182.59	-210	1	315	333	K.SIEECVKAGCYASNVVIQR.S	
1414.59	1414.29	-217	0	334	345	R.SGCTYPEKPDFN.-	
Spot ID: 2401; Gene: At3G12780; Protein: Phosphoglycerate kinase 1; UniProt ID: Q9LD57							
2015.94	2015.89	-31	0	17	34	R.ADLNVPLDDNQTITDDTR.I	
2285.13	2285.05	-39	1	17	36	R.ADLNVPLDDNQTITDDTRIR.A	**13**
999.59	999.55	-48	0	68	76	K.FSLAPLVPR.L	**8**
2062.06	2061.96	-54	1	130	148	K.KLASLADLYVNDAFGTAHR.A	**17**
1933.97	1933.88	-51	0	131	148	K.LASLADLYVNDAFGTAHR.A	**36**
1299.78	1299.97	139	1	241	252	K.LELATELLAKAK.A	
2356.28	2356.16	-48	1	255	277	K.GVSLLLPTDVVVADKFAPDANSK.I	
Spot ID: 3504; Gene: At3G04120; Protein: Glyceraldehyde-3-phosphate dehydrogenase; UniProt: P25858							
1101.64	1102.38	-240	1	6	15	K.IRIGINGFGR.I	
832.46	833.27	-227	0	6	15	R.IGINGFGR.I	
3367.64	3367.8	-250	1	23	50	R.VVLQRDDVELVAVNDPFITTEYMTYMFK.Y	
2772.26	2772.55	-257	0	28	50	R.DDVELVAVNDPFITTEYMTYMFK.Y	
1675.97	1676.56	-249	0	70	84	K.TLLFGEKPVTVFGIR.N	**51**
2645.72	2645.38	-254	1	167	190	K.VINDRFGIVEGLMTTVHSITATQK.T	
2048.06	2048.55	-255	0	172	190	R.FGIVEGLMTTVHSITATQK.T	
826.4	827.22	-224	0	232	238	K.LTGMSFR.V	
1497.84	1498.48	-246	0	239	252	R.VPTVDVSVVDLTVR.L	
1868.06	1868.6	-249	1	239	255	R.VPTVDVSVVDLTVRLEK.A	
2171	2171.46	-253	0	276	295	K.GILGYTEDDVVSTDFVGDNR.S	**117**
2919.38	2920.7	107	1	276	302	K.GILGYTEDDVVSTDFVGDNRSSIFDAK.A	
Spot ID: 9505, Gene: AtCG00490; Protein: Ribulose-1,5-bisphosphate carboxylase (large subunit); UniProt: O03042							
2409.17	2409.62	-234	1	22	41	K.LTYYTPEYETKDTDILAAFR.V	**35**
1020.52	1021.6	-226	0	33	41	K.DTDILAAFR.V	
1239.73	1240.45	-230	1	129	139	K.ALAALRLEDLR.I	
1414.78	1415.47	-223	1	135	146	R.LEDLRIPPAYTK.T	
1464.75	1465.43	-225	0	147	159	K.TFQGPPHGIQVER.D	**61**
1707.87	1708.49	-229	1	147	161	K.TFQGPPHGIQVERDK.L	
1501.84	1502.5	-231	0	165	177	K.YGRPLLGCTIKPK.L	
909.44	910.25	-218	0	188	194	R.AVYECLR.G	
2185.48	2185.48	-232	1	195	213	R.GGLDFTKDDENVNSQPFMR.W	
1531.75	1532.41	-224	1	216	227	R.DNGLLLHIHR.A	
3053.44	3053.73	-234	0	259	285	R.ELGVPIVMHDYLTGGFTANTSLSHYCR.D	
1186.66	1187.4	-226	0	286	295	R.DNGLLLHIHR.A	

1170.3	1170.3	-221	1	304	312	R.QKNHGMHFR.V	
913.4	914.19	-231	0	306	312	K.NHGMHFR.V	
1819.95	1819.53	-233	1	335	350	K.LEGDRESTLGFVDLLR.D	
1683.85	1684.48	-229	1	432	446	R.NEGRDLAVEGNEIIR.E	
1228.37	1228.37	-227	0	436	446	R.DLAVEGNEIIR.E	
1866.49	1866.49	-227	1	464	479	K.EITFNFPTIDKLDGQE.-	

Table 2-S2. Additional protein information with links to TAIR and UniProt.

IAA-Responsive Proteins			
Spot ID	Gene Link	UniProt Link	Annotation
3604	At3G03960	Q94K05	TCP-1, chaperonin T-complex protein 1, theta subunit
4607	At1G57720	Q9FVT2	eEF-1B gamma 2, Transcription elongation factor
2502	At1G04820	P29510	TUA4/TUBA4, Tubulin alpha-4 chain
2502	At1G05010	P29510	TUA2/TUBA2, Tubulin alpha-2 chain
1406	At5G03300	Q9LZG0	ADK2, Adenosine kinase 2
9505	AtCG00490	O03042	rbcL, RuBisCO, large subunit
9711	At1G78570	Q9SYM5	RHM1, Rhamnose biosynthesis 1
2401	At3G12780	Q9LD57	PGK1, Phosphoglycerate kinase 1
6504	At3G04120	P25858	GAPC, Glyceraldehyde-3-phosphate dehydrogenase
ACC-Responsive Proteins			
4306	At2G43750	P47999	OASB, Cysteine Synthase (plastid)
6203	At4G14880	P47998	OASA1, Cysteine Synthase (cytosolic)
6410	At4G38220	F4JTK8	Peptidase M20/M25/M40 family protein
3403	At3G13920	F4JEL4	EIF4A1, Translation Initiation factor 4A-1
4104	At3G16420	O04314	PBP1, PYK10-Binding Protein 1

VII. References

Alvarez, S., Berla, B. M., Sheffield, J., Cahoon, R. E., Jez, J. M., Hicks, L. M., 2009. Comprehensive analysis of the *Brassica juncea* root proteome in response to cadmium exposure by complementary proteomic approaches. *Proteomics* 9, 2419-2431.

Baron-Epel, O., Gharyal, P. K., Schindler, M., 1988. Pectins as mediators of wall porosity in soybean cells. *Planta* 175, 389-395.

Benjamins, R., Scheres, B., 2008. Auxin: the looping star in plant development. *Annual Review of Plant Biology* 59, 443-465.

Braun, P., Carvunis, A. R., Charloteaux, B., Dreze, M., Ecker, J. R., Hill, D. E., Roth, F. P., Vidal, M., Galli, M., et al, 2011. Evidence for network evolution in an *Arabidopsis* interactome map. *Science* 333, 601-607.

Buer, C. S., Muday, G. K., 2004. The *transparent testa4* mutation prevents flavonoid synthesis and alters auxin transport and the response of *Arabidopsis* roots to gravity and light. *Plant Cell* 16, 1191-1205.

Buer, C. S., Sukumar, P., Muday, G. K., 2006. Ethylene modulates flavonoid accumulation and gravitropic responses in roots of *Arabidopsis*. *Plant Physiology* 140, 1384-1396.

Chen, R., Binder, B. M., Garrett, W. M., Tucker, M. L., Chang, C., Cooper, B., 2011. Proteomic responses in *Arabidopsis thaliana* seedlings treated with ethylene. *Molecular BioSystems* 7, 2637-2650.

Chen, Y., Hoehenwarter, W., Weckwerth, W., 2010. Comparative analysis of phytohormone-responsive phosphoproteins in *Arabidopsis thaliana* using TiO_2-phosphopeptide enrichment and mass accuracy precursor alignment. *Plant Journal* 63, 1-17.

Chevalier, F., 2010. Highlights on the capacities of "Gel-based" proteomics. *Proteome Sci* 8.

Chory, J., Chatterjee, M., Cook, R. K., Elich, T., Fankhauser, C., Li, J., Nagpal, P., Neff, M., Pepper, A., Poole, D., Reed, J., Vitart, V., 1996. From seed germination to flowering, light controls plant development via the pigment phytochrome. *Proceedings of the National Academy of Sciences* 93, 12066-12071.

Cosgrove, D. J., 2005. Growth of the plant cell wall. *Nature Reviews Molecular Cell Biology* 6, 850-861.

De Grauwe, L., Vandenbussche, F., Tietz, O., Palme, K., Van Der Straeten, D., 2005. Auxin, ethylene and brassinosteroids: Tripartite control of growth in the *Arabidopsis* hypocotyl. *Plant Cell Physiology* 46, 827-836.

Diet, A., Link, B., Seifert, G. J., Schellenberg, B., Wagner, U., Pauly, M., Reiter, W. D., Ringli, C., 2006. The *Arabidopsis* root hair cell wall formation mutant lrx1 is suppressed by mutations in the RHM1 gene encoding a UDP-L-rhamnose synthase. *Plant Cell* 18, 1630-1641.

Guo, H., Li, L., Ye, H., Yu, X., Algreen, A., Yin, Y., 2009. Three related receptor-like kinases are required for optimal cell elongation in *Arabidopsis thaliana*. *Proceedings of the National Academy of Sciences* 106, 7648-7653.

Gygi, S. P., Corthals, G. L., Zhang, Y., Rochon, Y., Aebersold, R., 2000. Evaluation of two-dimensional gel electrophoresis-based proteome analysis technology. *Proceedings of the National Academy of Sciences* 97, 9390-9395.

Hurkman, W. J., Tanaka, C. K., 1986. Solubilization of plant membrane proteins for analysis by two-dimensional gel electrophoresis. *Plant Physiology* 81, 802-806.

Ishikawa, H., Evans, M. L., 1997. Novel software for analysis of root gravitropism: Comparative response patterns of *Arabidopsis* wild-type and axr1 seedlings. *Plant Cell Environment* 20, 919-928.

Kandasamy, M. K., Gilliland, L. U., McKinney, E. C., Meagher, R. B., 2001. One plant actin isovariant, ACT7, is induced by auxin and required for normal callus formation. *Plant Cell* 13, 1541-1554.

Khan, M., Takasaki, H., Komatsu, S., 2005. Comprehensive phosphoproteome analysis in rice and identification of phosphoproteins responsive to different hormones/stresses. *Journal of Proteome Research* 4, 1592-1599.

Kopczak, S. D., Haas, N. A., Hussey, P. J., Silflow, C. D., Snustad, D. P., 1992. The small genome of *Arabidopsis* contains at least six expressed alpha-tubulin genes. *Plant Cell* 4, 539-547.

Laskowski, M., Biller, S., Stanley, K., Kajstura, T., Prusty, R., 2006. Expression profiling of auxin-treated *Arabidopsis* roots: Toward a molecular analysis of lateral root emergence. *Plant Cell Physiology* 47, 788-792.

Lewis, D. R., Ramirez, M. V., Miller, N. D., Vallabhaneni, P., Ray, W. K., Helm, R. F., Winkel, B. S., Muday, G. K., 2011. Auxin and ethylene induce flavonol accumulation through distinct transcriptional networks. *Plant Physiology* 156, 144-164.

López-Bucio, J., Cruz-Ramírez, A., Herrera-Estrella, L., 2003. The role of nutrient availability in regulating root architecture. *Current Opinion Plant Biology* 6, 280-287.

Maher, E., Martindale, S., 1980. Mutants of *Arabidopsis thaliana* with altered responses to auxins and gravity. *Biochemical Genetics*, 1041-1053.

Mishra, B. S., Singh, M., Aggrawal, P., Laxmi, A., 2009. Glucose and auxin signaling interaction in controlling *Arabidopsis thaliana* seedlings root growth and development. *PLoS One* 4, e4502.

Moffatt, B. A., Stevens, Y. Y., Allen, M. S., Snider, J. D., Pereira, L. A., Todorova, M. I., Summers, P. S., Weretilnyk, E. A., Martin-McCaffrey, L., Wagner, C., 2002. Adenosine kinase deficiency is associated with developmental abnormalities and reduced transmethylation. *Plant Physiology* 128, 812-821.

Mooney, B. P., Miernyk, J. A., Michael Greenlief, C., Thelen, J. J., 2006. Using quantitative proteomics of *Arabidopsis* roots and leaves to predict metabolic activity. *Physiology Plantarum* 128, 237-250.

Moore, B., Zhou, L., Rolland, F., Hall, Q., Cheng, W. H., Liu, Y. X., Hwang, I., Jones, T., Sheen, J., 2003. Role of the *Arabidopsis* glucose sensor HXK1 in nutrient, light, and hormonal signaling. *Science* 300, 332-336.

Muday, G. K., Rahman, A., Binder, B. M., 2012. Auxin and ethylene: collaborators or competitors? *Trends in Plant Science.* 17, 181-195.

Negi, S., Ivanchenko, M. G., Muday, G. K., 2008. Ethylene regulates lateral root formation and auxin transport in *Arabidopsis thaliana*. *Plant Journal* 55, 175-187.

Nemhauser, J. L., Mockler, T. C., Chory, J., 2004. Interdependency of brassinosteroid and auxin signaling in *Arabidopsis*. *Plos Biology* 2, 1460-1471.

O'Neill, M. A., Eberhard, S., Albersheim, P., Darvill, A. G., 2001. Requirement of borate cross-linking of cell wall rhamnogalacturonan II for *Arabidopsis* growth. *Science* 294, 846-849.

Ohto, M. A., Hayashi, S., Sawa, S., Hashimoto-Ohta, A., Nakamura, K., 2006. Involvement of HLS1 in sugar and auxin signaling in *Arabidopsis* leaves. *Plant Cell Physiology* 47, 1603-1611.

Oka, T., Nemoto, T., Jigami, Y., 2007. Functional analysis of *Arabidopsis thaliana* RHM2/MUM4, a multidomain protein involved in UDP-D-glucose to UDP-L-rhamnose conversion. *Journal of Biological Chemistry* 282, 5389-5403.

Petricka, J. J., Schauer, M. A., Megraw, M., Breakfield, N. W., Thompson, J. W., Georgiev, S., Soderblom, E. J., Ohler, U., Moseley, M. A., Grossniklaus, U., Benfey, P. N., 2012. The protein expression landscape of the *Arabidopsi*s root. *Proceedings of the National Academy of Science* 109, 6811-6818.

Pitts, R. J., Cernac, A., Estelle, M., 1998. Auxin and ethylene promote root hair elongation in *Arabidopsis*. *Plant Journal* 16, 553-560.

Rabilloud, T., Chevallet, M., Luche, S., Lelong, C., 2010. Two-dimensional gel electrophoresis in proteomics: Past, present and future. *Journal of Proteomics* 73, 2064-2077.

Rahman, A., Hosokawa, S., Oono, Y., Amakawa, T., Goto, N., Tsurumi, S., 2002. Auxin and ethylene response interactions during *Arabidopsis* root hair development dissected by auxin influx modulators. *Plant Physiology* 130, 1908-1917.

Reed, R. C., Brady, S. R., Muday, G. K., 1998. Inhibition of auxin movement from the shoot into the root inhibits lateral root development in *Arabidopsis*. *Plant Physiology* 118, 1369-1378.

Reiter, W.-D., Vanzin, G. F., 2001. Molecular genetics of nucleotide sugar interconversion pathways in plants. *Plant Molecular Biology* 47, 95-113.

Ridley, B. L., O'Neill, M. A., Mohnen, D. A., 2001. Pectins: structure, biosynthesis, and oligogalacturonide-related signaling. *Phytochemistry* 57, 929-967.

Ringli, C., Bigler, L., Kuhn, B. M., Leiber, R. M., Diet, A., Santelia, D., Frey, B., Pollmann, S., Klein, M., 2008. The modified flavonol glycosylation profile in the *Arabidopsis* rol1 mutants results in alterations in plant growth and cell shape formation. *Plant Cell* 20, 1470-1481.

Rolland, F., Baena-Gonzalez, E., Sheen, J., 2006. Sugar sensing and signaling in plants: Conserved and novel mechanisms. *Annual Review of Plant Biology* 57, 675-709.

Rolland, F., Sheen, J., 2005. Sugar sensing and signalling networks in plants. *Biochemical Society Transactions* 33, 269-271.

Roman, G., Lubarsky, B., Kieber, J. J., Rothenberg, M., Ecker, J. R., 1995. Genetic-analysis of ethylene signal-transduction in *Arabidopsis-thaliana* - 5 novel mutant loci integrated into a stress-response pathway. *Genetics* 139, 1393-1409.

Saito, K., 2004. Sulfur assimilatory metabolism. The long and smelling road. *Plant Physiology* 136, 2443-2450.

Schoor, S., Farrow, S., Blaschke, H., Lee, S., Perry, G., von Schwartzenberg, K., Emery, N., Moffatt, B., 2011. Adenosine kinase contributes to cytokinin interconversion in *Arabidopsis*. *Plant Physiology* 157, 659-672.

Schwender, J., Goffman, F., Ohlrogge, J. B., Shachar-Hill, Y., 2004. Rubisco without the Calvin cycle improves the carbon efficiency of developing green seeds. *Nature* 432, 779-782.

Stepanova, A. N., Yun, J., Likhacheva, A. V., Alonso, J. M., 2007. Multilevel interactions between ethylene and auxin in *Arabidopsis* roots. *Plant Cell* 19, 2169-2185.

Stephenson, M. B., Hawes, M. C., 1994. Correlation of pectin methylesterase activity in root caps of pea with root border cell separation. *Plant Physiology* 106, 739-745.

Strader, L. C., Chen, G. L., Bartel, B., 2010. Ethylene directs auxin to control root cell expansion. *Plant Journal* 64, 874-884.

Tan, C., Wang, H., Zhang, Y., Qi, B., Xu, G., Zheng, H., 2011. A proteomic approach to analyzing responses of *Arabidopsis thaliana* root cells to different gravitational conditions using an agravitropic mutant, pin2 and its wild type. *Proteome Science* 9, 72.

Tang, W., Kim, T. W., Oses-Prieto, J. A., Sun, Y., Deng, Z., Zhu, S., Wang, R., Burlingame, A. L., Wang, Z. Y., 2008. BSKs mediate signal transduction from the receptor kinase BRI1 in *Arabidopsis*. *Science* 321, 557-560.

Tanimoto, M., Roberts, K., Dolan, L., 1995. Ethylene is a positive regulator of root hair development in *Arabidopsis thaliana*. *Plant Journal* 8, 943-948.

Tian, Q., Reed, J. W., 2001. Molecular links between light and auxin signaling pathways. *Journal of Plant Growth Regulation* 20, 274-280.

van Noorden, G. E., Kerim, T., Goffard, N., Wiblin, R., Pellerone, F. I., Rolfe, B. G., Mathesius, U., 2007. Overlap of proteome changes in *Medicago truncatula* in response to auxin and Sinorhizobium meliloti. *Plant Physiology* 144, 1115-1131.

Wasteneys, G. O., Galway, M. E., 2003. Remodeling the cytoskeleton for growth and form: an overview with some new views. *Annual Review of Plant Biology* 54, 691-722.

Watt, G., Leoff, C., Harper, A. D., Bar-Peled, M., 2004. A bifunctional 3,5-epimerase/4-keto reductase for nucleotide-rhamnose synthesis in *Arabidopsis*. *Plant Physiology* 134, 1337-1346.

Whitney, S. M., Houtz, R. L., Alonso, H., 2011. Advancing our understanding and capacity to engineer nature's CO_2-sequestering enzyme, Rubisco. *Plant Physiology* 155, 27-35.

Willats, W. G., McCartney, L., Mackie, W., Knox, J. P., 2001. Pectin: cell biology and prospects for functional analysis. *Plant Molecular Biology* 47, 9-27.

Xu, X. M., Wang, J., Xuan, Z., Goldshmidt, A., Borrill, P. G., Hariharan, N., Kim, J. Y., Jackson, D., 2011. Chaperonins facilitate KNOTTED1 cell-to-cell trafficking and stem cell function. *Science* 333, 1141-1144.

Yang, G., Inoue, A., Takasaki, H., Kaku, H., Akao, S., Komatsu, S., 2005. A proteomic approach to analyze auxin- and zinc-responsive protein in rice. *Journal of Proteome Research* 4, 456-463.

Young, L. S., Harrison, B. R., Narayana, M. U. M., Moffatt, B. A., Gilroy, S., Masson, P. H., 2006. Adenosine kinase modulates root gravitropism and cap morphogenesis in *Arabidopsis*. *Plant Physiology* 142, 564-573.

Chapter 3

Evaluation of selected-reaction monitoring for peptide quantification in the model plant, *Arabidopsis thaliana*.

William O. Slade[A], *W. Keith Ray*[B], *Brenda S.J. Winkel*[A], *Richard F. Helm*[B]

Departments of Biological Sciences[A] *and Biochemistry*[B], *Virginia Tech, Blacksburg, VA 24061-0406, United States*

Contributions

William O. Slade
Designed the experiments, optimized analytical methods, performed the experiments, analyzed the data, and wrote the manuscript.

W. Keith Ray
Provided technical support.

Brenda S.J. Winkel
Conceived the experimental idea, and wrote the manuscript.

Richard F. Helm
Conceived the experimental idea, designed the experiments, analyzed the data, and edited the manuscript.

I. Abstract

Mass spectrometry-based plant proteomics can be used to uncover how regulation of proteins at the molecular level is manifested into a coherent biological response. Initial published research efforts focused on data-dependent acquisition methods (Aebersold and Mann, 2003), which are limited in utility in complex organisms due to the presence of high abundance proteins that suppress detection of low abundance proteins of biological significance. Targeted proteomics, on the other hand, relies upon selected reaction monitoring (SRM) protocols where proteotypic peptides, or those unique to specific proteins of interest, are analyzed, using their detection responses as a surrogate for protein levels. Herein we describe the use of SRM in *Arabidopsis thaliana*. We selected 500 peptides from 102 proteins representing diverse physiochemical properties and assayed their amenability to detection and quantification. This report provides evidence that SRM is a robust platform for peptide quantification in *Arabidopsis*, and can serve as a paradigm shift for studying protein regulation in plants.

II. Introduction

Measurement of protein abundances in plant-based systems can be accomplished by either targeted or untargeted peptide-based approaches. In comparison to whole-protein strategies, peptides are usually more soluble, capable of chromatographic separation of higher resolution, and more amenable to study using mass spectrometry (Duncan et al., 2010). Peptide quantification has been successfully used to elucidate many molecular pathways in plants, including the seedling response to ethylene in *Arabidopsis* (Chen et al., 2011), the response to methyl jasmonate in *Brassica napus* (Zhu et al., 2012), and molecular control of the chloroplast-to-chromoplast transition in *Solanum lycopersicum* (Barsan et al., 2012).

Label-free or tagged data-dependent acquisition (DDA) methods are currently the most popular choice for peptide-level quantification in plants (Vaudel et al., 2010). DDA operates by first acquiring general ion information about a sample and then choosing specific ions to fragment based on specific, user-guided parameters. DDA methods are attractive due to their throughput, development speed, and ease-of-use. DDA methods have been applied to several biological questions including the analysis of the *Plasmodium falciparum* life cycle and the analysis of how protein-protein interactions affect differentiation of PC12 cells (Aebersold and Mann, 2003; Choudhary and Mann, 2010; Yates et al., 2005).

Despite its popularity, DDA methods for proteomics are limited by technical and computational challenges. Complex organisms, such as *Arabidopsis*, display a wide dynamic range (10^5) of protein concentrations (Arsova et al., 2012). This coupled with the stochastic sampling nature of DDA methods (Bell et al., 2009) means that most peptides in a sample are unavailable to DDA (Michalski et al., 2011b). Additionally, current computational algorithms bias peptide identifications from DDA datasets towards certain fragmentation patterns (Grewal et al., 2004; Michalski et al., 2011a; Schwartz and

Bursey, 1992), not necessarily the best targets for peptide quantification (Lange et al., 2008)

SRM is a targeted, hypothesis-based approach to protein quantification by mass spectrometry. In contrast to DDA, SRM consists of a two-stage mass filter for peptides, using the unique properties of a triple-quad (QQQ) mass spectrometer. Once an initial protein and proteotypic peptides are selected, the peptides are assayed for specific fragment ions, and the mass spectrometer is optimized for the selective detection of the parent ion and its fragments. A method is subsequently developed to detect and measure parent ion/fragment ion pairs, which can be monitored in parallel. SRM results in greater sensitivity (Onisko et al., 2007), selectivity (Lange et al., 2008), reproducibility (Addona et al., 2009), and dynamic range (Stahl-Zeng et al., 2007) than current, conventional DDA methods. Thus, SRM represents a hypothesis-driven methodology for analyzing plant proteomes. Given the advance of SRM, we were surprised to observe limited reports of its efficacy in plants in the literature.

In the current study we assessed the efficacy of SRM for peptide quantification in *Arabidopsis*. We selected 500 peptides from 102 proteins of diverse physiochemical properties for development of SRM assays. In *Arabidopsis* roots, we observed less than 1% of proteins and peptides using SRM without fractionation. Fractionating protein lysates using SDS-PAGE improved protein coverage to 60.2% and peptide coverage to 39.9 %. Thus, we conclude that SRM is a robust platform for peptide quantification in *Arabidopsis*, but fractionation is required to enhance the number of proteins detected.

III. Results

In order to evaluate selected-reaction monitoring for relative quantification of proteins in *Arabidopsis*, we selected 102 proteins exhibiting a wide range of physiochemical properties (Figure 3-1). From these proteins, we selected a diverse group of 511 peptides for development of SRM assays (Figure 3-2). Peptides were first screened for amenability to our LC-MS/MS set up. Out of 511 peptides, 291 were observed using direction infusion or LC-MS/MS (Figure 3-3). A peptide was considered not detectable if the signal was not above 500 counts at a concentration of 1 μM in a simple mixture. Of those 291, 126 had been observed by other researchers, as indicated by a search of the Global Proteome Database (GPM) (Figure 3-3). Additionally, we observed a wide distribution of Enhanced Signature Peptide (ESP) scores for screened and observed peptides (Figure 3-3). The ESP score is a prediction of how amenable peptides are to SRM analysis (Fusaro et al. 2009). A wide distribution suggests, at least for the peptides analyzed here, that the ESP score does not consider all of the important variables for SRM analysis in *Arabidopsis.*

To assess the efficacy of SRM for peptides in *Arabidopsis*, the program Skyline (MacLean et al., 2010) was used to select the five most abundant fragment ions per peptide and to optimize the collision energy and declustering potential for each peptide (Figure 3-4). We then analyzed the response of each SRM assay in *Arabidopsis* roots. We analyzed proteins lystates that were not fractionated, separated into eight fractions

(Ladder 1), or separated into 12 fractions (Ladder 2). In whole-cell lysates, out of 291 peptides, we observed six peptides, corresponding to four proteins (Figure 3-5, Table 3-S1). We observed that prefractionation of the lysates into eight and 12 fractions according to molecular weight using SDS-Page resulted in increased coverage to 83 and 116 peptides, representing 48 and 62 proteins, respectively. Additionally, resolution and signal were improved for peptides observed in both fractionation schemes (Figure 3-6).

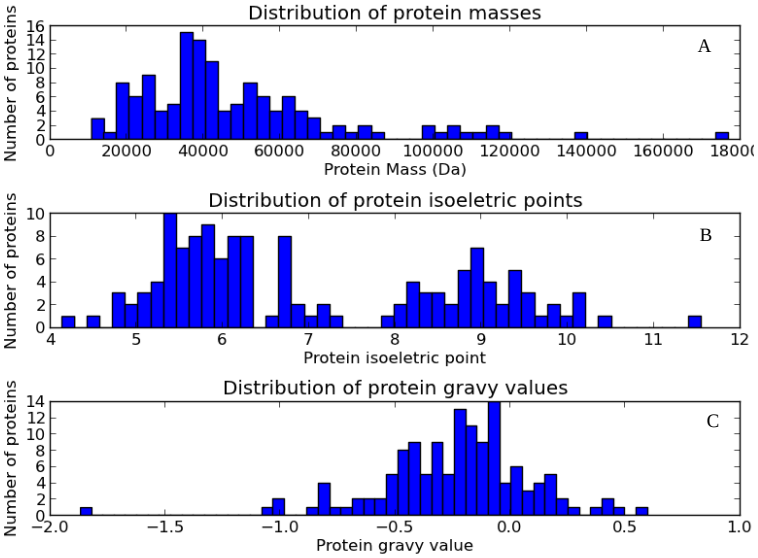

Figure 3-1. Distribution of physiochemical properties of the screened proteins. Shown are the distributions of protien mass (A), isoelectric point (B), and gravy (C, hydrophobicity).

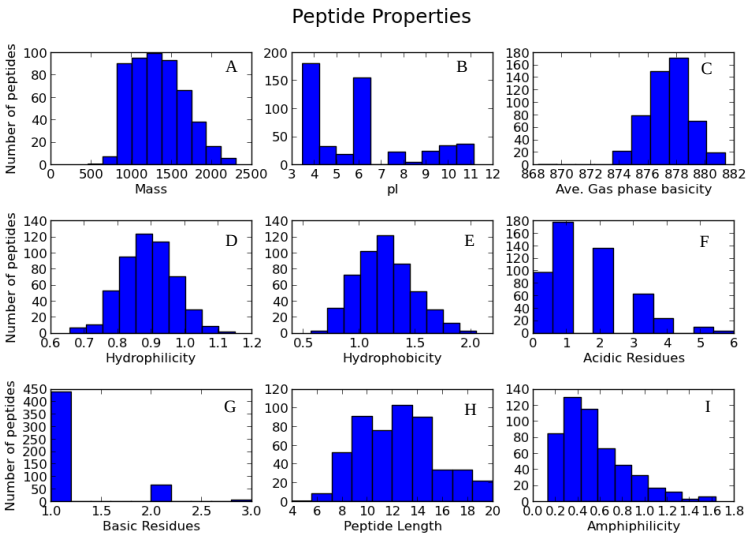

Figure 3-2. Distribution of physiochemical properties for screened peptides. Shown are the distributions of mass (A), pI (B), average gas-phase basicity (C), hydrophilicity (D), # of acidic residues (F), # of basic residues (G), peptide length (H), and amphiphilicity (I).

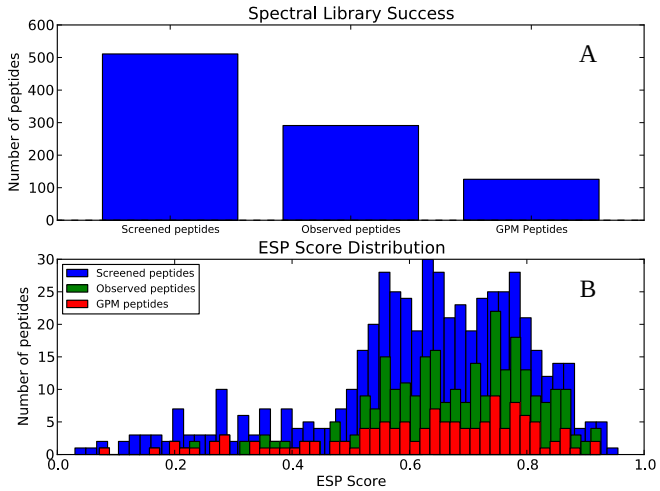

Figure 3-3. Spectral library success and ESP score distribution. Panel A shows total number of peptides screened (Screened peptides), those observed on the mass spectrometr (Observed peptides), and of the Observed peptides how many are in the GPM database (GPM peptides). Panel B shows the ESP score distributions for all peptides.

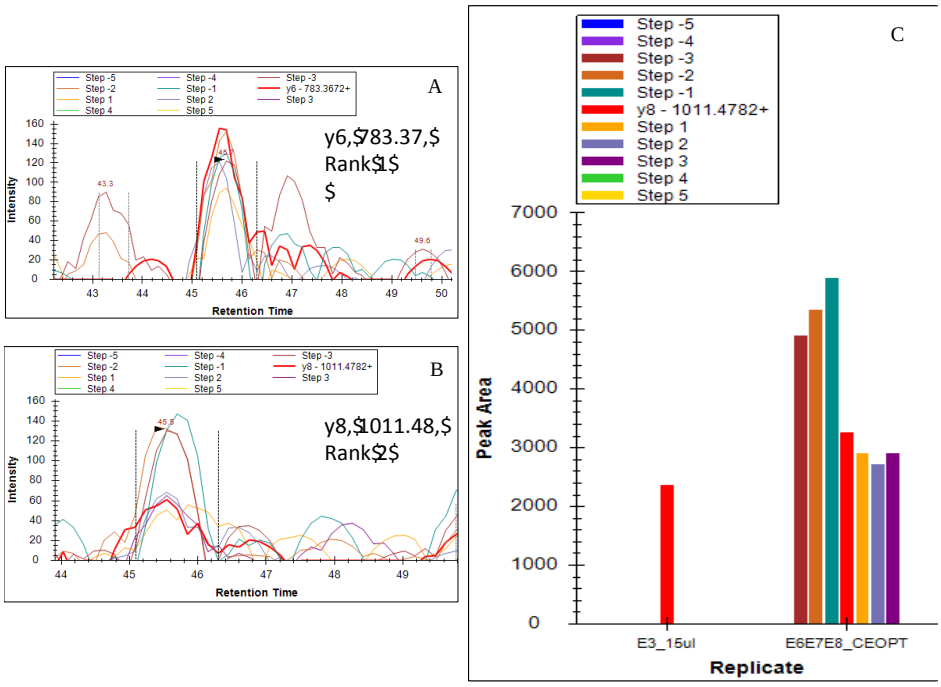

Figure 3-4. Collision energy (CE) and declustering potential (DP) optimization using Skyline. Shown are examples of CE optimization (A)

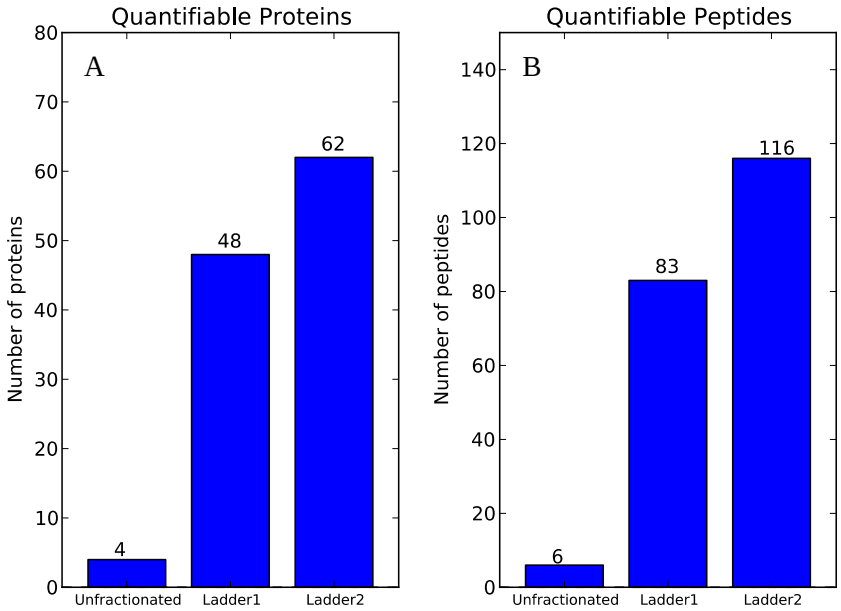

Figure 3-5. Protein and peptide response to SRM assays in *Arabidopsis* roots. Shown are the number of quantifable proteins (A) and peptides (B). Ladder 1 yields 8 fractions and Ladder 2 yields 12 fractions.

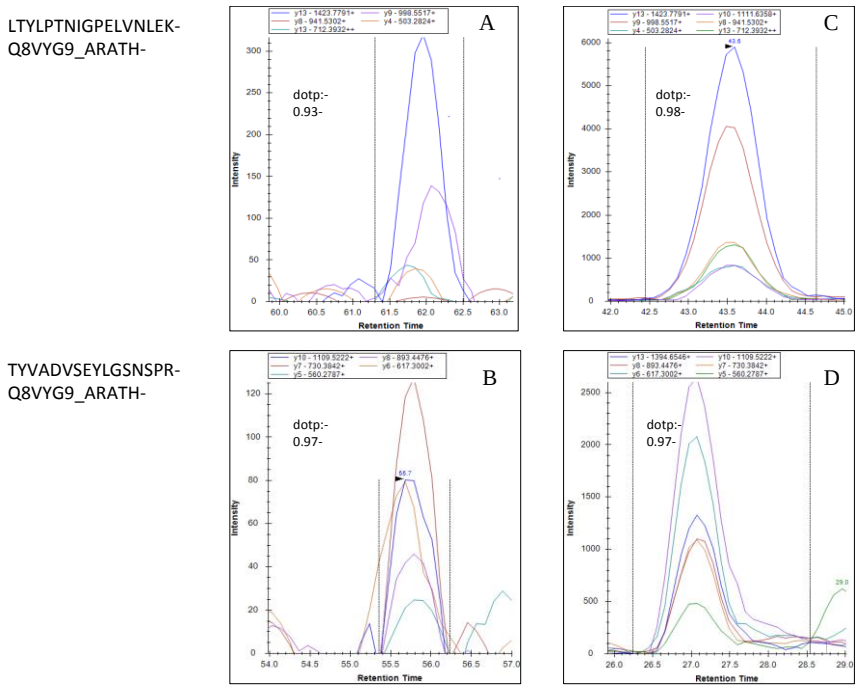

Figure 3-6. Increased fractionation improves resolution and sensitivity of SRM assays. Shown are example peptides using 8 fractions (A,B) and 12 fractions (C,B).

IV. Discussion

Our results indicate that SRM is a robust platform for quantification of proteins in *Arabidopsis.* We showed that 219 peptides of diverse physiochemical properties representing 68 diverse proteins are suitable for SRM analysis (See Appendix C for file information). The overall success rate 62 of 102 proteins, 61%, compares favorably with SRM analyses in other complex organisms (Mortstedt et al., 2013; Picotti et al., 2009; Schafer et al., 2012), indicating the SRM methodology can be applied to *Arabidopsis.* For example, Schafer et al. (2012) successfully developed SRM assays for 18 out of 27 proteins, or 67%. Additionally, we showed that fractionation (subproteome generation) is required for optimal SRM sensitivity and resolution, which concurs with reports of SRM in other complex systems.

The development of SRM assays is influenced by the effect of sample complexity on sensitivity and resolution. Sensitivity and resolution of SRM assays appear to be inversely proportional to sample complexity, and can only be mitigated by fractionation strategies. We observed fractionation is required for SRM assays of most peptides we screened. While researchers have reported the use of SRM assays with minimal fractionation to quantify the full dynamic range of proteins in yeast (Picotti et al., 2009) and human cell cultures (Ebhardt et al., 2012). More complex samples, such as mouse liver (Schafer et al., 2012) or nasal fluid (Mortstedt et al., 2013), required fractionation. Additionally, our results compare with Schafer et al (2012), in that fractionation of a complex sample improves not only sensitivity but also resolution of SRM assays.

While the development of SRM assays yields better sensitivity and selectivity compared to traditional discovery experiments, the process is laborious and lacks throughput (Picotti and Aebersold, 2012). Additionally, it is not yet known what physiochemical properties best predict amenability to mass spectrometry, or to a certain analytical workflow. Computational tools, such as the ESP Predictor, predicting peptide SRM robustness appear to alleviate some experimental burden (Fusaro et al., 2009). The ESP Predictor, based on a random forest classifier algorithm, predicts robust SRM peptides with high confidence in yeast and human cell lines (Fusaro et al., 2009). To our surprise, the peptides we screened displayed a poor correlation between the ESP prediction software and amenability to SRM analysis. The ESP software was trained primarily on discovery datasets using algorithms such as Mascot and Sequest that are biased towards certain types of peptides, not necessarily the best targets for quantitation. Many of the best SRM candidates we observed did not have high ESP scores or have previous spectral data in the GPM database. This discrepancy has been noted previously by Fusaro et al. (2009) and Lange et al. (2008).

Future work could attempt to assess what physiochemical properties best predict amenability of peptides to analyses by mass spectrometry, particularly SRM. The poor correlation between ESP score and SRM response observed in the current experiments indicates a substantial gap in our understanding of how to assess whether a peptide is amenable to SRM. To address this problem, a representative sample size of the potential *Arabidopsis* peptidome (tens of millions of peptides) would have to be studied. The

peptides screened in the current analysis represent 0.000022% of this potential peptidome, which is insufficiently large to draw conclusions about the physiochemical properties that best predict amenability for SRM applications.

In summary, our work suggests that SRM is a robust platform for protein quantification in *Arabidopsis*. We screened over 500 peptides for SRM assay robustness and observed success for a group of peptides with diverse physiochemical properties. Additionally, we observed no correlation among a certain physiochemical property and amenability to the SRM assay. Here we propose that SRM will replace discovery proteomics in plants due to improved sensitivity, reproducibility, dynamic range, and cost. Given that proteins are often the ultimate effectors of biological activity, SRM assays will help to elucidate how changes in protein levels are manifested in a coherent biological response.

V. Experimental

i. Plant Material

Plant material was prepared according to Slade et al. (2012) Briefly, seeds of the Columbia (Col-0) ecotype of *Arabidopsis* were obtained from Lehle Seeds (Round Rock, Texas, USA). Plants were grown on 1X Musharige and Skoog medium from Caisson labs (North Logan, Utah, USA) pH 5.7, 0.8% (w/v) agar, and supplemented with 1% (w/v) sucrose. After cold treatment for 48-72 h at 4°C, seeds were moved to a growth chamber and grown under 100 μmol $m^{-2}s^{-2}$ cool-white light (24h lighting). The growth chamber was maintained at 22°C and 60% relative humidity. All assays were conducted 5 d after germination, which was typically 6-7 d after the cold treatment.

ii. Protein extraction

Each biological replicate (~150 mg) of root tissue was ground to a fine powder and mixed with 3 volumes of Extraction Buffer (EB; 62.5 mM Tris-HCl, pH 6.8, 25% glycerol, 2% SDS, 710mM β-mercaptoethanol), then heated at 95°C for 10 min. Cellular debris were pelleted by centrifugation at 6710g for 20 min. After centrifugation, protein concentration was determined with the 2D-Quant Kit (GE Healthcare; Piscataway, NJ) using BSA as a standard. Protein concentrations were typically on the order of 4-6 mg/mL.

iii. SDS-Page

For each biological replicate, 60 μg of protein was loaded onto one lane of a 10.5-14% Tris-HCl gel (Criterion, Biorad). Electrophoresis was carried out at room temperature at 40 V for 20 min and then 120 V until the bromophenol dye front reached the bottom of the gel. Gels were stained with Coomassie blue (ProtoBlue Safe, National Diagnostics). Gels were cut into single-lane bands (Supplemental Figure 3-1) according to molecular weight, using either a ladder for eight fractions (Ladder 1), EZ-Run prestained *Rec* protein ladder (Fisher) or 12 fractions, PageRuler Unstained protein ladder (Ladder 2) (Pierce).

iv. In-gel tryptic digest
Gel slices were washed once with ultrapure H_2O followed by washes with ACN-H_2O (1:1,v/v) 50 mM NH_4CO_3, pH 8.0 until the slices were no longer colored. Following dehydration with CH_3CN, cores were rehydrated in 10 mM dithiothreitol (DTT) for 20 min at 55°C. Gel pieces were cooled to RT and then incubated in 10 mM iodoacetamide (IAA) for 20 min at RT in the dark. After one wash in ultrapure H_2O and two washes CH_3CN-H_2O (1:1,v/v) 50 mM NH_4CO_3, pH 8.0, the gel pieces were dehydrated with CH_3CN. Samples were dried in a vacuum centrifuge and then stored at -80°C until further use. Samples were rehydrated in 10 ng/nl trypsin (Promega, Wisconsin, MA, USA) at 4°C for 90 min and then incubated at 37°C for 16 h. Peptides were extracted twice using acetonitrile/H_2O/formic acid (50/40/10), lyophilized, and stored at -80°C until use.

v. Protein selection
Previous mRNA profiling work identified a group of 139 genes (Supplemental Figure 3-2) responsive to both auxin and ethylene over a 24 h time course in *Arabidopsis* roots (Lewis et al., submitted). Of the 139, proteins containing at least one unique peptide were considered for further analysis.

vi. Peptide selection and synthesis
Primary protein sequences were downloaded from UniProt and digested *in silico* using Peptide Cutter (Wilkins et al., 1999). Peptides were queried for SRM robustness using ESP Predictor and for SRM uniqueness using TAIR PatMatch. Ultimately, all unique peptides 6-20 amino acids in length were selected for synthesis, which were prepared commercially (JPT Technologies).

vii. Mass spectrometry and nanoLC set-up
The MS platform used was a 4000 QTRAP hybrid triple quadrupole/linear ion mass spectrometer equipped with a Phoenix SandT source coupled to an online nano liquid chromatography system (Tempo, Eksigient) with an autosampler (AS2, Eksigient). The following MS settings were used: Curtain gas: 10V, ion source: 2800V, gas source one (GS1): 35. Mobile phases were as follows: (A) 0.1% formic acid and (B) ACN. Analytical columns were prepared as follows: Fritted capillaries (PST-LC75-eFRIT, Phoenix ST) were packed to a length of 15 cm with Magic C18AQ Resin (3u, 200A, Michrom Bioresources) resuspended in chloroform using a pressure bomb. The mobile phases were (A) 0.1% Formic Acid and (B) 0.1% FA in ACN. Samples were separated on an in-house packed column at 300 nl/min using the following gradient steps: (A) 90% A for 10 min, (B) increase B to 60% over 50 min, (C) increase B to 90% over 10 min, (D) increase A to 90% over 5 min, (E) re-equilibrate at 90% A for 25 min.

viii. Spectral Library
Peptides were screened for amenability to analysis by mass spectrometry based on the methodology of Picotti et al. (2010). Briefly, peptides were resuspended in 20% ACN, 1% formic acid, vortexed for 30 sec, and sonicated for 15 min. Aliquots (~1 μM) of up to 12 peptides were mixed and evaporated on a vacuum centrifuge to complete dryness. Mixes were resuspended in 0.1% formic acid and analyzed using nanoLC-MS/MS. An

enhanced mass spec (EMS) scan was acquired in the 400-1500 Da mass range. Ions with charge +2 to +5 and exceeding 1000 counts were selected for an enhanced ion product (EPI) scan. Analyst 1.6 was then used to build a peak list given the following parameters: charge states: +2 to +5, minimum intensity: 1000, peak density: 20 per 100 m/z.

Mascot Daemon v 2.2.2 (Matrix Science, Inc., Boston, MA) was used to automatically submit peak lists to a local Mascot Server v 2.2.2 (Matrix Science, Inc., Boston, MA) search engine utilizing the *Arabidopsis* protein database (NCBInr 20100131) appended with its reverse decoy. Searches of MS/MS data used trypsin specificity with the possibility of one missed cleavage, a peptide mass tolerance of ± 150 ppm, a peptide fragment mass tolerance of ± 0.6 Da, and the possibility of carbidomethylation at cysteine, oxidation at methionine and tryptophan.

x. Design of SRM assays

Mascot search results were imported as .dat files into Skyline v. 1.4 with a cutoff score of 0.85. The tandem MS spectra were then validated manually to ensure the spectra contained at least 4 to 5 consecutive –b or –y ions matching the predicted sequence. Peptides not meeting this criterion were not considered further.

Skyline was used to automate the selection of transitions using the following parameters: monoisotopic precursor and product ions, ABI 4000 QTrap default collision energy values, precursor charges: 2,3, ion charges: 1,2, ion types: y, and five product ions per parent ion. Additionally, product ions with a greater m/z ratio than the parent were prioritized unless this was not possible.

xi. Validation of SRM assays

All SRM assays (Supplemental Figure 3-3) were screened in *Arabidopsis* roots. SRM assays were considered validated if the following criteria were met: (1) At least four co-eluting transitions were observed, (2) a dot-p score (reference) of ≥ 0.85, (3) a minimum intensity of 500 counts, and (4) a spectrum containing only one peak meeting the first three criteria.

VI. Supplemental Information

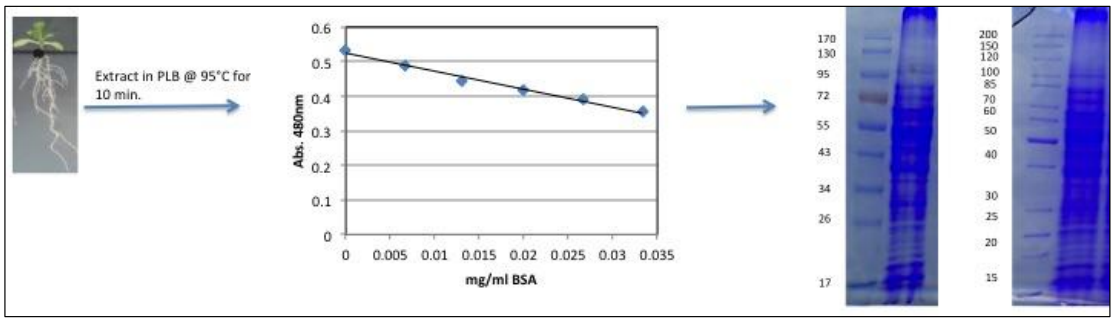

Figure 3-S1. Scheme for fractionation of protein lysates using SDS-Page. Show are the EZ-Run prestained ladder (Fisher, 8 fractions) and the Page ruler unstained protein ladder (Pierce, 12 fractions).

Figure 3-S2. Overlap between IAA- and ACC-regulated genes. Genes regualted by IAA and ACC were selected as targets for protein quantitation.

Table 3-S1. List of peptides and proteins identified in unfractionated lysates.

Mr Calc (Da)	MC	Start Seq.	End Seq.	Peptide Sequence
Uniprot: P46010; Gene: AT3G44320; Nitrilase 3				
1578.8679	0	59	72	LVLFPEAFIGGYPR
Uniprot: Q96330; Gene: At5g08640; Flavonol synthase				
1628.9469	0	168	183	LSETLLGILSDGLGLK
1661.8745	0	300	315	IVGPLPELTGDDNPPK
Uniprot: P24102; Gene: At2g38380; Peroxidase 22				
1517.7077	0	188	202	TSDLVALSGGHTFGR
Uniprot: P52577; Gene: At1g75280; Isoflavone homolog				
1190.7143	0	7	18	ILVIGGTGYIGK
1380.6794	0	108	119	FLPSEFGVDVDR

Table 3-S2. List of all peptides and transitions tested. Q1 and Q3 monoisotpic masses (MI), protein and peptide information, declustering potential (DP), and collision energy (CE).

Q1_MI	Q3_MI	Protein_information	DP	CE
551.31	887.48	sp|Q1JPL7|PME18_ARATH.ITASSDLAPVK.	71.3	27.2
551.31	816.45	sp|Q1JPL7|PME18_ARATH.ITASSDLAPVK.	71.3	27.2
551.31	527.36	sp|Q1JPL7|PME18_ARATH.ITASSDLAPVK.	71.3	27.2
551.31	414.27	sp|Q1JPL7|PME18_ARATH.ITASSDLAPVK.	71.3	27.2
551.31	343.23	sp|Q1JPL7|PME18_ARATH.ITASSDLAPVK.	71.3	27.2
595.86	964.55	sp|P52577|IFRH_ARATH.ILVIGGTGYIGK.	74.6	29.7
595.86	865.48	sp|P52577|IFRH_ARATH.ILVIGGTGYIGK.	74.6	29.7
595.86	752.39	sp|P52577|IFRH_ARATH.ILVIGGTGYIGK.	74.6	29.7
595.86	695.37	sp|P52577|IFRH_ARATH.ILVIGGTGYIGK.	74.6	29.7
595.86	317.22	sp|P52577|IFRH_ARATH.ILVIGGTGYIGK.	74.6	29.7
690.84	1120.53	sp|P52577|IFRH_ARATH.FLPSEFGVDVDR.	81.5	35.1
690.84	660.33	sp|P52577|IFRH_ARATH.FLPSEFGVDVDR.	81.5	35.1
690.84	504.24	sp|P52577|IFRH_ARATH.FLPSEFGVDVDR.	81.5	35.1
690.84	389.21	sp|P52577|IFRH_ARATH.FLPSEFGVDVDR.	81.5	35.1
690.84	175.12	sp|P52577|IFRH_ARATH.FLPSEFGVDVDR.	81.5	35.1
759.39	1002.51	sp|P24102|PER22_ARATH.TSDLVALSGGHTFGR.	86.5	39
759.39	931.47	sp|P24102|PER22_ARATH.TSDLVALSGGHTFGR.	86.5	39
759.39	818.39	sp|P24102|PER22_ARATH.TSDLVALSGGHTFGR.	86.5	39
759.39	731.36	sp|P24102|PER22_ARATH.TSDLVALSGGHTFGR.	86.5	39
759.39	480.26	sp|P24102|PER22_ARATH.TSDLVALSGGHTFGR.	86.5	39
965.04	1393.70	sp|O65355|GGH_ARATH.VIPLIFNEPEEILFQK.	101.5	50.7
965.04	1246.63	sp|O65355|GGH_ARATH.VIPLIFNEPEEILFQK.	101.5	50.7
965.04	1003.55	sp|O65355|GGH_ARATH.VIPLIFNEPEEILFQK.	101.5	50.7
965.04	535.32	sp|O65355|GGH_ARATH.VIPLIFNEPEEILFQK.	101.5	50.7
965.04	422.24	sp|O65355|GGH_ARATH.VIPLIFNEPEEILFQK.	101.5	50.7
571.83	1029.58	sp|Q9FRL8|DHAR2_ARATH.IFGAFVTFLK.	72.8	28.3
571.83	882.51	sp|Q9FRL8|DHAR2_ARATH.IFGAFVTFLK.	72.8	28.3
571.83	754.45	sp|Q9FRL8|DHAR2_ARATH.IFGAFVTFLK.	72.8	28.3
571.83	508.31	sp|Q9FRL8|DHAR2_ARATH.IFGAFVTFLK.	72.8	28.3
571.83	407.27	sp|Q9FRL8|DHAR2_ARATH.IFGAFVTFLK.	72.8	28.3
531.95	953.51	sp|Q9FRL8|DHAR2_ARATH.ALVDELEALENHLK.	69.9	23.6
531.95	824.46	sp|Q9FRL8|DHAR2_ARATH.ALVDELEALENHLK.	69.9	23.6
531.95	753.43	sp|Q9FRL8|DHAR2_ARATH.ALVDELEALENHLK.	69.9	23.6
531.95	640.34	sp|Q9FRL8|DHAR2_ARATH.ALVDELEALENHLK.	69.9	23.6
531.95	511.30	sp|Q9FRL8|DHAR2_ARATH.ALVDELEALENHLK.	69.9	23.6
957.53	1423.78	tr|Q8VYG9|Q8VYG9_ARATH.LTYLPTNIGPELVNLEK.	100.9	50.3

957.53	1111.64	tr|Q8VYG9|Q8VYG9_ARATH.LTYLPTNIGPELVNLEK.	100.9	50.3
957.53	998.55	tr|Q8VYG9|Q8VYG9_ARATH.LTYLPTNIGPELVNLEK.	100.9	50.3
957.53	941.53	tr|Q8VYG9|Q8VYG9_ARATH.LTYLPTNIGPELVNLEK.	100.9	50.3
957.53	503.28	tr|Q8VYG9|Q8VYG9_ARATH.LTYLPTNIGPELVNLEK.	100.9	50.3
639.02	998.55	tr|Q8VYG9|Q8VYG9_ARATH.LTYLPTN[+1_0]IGPELVNLEK.	77.7	26.9
639.02	941.53	tr|Q8VYG9|Q8VYG9_ARATH.LTYLPTN[+1_0]IGPELVNLEK.	77.7	26.9
639.02	715.43	tr|Q8VYG9|Q8VYG9_ARATH.LTYLPTN[+1_0]IGPELVNLEK.	77.7	26.9
639.02	602.35	tr|Q8VYG9|Q8VYG9_ARATH.LTYLPTN[+1_0]IGPELVNLEK.	77.7	26.9
639.02	503.28	tr|Q8VYG9|Q8VYG9_ARATH.LTYLPTN[+1_0]IGPELVNLEK.	77.7	26.9
879.42	1109.52	tr|Q8VYG9|Q8VYG9_ARATH.TYVADVSEYLGSNSPR.	95.2	45.9
879.42	893.45	tr|Q8VYG9|Q8VYG9_ARATH.TYVADVSEYLGSNSPR.	95.2	45.9
879.42	730.38	tr|Q8VYG9|Q8VYG9_ARATH.TYVADVSEYLGSNSPR.	95.2	45.9
879.42	617.30	tr|Q8VYG9|Q8VYG9_ARATH.TYVADVSEYLGSNSPR.	95.2	45.9
879.42	560.28	tr|Q8VYG9|Q8VYG9_ARATH.TYVADVSEYLGSNSPR.	95.2	45.9
637.84	1075.57	tr|Q9SF06|Q9SF06_ARATH.AQQETSAALLSR.	77.6	32.1
637.84	818.47	tr|Q9SF06|Q9SF06_ARATH.AQQETSAALLSR.	77.6	32.1
637.84	717.43	tr|Q9SF06|Q9SF06_ARATH.AQQETSAALLSR.	77.6	32.1
637.84	559.36	tr|Q9SF06|Q9SF06_ARATH.AQQETSAALLSR.	77.6	32.1
637.84	375.24	tr|Q9SF06|Q9SF06_ARATH.AQQETSAALLSR.	77.6	32.1
595.32	959.54	tr|Q9SF06|Q9SF06_ARATH.TETLVLEGEAK.	74.5	29.7
595.32	745.41	tr|Q9SF06|Q9SF06_ARATH.TETLVLEGEAK.	74.5	29.7
595.32	646.34	tr|Q9SF06|Q9SF06_ARATH.TETLVLEGEAK.	74.5	29.7
595.32	533.26	tr|Q9SF06|Q9SF06_ARATH.TETLVLEGEAK.	74.5	29.7
595.32	404.21	tr|Q9SF06|Q9SF06_ARATH.TETLVLEGEAK.	74.5	29.7
613.34	957.57	tr|Q9SF06|Q9SF06_ARATH.MHVDLLVVGSR.	75.8	30.7
613.34	858.50	tr|Q9SF06|Q9SF06_ARATH.MHVDLLVVGSR.	75.8	30.7
613.34	743.48	tr|Q9SF06|Q9SF06_ARATH.MHVDLLVVGSR.	75.8	30.7
613.34	630.39	tr|Q9SF06|Q9SF06_ARATH.MHVDLLVVGSR.	75.8	30.7
613.34	418.24	tr|Q9SF06|Q9SF06_ARATH.MHVDLLVVGSR.	75.8	30.7
789.94	1253.63	sp|P46010|NRL3_ARATH.LVLFPEAFIGGYPR.	88.7	40.8
789.94	1106.56	sp|P46010|NRL3_ARATH.LVLFPEAFIGGYPR.	88.7	40.8
789.94	880.47	sp|P46010|NRL3_ARATH.LVLFPEAFIGGYPR.	88.7	40.8
789.94	809.43	sp|P46010|NRL3_ARATH.LVLFPEAFIGGYPR.	88.7	40.8
789.94	549.28	sp|P46010|NRL3_ARATH.LVLFPEAFIGGYPR.	88.7	40.8
1015.07	1154.69	sp|Q9C5Y0|PLDD1_ARATH.VITSDPYVTVVVPQATLAR.	105.1	53.6
1015.07	1053.64	sp|Q9C5Y0|PLDD1_ARATH.VITSDPYVTVVVPQATLAR.	105.1	53.6
1015.07	954.57	sp|Q9C5Y0|PLDD1_ARATH.VITSDPYVTVVVPQATLAR.	105.1	53.6
1015.07	855.50	sp|Q9C5Y0|PLDD1_ARATH.VITSDPYVTVVVPQATLAR.	105.1	53.6
1015.07	756.44	sp|Q9C5Y0|PLDD1_ARATH.VITSDPYVTVVVPQATLAR.	105.1	53.6

725.36	1005.57	sp|Q9C5Y0|PLDD1_ARATH.DDDVFGAQIIGTAK.	84	37.1
725.36	858.50	sp|Q9C5Y0|PLDD1_ARATH.DDDVFGAQIIGTAK.	84	37.1
725.36	801.48	sp|Q9C5Y0|PLDD1_ARATH.DDDVFGAQIIGTAK.	84	37.1
725.36	489.30	sp|Q9C5Y0|PLDD1_ARATH.DDDVFGAQIIGTAK.	84	37.1
725.36	376.22	sp|Q9C5Y0|PLDD1_ARATH.DDDVFGAQIIGTAK.	84	37.1
681.39	981.53	tr|Q9FH82|Q9FH82_ARATH.AVPITYLESAVAK.	80.8	34.6
681.39	880.48	tr|Q9FH82|Q9FH82_ARATH.AVPITYLESAVAK.	80.8	34.6
681.39	717.41	tr|Q9FH82|Q9FH82_ARATH.AVPITYLESAVAK.	80.8	34.6
681.39	604.33	tr|Q9FH82|Q9FH82_ARATH.AVPITYLESAVAK.	80.8	34.6
681.39	475.29	tr|Q9FH82|Q9FH82_ARATH.AVPITYLESAVAK.	80.8	34.6
1043.57	830.46	tr|Q9FH82|Q9FH82_ARATH.NVLAPTSVDK.	107.2	55.2
1043.57	717.38	tr|Q9FH82|Q9FH82_ARATH.NVLAPTSVDK.	107.2	55.2
1043.57	646.34	tr|Q9FH82|Q9FH82_ARATH.NVLAPTSVDK.	107.2	55.2
1043.57	549.29	tr|Q9FH82|Q9FH82_ARATH.NVLAPTSVDK.	107.2	55.2
1043.57	448.24	tr|Q9FH82|Q9FH82_ARATH.NVLAPTSVDK.	107.2	55.2
563.77	956.43	tr|Q9FH82|Q9FH82_ARATH.AVGDWFFER.	72.2	27.9
563.77	784.38	tr|Q9FH82|Q9FH82_ARATH.AVGDWFFER.	72.2	27.9
563.77	598.30	tr|Q9FH82|Q9FH82_ARATH.AVGDWFFER.	72.2	27.9
563.77	451.23	tr|Q9FH82|Q9FH82_ARATH.AVGDWFFER.	72.2	27.9
563.77	175.12	tr|Q9FH82|Q9FH82_ARATH.AVGDWFFER.	72.2	27.9
835.42	1144.52	sp|Q9SYM4|TPS1_ARATH.ILGLEGTPEGVEDQGR.	92	43.4
835.42	986.45	sp|Q9SYM4|TPS1_ARATH.ILGLEGTPEGVEDQGR.	92	43.4
835.42	760.36	sp|Q9SYM4|TPS1_ARATH.ILGLEGTPEGVEDQGR.	92	43.4
835.42	604.27	sp|Q9SYM4|TPS1_ARATH.ILGLEGTPEGVEDQGR.	92	43.4
835.42	360.20	sp|Q9SYM4|TPS1_ARATH.ILGLEGTPEGVEDQGR.	92	43.4
575.80	937.49	tr|Q9STG9|Q9STG9_ARATH.NVQPFVAGYR.	73.1	28.6
575.80	809.43	tr|Q9STG9|Q9STG9_ARATH.NVQPFVAGYR.	73.1	28.6
575.80	712.38	tr|Q9STG9|Q9STG9_ARATH.NVQPFVAGYR.	73.1	28.6
575.80	466.24	tr|Q9STG9|Q9STG9_ARATH.NVQPFVAGYR.	73.1	28.6
575.80	395.20	tr|Q9STG9|Q9STG9_ARATH.NVQPFVAGYR.	73.1	28.6
804.39	1076.52	sp|P21240|CPNB1_ARATH.ETSTIVGDGSTQDAVK.	89.8	41.6
804.39	977.45	sp|P21240|CPNB1_ARATH.ETSTIVGDGSTQDAVK.	89.8	41.6
804.39	920.43	sp|P21240|CPNB1_ARATH.ETSTIVGDGSTQDAVK.	89.8	41.6
804.39	661.35	sp|P21240|CPNB1_ARATH.ETSTIVGDGSTQDAVK.	89.8	41.6
804.39	317.22	sp|P21240|CPNB1_ARATH.ETSTIVGDGSTQDAVK.	89.8	41.6
769.89	1295.68	tr|Q9SM08|Q9SM08_ARATH.DQYIGISTVQATDK.	87.2	39.6
769.89	1132.62	tr|Q9SM08|Q9SM08_ARATH.DQYIGISTVQATDK.	87.2	39.6
769.89	1019.54	tr|Q9SM08|Q9SM08_ARATH.DQYIGISTVQATDK.	87.2	39.6
769.89	962.52	tr|Q9SM08|Q9SM08_ARATH.DQYIGISTVQATDK.	87.2	39.6
769.89	849.43	tr|Q9SM08|Q9SM08_ARATH.DQYIGISTVQATDK.	87.2	39.6
482.76	704.37	tr|Q9SM08|Q9SM08_ARATH.FLLNGSASR.	66.3	23.3

482.76	591.28	tr|Q9SM08|Q9SM08_ARATH.FLLNGSASR.	66.3	23.3
482.76	477.24	tr|Q9SM08|Q9SM08_ARATH.FLLNGSASR.	66.3	23.3
482.76	420.22	tr|Q9SM08|Q9SM08_ARATH.FLLNGSASR.	66.3	23.3
482.76	333.19	tr|Q9SM08|Q9SM08_ARATH.FLLNGSASR.	66.3	23.3
619.30	1036.52	tr|Q9SM08|Q9SM08_ARATH.NSFPVGTC[+57_0]ISR.	76.3	31
619.30	889.46	tr|Q9SM08|Q9SM08_ARATH.NSFPVGTC[+57_0]ISR.	76.3	31
619.30	792.40	tr|Q9SM08|Q9SM08_ARATH.NSFPVGTC[+57_0]ISR.	76.3	31
619.30	693.33	tr|Q9SM08|Q9SM08_ARATH.NSFPVGTC[+57_0]ISR.	76.3	31
690.36	1115.59	tr|Q9SM08|Q9SM08_ARATH.YTEQILDLQEK.	81.4	35.1
690.36	858.49	tr|Q9SM08|Q9SM08_ARATH.YTEQILDLQEK.	81.4	35.1
690.36	745.41	tr|Q9SM08|Q9SM08_ARATH.YTEQILDLQEK.	81.4	35.1
690.36	632.32	tr|Q9SM08|Q9SM08_ARATH.YTEQILDLQEK.	81.4	35.1
690.36	517.30	tr|Q9SM08|Q9SM08_ARATH.YTEQILDLQEK.	81.4	35.1
884.91	1202.56	tr|Q9SM08|Q9SM08_ARATH.DNSHLVNAEGDVNEAGK.	95.6	46.2
884.91	1103.50	tr|Q9SM08|Q9SM08_ARATH.DNSHLVNAEGDVNEAGK.	95.6	46.2
884.91	789.37	tr|Q9SM08|Q9SM08_ARATH.DNSHLVNAEGDVNEAGK.	95.6	46.2
884.91	617.33	tr|Q9SM08|Q9SM08_ARATH.DNSHLVNAEGDVNEAGK.	95.6	46.2
884.91	518.26	tr|Q9SM08|Q9SM08_ARATH.DNSHLVNAEGDVNEAGK.	95.6	46.2
466.27	747.40	tr|Q3EBG3|Q3EBG3_ARATH.ALPVDAAFK.	65.1	22.3
466.27	650.35	tr|Q3EBG3|Q3EBG3_ARATH.ALPVDAAFK.	65.1	22.3
466.27	551.28	tr|Q3EBG3|Q3EBG3_ARATH.ALPVDAAFK.	65.1	22.3
466.27	436.26	tr|Q3EBG3|Q3EBG3_ARATH.ALPVDAAFK.	65.1	22.3
466.27	294.18	tr|Q3EBG3|Q3EBG3_ARATH.ALPVDAAFK.	65.1	22.3
707.85	1126.61	sp|Q6E263|CRR39_ARATH.QC[+57_0]DPLDANILQK.	82.7	36.1
707.85	914.53	sp|Q6E263|CRR39_ARATH.QC[+57_0]DPLDANILQK.	82.7	36.1
707.85	801.45	sp|Q6E263|CRR39_ARATH.QC[+57_0]DPLDANILQK.	82.7	36.1
707.85	686.42	sp|Q6E263|CRR39_ARATH.QC[+57_0]DPLDANILQK.	82.7	36.1
707.85	615.38	sp|Q6E263|CRR39_ARATH.QC[+57_0]DPLDANILQK.	82.7	36.1
726.87	1154.60	sp|Q6E263|CRR39_ARATH.SPNYSNQNLFLR.	84.1	37.2
726.87	991.53	sp|Q6E263|CRR39_ARATH.SPNYSNQNLFLR.	84.1	37.2
726.87	904.50	sp|Q6E263|CRR39_ARATH.SPNYSNQNLFLR.	84.1	37.2
726.87	662.40	sp|Q6E263|CRR39_ARATH.SPNYSNQNLFLR.	84.1	37.2
726.87	435.27	sp|Q6E263|CRR39_ARATH.SPNYSNQNLFLR.	84.1	37.2
496.78	793.46	sp|Q6E263|CRR39_ARATH.AQALSSFLR.	67.3	24.1
496.78	722.42	sp|Q6E263|CRR39_ARATH.AQALSSFLR.	67.3	24.1
496.78	609.34	sp|Q6E263|CRR39_ARATH.AQALSSFLR.	67.3	24.1
496.78	522.30	sp|Q6E263|CRR39_ARATH.AQALSSFLR.	67.3	24.1
496.78	435.27	sp|Q6E263|CRR39_ARATH.AQALSSFLR.	67.3	24.1
481.77	863.47	tr|Q84WS4|Q84WS4_ARATH.VVGTLFGNR.	66.2	23.2
481.77	764.40	tr|Q84WS4|Q84WS4_ARATH.VVGTLFGNR.	66.2	23.2
481.77	606.34	tr|Q84WS4|Q84WS4_ARATH.VVGTLFGNR.	66.2	23.2

481.77	493.25	tr|Q84WS4|Q84WS4_ARATH.VVGTLFGNR.	66.2	23.2
481.77	346.18	tr|Q84WS4|Q84WS4_ARATH.VVGTLFGNR.	66.2	23.2
490.28	866.46	tr|Q84WS4|Q84WS4_ARATH.IALETAAYK.	66.9	23.7
490.28	795.42	tr|Q84WS4|Q84WS4_ARATH.IALETAAYK.	66.9	23.7
490.28	682.34	tr|Q84WS4|Q84WS4_ARATH.IALETAAYK.	66.9	23.7
490.28	553.30	tr|Q84WS4|Q84WS4_ARATH.IALETAAYK.	66.9	23.7
490.28	381.21	tr|Q84WS4|Q84WS4_ARATH.IALETAAYK.	66.9	23.7
691.86	1168.58	sp|Q9XIA9|LACS2_ARATH.TIVSFGEVSSTQK.	81.6	35.2
691.86	1069.52	sp|Q9XIA9|LACS2_ARATH.TIVSFGEVSSTQK.	81.6	35.2
691.86	835.42	sp|Q9XIA9|LACS2_ARATH.TIVSFGEVSSTQK.	81.6	35.2
691.86	550.28	sp|Q9XIA9|LACS2_ARATH.TIVSFGEVSSTQK.	81.6	35.2
691.86	463.25	sp|Q9XIA9|LACS2_ARATH.TIVSFGEVSSTQK.	81.6	35.2
408.75	703.41	sp|Q9XIA9|LACS2_ARATH.ISASGLIR.	60.9	19
408.75	616.38	sp|Q9XIA9|LACS2_ARATH.ISASGLIR.	60.9	19
408.75	545.34	sp|Q9XIA9|LACS2_ARATH.ISASGLIR.	60.9	19
408.75	458.31	sp|Q9XIA9|LACS2_ARATH.ISASGLIR.	60.9	19
408.75	175.12	sp|Q9XIA9|LACS2_ARATH.ISASGLIR.	60.9	19
650.82	990.51	sp|Q9XIA9|LACS2_ARATH.YFLDELNSTAK.	78.6	32.8
650.82	877.43	sp|Q9XIA9|LACS2_ARATH.YFLDELNSTAK.	78.6	32.8
650.82	762.40	sp|Q9XIA9|LACS2_ARATH.YFLDELNSTAK.	78.6	32.8
650.82	633.36	sp|Q9XIA9|LACS2_ARATH.YFLDELNSTAK.	78.6	32.8
650.82	520.27	sp|Q9XIA9|LACS2_ARATH.YFLDELNSTAK.	78.6	32.8
775.90	1229.62	sp|Q9XIA9|LACS2_ARATH.AIHLEPNPFDIER.	87.7	40
775.90	1116.53	sp|Q9XIA9|LACS2_ARATH.AIHLEPNPFDIER.	87.7	40
775.90	987.49	sp|Q9XIA9|LACS2_ARATH.AIHLEPNPFDIER.	87.7	40
775.90	417.25	sp|Q9XIA9|LACS2_ARATH.AIHLEPNPFDIER.	87.7	40
775.90	304.16	sp|Q9XIA9|LACS2_ARATH.AIHLEPNPFDIER.	87.7	40
517.60	679.34	sp|Q9XIA9|LACS2_ARATH.AIHLEPNPFDIER.	68.9	23.1
517.60	532.27	sp|Q9XIA9|LACS2_ARATH.AIHLEPNPFDIER.	68.9	23.1
517.60	417.25	sp|Q9XIA9|LACS2_ARATH.AIHLEPNPFDIER.	68.9	23.1
517.60	304.16	sp|Q9XIA9|LACS2_ARATH.AIHLEPNPFDIER.	68.9	23.1
517.60	175.12	sp|Q9XIA9|LACS2_ARATH.AIHLEPNPFDIER.	68.9	23.1
934.52	819.50	sp|Q9XIA9|LACS2_ARATH.DLITPTFK.	99.2	49
934.52	593.33	sp|Q9XIA9|LACS2_ARATH.DLITPTFK.	99.2	49
934.52	492.28	sp|Q9XIA9|LACS2_ARATH.DLITPTFK.	99.2	49
934.52	395.23	sp|Q9XIA9|LACS2_ARATH.DLITPTFK.	99.2	49
934.52	294.18	sp|Q9XIA9|LACS2_ARATH.DLITPTFK.	99.2	49
611.82	1052.53	sp|Q9XIA9|LACS2_ARATH.GIVDQLYSEAK.	75.7	30.6
611.82	953.46	sp|Q9XIA9|LACS2_ARATH.GIVDQLYSEAK.	75.7	30.6
611.82	710.37	sp|Q9XIA9|LACS2_ARATH.GIVDQLYSEAK.	75.7	30.6
611.82	597.29	sp|Q9XIA9|LACS2_ARATH.GIVDQLYSEAK.	75.7	30.6

611.82	434.22	sp|Q9XIA9|LACS2_ARATH.GIVDQLYSEAK.	75.7	30.6
589.31	1064.54	tr|Q9SLI0|Q9SLI0_ARATH.LPSYEVNSLR.	74.1	29.3
589.31	967.48	tr|Q9SLI0|Q9SLI0_ARATH.LPSYEVNSLR.	74.1	29.3
589.31	880.45	tr|Q9SLI0|Q9SLI0_ARATH.LPSYEVNSLR.	74.1	29.3
589.31	717.39	tr|Q9SLI0|Q9SLI0_ARATH.LPSYEVNSLR.	74.1	29.3
589.31	489.28	tr|Q9SLI0|Q9SLI0_ARATH.LPSYEVNSLR.	74.1	29.3
422.26	730.42	tr|Q9SLI0|Q9SLI0_ARATH.LNVALTGR.	61.9	19.8
422.26	616.38	tr|Q9SLI0|Q9SLI0_ARATH.LNVALTGR.	61.9	19.8
422.26	517.31	tr|Q9SLI0|Q9SLI0_ARATH.LNVALTGR.	61.9	19.8
422.26	446.27	tr|Q9SLI0|Q9SLI0_ARATH.LNVALTGR.	61.9	19.8
422.26	333.19	tr|Q9SLI0|Q9SLI0_ARATH.LNVALTGR.	61.9	19.8
822.45	1217.65	tr|Q9SLI0|Q9SLI0_ARATH.LVVDSLSTNNNINIK.	91.1	42.6
822.45	1017.53	tr|Q9SLI0|Q9SLI0_ARATH.LVVDSLSTNNNINIK.	91.1	42.6
822.45	930.50	tr|Q9SLI0|Q9SLI0_ARATH.LVVDSLSTNNNINIK.	91.1	42.6
822.45	829.45	tr|Q9SLI0|Q9SLI0_ARATH.LVVDSLSTNNNINIK.	91.1	42.6
822.45	374.24	tr|Q9SLI0|Q9SLI0_ARATH.LVVDSLSTNNNINIK.	91.1	42.6
549.83	872.48	sp|Q3E9B8|AB23G_ARATH.ILAVVGPSGTGK.	71.2	27.1
549.83	801.45	sp|Q3E9B8|AB23G_ARATH.ILAVVGPSGTGK.	71.2	27.1
549.83	702.38	sp|Q3E9B8|AB23G_ARATH.ILAVVGPSGTGK.	71.2	27.1
549.83	603.31	sp|Q3E9B8|AB23G_ARATH.ILAVVGPSGTGK.	71.2	27.1
549.83	546.29	sp|Q3E9B8|AB23G_ARATH.ILAVVGPSGTGK.	71.2	27.1
702.35	1104.55	sp|Q3E9B8|AB23G_ARATH.ALDPSSAVLM[+16_0]NNR.	82.3	35.8
702.35	762.39	sp|Q3E9B8|AB23G_ARATH.ALDPSSAVLM[+16_0]NNR.	82.3	35.8
702.35	663.32	sp|Q3E9B8|AB23G_ARATH.ALDPSSAVLM[+16_0]NNR.	82.3	35.8
702.35	599.33	sp|Q3E9B8|AB23G_ARATH.ALDPSSAVLM[+16_0]NNR.	82.3	35.8
702.35	550.24	sp|Q3E9B8|AB23G_ARATH.ALDPSSAVLM[+16_0]NNR.	82.3	35.8
919.48	1302.65	sp|Q3E9B8|AB23G_ARATH.DPPILLLDEPTSGLDSR.	98.1	48.1
919.48	1189.57	sp|Q3E9B8|AB23G_ARATH.DPPILLLDEPTSGLDSR.	98.1	48.1
919.48	1076.49	sp|Q3E9B8|AB23G_ARATH.DPPILLLDEPTSGLDSR.	98.1	48.1
919.48	961.46	sp|Q3E9B8|AB23G_ARATH.DPPILLLDEPTSGLDSR.	98.1	48.1
919.48	832.42	sp|Q3E9B8|AB23G_ARATH.DPPILLLDEPTSGLDSR.	98.1	48.1
878.47	1414.76	sp|Q9SYQ8|CLV1_ARATH.NNLYGQIPEAIGELPK.	95.2	45.8
878.47	1251.69	sp|Q9SYQ8|CLV1_ARATH.NNLYGQIPEAIGELPK.	95.2	45.8
878.47	1066.61	sp|Q9SYQ8|CLV1_ARATH.NNLYGQIPEAIGELPK.	95.2	45.8
878.47	953.53	sp|Q9SYQ8|CLV1_ARATH.NNLYGQIPEAIGELPK.	95.2	45.8
878.47	543.31	sp|Q9SYQ8|CLV1_ARATH.NNLYGQIPEAIGELPK.	95.2	45.8
507.95	741.49	sp|Q9SYQ8|CLV1_ARATH.LDVSDNHLTGLIPK.	68.1	22.8
507.95	628.40	sp|Q9SYQ8|CLV1_ARATH.LDVSDNHLTGLIPK.	68.1	22.8
507.95	527.36	sp|Q9SYQ8|CLV1_ARATH.LDVSDNHLTGLIPK.	68.1	22.8
507.95	244.17	sp|Q9SYQ8|CLV1_ARATH.LDVSDNHLTGLIPK.	68.1	22.8
507.95	147.11	sp|Q9SYQ8|CLV1_ARATH.LDVSDNHLTGLIPK.	68.1	22.8

622.82	969.54	sp|Q9SYQ8|CLV1_ARATH.GSMPNNVDVAIK.	76.5	31.2
622.82	758.44	sp|Q9SYQ8|CLV1_ARATH.GSMPNNVDVAIK.	76.5	31.2
622.82	545.33	sp|Q9SYQ8|CLV1_ARATH.GSMPNNVDVAIK.	76.5	31.2
622.82	430.30	sp|Q9SYQ8|CLV1_ARATH.GSMPNNVDVAIK.	76.5	31.2
622.82	331.23	sp|Q9SYQ8|CLV1_ARATH.GSMPNNVDVAIK.	76.5	31.2
630.82	969.54	sp|Q9SYQ8|CLV1_ARATH.GSM[+16_0]PNNVDVAIK.	77.1	31.7
630.82	545.33	sp|Q9SYQ8|CLV1_ARATH.GSM[+16_0]PNNVDVAIK.	77.1	31.7
630.82	430.30	sp|Q9SYQ8|CLV1_ARATH.GSM[+16_0]PNNVDVAIK.	77.1	31.7
630.82	147.11	sp|Q9SYQ8|CLV1_ARATH.GSM[+16_0]PNNVDVAIK.	77.1	31.7
439.26	764.43	sp|Q9SYQ8|CLV1_ARATH.LLGYVANK.	63.1	20.8
439.26	651.35	sp|Q9SYQ8|CLV1_ARATH.LLGYVANK.	63.1	20.8
439.26	431.26	sp|Q9SYQ8|CLV1_ARATH.LLGYVANK.	63.1	20.8
439.26	332.19	sp|Q9SYQ8|CLV1_ARATH.LLGYVANK.	63.1	20.8
471.78	829.48	sp|C0LGT1|Y5129_ARATH.IPSTIGNLK.	65.5	22.6
471.78	732.43	sp|C0LGT1|Y5129_ARATH.IPSTIGNLK.	65.5	22.6
471.78	645.39	sp|C0LGT1|Y5129_ARATH.IPSTIGNLK.	65.5	22.6
471.78	544.35	sp|C0LGT1|Y5129_ARATH.IPSTIGNLK.	65.5	22.6
471.78	431.26	sp|C0LGT1|Y5129_ARATH.IPSTIGNLK.	65.5	22.6
697.84	1024.49	sp|C0LGT1|Y5129_ARATH.ELQLATDNFSEK.	82	35.5
697.84	911.41	sp|C0LGT1|Y5129_ARATH.ELQLATDNFSEK.	82	35.5
697.84	840.37	sp|C0LGT1|Y5129_ARATH.ELQLATDNFSEK.	82	35.5
697.84	739.33	sp|C0LGT1|Y5129_ARATH.ELQLATDNFSEK.	82	35.5
697.84	363.19	sp|C0LGT1|Y5129_ARATH.ELQLATDNFSEK.	82	35.5
805.88	1134.52	sp|C0LGT1|Y5129_ARATH.LTDFESPGGDAAFQR.	89.9	41.7
805.88	1005.47	sp|C0LGT1|Y5129_ARATH.LTDFESPGGDAAFQR.	89.9	41.7
805.88	918.44	sp|C0LGT1|Y5129_ARATH.LTDFESPGGDAAFQR.	89.9	41.7
805.88	821.39	sp|C0LGT1|Y5129_ARATH.LTDFESPGGDAAFQR.	89.9	41.7
805.88	592.32	sp|C0LGT1|Y5129_ARATH.LTDFESPGGDAAFQR.	89.9	41.7
629.81	1015.52	sp|C0LGT1|Y5129_ARATH.AGDPVLDWETR.	77	31.6
629.81	918.47	sp|C0LGT1|Y5129_ARATH.AGDPVLDWETR.	77	31.6
629.81	819.40	sp|C0LGT1|Y5129_ARATH.AGDPVLDWETR.	77	31.6
629.81	706.32	sp|C0LGT1|Y5129_ARATH.AGDPVLDWETR.	77	31.6
629.81	591.29	sp|C0LGT1|Y5129_ARATH.AGDPVLDWETR.	77	31.6
789.39	1078.58	sp|C0LGT1|Y5129_ARATH.GTM[	88.7	40.7
789.39	965.49	sp|C0LGT1|Y5129_ARATH.GTM[	88.7	40.7
789.39	894.46	sp|C0LGT1|Y5129_ARATH.GTM[	88.7	40.7
789.39	668.36	sp|C0LGT1|Y5129_ARATH.GTM[	88.7	40.7
789.39	392.21	sp|C0LGT1|Y5129_ARATH.GTM[	88.7	40.7
781.39	1078.58	sp|C0LGT1|Y5129_ARATH.GTMGHIAPEYLSTGK.	88.1	40.3
781.39	965.49	sp|C0LGT1|Y5129_ARATH.GTMGHIAPEYLSTGK.	88.1	40.3
781.39	894.46	sp|C0LGT1|Y5129_ARATH.GTMGHIAPEYLSTGK.	88.1	40.3

781.39	668.36	sp|C0LGT1|Y5129_ARATH.GTMGHIAPEYLSTGK.	88.1	40.3
781.39	392.21	sp|C0LGT1|Y5129_ARATH.GTMGHIAPEYLSTGK.	88.1	40.3
890.95	1204.61	sp|Q9FLB0|RH18_ARATH.TGLFSATQTEGVEELAK.	96.1	46.5
890.95	975.50	sp|Q9FLB0|RH18_ARATH.TGLFSATQTEGVEELAK.	96.1	46.5
890.95	745.41	sp|Q9FLB0|RH18_ARATH.TGLFSATQTEGVEELAK.	96.1	46.5
890.95	460.28	sp|Q9FLB0|RH18_ARATH.TGLFSATQTEGVEELAK.	96.1	46.5
890.95	331.23	sp|Q9FLB0|RH18_ARATH.TGLFSATQTEGVEELAK.	96.1	46.5
675.35	933.50	sp|Q9FLB0|RH18_ARATH.LSSEGFTPVEGVK.	80.4	34.2
675.35	876.48	sp|Q9FLB0|RH18_ARATH.LSSEGFTPVEGVK.	80.4	34.2
675.35	729.41	sp|Q9FLB0|RH18_ARATH.LSSEGFTPVEGVK.	80.4	34.2
675.35	628.37	sp|Q9FLB0|RH18_ARATH.LSSEGFTPVEGVK.	80.4	34.2
675.35	303.20	sp|Q9FLB0|RH18_ARATH.LSSEGFTPVEGVK.	80.4	34.2
683.84	1181.58	sp|Q8VYB2|UKL3_ARATH.GQAVDIPNYDFK.	81	34.7
683.84	1110.55	sp|Q8VYB2|UKL3_ARATH.GQAVDIPNYDFK.	81	34.7
683.84	1011.48	sp|Q8VYB2|UKL3_ARATH.GQAVDIPNYDFK.	81	34.7
683.84	896.45	sp|Q8VYB2|UKL3_ARATH.GQAVDIPNYDFK.	81	34.7
683.84	783.37	sp|Q8VYB2|UKL3_ARATH.GQAVDIPNYDFK.	81	34.7
560.79	1007.48	sp|Q8VYB2|UKL3_ARATH.IFVDADADVR.	72	27.7
560.79	860.41	sp|Q8VYB2|UKL3_ARATH.IFVDADADVR.	72	27.7
560.79	761.34	sp|Q8VYB2|UKL3_ARATH.IFVDADADVR.	72	27.7
560.79	646.32	sp|Q8VYB2|UKL3_ARATH.IFVDADADVR.	72	27.7
560.79	274.19	sp|Q8VYB2|UKL3_ARATH.IFVDADADVR.	72	27.7
626.82	1024.53	sp|Q8VYB2|UKL3_ARATH.DIATVLDQYSK.	76.8	31.5
626.82	852.45	sp|Q8VYB2|UKL3_ARATH.DIATVLDQYSK.	76.8	31.5
626.82	753.38	sp|Q8VYB2|UKL3_ARATH.DIATVLDQYSK.	76.8	31.5
626.82	640.29	sp|Q8VYB2|UKL3_ARATH.DIATVLDQYSK.	76.8	31.5
626.82	525.27	sp|Q8VYB2|UKL3_ARATH.DIATVLDQYSK.	76.8	31.5
590.28	981.41	sp|Q8VYB2|UKL3_ARATH.VVPGM[+16_0]GEFGDR.	74.1	29.4
590.28	917.41	sp|Q8VYB2|UKL3_ARATH.VVPGM[+16_0]GEFGDR.	74.1	29.4
590.28	820.36	sp|Q8VYB2|UKL3_ARATH.VVPGM[+16_0]GEFGDR.	74.1	29.4
590.28	680.30	sp|Q8VYB2|UKL3_ARATH.VVPGM[+16_0]GEFGDR.	74.1	29.4
590.28	494.24	sp|Q8VYB2|UKL3_ARATH.VVPGM[+16_0]GEFGDR.	74.1	29.4
764.88	1268.67	tr|Q7XZS3|Q7XZS3_ARATH.MEGVTSYTIDLATK.	86.9	39.3
764.88	1112.58	tr|Q7XZS3|Q7XZS3_ARATH.MEGVTSYTIDLATK.	86.9	39.3
764.88	1011.54	tr|Q7XZS3|Q7XZS3_ARATH.MEGVTSYTIDLATK.	86.9	39.3
764.88	924.50	tr|Q7XZS3|Q7XZS3_ARATH.MEGVTSYTIDLATK.	86.9	39.3
764.88	432.28	tr|Q7XZS3|Q7XZS3_ARATH.MEGVTSYTIDLATK.	86.9	39.3
772.88	1112.58	tr|Q7XZS3|Q7XZS3_ARATH.M[	87.5	39.8
772.88	1011.54	tr|Q7XZS3|Q7XZS3_ARATH.M[	87.5	39.8
772.88	761.44	tr|Q7XZS3|Q7XZS3_ARATH.M[	87.5	39.8
772.88	432.28	tr|Q7XZS3|Q7XZS3_ARATH.M[	87.5	39.8

772.88	319.20	tr|Q7XZS3|Q7XZS3_ARATH.M[	87.5	39.8
621.87	1028.60	tr|Q7XZS3|Q7XZS3_ARATH.ITPVGLVESISK.	76.5	31.2
621.87	832.48	tr|Q7XZS3|Q7XZS3_ARATH.ITPVGLVESISK.	76.5	31.2
621.87	662.37	tr|Q7XZS3|Q7XZS3_ARATH.ITPVGLVESISK.	76.5	31.2
621.87	563.30	tr|Q7XZS3|Q7XZS3_ARATH.ITPVGLVESISK.	76.5	31.2
621.87	434.26	tr|Q7XZS3|Q7XZS3_ARATH.ITPVGLVESISK.	76.5	31.2
523.81	933.53	tr|F4HR96|F4HR96_ARATH.ISLGLSTIDK.	69.3	25.6
523.81	846.49	tr|F4HR96|F4HR96_ARATH.ISLGLSTIDK.	69.3	25.6
523.81	733.41	tr|F4HR96|F4HR96_ARATH.ISLGLSTIDK.	69.3	25.6
523.81	676.39	tr|F4HR96|F4HR96_ARATH.ISLGLSTIDK.	69.3	25.6
523.81	563.30	tr|F4HR96|F4HR96_ARATH.ISLGLSTIDK.	69.3	25.6
842.92	856.53	tr|F4HR96|F4HR96_ARATH.NDQDQNNVALDILGR.	92.6	43.8
842.92	757.46	tr|F4HR96|F4HR96_ARATH.NDQDQNNVALDILGR.	92.6	43.8
842.92	686.42	tr|F4HR96|F4HR96_ARATH.NDQDQNNVALDILGR.	92.6	43.8
842.92	573.34	tr|F4HR96|F4HR96_ARATH.NDQDQNNVALDILGR.	92.6	43.8
842.92	458.31	tr|F4HR96|F4HR96_ARATH.NDQDQNNVALDILGR.	92.6	43.8
704.33	932.45	tr|F4HR96|F4HR96_ARATH.DFAAAVLM[+16_0]HDSSK.	82.5	35.9
704.33	833.38	tr|F4HR96|F4HR96_ARATH.DFAAAVLM[+16_0]HDSSK.	82.5	35.9
704.33	769.38	tr|F4HR96|F4HR96_ARATH.DFAAAVLM[+16_0]HDSSK.	82.5	35.9
704.33	573.26	tr|F4HR96|F4HR96_ARATH.DFAAAVLM[+16_0]HDSSK.	82.5	35.9
704.33	321.18	tr|F4HR96|F4HR96_ARATH.DFAAAVLM[+16_0]HDSSK.	82.5	35.9
696.33	987.49	tr|F4HR96|F4HR96_ARATH.DFAAAVLMHDSSK.	81.9	35.4
696.33	817.39	tr|F4HR96|F4HR96_ARATH.DFAAAVLMHDSSK.	81.9	35.4
696.33	704.30	tr|F4HR96|F4HR96_ARATH.DFAAAVLMHDSSK.	81.9	35.4
696.33	436.20	tr|F4HR96|F4HR96_ARATH.DFAAAVLMHDSSK.	81.9	35.4
696.33	321.18	tr|F4HR96|F4HR96_ARATH.DFAAAVLMHDSSK.	81.9	35.4
620.80	882.43	tr|F4HR96|F4HR96_ARATH.QVMSSGEFVTR.	76.4	31.1
620.80	708.37	tr|F4HR96|F4HR96_ARATH.QVMSSGEFVTR.	76.4	31.1
620.80	522.30	tr|F4HR96|F4HR96_ARATH.QVMSSGEFVTR.	76.4	31.1
620.80	276.17	tr|F4HR96|F4HR96_ARATH.QVMSSGEFVTR.	76.4	31.1
620.80	175.12	tr|F4HR96|F4HR96_ARATH.QVMSSGEFVTR.	76.4	31.1
628.80	1029.47	tr|F4HR96|F4HR96_ARATH.QVM[+16_0]SSGEFVTR.	77	31.6
628.80	965.47	tr|F4HR96|F4HR96_ARATH.QVM[+16_0]SSGEFVTR.	77	31.6
628.80	882.43	tr|F4HR96|F4HR96_ARATH.QVM[+16_0]SSGEFVTR.	77	31.6
628.80	795.40	tr|F4HR96|F4HR96_ARATH.QVM[+16_0]SSGEFVTR.	77	31.6
628.80	522.30	tr|F4HR96|F4HR96_ARATH.QVM[+16_0]SSGEFVTR.	77	31.6
1249.64	936.48	tr|F4HR96|F4HR96_ARATH.DVVATGDLNFAK.	122.2	67
1249.64	865.44	tr|F4HR96|F4HR96_ARATH.DVVATGDLNFAK.	122.2	67
1249.64	592.35	tr|F4HR96|F4HR96_ARATH.DVVATGDLNFAK.	122.2	67
1249.64	479.26	tr|F4HR96|F4HR96_ARATH.DVVATGDLNFAK.	122.2	67
1249.64	365.22	tr|F4HR96|F4HR96_ARATH.DVVATGDLNFAK.	122.2	67

625.32	936.48	tr|F4HR96|F4HR96_ARATH.DVVATGDLNFAK.	76.7	31.4
625.32	865.44	tr|F4HR96|F4HR96_ARATH.DVVATGDLNFAK.	76.7	31.4
625.32	764.39	tr|F4HR96|F4HR96_ARATH.DVVATGDLNFAK.	76.7	31.4
625.32	592.35	tr|F4HR96|F4HR96_ARATH.DVVATGDLNFAK.	76.7	31.4
625.32	479.26	tr|F4HR96|F4HR96_ARATH.DVVATGDLNFAK.	76.7	31.4
734.86	812.43	tr|F4HR96|F4HR96_ARATH.EIGDNGAAVYFNAK.	84.7	37.6
734.86	741.39	tr|F4HR96|F4HR96_ARATH.EIGDNGAAVYFNAK.	84.7	37.6
734.86	642.32	tr|F4HR96|F4HR96_ARATH.EIGDNGAAVYFNAK.	84.7	37.6
734.86	479.26	tr|F4HR96|F4HR96_ARATH.EIGDNGAAVYFNAK.	84.7	37.6
734.86	332.19	tr|F4HR96|F4HR96_ARATH.EIGDNGAAVYFNAK.	84.7	37.6
713.83	1254.57	tr|F4HR96|F4HR96_ARATH.TASGIYEAAWSDR.	83.2	36.4
713.83	997.44	tr|F4HR96|F4HR96_ARATH.TASGIYEAAWSDR.	83.2	36.4
713.83	705.33	tr|F4HR96|F4HR96_ARATH.TASGIYEAAWSDR.	83.2	36.4
713.83	563.26	tr|F4HR96|F4HR96_ARATH.TASGIYEAAWSDR.	83.2	36.4
713.83	377.18	tr|F4HR96|F4HR96_ARATH.TASGIYEAAWSDR.	83.2	36.4
820.39	992.48	sp|Q9FIF3|RS82_ARATH.LDTGNFSWGSEAVTR.	90.9	42.5
820.39	905.45	sp|Q9FIF3|RS82_ARATH.LDTGNFSWGSEAVTR.	90.9	42.5
820.39	719.37	sp|Q9FIF3|RS82_ARATH.LDTGNFSWGSEAVTR.	90.9	42.5
820.39	662.35	sp|Q9FIF3|RS82_ARATH.LDTGNFSWGSEAVTR.	90.9	42.5
820.39	446.27	sp|Q9FIF3|RS82_ARATH.LDTGNFSWGSEAVTR.	90.9	42.5
845.94	1250.61	sp|Q9FIF3|RS82_ARATH.ILDVAYNASNNELVR.	92.8	44
845.94	1179.58	sp|Q9FIF3|RS82_ARATH.ILDVAYNASNNELVR.	92.8	44
845.94	1016.51	sp|Q9FIF3|RS82_ARATH.ILDVAYNASNNELVR.	92.8	44
845.94	902.47	sp|Q9FIF3|RS82_ARATH.ILDVAYNASNNELVR.	92.8	44
845.94	831.43	sp|Q9FIF3|RS82_ARATH.ILDVAYNASNNELVR.	92.8	44
564.30	831.43	sp|Q9FIF3|RS82_ARATH.ILDVAYNASNNELVR.	72.3	24.6
564.30	744.40	sp|Q9FIF3|RS82_ARATH.ILDVAYNASNNELVR.	72.3	24.6
564.30	516.31	sp|Q9FIF3|RS82_ARATH.ILDVAYNASNNELVR.	72.3	24.6
564.30	387.27	sp|Q9FIF3|RS82_ARATH.ILDVAYNASNNELVR.	72.3	24.6
564.30	175.12	sp|Q9FIF3|RS82_ARATH.ILDVAYNASNNELVR.	72.3	24.6
788.37	1052.50	sp|Q9FIF3|RS82_ARATH.ALDSHLEEQFSSGR.	88.6	40.7
788.37	939.42	sp|Q9FIF3|RS82_ARATH.ALDSHLEEQFSSGR.	88.6	40.7
788.37	810.37	sp|Q9FIF3|RS82_ARATH.ALDSHLEEQFSSGR.	88.6	40.7
788.37	553.27	sp|Q9FIF3|RS82_ARATH.ALDSHLEEQFSSGR.	88.6	40.7
788.37	406.20	sp|Q9FIF3|RS82_ARATH.ALDSHLEEQFSSGR.	88.6	40.7
525.92	939.42	sp|Q9FIF3|RS82_ARATH.ALDSHLEEQFSSGR.	69.5	23.4
525.92	681.33	sp|Q9FIF3|RS82_ARATH.ALDSHLEEQFSSGR.	69.5	23.4
525.92	553.27	sp|Q9FIF3|RS82_ARATH.ALDSHLEEQFSSGR.	69.5	23.4
525.92	406.20	sp|Q9FIF3|RS82_ARATH.ALDSHLEEQFSSGR.	69.5	23.4
525.92	319.17	sp|Q9FIF3|RS82_ARATH.ALDSHLEEQFSSGR.	69.5	23.4
819.42	1192.60	sp|Q94AL9|AGT22_ARATH.AGGLFIADEVQSGFAR.	90.9	42.4

819.42	1079.51	sp|Q94AL9|AGT22_ARATH.AGGLFIADEVQSGFAR.	90.9	42.4
819.42	1008.47	sp|Q94AL9|AGT22_ARATH.AGGLFIADEVQSGFAR.	90.9	42.4
819.42	893.45	sp|Q94AL9|AGT22_ARATH.AGGLFIADEVQSGFAR.	90.9	42.4
819.42	537.28	sp|Q94AL9|AGT22_ARATH.AGGLFIADEVQSGFAR.	90.9	42.4
720.36	1198.58	sp|Q94AL9|AGT22_ARATH.LQENAAM[	83.6	36.8
720.36	1069.53	sp|Q94AL9|AGT22_ARATH.LQENAAM[	83.6	36.8
720.36	884.45	sp|Q94AL9|AGT22_ARATH.LQENAAM[	83.6	36.8
720.36	666.38	sp|Q94AL9|AGT22_ARATH.LQENAAM[	83.6	36.8
720.36	567.31	sp|Q94AL9|AGT22_ARATH.LQENAAM[	83.6	36.8
712.37	1182.58	sp|Q94AL9|AGT22_ARATH.LQENAAMVGSYLK.	83	36.3
712.37	868.46	sp|Q94AL9|AGT22_ARATH.LQENAAMVGSYLK.	83	36.3
712.37	797.42	sp|Q94AL9|AGT22_ARATH.LQENAAMVGSYLK.	83	36.3
712.37	666.38	sp|Q94AL9|AGT22_ARATH.LQENAAMVGSYLK.	83	36.3
712.37	567.31	sp|Q94AL9|AGT22_ARATH.LQENAAMVGSYLK.	83	36.3
650.64	1210.64	sp|O22967|DOF23_ARATH.NEEETHPPEQEATIAVR.	78.5	27.3
650.64	630.39	sp|O22967|DOF23_ARATH.NEEETHPPEQEATIAVR.	78.5	27.3
650.64	559.36	sp|O22967|DOF23_ARATH.NEEETHPPEQEATIAVR.	78.5	27.3
650.64	458.31	sp|O22967|DOF23_ARATH.NEEETHPPEQEATIAVR.	78.5	27.3
650.64	345.22	sp|O22967|DOF23_ARATH.NEEETHPPEQEATIAVR.	78.5	27.3
644.84	991.46	sp|O22967|DOF23_ARATH.VVVGM[+16_0]LGDGNGVR.	78.1	32.5
644.84	674.32	sp|O22967|DOF23_ARATH.VVVGM[+16_0]LGDGNGVR.	78.1	32.5
644.84	502.27	sp|O22967|DOF23_ARATH.VVVGM[+16_0]LGDGNGVR.	78.1	32.5
644.84	331.21	sp|O22967|DOF23_ARATH.VVVGM[+16_0]LGDGNGVR.	78.1	32.5
644.84	175.12	sp|O22967|DOF23_ARATH.VVVGM[+16_0]LGDGNGVR.	78.1	32.5
611.31	1007.52	sp|Q9M0G2|C3H49_ARATH.VDSFDVSSPIR.	75.7	30.6
611.31	773.42	sp|Q9M0G2|C3H49_ARATH.VDSFDVSSPIR.	75.7	30.6
611.31	658.39	sp|Q9M0G2|C3H49_ARATH.VDSFDVSSPIR.	75.7	30.6
611.31	559.32	sp|Q9M0G2|C3H49_ARATH.VDSFDVSSPIR.	75.7	30.6
611.31	472.29	sp|Q9M0G2|C3H49_ARATH.VDSFDVSSPIR.	75.7	30.6
937.48	1214.58	sp|Q9M0G2|C3H49_ARATH.AFQLSISPVSGSPPM[+16_0]SPR.	99.5	49.2
937.48	1127.55	sp|Q9M0G2|C3H49_ARATH.AFQLSISPVSGSPPM[+16_0]SPR.	99.5	49.2
937.48	1063.55	sp|Q9M0G2|C3H49_ARATH.AFQLSISPVSGSPPM[+16_0]SPR.	99.5	49.2
937.48	700.34	sp|Q9M0G2|C3H49_ARATH.AFQLSISPVSGSPPM[+16_0]SPR.	99.5	49.2
937.48	636.35	sp|Q9M0G2|C3H49_ARATH.AFQLSISPVSGSPPM[+16_0]SPR.	99.5	49.2
819.40	933.48	sp|Q9M0G2|C3H49_ARATH.SLGSC[+57_0]SINDVVPSFR.	90.9	42.4
819.40	704.41	sp|Q9M0G2|C3H49_ARATH.SLGSC[+57_0]SINDVVPSFR.	90.9	42.4
819.40	605.34	sp|Q9M0G2|C3H49_ARATH.SLGSC[+57_0]SINDVVPSFR.	90.9	42.4
819.40	506.27	sp|Q9M0G2|C3H49_ARATH.SLGSC[+57_0]SINDVVPSFR.	90.9	42.4
819.40	322.19	sp|Q9M0G2|C3H49_ARATH.SLGSC[+57_0]SINDVVPSFR.	90.9	42.4

813.91	963.53	sp|Q9LPM9|BCAT6_ARATH.SAGFSDVLFLDAATGR.	90.5	42.1
813.91	850.44	sp|Q9LPM9|BCAT6_ARATH.SAGFSDVLFLDAATGR.	90.5	42.1
813.91	475.26	sp|Q9LPM9|BCAT6_ARATH.SAGFSDVLFLDAATGR.	90.5	42.1
813.91	404.23	sp|Q9LPM9|BCAT6_ARATH.SAGFSDVLFLDAATGR.	90.5	42.1
813.91	333.19	sp|Q9LPM9|BCAT6_ARATH.SAGFSDVLFLDAATGR.	90.5	42.1
934.02	1295.73	sp|Q9LPM9|BCAT6_ARATH.GNIVSTPPTSGTILPGVTR.	99.2	49
934.02	1198.68	sp|Q9LPM9|BCAT6_ARATH.GNIVSTPPTSGTILPGVTR.	99.2	49
934.02	913.55	sp|Q9LPM9|BCAT6_ARATH.GNIVSTPPTSGTILPGVTR.	99.2	49
934.02	642.39	sp|Q9LPM9|BCAT6_ARATH.GNIVSTPPTSGTILPGVTR.	99.2	49
934.02	529.31	sp|Q9LPM9|BCAT6_ARATH.GNIVSTPPTSGTILPGVTR.	99.2	49
594.81	886.50	sp|A0MFH4|LOR16_ARATH.SSQTVDPVLSR.	74.5	29.6
594.81	785.45	sp|A0MFH4|LOR16_ARATH.SSQTVDPVLSR.	74.5	29.6
594.81	686.38	sp|A0MFH4|LOR16_ARATH.SSQTVDPVLSR.	74.5	29.6
594.81	571.36	sp|A0MFH4|LOR16_ARATH.SSQTVDPVLSR.	74.5	29.6
594.81	262.15	sp|A0MFH4|LOR16_ARATH.SSQTVDPVLSR.	74.5	29.6
600.32	913.55	sp|A0MFH4|LOR16_ARATH.NGDGNDLLLIR.	74.9	30
600.32	627.46	sp|A0MFH4|LOR16_ARATH.NGDGNDLLLIR.	74.9	30
600.32	514.37	sp|A0MFH4|LOR16_ARATH.NGDGNDLLLIR.	74.9	30
600.32	401.29	sp|A0MFH4|LOR16_ARATH.NGDGNDLLLIR.	74.9	30
600.32	175.12	sp|A0MFH4|LOR16_ARATH.NGDGNDLLLIR.	74.9	30
642.82	1066.56	tr|Q9C9L7|Q9C9L7_ARATH.M[+16_0]AETTTVTSSLK.	78	32.4
642.82	937.52	tr|Q9C9L7|Q9C9L7_ARATH.M[+16_0]AETTTVTSSLK.	78	32.4
642.82	735.42	tr|Q9C9L7|Q9C9L7_ARATH.M[+16_0]AETTTVTSSLK.	78	32.4
642.82	634.38	tr|Q9C9L7|Q9C9L7_ARATH.M[+16_0]AETTTVTSSLK.	78	32.4
642.82	535.31	tr|Q9C9L7|Q9C9L7_ARATH.M[+16_0]AETTTVTSSLK.	78	32.4
634.82	1066.56	tr|Q9C9L7|Q9C9L7_ARATH.MAETTTVTSSLK.	77.4	31.9
634.82	937.52	tr|Q9C9L7|Q9C9L7_ARATH.MAETTTVTSSLK.	77.4	31.9
634.82	836.47	tr|Q9C9L7|Q9C9L7_ARATH.MAETTTVTSSLK.	77.4	31.9
634.82	735.42	tr|Q9C9L7|Q9C9L7_ARATH.MAETTTVTSSLK.	77.4	31.9
634.82	535.31	tr|Q9C9L7|Q9C9L7_ARATH.MAETTTVTSSLK.	77.4	31.9
705.86	1096.55	tr|F4JI53|F4JI53_ARATH.SNIASTNMFQIGK.	82.6	36
705.86	1025.51	tr|F4JI53|F4JI53_ARATH.SNIASTNMFQIGK.	82.6	36
705.86	938.48	tr|F4JI53|F4JI53_ARATH.SNIASTNMFQIGK.	82.6	36
705.86	837.43	tr|F4JI53|F4JI53_ARATH.SNIASTNMFQIGK.	82.6	36
705.86	317.22	tr|F4JI53|F4JI53_ARATH.SNIASTNMFQIGK.	82.6	36
713.85	1112.54	tr|F4JI53|F4JI53_ARATH.SNIASTNM[+16_0]FQIGK.	83.2	36.4
713.85	1041.50	tr|F4JI53|F4JI53_ARATH.SNIASTNM[+16_0]FQIGK.	83.2	36.4
713.85	977.51	tr|F4JI53|F4JI53_ARATH.SNIASTNM[+16_0]FQIGK.	83.2	36.4
713.85	954.47	tr|F4JI53|F4JI53_ARATH.SNIASTNM[+16_0]FQIGK.	83.2	36.4
713.85	317.22	tr|F4JI53|F4JI53_ARATH.SNIASTNM[+16_0]FQIGK.	83.2	36.4
572.34	860.48	tr|F4JI53|F4JI53_ARATH.VALITGGASGIGK.	72.8	28.4

572.34	747.40	tr|F4JI53|F4JI53_ARATH.VALITGGASGIGK.	72.8	28.4
572.34	646.35	tr|F4JI53|F4JI53_ARATH.VALITGGASGIGK.	72.8	28.4
572.34	589.33	tr|F4JI53|F4JI53_ARATH.VALITGGASGIGK.	72.8	28.4
572.34	461.27	tr|F4JI53|F4JI53_ARATH.VALITGGASGIGK.	72.8	28.4
661.89	1110.63	tr|F4JI53|F4JI53_ARATH.VIIADIQPQIGR.	79.4	33.5
661.89	997.54	tr|F4JI53|F4JI53_ARATH.VIIADIQPQIGR.	79.4	33.5
661.89	926.51	tr|F4JI53|F4JI53_ARATH.VIIADIQPQIGR.	79.4	33.5
661.89	698.39	tr|F4JI53|F4JI53_ARATH.VIIADIQPQIGR.	79.4	33.5
661.89	570.34	tr|F4JI53|F4JI53_ARATH.VIIADIQPQIGR.	79.4	33.5
836.94	1177.61	tr|F4JI53|F4JI53_ARATH.TPPSIVDLDLNVFDK.	92.1	43.4
836.94	1078.54	tr|F4JI53|F4JI53_ARATH.TPPSIVDLDLNVFDK.	92.1	43.4
836.94	850.43	tr|F4JI53|F4JI53_ARATH.TPPSIVDLDLNVFDK.	92.1	43.4
836.94	735.40	tr|F4JI53|F4JI53_ARATH.TPPSIVDLDLNVFDK.	92.1	43.4
836.94	409.21	tr|F4JI53|F4JI53_ARATH.TPPSIVDLDLNVFDK.	92.1	43.4
407.76	656.45	tr|F4JI53|F4JI53_ARATH.SAVIGIVR.	60.8	19
407.76	557.38	tr|F4JI53|F4JI53_ARATH.SAVIGIVR.	60.8	19
407.76	444.29	tr|F4JI53|F4JI53_ARATH.SAVIGIVR.	60.8	19
407.76	387.27	tr|F4JI53|F4JI53_ARATH.SAVIGIVR.	60.8	19
407.76	175.12	tr|F4JI53|F4JI53_ARATH.SAVIGIVR.	60.8	19
615.82	1016.50	tr|F4JI53|F4JI53_ARATH.TLDFPAPDQVK.	76	30.8
615.82	901.48	tr|F4JI53|F4JI53_ARATH.TLDFPAPDQVK.	76	30.8
615.82	754.41	tr|F4JI53|F4JI53_ARATH.TLDFPAPDQVK.	76	30.8
615.82	586.32	tr|F4JI53|F4JI53_ARATH.TLDFPAPDQVK.	76	30.8
615.82	374.24	tr|F4JI53|F4JI53_ARATH.TLDFPAPDQVK.	76	30.8
475.27	765.45	tr|F4JSV2|F4JSV2_ARATH.SPASFSLLK.	65.8	22.8
475.27	694.41	tr|F4JSV2|F4JSV2_ARATH.SPASFSLLK.	65.8	22.8
475.27	607.38	tr|F4JSV2|F4JSV2_ARATH.SPASFSLLK.	65.8	22.8
475.27	460.31	tr|F4JSV2|F4JSV2_ARATH.SPASFSLLK.	65.8	22.8
475.27	147.11	tr|F4JSV2|F4JSV2_ARATH.SPASFSLLK.	65.8	22.8
852.93	969.57	tr|F4JSV2|F4JSV2_ARATH.VYNDDEPLISSPISR.	93.3	44.4
852.93	759.44	tr|F4JSV2|F4JSV2_ARATH.VYNDDEPLISSPISR.	93.3	44.4
852.93	646.35	tr|F4JSV2|F4JSV2_ARATH.VYNDDEPLISSPISR.	93.3	44.4
852.93	559.32	tr|F4JSV2|F4JSV2_ARATH.VYNDDEPLISSPISR.	93.3	44.4
852.93	472.29	tr|F4JSV2|F4JSV2_ARATH.VYNDDEPLISSPISR.	93.3	44.4
712.87	1057.59	tr|F4JSV2|F4JSV2_ARATH.GFYVNTPSPLTTK.	83.1	36.4
712.87	958.52	tr|F4JSV2|F4JSV2_ARATH.GFYVNTPSPLTTK.	83.1	36.4
712.87	844.48	tr|F4JSV2|F4JSV2_ARATH.GFYVNTPSPLTTK.	83.1	36.4
712.87	743.43	tr|F4JSV2|F4JSV2_ARATH.GFYVNTPSPLTTK.	83.1	36.4
712.87	559.34	tr|F4JSV2|F4JSV2_ARATH.GFYVNTPSPLTTK.	83.1	36.4
709.35	1157.58	tr|F4JSV2|F4JSV2_ARATH.M[+16_0]LTDSVTGHVDVK.	82.8	36.2
709.35	1056.53	tr|F4JSV2|F4JSV2_ARATH.M[+16_0]LTDSVTGHVDVK.	82.8	36.2

709.35	941.51	tr|F4JSV2|F4JSV2_ARATH.M[+16_0]LTDSVTGHVDVK.	82.8	36.2
709.35	854.47	tr|F4JSV2|F4JSV2_ARATH.M[+16_0]LTDSVTGHVDVK.	82.8	36.2
709.35	755.40	tr|F4JSV2|F4JSV2_ARATH.M[+16_0]LTDSVTGHVDVK.	82.8	36.2
586.84	972.55	tr|F4JSV2|F4JSV2_ARATH.LSSEAAIVAVGR.	73.9	29.2
586.84	614.40	tr|F4JSV2|F4JSV2_ARATH.LSSEAAIVAVGR.	73.9	29.2
586.84	501.31	tr|F4JSV2|F4JSV2_ARATH.LSSEAAIVAVGR.	73.9	29.2
586.84	402.25	tr|F4JSV2|F4JSV2_ARATH.LSSEAAIVAVGR.	73.9	29.2
586.84	331.21	tr|F4JSV2|F4JSV2_ARATH.LSSEAAIVAVGR.	73.9	29.2
579.28	857.44	tr|F4JSV2|F4JSV2_ARATH.GNETYSVLM[+16_0]K.	73.3	28.8
579.28	756.40	tr|F4JSV2|F4JSV2_ARATH.GNETYSVLM[+16_0]K.	73.3	28.8
579.28	593.33	tr|F4JSV2|F4JSV2_ARATH.GNETYSVLM[+16_0]K.	73.3	28.8
579.28	529.33	tr|F4JSV2|F4JSV2_ARATH.GNETYSVLM[+16_0]K.	73.3	28.8
579.28	407.23	tr|F4JSV2|F4JSV2_ARATH.GNETYSVLM[+16_0]K.	73.3	28.8
657.66	922.46	tr|F4JSV2|F4JSV2_ARATH.NSAHQAQLAQPDFVTSTR.	79.1	27.5
657.66	825.41	tr|F4JSV2|F4JSV2_ARATH.NSAHQAQLAQPDFVTSTR.	79.1	27.5
657.66	710.38	tr|F4JSV2|F4JSV2_ARATH.NSAHQAQLAQPDFVTSTR.	79.1	27.5
657.66	563.31	tr|F4JSV2|F4JSV2_ARATH.NSAHQAQLAQPDFVTSTR.	79.1	27.5
657.66	464.25	tr|F4JSV2|F4JSV2_ARATH.NSAHQAQLAQPDFVTSTR.	79.1	27.5
676.33	1139.50	tr|F4JSV2|F4JSV2_ARATH.LVEVNDYSGAER.	80.4	34.3
676.33	1010.45	tr|F4JSV2|F4JSV2_ARATH.LVEVNDYSGAER.	80.4	34.3
676.33	911.39	tr|F4JSV2|F4JSV2_ARATH.LVEVNDYSGAER.	80.4	34.3
676.33	682.32	tr|F4JSV2|F4JSV2_ARATH.LVEVNDYSGAER.	80.4	34.3
676.33	519.25	tr|F4JSV2|F4JSV2_ARATH.LVEVNDYSGAER.	80.4	34.3
600.81	901.47	tr|F4JSV2|F4JSV2_ARATH.GLEAELADLNR.	74.9	30
600.81	830.44	tr|F4JSV2|F4JSV2_ARATH.GLEAELADLNR.	74.9	30
600.81	588.31	tr|F4JSV2|F4JSV2_ARATH.GLEAELADLNR.	74.9	30
600.81	517.27	tr|F4JSV2|F4JSV2_ARATH.GLEAELADLNR.	74.9	30
600.81	402.25	tr|F4JSV2|F4JSV2_ARATH.GLEAELADLNR.	74.9	30
622.82	1028.55	tr|F4JSV2|F4JSV2_ARATH.SEPLTPTSAWR.	76.5	31.2
622.82	931.50	tr|F4JSV2|F4JSV2_ARATH.SEPLTPTSAWR.	76.5	31.2
622.82	818.42	tr|F4JSV2|F4JSV2_ARATH.SEPLTPTSAWR.	76.5	31.2
622.82	717.37	tr|F4JSV2|F4JSV2_ARATH.SEPLTPTSAWR.	76.5	31.2
622.82	519.27	tr|F4JSV2|F4JSV2_ARATH.SEPLTPTSAWR.	76.5	31.2
594.83	962.48	tr|Q9M682|Q9M682_ARATH.ILIQETGEGTK.	74.5	29.6
594.83	849.39	tr|Q9M682|Q9M682_ARATH.ILIQETGEGTK.	74.5	29.6
594.83	721.34	tr|Q9M682|Q9M682_ARATH.ILIQETGEGTK.	74.5	29.6
594.83	592.29	tr|Q9M682|Q9M682_ARATH.ILIQETGEGTK.	74.5	29.6
594.83	305.18	tr|Q9M682|Q9M682_ARATH.ILIQETGEGTK.	74.5	29.6
808.43	1256.66	tr|Q9M682|Q9M682_ARATH.M[+16_0]IVLDLSSINGGAPGR.	90.1	41.8
808.43	1028.55	tr|Q9M682|Q9M682_ARATH.M[+16_0]IVLDLSSINGGAPGR.	90.1	41.8

808.43	915.46	tr|Q9M682|Q9M682_ARATH.M[+16_0]IVLDLSSINGGAPGR.	90.1	41.8
808.43	514.27	tr|Q9M682|Q9M682_ARATH.M[+16_0]IVLDLSSINGGAPGR.	90.1	41.8
808.43	329.19	tr|Q9M682|Q9M682_ARATH.M[+16_0]IVLDLSSINGGAPGR.	90.1	41.8
491.31	868.53	tr|Q8RWL5|Q8RWL5_ARATH.LPLIVPSSR.	66.9	23.7
491.31	771.47	tr|Q8RWL5|Q8RWL5_ARATH.LPLIVPSSR.	66.9	23.7
491.31	658.39	tr|Q8RWL5|Q8RWL5_ARATH.LPLIVPSSR.	66.9	23.7
491.31	545.30	tr|Q8RWL5|Q8RWL5_ARATH.LPLIVPSSR.	66.9	23.7
491.31	446.24	tr|Q8RWL5|Q8RWL5_ARATH.LPLIVPSSR.	66.9	23.7
770.33	1266.55	tr|Q8RWL5|Q8RWL5_ARATH.SWDGFDDGAEAEIK.	87.3	39.6
770.33	1151.52	tr|Q8RWL5|Q8RWL5_ARATH.SWDGFDDGAEAEIK.	87.3	39.6
770.33	1094.50	tr|Q8RWL5|Q8RWL5_ARATH.SWDGFDDGAEAEIK.	87.3	39.6
770.33	947.43	tr|Q8RWL5|Q8RWL5_ARATH.SWDGFDDGAEAEIK.	87.3	39.6
770.33	717.38	tr|Q8RWL5|Q8RWL5_ARATH.SWDGFDDGAEAEIK.	87.3	39.6
553.80	878.47	tr|Q8RWL5|Q8RWL5_ARATH.EVIFIDSQR.	71.5	27.3
553.80	765.39	tr|Q8RWL5|Q8RWL5_ARATH.EVIFIDSQR.	71.5	27.3
553.80	618.32	tr|Q8RWL5|Q8RWL5_ARATH.EVIFIDSQR.	71.5	27.3
553.80	505.24	tr|Q8RWL5|Q8RWL5_ARATH.EVIFIDSQR.	71.5	27.3
553.80	390.21	tr|Q8RWL5|Q8RWL5_ARATH.EVIFIDSQR.	71.5	27.3
755.37	1167.58	tr|Q8RWL5|Q8RWL5_ARATH.DGAVC[+57_0]FLNNGTITK.	86.2	38.8
755.37	1007.55	tr|Q8RWL5|Q8RWL5_ARATH.DGAVC[+57_0]FLNNGTITK.	86.2	38.8
755.37	860.48	tr|Q8RWL5|Q8RWL5_ARATH.DGAVC[+57_0]FLNNGTITK.	86.2	38.8
755.37	747.40	tr|Q8RWL5|Q8RWL5_ARATH.DGAVC[+57_0]FLNNGTITK.	86.2	38.8
755.37	519.31	tr|Q8RWL5|Q8RWL5_ARATH.DGAVC[+57_0]FLNNGTITK.	86.2	38.8
565.33	959.55	tr|Q9LW35|Q9LW35_ARATH.VAVITGGASGIGK.	72.3	28
565.33	860.48	tr|Q9LW35|Q9LW35_ARATH.VAVITGGASGIGK.	72.3	28
565.33	747.40	tr|Q9LW35|Q9LW35_ARATH.VAVITGGASGIGK.	72.3	28
565.33	646.35	tr|Q9LW35|Q9LW35_ARATH.VAVITGGASGIGK.	72.3	28
565.33	589.33	tr|Q9LW35|Q9LW35_ARATH.VAVITGGASGIGK.	72.3	28
861.98	1222.72	tr|Q9LW35|Q9LW35_ARATH.INC[+57_0]ISPAGIPTPLTLR.	94	44.9
861.98	1135.68	tr|Q9LW35|Q9LW35_ARATH.INC[+57_0]ISPAGIPTPLTLR.	94	44.9
861.98	1038.63	tr|Q9LW35|Q9LW35_ARATH.INC[+57_0]ISPAGIPTPLTLR.	94	44.9
861.98	797.49	tr|Q9LW35|Q9LW35_ARATH.INC[+57_0]ISPAGIPTPLTLR.	94	44.9
861.98	599.39	tr|Q9LW35|Q9LW35_ARATH.INC[+57_0]ISPAGIPTPLTLR.	94	44.9
574.99	797.49	tr|Q9LW35|Q9LW35_ARATH.INC[+57_0]ISPAGIPTPLTLR.	73	24.9
574.99	599.39	tr|Q9LW35|Q9LW35_ARATH.INC[+57_0]ISPAGIPTPLTLR.	73	24.9
574.99	389.25	tr|Q9LW35|Q9LW35_ARATH.INC[+57_0]ISPAGIPTPLTLR.	73	24.9
574.99	175.12	tr|Q9LW35|Q9LW35_ARATH.INC[+57_0]ISPAGIPTPLTLR.	73	24.9

814.45	1128.66	tr|Q9LW35|Q9LW35_ARATH.EEQLLAIVNATGELK.	90.5	42.2
814.45	1015.58	tr|Q9LW35|Q9LW35_ARATH.EEQLLAIVNATGELK.	90.5	42.2
814.45	944.54	tr|Q9LW35|Q9LW35_ARATH.EEQLLAIVNATGELK.	90.5	42.2
814.45	831.46	tr|Q9LW35|Q9LW35_ARATH.EEQLLAIVNATGELK.	90.5	42.2
814.45	446.26	tr|Q9LW35|Q9LW35_ARATH.EEQLLAIVNATGELK.	90.5	42.2
569.29	995.50	tr|Q9LW35|Q9LW35_ARATH.AALYLASDDAK.	72.6	28.2
569.29	882.42	tr|Q9LW35|Q9LW35_ARATH.AALYLASDDAK.	72.6	28.2
569.29	719.36	tr|Q9LW35|Q9LW35_ARATH.AALYLASDDAK.	72.6	28.2
569.29	606.27	tr|Q9LW35|Q9LW35_ARATH.AALYLASDDAK.	72.6	28.2
569.29	535.24	tr|Q9LW35|Q9LW35_ARATH.AALYLASDDAK.	72.6	28.2
543.26	986.45	sp|Q9C6M2|LHTL6_ARATH.VPDVSYDYK.	70.7	26.7
543.26	889.39	sp|Q9C6M2|LHTL6_ARATH.VPDVSYDYK.	70.7	26.7
543.26	774.37	sp|Q9C6M2|LHTL6_ARATH.VPDVSYDYK.	70.7	26.7
543.26	675.30	sp|Q9C6M2|LHTL6_ARATH.VPDVSYDYK.	70.7	26.7
543.26	310.18	sp|Q9C6M2|LHTL6_ARATH.VPDVSYDYK.	70.7	26.7
563.27	953.45	sp|Q9C6M2|LHTL6_ARATH.ATNPGDFTFR.	72.2	27.8
563.27	839.40	sp|Q9C6M2|LHTL6_ARATH.ATNPGDFTFR.	72.2	27.8
563.27	742.35	sp|Q9C6M2|LHTL6_ARATH.ATNPGDFTFR.	72.2	27.8
563.27	685.33	sp|Q9C6M2|LHTL6_ARATH.ATNPGDFTFR.	72.2	27.8
563.27	570.30	sp|Q9C6M2|LHTL6_ARATH.ATNPGDFTFR.	72.2	27.8
527.28	835.45	sp|Q84JA6|CESA4_ARATH.AFSSTGSVLGK.	69.6	25.8
527.28	748.42	sp|Q84JA6|CESA4_ARATH.AFSSTGSVLGK.	69.6	25.8
527.28	661.39	sp|Q84JA6|CESA4_ARATH.AFSSTGSVLGK.	69.6	25.8
527.28	560.34	sp|Q84JA6|CESA4_ARATH.AFSSTGSVLGK.	69.6	25.8
527.28	317.22	sp|Q84JA6|CESA4_ARATH.AFSSTGSVLGK.	69.6	25.8
716.84	1028.50	sp|Q84JA6|CESA4_ARATH.EGAFDIDGNELPR.	83.4	36.6
716.84	913.47	sp|Q84JA6|CESA4_ARATH.EGAFDIDGNELPR.	83.4	36.6
716.84	800.39	sp|Q84JA6|CESA4_ARATH.EGAFDIDGNELPR.	83.4	36.6
716.84	685.36	sp|Q84JA6|CESA4_ARATH.EGAFDIDGNELPR.	83.4	36.6
716.84	385.26	sp|Q84JA6|CESA4_ARATH.EGAFDIDGNELPR.	83.4	36.6
519.79	782.46	sp|Q8LEE9|FLA12_ARATH.AGQFTVFIR.	69	25.4
519.79	635.39	sp|Q8LEE9|FLA12_ARATH.AGQFTVFIR.	69	25.4
519.79	534.34	sp|Q8LEE9|FLA12_ARATH.AGQFTVFIR.	69	25.4
519.79	435.27	sp|Q8LEE9|FLA12_ARATH.AGQFTVFIR.	69	25.4
519.79	175.12	sp|Q8LEE9|FLA12_ARATH.AGQFTVFIR.	69	25.4
979.40	1034.53	sp|Q8LEE9|FLA12_ARATH.DDSDSSSDDSPADASFALR.	102.5	51.6
979.40	947.49	sp|Q8LEE9|FLA12_ARATH.DDSDSSSDDSPADASFALR.	102.5	51.6
979.40	664.38	sp|Q8LEE9|FLA12_ARATH.DDSDSSSDDSPADASFALR.	102.5	51.6
979.40	593.34	sp|Q8LEE9|FLA12_ARATH.DDSDSSSDDSPADASFALR.	102.5	51.6
979.40	359.24	sp|Q8LEE9|FLA12_ARATH.DDSDSSSDDSPADASFALR.	102.5	51.6
714.36	1168.60	tr|Q9ZT92|Q9ZT92_ARATH.SATGFNPAYVTTAK.	83.2	36.5

714.36	964.51	tr|Q9ZT92|Q9ZT92_ARATH.SATGFNPAYVTTAK.	83.2	36.5
714.36	850.47	tr|Q9ZT92|Q9ZT92_ARATH.SATGFNPAYVTTAK.	83.2	36.5
714.36	519.31	tr|Q9ZT92|Q9ZT92_ARATH.SATGFNPAYVTTAK.	83.2	36.5
714.36	420.25	tr|Q9ZT92|Q9ZT92_ARATH.SATGFNPAYVTTAK.	83.2	36.5
967.55	1253.71	tr|Q9ZT92|Q9ZT92_ARATH.AVSVPVQVPPATVVSEGLGK.	101.7	50.9
967.55	1154.64	tr|Q9ZT92|Q9ZT92_ARATH.AVSVPVQVPPATVVSEGLGK.	101.7	50.9
967.55	689.38	tr|Q9ZT92|Q9ZT92_ARATH.AVSVPVQVPPATVVSEGLGK.	101.7	50.9
967.55	590.31	tr|Q9ZT92|Q9ZT92_ARATH.AVSVPVQVPPATVVSEGLGK.	101.7	50.9
967.55	374.24	tr|Q9ZT92|Q9ZT92_ARATH.AVSVPVQVPPATVVSEGLGK.	101.7	50.9
626.30	1025.43	tr|Q9ZT92|Q9ZT92_ARATH.ILSSDNEGNFR.	76.8	31.4
626.30	938.40	tr|Q9ZT92|Q9ZT92_ARATH.ILSSDNEGNFR.	76.8	31.4
626.30	851.36	tr|Q9ZT92|Q9ZT92_ARATH.ILSSDNEGNFR.	76.8	31.4
626.30	736.34	tr|Q9ZT92|Q9ZT92_ARATH.ILSSDNEGNFR.	76.8	31.4
626.30	493.25	tr|Q9ZT92|Q9ZT92_ARATH.ILSSDNEGNFR.	76.8	31.4
599.77	940.45	sp|F4KCL7|OE64M_ARATH.EEDFGAFLDR.	74.8	29.9
599.77	678.36	sp|F4KCL7|OE64M_ARATH.EEDFGAFLDR.	74.8	29.9
599.77	550.30	sp|F4KCL7|OE64M_ARATH.EEDFGAFLDR.	74.8	29.9
599.77	403.23	sp|F4KCL7|OE64M_ARATH.EEDFGAFLDR.	74.8	29.9
599.77	175.12	sp|F4KCL7|OE64M_ARATH.EEDFGAFLDR.	74.8	29.9
994.52	681.36	sp|F4KCL7|OE64M_ARATH.AIENLSGYK.	103.6	52.4
994.52	567.31	sp|F4KCL7|OE64M_ARATH.AIENLSGYK.	103.6	52.4
994.52	454.23	sp|F4KCL7|OE64M_ARATH.AIENLSGYK.	103.6	52.4
994.52	367.20	sp|F4KCL7|OE64M_ARATH.AIENLSGYK.	103.6	52.4
994.52	310.18	sp|F4KCL7|OE64M_ARATH.AIENLSGYK.	103.6	52.4
547.30	859.49	sp|F4KCL7|OE64M_ARATH.FSNDVVTALK.	71	26.9
547.30	745.45	sp|F4KCL7|OE64M_ARATH.FSNDVVTALK.	71	26.9
547.30	630.42	sp|F4KCL7|OE64M_ARATH.FSNDVVTALK.	71	26.9
547.30	531.35	sp|F4KCL7|OE64M_ARATH.FSNDVVTALK.	71	26.9
547.30	432.28	sp|F4KCL7|OE64M_ARATH.FSNDVVTALK.	71	26.9
844.96	1062.59	sp|F4KCL7|OE64M_ARATH.EDGILVIPTVADPPPR.	92.7	43.9
844.96	949.51	sp|F4KCL7|OE64M_ARATH.EDGILVIPTVADPPPR.	92.7	43.9
844.96	466.28	sp|F4KCL7|OE64M_ARATH.EDGILVIPTVADPPPR.	92.7	43.9
844.96	369.22	sp|F4KCL7|OE64M_ARATH.EDGILVIPTVADPPPR.	92.7	43.9
497.25	793.38	sp|F4KCL7|OE64M_ARATH.SLNEFLDR.	67.4	24.1
497.25	550.30	sp|F4KCL7|OE64M_ARATH.SLNEFLDR.	67.4	24.1
497.25	403.23	sp|F4KCL7|OE64M_ARATH.SLNEFLDR.	67.4	24.1
497.25	290.15	sp|F4KCL7|OE64M_ARATH.SLNEFLDR.	67.4	24.1
497.25	175.12	sp|F4KCL7|OE64M_ARATH.SLNEFLDR.	67.4	24.1
752.88	1134.56	sp|Q9LW86|SUT34_ARATH.VGDVFFPDDPLQR.	86	38.6

752.88	987.49	sp|Q9LW86|SUT34_ARATH.VGDVFFPDDPLQR.	86	38.6
752.88	840.42	sp|Q9LW86|SUT34_ARATH.VGDVFFPDDPLQR.	86	38.6
752.88	628.34	sp|Q9LW86|SUT34_ARATH.VGDVFFPDDPLQR.	86	38.6
752.88	513.31	sp|Q9LW86|SUT34_ARATH.VGDVFFPDDPLQR.	86	38.6
571.34	858.48	sp|Q9LW86|SUT34_ARATH.GLLGIVHFTGK.	72.8	28.3
571.34	688.38	sp|Q9LW86|SUT34_ARATH.GLLGIVHFTGK.	72.8	28.3
571.34	589.31	sp|Q9LW86|SUT34_ARATH.GLLGIVHFTGK.	72.8	28.3
571.34	452.25	sp|Q9LW86|SUT34_ARATH.GLLGIVHFTGK.	72.8	28.3
571.34	305.18	sp|Q9LW86|SUT34_ARATH.GLLGIVHFTGK.	72.8	28.3
440.92	664.41	sp|Q9LW86|SUT34_ARATH.THAISFIGHLPK.	63.3	20.8
440.92	551.33	sp|Q9LW86|SUT34_ARATH.THAISFIGHLPK.	63.3	20.8
440.92	494.31	sp|Q9LW86|SUT34_ARATH.THAISFIGHLPK.	63.3	20.8
440.92	357.25	sp|Q9LW86|SUT34_ARATH.THAISFIGHLPK.	63.3	20.8
440.92	244.17	sp|Q9LW86|SUT34_ARATH.THAISFIGHLPK.	63.3	20.8
453.26	806.44	tr|Q8VY59|Q8VY59_ARATH.VGDQIVFK.	64.2	21.6
453.26	749.42	tr|Q8VY59|Q8VY59_ARATH.VGDQIVFK.	64.2	21.6
453.26	506.33	tr|Q8VY59|Q8VY59_ARATH.VGDQIVFK.	64.2	21.6
453.26	393.25	tr|Q8VY59|Q8VY59_ARATH.VGDQIVFK.	64.2	21.6
453.26	294.18	tr|Q8VY59|Q8VY59_ARATH.VGDQIVFK.	64.2	21.6
707.82	1180.56	tr|B9DGC0|B9DGC0_ARATH.SM[+16_0]FPPFESAETR.	82.7	36.1
707.82	1033.49	tr|B9DGC0|B9DGC0_ARATH.SM[+16_0]FPPFESAETR.	82.7	36.1
707.82	936.44	tr|B9DGC0|B9DGC0_ARATH.SM[+16_0]FPPFESAETR.	82.7	36.1
707.82	692.32	tr|B9DGC0|B9DGC0_ARATH.SM[+16_0]FPPFESAETR.	82.7	36.1
707.82	563.28	tr|B9DGC0|B9DGC0_ARATH.SM[+16_0]FPPFESAETR.	82.7	36.1
702.87	1061.57	tr|B9DGC0|B9DGC0_ARATH.TELLIQM[+16_0]DGLQK.	82.4	35.8
702.87	948.48	tr|B9DGC0|B9DGC0_ARATH.TELLIQM[+16_0]DGLQK.	82.4	35.8
702.87	884.48	tr|B9DGC0|B9DGC0_ARATH.TELLIQM[+16_0]DGLQK.	82.4	35.8
702.87	835.40	tr|B9DGC0|B9DGC0_ARATH.TELLIQM[+16_0]DGLQK.	82.4	35.8
702.87	445.28	tr|B9DGC0|B9DGC0_ARATH.TELLIQM[+16_0]DGLQK.	82.4	35.8
694.88	932.49	tr|B9DGC0|B9DGC0_ARATH.TELLIQMDGLQK.	81.8	35.3
694.88	819.40	tr|B9DGC0|B9DGC0_ARATH.TELLIQMDGLQK.	81.8	35.3
694.88	691.34	tr|B9DGC0|B9DGC0_ARATH.TELLIQMDGLQK.	81.8	35.3
694.88	560.30	tr|B9DGC0|B9DGC0_ARATH.TELLIQMDGLQK.	81.8	35.3
694.88	445.28	tr|B9DGC0|B9DGC0_ARATH.TELLIQMDGLQK.	81.8	35.3
610.36	993.54	tr|B9DGC0|B9DGC0_ARATH.ILVPLPDPEAR.	75.6	30.5
610.36	894.47	tr|B9DGC0|B9DGC0_ARATH.ILVPLPDPEAR.	75.6	30.5
610.36	684.33	tr|B9DGC0|B9DGC0_ARATH.ILVPLPDPEAR.	75.6	30.5
610.36	472.25	tr|B9DGC0|B9DGC0_ARATH.ILVPLPDPEAR.	75.6	30.5
610.36	246.16	tr|B9DGC0|B9DGC0_ARATH.ILVPLPDPEAR.	75.6	30.5
465.77	716.39	tr|B9DGC0|B9DGC0_ARATH.TLAILEDR.	65.1	22.3
465.77	645.36	tr|B9DGC0|B9DGC0_ARATH.TLAILEDR.	65.1	22.3

465.77	532.27	tr|B9DGC0|B9DGC0_ARATH.TLAILEDR.	65.1	22.3
465.77	290.15	tr|B9DGC0|B9DGC0_ARATH.TLAILEDR.	65.1	22.3
465.77	175.12	tr|B9DGC0|B9DGC0_ARATH.TLAILEDR.	65.1	22.3
619.34	857.44	tr|B9DGC0|B9DGC0_ARATH.IGPILPEDIDR.	76.3	31
619.34	744.35	tr|B9DGC0|B9DGC0_ARATH.IGPILPEDIDR.	76.3	31
619.34	518.26	tr|B9DGC0|B9DGC0_ARATH.IGPILPEDIDR.	76.3	31
619.34	403.23	tr|B9DGC0|B9DGC0_ARATH.IGPILPEDIDR.	76.3	31
619.34	175.12	tr|B9DGC0|B9DGC0_ARATH.IGPILPEDIDR.	76.3	31
650.31	1038.51	tr|B9DGC0|B9DGC0_ARATH.FNDDYGSQILK.	78.5	32.8
650.31	923.48	tr|B9DGC0|B9DGC0_ARATH.FNDDYGSQILK.	78.5	32.8
650.31	808.46	tr|B9DGC0|B9DGC0_ARATH.FNDDYGSQILK.	78.5	32.8
650.31	645.39	tr|B9DGC0|B9DGC0_ARATH.FNDDYGSQILK.	78.5	32.8
650.31	147.11	tr|B9DGC0|B9DGC0_ARATH.FNDDYGSQILK.	78.5	32.8
1320.74	1108.59	sp|Q9LFW3|COBL4_ARATH.IVPSTVFLTTDK.	127.4	71
1320.74	924.50	sp|Q9LFW3|COBL4_ARATH.IVPSTVFLTTDK.	127.4	71
1320.74	823.46	sp|Q9LFW3|COBL4_ARATH.IVPSTVFLTTDK.	127.4	71
1320.74	724.39	sp|Q9LFW3|COBL4_ARATH.IVPSTVFLTTDK.	127.4	71
1320.74	464.24	sp|Q9LFW3|COBL4_ARATH.IVPSTVFLTTDK.	127.4	71
660.87	1108.59	sp|Q9LFW3|COBL4_ARATH.IVPSTVFLTTDK.	79.3	33.4
660.87	1011.54	sp|Q9LFW3|COBL4_ARATH.IVPSTVFLTTDK.	79.3	33.4
660.87	924.50	sp|Q9LFW3|COBL4_ARATH.IVPSTVFLTTDK.	79.3	33.4
660.87	823.46	sp|Q9LFW3|COBL4_ARATH.IVPSTVFLTTDK.	79.3	33.4
660.87	724.39	sp|Q9LFW3|COBL4_ARATH.IVPSTVFLTTDK.	79.3	33.4
431.26	714.45	tr|Q9M2T7|Q9M2T7_ARATH.FGGQIIVK.	62.6	20.3
431.26	657.43	tr|Q9M2T7|Q9M2T7_ARATH.FGGQIIVK.	62.6	20.3
431.26	472.35	tr|Q9M2T7|Q9M2T7_ARATH.FGGQIIVK.	62.6	20.3
431.26	359.27	tr|Q9M2T7|Q9M2T7_ARATH.FGGQIIVK.	62.6	20.3
431.26	147.11	tr|Q9M2T7|Q9M2T7_ARATH.FGGQIIVK.	62.6	20.3
527.36	841.55	tr|Q9M2T7|Q9M2T7_ARATH.VILQAVVALK.	69.6	25.8
527.36	728.47	tr|Q9M2T7|Q9M2T7_ARATH.VILQAVVALK.	69.6	25.8
527.36	600.41	tr|Q9M2T7|Q9M2T7_ARATH.VILQAVVALK.	69.6	25.8
527.36	147.11	tr|Q9M2T7|Q9M2T7_ARATH.VILQAVVALK.	69.6	25.8
636.84	830.50	sp|Q9LK32|Y3721_ARATH.NDNVSILSPSVK.	77.5	32
636.84	743.47	sp|Q9LK32|Y3721_ARATH.NDNVSILSPSVK.	77.5	32
636.84	630.38	sp|Q9LK32|Y3721_ARATH.NDNVSILSPSVK.	77.5	32
636.84	517.30	sp|Q9LK32|Y3721_ARATH.NDNVSILSPSVK.	77.5	32
636.84	430.27	sp|Q9LK32|Y3721_ARATH.NDNVSILSPSVK.	77.5	32
1000.46	1265.65	sp|Q9LK32|Y3721_ARATH.EESGSSSAISTPYLSGANSR.	104.1	52.8
1000.46	1152.56	sp|Q9LK32|Y3721_ARATH.EESGSSSAISTPYLSGANSR.	104.1	52.8
1000.46	1065.53	sp|Q9LK32|Y3721_ARATH.EESGSSSAISTPYLSGANSR.	104.1	52.8
1000.46	964.48	sp|Q9LK32|Y3721_ARATH.EESGSSSAISTPYLSGANSR.	104.1	52.8

1000.46	591.28	sp|Q9LK32|Y3721_ARATH.EESGSSSAISTPYLSGANSR.	104.1	52.8
582.30	929.53	sp|Q9LK32|Y3721_ARATH.M[+16_0]SSETPVVAVK.	73.6	28.9
582.30	842.50	sp|Q9LK32|Y3721_ARATH.M[+16_0]SSETPVVAVK.	73.6	28.9
582.30	713.46	sp|Q9LK32|Y3721_ARATH.M[+16_0]SSETPVVAVK.	73.6	28.9
582.30	612.41	sp|Q9LK32|Y3721_ARATH.M[+16_0]SSETPVVAVK.	73.6	28.9
582.30	317.22	sp|Q9LK32|Y3721_ARATH.M[+16_0]SSETPVVAVK.	73.6	28.9
521.30	897.54	tr|Q9ZQ51|Q9ZQ51_ARATH.GSLVPLNVDK.	69.1	25.4
521.30	784.46	tr|Q9ZQ51|Q9ZQ51_ARATH.GSLVPLNVDK.	69.1	25.4
521.30	685.39	tr|Q9ZQ51|Q9ZQ51_ARATH.GSLVPLNVDK.	69.1	25.4
521.30	588.34	tr|Q9ZQ51|Q9ZQ51_ARATH.GSLVPLNVDK.	69.1	25.4
521.30	475.25	tr|Q9ZQ51|Q9ZQ51_ARATH.GSLVPLNVDK.	69.1	25.4
788.91	1051.49	tr|Q9ZQ51|Q9ZQ51_ARATH.EAVLLTNPSNPM[+16_0]FK.	88.6	40.7
788.91	950.44	tr|Q9ZQ51|Q9ZQ51_ARATH.EAVLLTNPSNPM[+16_0]FK.	88.6	40.7
788.91	836.40	tr|Q9ZQ51|Q9ZQ51_ARATH.EAVLLTNPSNPM[+16_0]FK.	88.6	40.7
788.91	538.27	tr|Q9ZQ51|Q9ZQ51_ARATH.EAVLLTNPSNPM[+16_0]FK.	88.6	40.7
788.91	474.27	tr|Q9ZQ51|Q9ZQ51_ARATH.EAVLLTNPSNPM[+16_0]FK.	88.6	40.7
795.95	1091.61	tr|Q9ZQ51|Q9ZQ51_ARATH.VFGPVLAYLNSVSPK.	89.1	41.1
795.95	978.53	tr|Q9ZQ51|Q9ZQ51_ARATH.VFGPVLAYLNSVSPK.	89.1	41.1
795.95	907.49	tr|Q9ZQ51|Q9ZQ51_ARATH.VFGPVLAYLNSVSPK.	89.1	41.1
795.95	744.43	tr|Q9ZQ51|Q9ZQ51_ARATH.VFGPVLAYLNSVSPK.	89.1	41.1
795.95	331.20	tr|Q9ZQ51|Q9ZQ51_ARATH.VFGPVLAYLNSVSPK.	89.1	41.1
553.32	834.47	tr|Q9ZQ51|Q9ZQ51_ARATH.GTLEGQFLIK.	71.5	27.3
553.32	705.43	tr|Q9ZQ51|Q9ZQ51_ARATH.GTLEGQFLIK.	71.5	27.3
553.32	520.35	tr|Q9ZQ51|Q9ZQ51_ARATH.GTLEGQFLIK.	71.5	27.3
553.32	373.28	tr|Q9ZQ51|Q9ZQ51_ARATH.GTLEGQFLIK.	71.5	27.3
553.32	147.11	tr|Q9ZQ51|Q9ZQ51_ARATH.GTLEGQFLIK.	71.5	27.3
727.38	971.49	tr|Q9ZQ51|Q9ZQ51_ARATH.NGPTLWEIGVPDR.	84.1	37.2
727.38	785.42	tr|Q9ZQ51|Q9ZQ51_ARATH.NGPTLWEIGVPDR.	84.1	37.2
727.38	656.37	tr|Q9ZQ51|Q9ZQ51_ARATH.NGPTLWEIGVPDR.	84.1	37.2
727.38	543.29	tr|Q9ZQ51|Q9ZQ51_ARATH.NGPTLWEIGVPDR.	84.1	37.2
727.38	387.20	tr|Q9ZQ51|Q9ZQ51_ARATH.NGPTLWEIGVPDR.	84.1	37.2
559.30	841.45	tr|Q9ZQ51|Q9ZQ51_ARATH.LYVNPLQDR.	71.9	27.6
559.30	742.38	tr|Q9ZQ51|Q9ZQ51_ARATH.LYVNPLQDR.	71.9	27.6
559.30	628.34	tr|Q9ZQ51|Q9ZQ51_ARATH.LYVNPLQDR.	71.9	27.6
559.30	418.20	tr|Q9ZQ51|Q9ZQ51_ARATH.LYVNPLQDR.	71.9	27.6
559.30	175.12	tr|Q9ZQ51|Q9ZQ51_ARATH.LYVNPLQDR.	71.9	27.6
729.40	1089.55	tr|Q9ZQ51|Q9ZQ51_ARATH.IALASAADSELQIR.	84.3	37.3
729.40	931.48	tr|Q9ZQ51|Q9ZQ51_ARATH.IALASAADSELQIR.	84.3	37.3
729.40	860.45	tr|Q9ZQ51|Q9ZQ51_ARATH.IALASAADSELQIR.	84.3	37.3
729.40	745.42	tr|Q9ZQ51|Q9ZQ51_ARATH.IALASAADSELQIR.	84.3	37.3
729.40	529.35	tr|Q9ZQ51|Q9ZQ51_ARATH.IALASAADSELQIR.	84.3	37.3

486.60	745.42	tr|Q9ZQ51|Q9ZQ51_ARATH.IALASAADSELQIR.	66.6	22.2
486.60	658.39	tr|Q9ZQ51|Q9ZQ51_ARATH.IALASAADSELQIR.	66.6	22.2
486.60	529.35	tr|Q9ZQ51|Q9ZQ51_ARATH.IALASAADSELQIR.	66.6	22.2
486.60	416.26	tr|Q9ZQ51|Q9ZQ51_ARATH.IALASAADSELQIR.	66.6	22.2
486.60	175.12	tr|Q9ZQ51|Q9ZQ51_ARATH.IALASAADSELQIR.	66.6	22.2
628.83	870.47	tr|Q9ZQ51|Q9ZQ51_ARATH.SDAIFTTGFIGK.	77	31.6
628.83	723.40	tr|Q9ZQ51|Q9ZQ51_ARATH.SDAIFTTGFIGK.	77	31.6
628.83	622.36	tr|Q9ZQ51|Q9ZQ51_ARATH.SDAIFTTGFIGK.	77	31.6
628.83	521.31	tr|Q9ZQ51|Q9ZQ51_ARATH.SDAIFTTGFIGK.	77	31.6
628.83	317.22	tr|Q9ZQ51|Q9ZQ51_ARATH.SDAIFTTGFIGK.	77	31.6
732.37	1264.64	tr|Q9SKM9|Q9SKM9_ARATH.AQESDIVSISTGTR.	84.5	37.5
732.37	933.54	tr|Q9SKM9|Q9SKM9_ARATH.AQESDIVSISTGTR.	84.5	37.5
732.37	820.45	tr|Q9SKM9|Q9SKM9_ARATH.AQESDIVSISTGTR.	84.5	37.5
732.37	721.38	tr|Q9SKM9|Q9SKM9_ARATH.AQESDIVSISTGTR.	84.5	37.5
732.37	521.27	tr|Q9SKM9|Q9SKM9_ARATH.AQESDIVSISTGTR.	84.5	37.5
826.91	1216.65	sp|Q42400|AAP1_ARATH.TSM[+16_0]TGTAVGVDVTAAQK.	91.4	42.9
826.91	1058.58	sp|Q42400|AAP1_ARATH.TSM[+16_0]TGTAVGVDVTAAQK.	91.4	42.9
826.91	987.55	sp|Q42400|AAP1_ARATH.TSM[+16_0]TGTAVGVDVTAAQK.	91.4	42.9
826.91	888.48	sp|Q42400|AAP1_ARATH.TSM[+16_0]TGTAVGVDVTAAQK.	91.4	42.9
826.91	346.21	sp|Q42400|AAP1_ARATH.TSM[+16_0]TGTAVGVDVTAAQK.	91.4	42.9
686.88	1058.58	tr|Q9M7Y3|Q9M7Y3_ARATH.LSNISGENIGIAGK.	81.2	34.9
686.88	945.50	tr|Q9M7Y3|Q9M7Y3_ARATH.LSNISGENIGIAGK.	81.2	34.9
686.88	858.47	tr|Q9M7Y3|Q9M7Y3_ARATH.LSNISGENIGIAGK.	81.2	34.9
686.88	445.28	tr|Q9M7Y3|Q9M7Y3_ARATH.LSNISGENIGIAGK.	81.2	34.9
686.88	275.17	tr|Q9M7Y3|Q9M7Y3_ARATH.LSNISGENIGIAGK.	81.2	34.9
1346.69	974.49	sp|Q8H191|PAO4_ARATH.TSAISGLGVGNENK.	129.3	72.5
1346.69	887.46	sp|Q8H191|PAO4_ARATH.TSAISGLGVGNENK.	129.3	72.5
1346.69	717.35	sp|Q8H191|PAO4_ARATH.TSAISGLGVGNENK.	129.3	72.5
1346.69	660.33	sp|Q8H191|PAO4_ARATH.TSAISGLGVGNENK.	129.3	72.5
1346.69	561.26	sp|Q8H191|PAO4_ARATH.TSAISGLGVGNENK.	129.3	72.5
673.85	1087.57	sp|Q8H191|PAO4_ARATH.TSAISGLGVGNENK.	80.2	34.1
673.85	974.49	sp|Q8H191|PAO4_ARATH.TSAISGLGVGNENK.	80.2	34.1
673.85	887.46	sp|Q8H191|PAO4_ARATH.TSAISGLGVGNENK.	80.2	34.1
673.85	717.35	sp|Q8H191|PAO4_ARATH.TSAISGLGVGNENK.	80.2	34.1
673.85	561.26	sp|Q8H191|PAO4_ARATH.TSAISGLGVGNENK.	80.2	34.1
868.92	1442.73	sp|Q8H191|PAO4_ARATH.M[	94.5	45.3
868.92	1159.61	sp|Q8H191|PAO4_ARATH.M[	94.5	45.3
868.92	947.53	sp|Q8H191|PAO4_ARATH.M[	94.5	45.3
868.92	651.38	sp|Q8H191|PAO4_ARATH.M[	94.5	45.3

868.92	488.32	sp|Q8H191|PAO4_ARATH.M[	94.5	45.3
868.92	1442.73	sp|Q8H191|PAO4_ARATH.M[	94.5	45.3
868.92	1159.61	sp|Q8H191|PAO4_ARATH.M[	94.5	45.3
868.92	947.53	sp|Q8H191|PAO4_ARATH.M[	94.5	45.3
868.92	651.38	sp|Q8H191|PAO4_ARATH.M[	94.5	45.3
868.92	488.32	sp|Q8H191|PAO4_ARATH.M[	94.5	45.3
812.39	800.46	tr|Q8S4F6|Q8S4F6_ARATH.EAVSGSNDM[+16_0]TITQVR.	90.3	42
812.39	717.43	tr|Q8S4F6|Q8S4F6_ARATH.EAVSGSNDM[+16_0]TITQVR.	90.3	42
812.39	616.38	tr|Q8S4F6|Q8S4F6_ARATH.EAVSGSNDM[+16_0]TITQVR.	90.3	42
812.39	503.29	tr|Q8S4F6|Q8S4F6_ARATH.EAVSGSNDM[+16_0]TITQVR.	90.3	42
812.39	402.25	tr|Q8S4F6|Q8S4F6_ARATH.EAVSGSNDM[+16_0]TITQVR.	90.3	42
804.39	717.43	tr|Q8S4F6|Q8S4F6_ARATH.EAVSGSNDMTITQVR.	89.8	41.6
804.39	616.38	tr|Q8S4F6|Q8S4F6_ARATH.EAVSGSNDMTITQVR.	89.8	41.6
804.39	503.29	tr|Q8S4F6|Q8S4F6_ARATH.EAVSGSNDMTITQVR.	89.8	41.6
804.39	402.25	tr|Q8S4F6|Q8S4F6_ARATH.EAVSGSNDMTITQVR.	89.8	41.6
804.39	175.12	tr|Q8S4F6|Q8S4F6_ARATH.EAVSGSNDMTITQVR.	89.8	41.6
663.89	956.58	tr|Q8S4F6|Q8S4F6_ARATH.AADLTLVPSAAIGK.	79.5	33.6
663.89	855.53	tr|Q8S4F6|Q8S4F6_ARATH.AADLTLVPSAAIGK.	79.5	33.6
663.89	742.45	tr|Q8S4F6|Q8S4F6_ARATH.AADLTLVPSAAIGK.	79.5	33.6
663.89	643.38	tr|Q8S4F6|Q8S4F6_ARATH.AADLTLVPSAAIGK.	79.5	33.6
663.89	317.22	tr|Q8S4F6|Q8S4F6_ARATH.AADLTLVPSAAIGK.	79.5	33.6
692.88	972.52	tr|Q8S4F6|Q8S4F6_ARATH.DLIAAGATAANQLR.	81.6	35.2
692.88	901.49	tr|Q8S4F6|Q8S4F6_ARATH.DLIAAGATAANQLR.	81.6	35.2
692.88	672.38	tr|Q8S4F6|Q8S4F6_ARATH.DLIAAGATAANQLR.	81.6	35.2
692.88	601.34	tr|Q8S4F6|Q8S4F6_ARATH.DLIAAGATAANQLR.	81.6	35.2
692.88	530.30	tr|Q8S4F6|Q8S4F6_ARATH.DLIAAGATAANQLR.	81.6	35.2
554.26	951.42	tr|Q8S4F6|Q8S4F6_ARATH.GVDSESFNPR.	71.5	27.3
554.26	836.39	tr|Q8S4F6|Q8S4F6_ARATH.GVDSESFNPR.	71.5	27.3
554.26	620.32	tr|Q8S4F6|Q8S4F6_ARATH.GVDSESFNPR.	71.5	27.3
554.26	386.21	tr|Q8S4F6|Q8S4F6_ARATH.GVDSESFNPR.	71.5	27.3
554.26	272.17	tr|Q8S4F6|Q8S4F6_ARATH.GVDSESFNPR.	71.5	27.3
540.79	967.49	tr|Q8S4F6|Q8S4F6_ARATH.IAFIGDGPYK.	70.5	26.6
540.79	896.45	tr|Q8S4F6|Q8S4F6_ARATH.IAFIGDGPYK.	70.5	26.6
540.79	749.38	tr|Q8S4F6|Q8S4F6_ARATH.IAFIGDGPYK.	70.5	26.6
540.79	636.30	tr|Q8S4F6|Q8S4F6_ARATH.IAFIGDGPYK.	70.5	26.6
540.79	464.25	tr|Q8S4F6|Q8S4F6_ARATH.IAFIGDGPYK.	70.5	26.6
453.74	664.38	sp|Q8LAL0|SCO12_ARATH.NQAASFLR.	64.2	21.6
453.74	593.34	sp|Q8LAL0|SCO12_ARATH.NQAASFLR.	64.2	21.6
453.74	522.30	sp|Q8LAL0|SCO12_ARATH.NQAASFLR.	64.2	21.6
453.74	435.27	sp|Q8LAL0|SCO12_ARATH.NQAASFLR.	64.2	21.6
453.74	175.12	sp|Q8LAL0|SCO12_ARATH.NQAASFLR.	64.2	21.6

815.45	1362.73	sp|Q8LAL0|SCO12_ARATH.GPIIGGPFTLVSTENK.	90.6	42.2
815.45	1249.64	sp|Q8LAL0|SCO12_ARATH.GPIIGGPFTLVSTENK.	90.6	42.2
815.45	1192.62	sp|Q8LAL0|SCO12_ARATH.GPIIGGPFTLVSTENK.	90.6	42.2
815.45	1135.60	sp|Q8LAL0|SCO12_ARATH.GPIIGGPFTLVSTENK.	90.6	42.2
815.45	578.28	sp|Q8LAL0|SCO12_ARATH.GPIIGGPFTLVSTENK.	90.6	42.2
603.83	916.48	sp|Q8LAL0|SCO12_ARATH.ILGLTGTASAM[+16_0]R.	75.1	30.2
603.83	810.38	sp|Q8LAL0|SCO12_ARATH.ILGLTGTASAM[+16_0]R.	75.1	30.2
603.83	746.38	sp|Q8LAL0|SCO12_ARATH.ILGLTGTASAM[+16_0]R.	75.1	30.2
603.83	709.33	sp|Q8LAL0|SCO12_ARATH.ILGLTGTASAM[+16_0]R.	75.1	30.2
603.83	645.33	sp|Q8LAL0|SCO12_ARATH.ILGLTGTASAM[+16_0]R.	75.1	30.2
639.83	1002.57	tr|Q9C891|Q9C891_ARATH.EM[+16_0]PIVGGSGLFR.	77.8	32.2
639.83	792.44	tr|Q9C891|Q9C891_ARATH.EM[+16_0]PIVGGSGLFR.	77.8	32.2
639.83	693.37	tr|Q9C891|Q9C891_ARATH.EM[+16_0]PIVGGSGLFR.	77.8	32.2
639.83	636.35	tr|Q9C891|Q9C891_ARATH.EM[+16_0]PIVGGSGLFR.	77.8	32.2
639.83	492.29	tr|Q9C891|Q9C891_ARATH.EM[+16_0]PIVGGSGLFR.	77.8	32.2
612.82	978.53	tr|O48916|O48916_ARATH.M[+16_0]VAQGFTVDLK.	75.8	30.7
612.82	907.49	tr|O48916|O48916_ARATH.M[+16_0]VAQGFTVDLK.	75.8	30.7
612.82	779.43	tr|O48916|O48916_ARATH.M[+16_0]VAQGFTVDLK.	75.8	30.7
612.82	575.34	tr|O48916|O48916_ARATH.M[+16_0]VAQGFTVDLK.	75.8	30.7
612.82	375.22	tr|O48916|O48916_ARATH.M[+16_0]VAQGFTVDLK.	75.8	30.7
597.81	979.52	tr|Q9XI75|Q9XI75_ARATH.NTDVLLGSGYR.	74.7	29.8
597.81	765.43	tr|Q9XI75|Q9XI75_ARATH.NTDVLLGSGYR.	74.7	29.8
597.81	652.34	tr|Q9XI75|Q9XI75_ARATH.NTDVLLGSGYR.	74.7	29.8
597.81	539.26	tr|Q9XI75|Q9XI75_ARATH.NTDVLLGSGYR.	74.7	29.8
597.81	482.24	tr|Q9XI75|Q9XI75_ARATH.NTDVLLGSGYR.	74.7	29.8
557.81	816.46	tr|Q9XI75|Q9XI75_ARATH.AINGLATDLAR.	71.8	27.5
557.81	646.35	tr|Q9XI75|Q9XI75_ARATH.AINGLATDLAR.	71.8	27.5
557.81	575.31	tr|Q9XI75|Q9XI75_ARATH.AINGLATDLAR.	71.8	27.5
557.81	474.27	tr|Q9XI75|Q9XI75_ARATH.AINGLATDLAR.	71.8	27.5
557.81	359.24	tr|Q9XI75|Q9XI75_ARATH.AINGLATDLAR.	71.8	27.5
484.28	741.39	tr|Q9XI75|Q9XI75_ARATH.LITHAGLDK.	66.4	23.3
484.28	640.34	tr|Q9XI75|Q9XI75_ARATH.LITHAGLDK.	66.4	23.3
484.28	503.28	tr|Q9XI75|Q9XI75_ARATH.LITHAGLDK.	66.4	23.3
484.28	432.25	tr|Q9XI75|Q9XI75_ARATH.LITHAGLDK.	66.4	23.3
765.41	1274.69	sp|P41088|CFI1_ARATH.SPASSNPLFLGGAGVR.	86.9	39.4
765.41	986.58	sp|P41088|CFI1_ARATH.SPASSNPLFLGGAGVR.	86.9	39.4
765.41	776.44	sp|P41088|CFI1_ARATH.SPASSNPLFLGGAGVR.	86.9	39.4
765.41	629.37	sp|P41088|CFI1_ARATH.SPASSNPLFLGGAGVR.	86.9	39.4
765.41	516.29	sp|P41088|CFI1_ARATH.SPASSNPLFLGGAGVR.	86.9	39.4
785.39	996.51	sp|P41088|CFI1_ARATH.TTEELTESIPFFR.	88.4	40.5
785.39	895.47	sp|P41088|CFI1_ARATH.TTEELTESIPFFR.	88.4	40.5

785.39	766.42	sp|P41088|CFI1_ARATH.TTEELTESIPFFR.	88.4	40.5
785.39	679.39	sp|P41088|CFI1_ARATH.TTEELTESIPFFR.	88.4	40.5
785.39	566.31	sp|P41088|CFI1_ARATH.TTEELTESIPFFR.	88.4	40.5
678.41	1129.65	sp|P41088|CFI1_ARATH.LLAEAVLESIIGK.	80.6	34.4
678.41	759.46	sp|P41088|CFI1_ARATH.LLAEAVLESIIGK.	80.6	34.4
678.41	517.33	sp|P41088|CFI1_ARATH.LLAEAVLESIIGK.	80.6	34.4
678.41	317.22	sp|P41088|CFI1_ARATH.LLAEAVLESIIGK.	80.6	34.4
678.41	204.13	sp|P41088|CFI1_ARATH.LLAEAVLESIIGK.	80.6	34.4
835.92	1244.59	sp|Q9S818|FL3H_ARATH.AILEEPITFAEM[	92.1	43.4
835.92	1115.54	sp|Q9S818|FL3H_ARATH.AILEEPITFAEM[	92.1	43.4
835.92	1051.55	sp|Q9S818|FL3H_ARATH.AILEEPITFAEM[	92.1	43.4
835.92	657.29	sp|Q9S818|FL3H_ARATH.AILEEPITFAEM[	92.1	43.4
835.92	457.21	sp|Q9S818|FL3H_ARATH.AILEEPITFAEM[	92.1	43.4
827.92	1228.59	sp|Q9S818|FL3H_ARATH.AILEEPITFAEMYK.	91.5	42.9
827.92	1099.55	sp|Q9S818|FL3H_ARATH.AILEEPITFAEMYK.	91.5	42.9
827.92	788.36	sp|Q9S818|FL3H_ARATH.AILEEPITFAEMYK.	91.5	42.9
827.92	641.30	sp|Q9S818|FL3H_ARATH.AILEEPITFAEMYK.	91.5	42.9
827.92	441.22	sp|Q9S818|FL3H_ARATH.AILEEPITFAEMYK.	91.5	42.9
787.86	1376.62	sp|Q96323|LDOX_ARATH.TPSDYIEATSEYAK.	88.6	40.6
787.86	1174.56	sp|Q96323|LDOX_ARATH.TPSDYIEATSEYAK.	88.6	40.6
787.86	898.42	sp|Q96323|LDOX_ARATH.TPSDYIEATSEYAK.	88.6	40.6
787.86	769.37	sp|Q96323|LDOX_ARATH.TPSDYIEATSEYAK.	88.6	40.6
787.86	381.21	sp|Q96323|LDOX_ARATH.TPSDYIEATSEYAK.	88.6	40.6
613.84	1042.55	sp|Q96323|LDOX_ARATH.ALSVGLGLEPDR.	75.9	30.7
613.84	856.45	sp|Q96323|LDOX_ARATH.ALSVGLGLEPDR.	75.9	30.7
613.84	686.35	sp|Q96323|LDOX_ARATH.ALSVGLGLEPDR.	75.9	30.7
613.84	516.24	sp|Q96323|LDOX_ARATH.ALSVGLGLEPDR.	75.9	30.7
613.84	387.20	sp|Q96323|LDOX_ARATH.ALSVGLGLEPDR.	75.9	30.7
1047.02	1261.55	sp|Q96330|FLS1_ARATH.GPTPAIPVVDLSDPDEESVR.	107.4	55.4
1047.02	831.38	sp|Q96330|FLS1_ARATH.GPTPAIPVVDLSDPDEESVR.	107.4	55.4
1047.02	619.30	sp|Q96330|FLS1_ARATH.GPTPAIPVVDLSDPDEESVR.	107.4	55.4
1047.02	490.26	sp|Q96330|FLS1_ARATH.GPTPAIPVVDLSDPDEESVR.	107.4	55.4
1047.02	361.22	sp|Q96330|FLS1_ARATH.GPTPAIPVVDLSDPDEESVR.	107.4	55.4
814.98	1085.66	sp|Q96330|FLS1_ARATH.LSETLLGILSDGLGLK.	90.5	42.2
814.98	972.57	sp|Q96330|FLS1_ARATH.LSETLLGILSDGLGLK.	90.5	42.2
814.98	689.38	sp|Q96330|FLS1_ARATH.LSETLLGILSDGLGLK.	90.5	42.2
814.98	602.35	sp|Q96330|FLS1_ARATH.LSETLLGILSDGLGLK.	90.5	42.2
814.98	487.32	sp|Q96330|FLS1_ARATH.LSETLLGILSDGLGLK.	90.5	42.2
831.44	1182.56	sp|Q96330|FLS1_ARATH.IVGPLPELTGDDNPPK.	91.7	43.1
831.44	956.47	sp|Q96330|FLS1_ARATH.IVGPLPELTGDDNPPK.	91.7	43.1
831.44	843.38	sp|Q96330|FLS1_ARATH.IVGPLPELTGDDNPPK.	91.7	43.1

831.44	455.26	sp|Q96330|FLS1_ARATH.IVGPLPELTGDDNPPK.	91.7	43.1
831.44	341.22	sp|Q96330|FLS1_ARATH.IVGPLPELTGDDNPPK.	91.7	43.1
539.29	1158.59	sp|Q9SEV0|BAN_ARATH.LSGSISFVHVDDLAR.	70.4	23.8
539.29	825.42	sp|Q9SEV0|BAN_ARATH.LSGSISFVHVDDLAR.	70.4	23.8
539.29	589.29	sp|Q9SEV0|BAN_ARATH.LSGSISFVHVDDLAR.	70.4	23.8
539.29	359.24	sp|Q9SEV0|BAN_ARATH.LSGSISFVHVDDLAR.	70.4	23.8
539.29	175.12	sp|Q9SEV0|BAN_ARATH.LSGSISFVHVDDLAR.	70.4	23.8
645.32	977.48	tr|Q94K05|Q94K05_ARATH.NPTNFNVDNVR.	78.2	32.5
645.32	863.44	tr|Q94K05|Q94K05_ARATH.NPTNFNVDNVR.	78.2	32.5
645.32	716.37	tr|Q94K05|Q94K05_ARATH.NPTNFNVDNVR.	78.2	32.5
645.32	503.26	tr|Q94K05|Q94K05_ARATH.NPTNFNVDNVR.	78.2	32.5
645.32	388.23	tr|Q94K05|Q94K05_ARATH.NPTNFNVDNVR.	78.2	32.5
783.90	1150.56	tr|Q94K05|Q94K05_ARATH.VAVFAGGVDTTATETK.	88.3	40.4
783.90	1079.52	tr|Q94K05|Q94K05_ARATH.VAVFAGGVDTTATETK.	88.3	40.4
783.90	1022.50	tr|Q94K05|Q94K05_ARATH.VAVFAGGVDTTATETK.	88.3	40.4
783.90	866.41	tr|Q94K05|Q94K05_ARATH.VAVFAGGVDTTATETK.	88.3	40.4
783.90	478.25	tr|Q94K05|Q94K05_ARATH.VAVFAGGVDTTATETK.	88.3	40.4
591.97	737.38	tr|Q94K05|Q94K05_ARATH.GTVLIHSAEQ[	74.3	25.4
591.97	624.30	tr|Q94K05|Q94K05_ARATH.GTVLIHSAEQ[	74.3	25.4
591.97	495.26	tr|Q94K05|Q94K05_ARATH.GTVLIHSAEQ[	74.3	25.4
591.97	381.21	tr|Q94K05|Q94K05_ARATH.GTVLIHSAEQ[	74.3	25.4
591.97	147.11	tr|Q94K05|Q94K05_ARATH.GTVLIHSAEQ[	74.3	25.4
591.64	994.48	tr|Q94K05|Q94K05_ARATH.GTVLIHSAEQLENYAK.	74.2	25.4
591.64	737.38	tr|Q94K05|Q94K05_ARATH.GTVLIHSAEQLENYAK.	74.2	25.4
591.64	624.30	tr|Q94K05|Q94K05_ARATH.GTVLIHSAEQLENYAK.	74.2	25.4
591.64	495.26	tr|Q94K05|Q94K05_ARATH.GTVLIHSAEQLENYAK.	74.2	25.4
591.64	381.21	tr|Q94K05|Q94K05_ARATH.GTVLIHSAEQLENYAK.	74.2	25.4
608.80	982.49	tr|Q94K05|Q94K05_ARATH.YAESFEFVPK.	75.5	30.4
608.80	853.45	tr|Q94K05|Q94K05_ARATH.YAESFEFVPK.	75.5	30.4
608.80	766.41	tr|Q94K05|Q94K05_ARATH.YAESFEFVPK.	75.5	30.4
608.80	490.30	tr|Q94K05|Q94K05_ARATH.YAESFEFVPK.	75.5	30.4
608.80	244.17	tr|Q94K05|Q94K05_ARATH.YAESFEFVPK.	75.5	30.4
483.92	841.39	sp|Q9SYM5|RHM1_ARATH.GQ[+1_0]VLPIHGDGSNVR.	66.4	22.1
483.92	704.33	sp|Q9SYM5|RHM1_ARATH.GQ[+1_0]VLPIHGDGSNVR.	66.4	22.1
483.92	647.31	sp|Q9SYM5|RHM1_ARATH.GQ[+1_0]VLPIHGDGSNVR.	66.4	22.1
483.92	532.28	sp|Q9SYM5|RHM1_ARATH.GQ[+1_0]VLPIHGDGSNVR.	66.4	22.1
483.92	175.12	sp|Q9SYM5|RHM1_ARATH.GQ[+1_0]VLPIHGDGSNVR.	66.4	22.1
724.88	1051.53	sp|Q9SYM5|RHM1_ARATH.GQVLPIHGDGSNVR.	84	37.1
724.88	841.39	sp|Q9SYM5|RHM1_ARATH.GQVLPIHGDGSNVR.	84	37.1
724.88	704.33	sp|Q9SYM5|RHM1_ARATH.GQVLPIHGDGSNVR.	84	37.1
724.88	647.31	sp|Q9SYM5|RHM1_ARATH.GQVLPIHGDGSNVR.	84	37.1

724.88	532.28	sp|Q9SYM5|RHM1_ARATH.GQVLPIHGDGSNVR.	84	37.1
483.92	841.39	sp|Q9SYM5|RHM1_ARATH.GQ[+1_0]VLPIHGDGSNVR.	66.4	22.1
483.92	704.33	sp|Q9SYM5|RHM1_ARATH.GQ[+1_0]VLPIHGDGSNVR.	66.4	22.1
483.92	647.31	sp|Q9SYM5|RHM1_ARATH.GQ[+1_0]VLPIHGDGSNVR.	66.4	22.1
483.92	532.28	sp|Q9SYM5|RHM1_ARATH.GQ[+1_0]VLPIHGDGSNVR.	66.4	22.1
483.92	175.12	sp|Q9SYM5|RHM1_ARATH.GQ[+1_0]VLPIHGDGSNVR.	66.4	22.1
637.33	794.44	sp|Q9SYM5|RHM1_ARATH.GEVGHVYNIGTK.	77.6	32.1
637.33	695.37	sp|Q9SYM5|RHM1_ARATH.GEVGHVYNIGTK.	77.6	32.1
637.33	532.31	sp|Q9SYM5|RHM1_ARATH.GEVGHVYNIGTK.	77.6	32.1
637.33	418.27	sp|Q9SYM5|RHM1_ARATH.GEVGHVYNIGTK.	77.6	32.1
637.33	305.18	sp|Q9SYM5|RHM1_ARATH.GEVGHVYNIGTK.	77.6	32.1
976.45	1284.59	sp|Q9LZG0|ADK2_ARATH.FLPYM[+16_0]DFVFGNETEAR.	102.3	51.4
976.45	1022.49	sp|Q9LZG0|ADK2_ARATH.FLPYM[+16_0]DFVFGNETEAR.	102.3	51.4
976.45	923.42	sp|Q9LZG0|ADK2_ARATH.FLPYM[+16_0]DFVFGNETEAR.	102.3	51.4
976.45	776.35	sp|Q9LZG0|ADK2_ARATH.FLPYM[+16_0]DFVFGNETEAR.	102.3	51.4
976.45	476.25	sp|Q9LZG0|ADK2_ARATH.FLPYM[+16_0]DFVFGNETEAR.	102.3	51.4
1008.48	1293.56	sp|Q9LD57|PGKH1_ARATH.ADLNVPLDDNQTITDDTR.	104.6	53.2
1008.48	1178.53	sp|Q9LD57|PGKH1_ARATH.ADLNVPLDDNQTITDDTR.	104.6	53.2
1008.48	1063.50	sp|Q9LD57|PGKH1_ARATH.ADLNVPLDDNQTITDDTR.	104.6	53.2
1008.48	607.27	sp|Q9LD57|PGKH1_ARATH.ADLNVPLDDNQTITDDTR.	104.6	53.2
1008.48	391.19	sp|Q9LD57|PGKH1_ARATH.ADLNVPLDDNQTITDDTR.	104.6	53.2
763.45	1169.68	sp|Q9LD57|PGKH1_ARATH.GVSLLLPTDVVVADK.	86.8	39.3
763.45	1056.59	sp|Q9LD57|PGKH1_ARATH.GVSLLLPTDVVVADK.	86.8	39.3
763.45	943.51	sp|Q9LD57|PGKH1_ARATH.GVSLLLPTDVVVADK.	86.8	39.3
763.45	432.25	sp|Q9LD57|PGKH1_ARATH.GVSLLLPTDVVVADK.	86.8	39.3
763.45	333.18	sp|Q9LD57|PGKH1_ARATH.GVSLLLPTDVVVADK.	86.8	39.3
678.37	1079.58	sp|P47999|CYSKP_ARATH.YLSTQLFQSIR.	80.6	34.4
678.37	992.55	sp|P47999|CYSKP_ARATH.YLSTQLFQSIR.	80.6	34.4
678.37	650.36	sp|P47999|CYSKP_ARATH.YLSTQLFQSIR.	80.6	34.4
678.37	503.29	sp|P47999|CYSKP_ARATH.YLSTQLFQSIR.	80.6	34.4
678.37	375.24	sp|P47999|CYSKP_ARATH.YLSTQLFQSIR.	80.6	34.4
741.37	1142.48	sp|P47998|CYSK1_ARATH.LIITM[+16_0]PASM[+16_0]STER.	85.2	38
741.37	1041.43	sp|P47998|CYSK1_ARATH.LIITM[+16_0]PASM[+16_0]STER.	85.2	38
741.37	894.40	sp|P47998|CYSK1_ARATH.LIITM[+16_0]PASM[+16_0]STER.	85.2	38
741.37	830.40	sp|P47998|CYSK1_ARATH.LIITM[+16_0]PASM[+16_0]STER.	85.2	38
741.37	726.31	sp|P47998|CYSK1_ARATH.LIITM[+16_0]PASM[+16_0]STER.	85.2	38

725.38	1223.58	sp|P47998|CYSK1_ARATH.LIITMPASMSTER.	84	37.1
725.38	1110.49	sp|P47998|CYSK1_ARATH.LIITMPASMSTER.	84	37.1
725.38	1009.44	sp|P47998|CYSK1_ARATH.LIITMPASMSTER.	84	37.1
725.38	878.40	sp|P47998|CYSK1_ARATH.LIITMPASMSTER.	84	37.1
725.38	710.31	sp|P47998|CYSK1_ARATH.LIITMPASMSTER.	84	37.1
733.37	1126.49	sp|P47998|CYSK1_ARATH.LIITM[+16_0]PASMSTER.	84.6	37.5
733.37	1062.49	sp|P47998|CYSK1_ARATH.LIITM[+16_0]PASMSTER.	84.6	37.5
733.37	1025.44	sp|P47998|CYSK1_ARATH.LIITM[+16_0]PASMSTER.	84.6	37.5
733.37	878.40	sp|P47998|CYSK1_ARATH.LIITM[+16_0]PASMSTER.	84.6	37.5
733.37	492.24	sp|P47998|CYSK1_ARATH.LIITM[+16_0]PASMSTER.	84.6	37.5
643.34	1009.53	sp|P47998|CYSK1_ARATH.YLSTVLFDATR.	78	32.4
643.34	722.38	sp|P47998|CYSK1_ARATH.YLSTVLFDATR.	78	32.4
643.34	609.30	sp|P47998|CYSK1_ARATH.YLSTVLFDATR.	78	32.4
643.34	462.23	sp|P47998|CYSK1_ARATH.YLSTVLFDATR.	78	32.4
643.34	347.20	sp|P47998|CYSK1_ARATH.YLSTVLFDATR.	78	32.4
521.76	814.41	sp|Q8LPK5|CESA8_ARATH.DIEGNELPR.	69.2	25.5
521.76	685.36	sp|Q8LPK5|CESA8_ARATH.DIEGNELPR.	69.2	25.5
521.76	514.30	sp|Q8LPK5|CESA8_ARATH.DIEGNELPR.	69.2	25.5
521.76	385.26	sp|Q8LPK5|CESA8_ARATH.DIEGNELPR.	69.2	25.5
521.76	272.17	sp|Q8LPK5|CESA8_ARATH.DIEGNELPR.	69.2	25.5
450.75	701.39	sp|Q8LPK5|CESA8_ARATH.AGAENALVR.	64	21.4
450.75	572.35	sp|Q8LPK5|CESA8_ARATH.AGAENALVR.	64	21.4
450.75	458.31	sp|Q8LPK5|CESA8_ARATH.AGAENALVR.	64	21.4
450.75	387.27	sp|Q8LPK5|CESA8_ARATH.AGAENALVR.	64	21.4
450.75	175.12	sp|Q8LPK5|CESA8_ARATH.AGAENALVR.	64	21.4
789.46	1023.57	tr|O82219|O82219_ARATH.LVQTLSPLIPM[+16_0]PPR.	88.7	40.7
789.46	959.57	tr|O82219|O82219_ARATH.LVQTLSPLIPM[+16_0]PPR.	88.7	40.7
789.46	936.53	tr|O82219|O82219_ARATH.LVQTLSPLIPM[+16_0]PPR.	88.7	40.7
789.46	872.54	tr|O82219|O82219_ARATH.LVQTLSPLIPM[+16_0]PPR.	88.7	40.7
789.46	613.31	tr|O82219|O82219_ARATH.LVQTLSPLIPM[+16_0]PPR.	88.7	40.7
781.46	1221.70	tr|O82219|O82219_ARATH.LVQTLSPLIPMPPR.	88.1	40.3
781.46	1007.57	tr|O82219|O82219_ARATH.LVQTLSPLIPMPPR.	88.1	40.3
781.46	920.54	tr|O82219|O82219_ARATH.LVQTLSPLIPMPPR.	88.1	40.3
781.46	597.32	tr|O82219|O82219_ARATH.LVQTLSPLIPMPPR.	88.1	40.3
781.46	369.22	tr|O82219|O82219_ARATH.LVQTLSPLIPMPPR.	88.1	40.3
843.89	1331.59	tr|O04314|O04314_ARATH.GANLWDDGSTHDAVTK.	92.6	43.8
843.89	1145.51	tr|O04314|O04314_ARATH.GANLWDDGSTHDAVTK.	92.6	43.8
843.89	1030.48	tr|O04314|O04314_ARATH.GANLWDDGSTHDAVTK.	92.6	43.8
843.89	915.45	tr|O04314|O04314_ARATH.GANLWDDGSTHDAVTK.	92.6	43.8
843.89	418.27	tr|O04314|O04314_ARATH.GANLWDDGSTHDAVTK.	92.6	43.8
701.37	1017.53	sp|P41376|IF4A1_ARATH.GLDVIQQAQSGTGK.	82.2	35.7

701.37	904.45	sp|P41376|IF4A1_ARATH.GLDVIQQAQSGTGK.	82.2	35.7
701.37	776.39	sp|P41376|IF4A1_ARATH.GLDVIQQAQSGTGK.	82.2	35.7
701.37	648.33	sp|P41376|IF4A1_ARATH.GLDVIQQAQSGTGK.	82.2	35.7
701.37	449.24	sp|P41376|IF4A1_ARATH.GLDVIQQAQSGTGK.	82.2	35.7
762.91	1238.68	sp|Q8L9A9|XTH8_ARATH.TGQPYIIQTNVYK.	86.7	39.2
762.91	978.56	sp|Q8L9A9|XTH8_ARATH.TGQPYIIQTNVYK.	86.7	39.2
762.91	865.48	sp|Q8L9A9|XTH8_ARATH.TGQPYIIQTNVYK.	86.7	39.2
762.91	752.39	sp|Q8L9A9|XTH8_ARATH.TGQPYIIQTNVYK.	86.7	39.2
762.91	624.34	sp|Q8L9A9|XTH8_ARATH.TGQPYIIQTNVYK.	86.7	39.2
449.74	730.38	sp|Q8L9A9|XTH8_ARATH.APFVSSYK.	63.9	21.4
449.74	583.31	sp|Q8L9A9|XTH8_ARATH.APFVSSYK.	63.9	21.4
449.74	484.24	sp|Q8L9A9|XTH8_ARATH.APFVSSYK.	63.9	21.4
449.74	397.21	sp|Q8L9A9|XTH8_ARATH.APFVSSYK.	63.9	21.4
449.74	147.11	sp|Q8L9A9|XTH8_ARATH.APFVSSYK.	63.9	21.4
594.31	1003.48	sp|Q56YN3|NADK1_ARATH.ALAQAEAAEWK.	74.4	29.6
594.31	804.39	sp|Q56YN3|NADK1_ARATH.ALAQAEAAEWK.	74.4	29.6
594.31	733.35	sp|Q56YN3|NADK1_ARATH.ALAQAEAAEWK.	74.4	29.6
594.31	604.31	sp|Q56YN3|NADK1_ARATH.ALAQAEAAEWK.	74.4	29.6
594.31	333.19	sp|Q56YN3|NADK1_ARATH.ALAQAEAAEWK.	74.4	29.6
552.31	903.50	sp|Q43295|KAP1_ARATH.SLLGLSMASPK.	71.4	27.2
552.31	790.41	sp|Q43295|KAP1_ARATH.SLLGLSMASPK.	71.4	27.2
552.31	733.39	sp|Q43295|KAP1_ARATH.SLLGLSMASPK.	71.4	27.2
552.31	620.31	sp|Q43295|KAP1_ARATH.SLLGLSMASPK.	71.4	27.2
552.31	331.20	sp|Q43295|KAP1_ARATH.SLLGLSMASPK.	71.4	27.2
560.31	919.49	sp|Q43295|KAP1_ARATH.SLLGLSM[+16_0]ASPK.	72	27.7
560.31	806.41	sp|Q43295|KAP1_ARATH.SLLGLSM[+16_0]ASPK.	72	27.7
560.31	742.41	sp|Q43295|KAP1_ARATH.SLLGLSM[+16_0]ASPK.	72	27.7
560.31	636.30	sp|Q43295|KAP1_ARATH.SLLGLSM[+16_0]ASPK.	72	27.7
560.31	331.20	sp|Q43295|KAP1_ARATH.SLLGLSM[+16_0]ASPK.	72	27.7
708.38	1020.53	sp|Q43295|KAP1_ARATH.QGPLSTVGNSTNIK.	82.8	36.1
708.38	933.50	sp|Q43295|KAP1_ARATH.QGPLSTVGNSTNIK.	82.8	36.1
708.38	832.45	sp|Q43295|KAP1_ARATH.QGPLSTVGNSTNIK.	82.8	36.1
708.38	733.38	sp|Q43295|KAP1_ARATH.QGPLSTVGNSTNIK.	82.8	36.1
708.38	562.32	sp|Q43295|KAP1_ARATH.QGPLSTVGNSTNIK.	82.8	36.1
624.79	904.44	sp|Q43295|KAP1_ARATH.EGGTSPIEMAEK.	76.7	31.3
624.79	817.41	sp|Q43295|KAP1_ARATH.EGGTSPIEMAEK.	76.7	31.3
624.79	607.28	sp|Q43295|KAP1_ARATH.EGGTSPIEMAEK.	76.7	31.3
624.79	478.23	sp|Q43295|KAP1_ARATH.EGGTSPIEMAEK.	76.7	31.3
624.79	347.19	sp|Q43295|KAP1_ARATH.EGGTSPIEMAEK.	76.7	31.3
623.30	974.44	tr|Q94BV7|Q94BV7_ARATH.ASLPELSDEER.	76.6	31.3
623.30	748.35	tr|Q94BV7|Q94BV7_ARATH.ASLPELSDEER.	76.6	31.3

623.30	635.26	tr|Q94BV7|Q94BV7_ARATH.ASLPELSDEER.	76.6	31.3
623.30	433.20	tr|Q94BV7|Q94BV7_ARATH.ASLPELSDEER.	76.6	31.3
623.30	304.16	tr|Q94BV7|Q94BV7_ARATH.ASLPELSDEER.	76.6	31.3
581.31	890.46	tr|Q94BV7|Q94BV7_ARATH.SALSQVDSQVK.	73.5	28.9
581.31	675.37	tr|Q94BV7|Q94BV7_ARATH.SALSQVDSQVK.	73.5	28.9
581.31	576.30	tr|Q94BV7|Q94BV7_ARATH.SALSQVDSQVK.	73.5	28.9
581.31	461.27	tr|Q94BV7|Q94BV7_ARATH.SALSQVDSQVK.	73.5	28.9
581.31	147.11	tr|Q94BV7|Q94BV7_ARATH.SALSQVDSQVK.	73.5	28.9
742.87	1185.54	sp|C0LGQ5|GSO1_ARATH.SLVTNPQ[+1_0]EDDPLR.	85.3	38.1
742.87	970.45	sp|C0LGQ5|GSO1_ARATH.SLVTNPQ[+1_0]EDDPLR.	85.3	38.1
742.87	500.28	sp|C0LGQ5|GSO1_ARATH.SLVTNPQ[+1_0]EDDPLR.	85.3	38.1
742.87	385.26	sp|C0LGQ5|GSO1_ARATH.SLVTNPQ[+1_0]EDDPLR.	85.3	38.1
742.87	175.12	sp|C0LGQ5|GSO1_ARATH.SLVTNPQ[+1_0]EDDPLR.	85.3	38.1
742.37	1184.55	sp|C0LGQ5|GSO1_ARATH.SLVTNPQEDDPLR.	85.2	38.1
742.37	1083.51	sp|C0LGQ5|GSO1_ARATH.SLVTNPQEDDPLR.	85.2	38.1
742.37	969.46	sp|C0LGQ5|GSO1_ARATH.SLVTNPQEDDPLR.	85.2	38.1
742.37	500.28	sp|C0LGQ5|GSO1_ARATH.SLVTNPQEDDPLR.	85.2	38.1
742.37	385.26	sp|C0LGQ5|GSO1_ARATH.SLVTNPQEDDPLR.	85.2	38.1
742.87	1185.54	sp|C0LGQ5|GSO1_ARATH.SLVTN[+1_0]PQEDDPLR.	85.3	38.1
742.87	969.46	sp|C0LGQ5|GSO1_ARATH.SLVTN[+1_0]PQEDDPLR.	85.3	38.1
742.87	500.28	sp|C0LGQ5|GSO1_ARATH.SLVTN[+1_0]PQEDDPLR.	85.3	38.1
742.87	385.26	sp|C0LGQ5|GSO1_ARATH.SLVTN[+1_0]PQEDDPLR.	85.3	38.1
742.87	175.12	sp|C0LGQ5|GSO1_ARATH.SLVTN[+1_0]PQEDDPLR.	85.3	38.1
444.26	774.44	sp|C0LGQ5|GSO1_ARATH.LSQLGELK.	63.5	21.1
444.26	687.40	sp|C0LGQ5|GSO1_ARATH.LSQLGELK.	63.5	21.1
444.26	559.34	sp|C0LGQ5|GSO1_ARATH.LSQLGELK.	63.5	21.1
444.26	446.26	sp|C0LGQ5|GSO1_ARATH.LSQLGELK.	63.5	21.1
444.26	260.20	sp|C0LGQ5|GSO1_ARATH.LSQLGELK.	63.5	21.1
690.83	1138.56	sp|C0LGQ5|GSO1_ARATH.NQFSGSLPQAM[+16_0]GK.	81.5	35.1
690.83	760.40	sp|C0LGQ5|GSO1_ARATH.NQFSGSLPQAM[+16_0]GK.	81.5	35.1
690.83	647.32	sp|C0LGQ5|GSO1_ARATH.NQFSGSLPQAM[+16_0]GK.	81.5	35.1
690.83	583.32	sp|C0LGQ5|GSO1_ARATH.NQFSGSLPQAM[+16_0]GK.	81.5	35.1
690.83	422.21	sp|C0LGQ5|GSO1_ARATH.NQFSGSLPQAM[+16_0]GK.	81.5	35.1
682.83	1122.56	sp|C0LGQ5|GSO1_ARATH.NQFSGSLPQAMGK.	80.9	34.7
682.83	975.49	sp|C0LGQ5|GSO1_ARATH.NQFSGSLPQAMGK.	80.9	34.7
682.83	888.46	sp|C0LGQ5|GSO1_ARATH.NQFSGSLPQAMGK.	80.9	34.7
682.83	631.32	sp|C0LGQ5|GSO1_ARATH.NQFSGSLPQAMGK.	80.9	34.7
682.83	335.17	sp|C0LGQ5|GSO1_ARATH.NQFSGSLPQAMGK.	80.9	34.7
700.34	910.49	sp|Q9SWW6|CESA7_ARATH.MEASAGLVAGSHNR.	82.2	35.7
700.34	740.38	sp|Q9SWW6|CESA7_ARATH.MEASAGLVAGSHNR.	82.2	35.7
700.34	641.31	sp|Q9SWW6|CESA7_ARATH.MEASAGLVAGSHNR.	82.2	35.7

700.34	570.27	sp|Q9SWW6|CESA7_ARATH.MEASAGLVAGSHNR.	82.2	35.7
700.34	513.25	sp|Q9SWW6|CESA7_ARATH.MEASAGLVAGSHNR.	82.2	35.7
467.23	740.38	sp|Q9SWW6|CESA7_ARATH.MEASAGLVAGSHNR.	65.2	21.6
467.23	641.31	sp|Q9SWW6|CESA7_ARATH.MEASAGLVAGSHNR.	65.2	21.6
467.23	570.27	sp|Q9SWW6|CESA7_ARATH.MEASAGLVAGSHNR.	65.2	21.6
467.23	513.25	sp|Q9SWW6|CESA7_ARATH.MEASAGLVAGSHNR.	65.2	21.6
467.23	289.16	sp|Q9SWW6|CESA7_ARATH.MEASAGLVAGSHNR.	65.2	21.6
526.27	1163.60	tr|Q9FGK4|Q9FGK4_ARATH.LGNESAGIQFTFHR.	69.5	23.4
526.27	835.42	tr|Q9FGK4|Q9FGK4_ARATH.LGNESAGIQFTFHR.	69.5	23.4
526.27	707.36	tr|Q9FGK4|Q9FGK4_ARATH.LGNESAGIQFTFHR.	69.5	23.4
526.27	560.29	tr|Q9FGK4|Q9FGK4_ARATH.LGNESAGIQFTFHR.	69.5	23.4
526.27	459.25	tr|Q9FGK4|Q9FGK4_ARATH.LGNESAGIQFTFHR.	69.5	23.4
718.34	1265.57	sp|Q708Y0|EBF2_ARATH.VAATSFYSGFEEK.	83.5	36.7
718.34	1093.48	sp|Q708Y0|EBF2_ARATH.VAATSFYSGFEEK.	83.5	36.7
718.34	1006.45	sp|Q708Y0|EBF2_ARATH.VAATSFYSGFEEK.	83.5	36.7
718.34	696.32	sp|Q708Y0|EBF2_ARATH.VAATSFYSGFEEK.	83.5	36.7
718.34	609.29	sp|Q708Y0|EBF2_ARATH.VAATSFYSGFEEK.	83.5	36.7
523.30	861.48	sp|Q708Y0|EBF2_ARATH.LAAIAVGTSSR.	69.3	25.6
523.30	677.36	sp|Q708Y0|EBF2_ARATH.LAAIAVGTSSR.	69.3	25.6
523.30	606.32	sp|Q708Y0|EBF2_ARATH.LAAIAVGTSSR.	69.3	25.6
523.30	507.25	sp|Q708Y0|EBF2_ARATH.LAAIAVGTSSR.	69.3	25.6
523.30	450.23	sp|Q708Y0|EBF2_ARATH.LAAIAVGTSSR.	69.3	25.6
657.37	958.53	sp|Q708Y0|EBF2_ARATH.ELLQSNNVGLVK.	79	33.2
657.37	830.47	sp|Q708Y0|EBF2_ARATH.ELLQSNNVGLVK.	79	33.2
657.37	743.44	sp|Q708Y0|EBF2_ARATH.ELLQSNNVGLVK.	79	33.2
657.37	416.29	sp|Q708Y0|EBF2_ARATH.ELLQSNNVGLVK.	79	33.2
657.37	147.11	sp|Q708Y0|EBF2_ARATH.ELLQSNNVGLVK.	79	33.2
601.34	973.57	sp|Q708Y0|EBF2_ARATH.N[+1_0]ITNASLVAVAK.	75	30
601.34	872.52	sp|Q708Y0|EBF2_ARATH.N[+1_0]ITNASLVAVAK.	75	30
601.34	687.44	sp|Q708Y0|EBF2_ARATH.N[+1_0]ITNASLVAVAK.	75	30
601.34	487.32	sp|Q708Y0|EBF2_ARATH.N[+1_0]ITNASLVAVAK.	75	30
601.34	388.26	sp|Q708Y0|EBF2_ARATH.N[+1_0]ITNASLVAVAK.	75	30
758.41	841.45	sp|Q56YP2|PI5K1_ARATH.DGLVLLAQSTPM[+16_0]VR.	86.4	39
758.41	706.36	sp|Q56YP2|PI5K1_ARATH.DGLVLLAQSTPM[+16_0]VR.	86.4	39
758.41	619.32	sp|Q56YP2|PI5K1_ARATH.DGLVLLAQSTPM[+16_0]VR.	86.4	39
758.41	518.28	sp|Q56YP2|PI5K1_ARATH.DGLVLLAQSTPM[+16_0]VR.	86.4	39
758.41	454.28	sp|Q56YP2|PI5K1_ARATH.DGLVLLAQSTPM[+16_0]VR.	86.4	39
514.77	657.36	sp|Q56YP2|PI5K1_ARATH.E[-18_0]LFQVDPAK.	68.6	25.1
514.77	529.30	sp|Q56YP2|PI5K1_ARATH.E[-18_0]LFQVDPAK.	68.6	25.1
514.77	430.23	sp|Q56YP2|PI5K1_ARATH.E[-18_0]LFQVDPAK.	68.6	25.1
514.77	315.20	sp|Q56YP2|PI5K1_ARATH.E[-18_0]LFQVDPAK.	68.6	25.1

514.77	147.11	sp|Q56YP2|PI5K1_ARATH.E[-18_0]LFQVDPAK.	68.6	25.1
746.87	1046.55	sp|Q38846|ERS1_ARATH.EM[+16_0]GLILTQEETGR.	85.6	38.3
746.87	933.46	sp|Q38846|ERS1_ARATH.EM[+16_0]GLILTQEETGR.	85.6	38.3
746.87	820.38	sp|Q38846|ERS1_ARATH.EM[+16_0]GLILTQEETGR.	85.6	38.3
746.87	591.27	sp|Q38846|ERS1_ARATH.EM[+16_0]GLILTQEETGR.	85.6	38.3
746.87	333.19	sp|Q38846|ERS1_ARATH.EM[+16_0]GLILTQEETGR.	85.6	38.3
737.86	1046.55	sp|Q38846|ERS1_ARATH.E[-18_0]M[+16_0]GLILTQEETGR.	84.9	37.8
737.86	933.46	sp|Q38846|ERS1_ARATH.E[-18_0]M[+16_0]GLILTQEETGR.	84.9	37.8
737.86	820.38	sp|Q38846|ERS1_ARATH.E[-18_0]M[+16_0]GLILTQEETGR.	84.9	37.8
737.86	462.23	sp|Q38846|ERS1_ARATH.E[-18_0]M[+16_0]GLILTQEETGR.	84.9	37.8
737.86	333.19	sp|Q38846|ERS1_ARATH.E[-18_0]M[+16_0]GLILTQEETGR.	84.9	37.8
739.36	1047.53	sp|Q38846|ERS1_ARATH.EMGLILTQ[+1_0]EETGR.	85	37.9
739.36	934.45	sp|Q38846|ERS1_ARATH.EMGLILTQ[+1_0]EETGR.	85	37.9
739.36	821.36	sp|Q38846|ERS1_ARATH.EMGLILTQ[+1_0]EETGR.	85	37.9
739.36	462.23	sp|Q38846|ERS1_ARATH.EMGLILTQ[+1_0]EETGR.	85	37.9
739.36	333.19	sp|Q38846|ERS1_ARATH.EMGLILTQ[+1_0]EETGR.	85	37.9
738.87	1046.55	sp|Q38846|ERS1_ARATH.EMGLILTQEETGR.	85	37.9
738.87	933.46	sp|Q38846|ERS1_ARATH.EMGLILTQEETGR.	85	37.9
738.87	820.38	sp|Q38846|ERS1_ARATH.EMGLILTQEETGR.	85	37.9
738.87	591.27	sp|Q38846|ERS1_ARATH.EMGLILTQEETGR.	85	37.9
738.87	333.19	sp|Q38846|ERS1_ARATH.EMGLILTQEETGR.	85	37.9
747.36	1047.53	sp|Q38846|ERS1_ARATH.EM[+16_0]GLILTQ[+1_0]EETGR.	85.6	38.3
747.36	934.45	sp|Q38846|ERS1_ARATH.EM[+16_0]GLILTQ[+1_0]EETGR.	85.6	38.3
747.36	821.36	sp|Q38846|ERS1_ARATH.EM[+16_0]GLILTQ[+1_0]EETGR.	85.6	38.3
747.36	591.27	sp|Q38846|ERS1_ARATH.EM[+16_0]GLILTQ[+1_0]EETGR.	85.6	38.3
747.36	333.19	sp|Q38846|ERS1_ARATH.EM[+16_0]GLILTQ[+1_0]EETGR.	85.6	38.3
566.80	882.50	sp|Q38846|ERS1_ARATH.YSPPEVVSVR.	72.4	28
566.80	785.45	sp|Q38846|ERS1_ARATH.YSPPEVVSVR.	72.4	28
566.80	688.40	sp|Q38846|ERS1_ARATH.YSPPEVVSVR.	72.4	28
566.80	559.36	sp|Q38846|ERS1_ARATH.YSPPEVVSVR.	72.4	28
566.80	175.12	sp|Q38846|ERS1_ARATH.YSPPEVVSVR.	72.4	28
726.35	1208.60	sp|Q38846|ERS1_ARATH.DQLMEQNFALDK.	84.1	37.1
726.35	1095.51	sp|Q38846|ERS1_ARATH.DQLMEQNFALDK.	84.1	37.1
726.35	964.47	sp|Q38846|ERS1_ARATH.DQLMEQNFALDK.	84.1	37.1
726.35	446.26	sp|Q38846|ERS1_ARATH.DQLMEQNFALDK.	84.1	37.1
726.35	375.22	sp|Q38846|ERS1_ARATH.DQLMEQNFALDK.	84.1	37.1

599.79	982.50	tr|Q9SG11|Q9SG11_ARATH.TDGSSWFTAVK.	74.8	29.9
599.79	565.33	tr|Q9SG11|Q9SG11_ARATH.TDGSSWFTAVK.	74.8	29.9
599.79	418.27	tr|Q9SG11|Q9SG11_ARATH.TDGSSWFTAVK.	74.8	29.9
599.79	317.22	tr|Q9SG11|Q9SG11_ARATH.TDGSSWFTAVK.	74.8	29.9
599.79	147.11	tr|Q9SG11|Q9SG11_ARATH.TDGSSWFTAVK.	74.8	29.9
589.78	1004.49	tr|Q84VY2|Q84VY2_ARATH.SSELTEEVER.	74.1	29.4
589.78	875.45	tr|Q84VY2|Q84VY2_ARATH.SSELTEEVER.	74.1	29.4
589.78	762.36	tr|Q84VY2|Q84VY2_ARATH.SSELTEEVER.	74.1	29.4
589.78	661.32	tr|Q84VY2|Q84VY2_ARATH.SSELTEEVER.	74.1	29.4
589.78	175.12	tr|Q84VY2|Q84VY2_ARATH.SSELTEEVER.	74.1	29.4
707.88	602.36	sp|Q9LRZ4|P2C41_ARATH.VGMPNGGSLGLAVSR.	82.7	36.1
707.88	432.26	sp|Q9LRZ4|P2C41_ARATH.VGMPNGGSLGLAVSR.	82.7	36.1
707.88	361.22	sp|Q9LRZ4|P2C41_ARATH.VGMPNGGSLGLAVSR.	82.7	36.1
707.88	262.15	sp|Q9LRZ4|P2C41_ARATH.VGMPNGGSLGLAVSR.	82.7	36.1
707.88	175.12	sp|Q9LRZ4|P2C41_ARATH.VGMPNGGSLGLAVSR.	82.7	36.1
715.87	1127.62	sp|Q9LRZ4|P2C41_ARATH.VGM[+16_0]PNGGSLGLAVSR.	83.3	36.5
715.87	916.52	sp|Q9LRZ4|P2C41_ARATH.VGM[+16_0]PNGGSLGLAVSR.	83.3	36.5
715.87	602.36	sp|Q9LRZ4|P2C41_ARATH.VGM[+16_0]PNGGSLGLAVSR.	83.3	36.5
715.87	432.26	sp|Q9LRZ4|P2C41_ARATH.VGM[+16_0]PNGGSLGLAVSR.	83.3	36.5
715.87	361.22	sp|Q9LRZ4|P2C41_ARATH.VGM[+16_0]PNGGSLGLAVSR.	83.3	36.5
756.37	1079.54	sp|Q9LRZ4|P2C41_ARATH.DFGLVSEPEVTYR.	86.3	38.8
756.37	980.47	sp|Q9LRZ4|P2C41_ARATH.DFGLVSEPEVTYR.	86.3	38.8
756.37	764.39	sp|Q9LRZ4|P2C41_ARATH.DFGLVSEPEVTYR.	86.3	38.8
756.37	538.30	sp|Q9LRZ4|P2C41_ARATH.DFGLVSEPEVTYR.	86.3	38.8
694.86	1128.60	sp|Q9CA67|CHLP_ARATH.M[+16_0]ISPSNIAVDIGR.	81.8	35.3
694.86	1041.57	sp|Q9CA67|CHLP_ARATH.M[+16_0]ISPSNIAVDIGR.	81.8	35.3
694.86	630.36	sp|Q9CA67|CHLP_ARATH.M[+16_0]ISPSNIAVDIGR.	81.8	35.3
694.86	460.25	sp|Q9CA67|CHLP_ARATH.M[+16_0]ISPSNIAVDIGR.	81.8	35.3
694.86	345.22	sp|Q9CA67|CHLP_ARATH.M[+16_0]ISPSNIAVDIGR.	81.8	35.3
811.38	1030.53	sp|Q9CA67|CHLP_ARATH.TM[+16_0]EVDAVIGADGANSR.	90.3	42
811.38	860.42	sp|Q9CA67|CHLP_ARATH.TM[+16_0]EVDAVIGADGANSR.	90.3	42
811.38	747.34	sp|Q9CA67|CHLP_ARATH.TM[+16_0]EVDAVIGADGANSR.	90.3	42
811.38	619.28	sp|Q9CA67|CHLP_ARATH.TM[+16_0]EVDAVIGADGANSR.	90.3	42
811.38	504.25	sp|Q9CA67|CHLP_ARATH.TM[+16_0]EVDAVIGADGANSR.	90.3	42
571.85	958.57	sp|Q9CA67|CHLP_ARATH.LAVNTIGSLVR.	72.8	28.3
571.85	859.50	sp|Q9CA67|CHLP_ARATH.LAVNTIGSLVR.	72.8	28.3

571.85	644.41	sp|Q9CA67|CHLP_ARATH.LAVNTIGSLVR.	72.8	28.3
571.85	531.32	sp|Q9CA67|CHLP_ARATH.LAVNTIGSLVR.	72.8	28.3
571.85	474.30	sp|Q9CA67|CHLP_ARATH.LAVNTIGSLVR.	72.8	28.3
654.32	904.51	sp|Q9LT91|PER66_ARATH.GC[+57_0]DASILLDSTR.	78.8	33
654.32	704.39	sp|Q9LT91|PER66_ARATH.GC[+57_0]DASILLDSTR.	78.8	33
654.32	591.31	sp|Q9LT91|PER66_ARATH.GC[+57_0]DASILLDSTR.	78.8	33
654.32	478.23	sp|Q9LT91|PER66_ARATH.GC[+57_0]DASILLDSTR.	78.8	33
654.32	363.20	sp|Q9LT91|PER66_ARATH.GC[+57_0]DASILLDSTR.	78.8	33
477.75	685.40	sp|Q9LT91|PER66_ARATH.DGPPNISVR.	65.9	23
477.75	588.35	sp|Q9LT91|PER66_ARATH.DGPPNISVR.	65.9	23
477.75	474.30	sp|Q9LT91|PER66_ARATH.DGPPNISVR.	65.9	23
477.75	361.22	sp|Q9LT91|PER66_ARATH.DGPPNISVR.	65.9	23
477.75	175.12	sp|Q9LT91|PER66_ARATH.DGPPNISVR.	65.9	23
711.35	859.46	sp|Q9LT91|PER66_ARATH.GVFGSDQALLGDSR.	83	36.3
711.35	731.40	sp|Q9LT91|PER66_ARATH.GVFGSDQALLGDSR.	83	36.3
711.35	660.37	sp|Q9LT91|PER66_ARATH.GVFGSDQALLGDSR.	83	36.3
711.35	547.28	sp|Q9LT91|PER66_ARATH.GVFGSDQALLGDSR.	83	36.3
711.35	262.15	sp|Q9LT91|PER66_ARATH.GVFGSDQALLGDSR.	83	36.3
495.26	716.40	sp|Q9FY54|SPSA2_ARATH.SWVQAAATR.	67.2	24
495.26	617.34	sp|Q9FY54|SPSA2_ARATH.SWVQAAATR.	67.2	24
495.26	489.28	sp|Q9FY54|SPSA2_ARATH.SWVQAAATR.	67.2	24
495.26	418.24	sp|Q9FY54|SPSA2_ARATH.SWVQAAATR.	67.2	24
495.26	347.20	sp|Q9FY54|SPSA2_ARATH.SWVQAAATR.	67.2	24
844.35	811.35	sp|Q9FY54|SPSA2_ARATH.EVTAEMSEDFSEGEK.	92.7	43.9
844.35	696.32	sp|Q9FY54|SPSA2_ARATH.EVTAEMSEDFSEGEK.	92.7	43.9
844.35	549.25	sp|Q9FY54|SPSA2_ARATH.EVTAEMSEDFSEGEK.	92.7	43.9
844.35	462.22	sp|Q9FY54|SPSA2_ARATH.EVTAEMSEDFSEGEK.	92.7	43.9
844.35	333.18	sp|Q9FY54|SPSA2_ARATH.EVTAEMSEDFSEGEK.	92.7	43.9
832.85	1048.45	sp|Q9FY54|SPSA2_ARATH.SGSNN[+1_0]GVDTNLDAEDR.	91.8	43.2
832.85	933.43	sp|Q9FY54|SPSA2_ARATH.SGSNN[+1_0]GVDTNLDAEDR.	91.8	43.2
832.85	605.25	sp|Q9FY54|SPSA2_ARATH.SGSNN[+1_0]GVDTNLDAEDR.	91.8	43.2
832.85	490.23	sp|Q9FY54|SPSA2_ARATH.SGSNN[+1_0]GVDTNLDAEDR.	91.8	43.2
832.85	290.15	sp|Q9FY54|SPSA2_ARATH.SGSNN[+1_0]GVDTNLDAEDR.	91.8	43.2
888.44	1256.65	sp|Q96292|ACT2_ARATH.NYELPDGQ[+1_0]VITIGAER.	95.9	46.4
888.44	858.50	sp|Q96292|ACT2_ARATH.NYELPDGQ[+1_0]VITIGAER.	95.9	46.4
888.44	759.44	sp|Q96292|ACT2_ARATH.NYELPDGQ[+1_0]VITIGAER.	95.9	46.4
888.44	646.35	sp|Q96292|ACT2_ARATH.NYELPDGQ[+1_0]VITIGAER.	95.9	46.4
888.44	432.22	sp|Q96292|ACT2_ARATH.NYELPDGQ[+1_0]VITIGAER.	95.9	46.4
468.25	788.43	tr|Q9SG17|Q9SG17_ARATH.FSDAQIVR.	65.3	22.4

468.25	701.39	tr|Q9SG17|Q9SG17_ARATH.FSDAQIVR.	65.3	22.4
468.25	586.37	tr|Q9SG17|Q9SG17_ARATH.FSDAQIVR.	65.3	22.4
468.25	515.33	tr|Q9SG17|Q9SG17_ARATH.FSDAQIVR.	65.3	22.4
468.25	387.27	tr|Q9SG17|Q9SG17_ARATH.FSDAQIVR.	65.3	22.4
902.94	1321.60	tr|Q9SG17|Q9SG17_ARATH.LDAALDVGGVYDPQSER.	96.9	47.2
902.94	1206.57	tr|Q9SG17|Q9SG17_ARATH.LDAALDVGGVYDPQSER.	96.9	47.2
902.94	1107.51	tr|Q9SG17|Q9SG17_ARATH.LDAALDVGGVYDPQSER.	96.9	47.2
902.94	894.40	tr|Q9SG17|Q9SG17_ARATH.LDAALDVGGVYDPQSER.	96.9	47.2
902.94	616.30	tr|Q9SG17|Q9SG17_ARATH.LDAALDVGGVYDPQSER.	96.9	47.2
808.40	1160.56	tr|Q9SG17|Q9SG17_ARATH.LNLDWIEPDQSSAK.	90	41.8
808.40	974.48	tr|Q9SG17|Q9SG17_ARATH.LNLDWIEPDQSSAK.	90	41.8
808.40	861.39	tr|Q9SG17|Q9SG17_ARATH.LNLDWIEPDQSSAK.	90	41.8
808.40	732.35	tr|Q9SG17|Q9SG17_ARATH.LNLDWIEPDQSSAK.	90	41.8
808.40	392.21	tr|Q9SG17|Q9SG17_ARATH.LNLDWIEPDQSSAK.	90	41.8
543.30	844.45	tr|Q9SG17|Q9SG17_ARATH.IQAVSVSPER.	70.7	26.7
543.30	773.42	tr|Q9SG17|Q9SG17_ARATH.IQAVSVSPER.	70.7	26.7
543.30	674.35	tr|Q9SG17|Q9SG17_ARATH.IQAVSVSPER.	70.7	26.7
543.30	488.25	tr|Q9SG17|Q9SG17_ARATH.IQAVSVSPER.	70.7	26.7
543.30	401.21	tr|Q9SG17|Q9SG17_ARATH.IQAVSVSPER.	70.7	26.7
765.36	1102.50	sp|Q56WF8|SCP48_ARATH.DVNVIDEEGSEAPR.	86.9	39.4
765.36	989.42	sp|Q56WF8|SCP48_ARATH.DVNVIDEEGSEAPR.	86.9	39.4
765.36	874.39	sp|Q56WF8|SCP48_ARATH.DVNVIDEEGSEAPR.	86.9	39.4
765.36	616.30	sp|Q56WF8|SCP48_ARATH.DVNVIDEEGSEAPR.	86.9	39.4
765.36	343.21	sp|Q56WF8|SCP48_ARATH.DVNVIDEEGSEAPR.	86.9	39.4
537.78	856.45	sp|Q56WF8|SCP48_ARATH.AFDLPAAVDR.	70.3	26.4
537.78	741.43	sp|Q56WF8|SCP48_ARATH.AFDLPAAVDR.	70.3	26.4
537.78	628.34	sp|Q56WF8|SCP48_ARATH.AFDLPAAVDR.	70.3	26.4
537.78	531.29	sp|Q56WF8|SCP48_ARATH.AFDLPAAVDR.	70.3	26.4
537.78	175.12	sp|Q56WF8|SCP48_ARATH.AFDLPAAVDR.	70.3	26.4
790.46	1223.74	sp|Q56WF8|SCP48_ARATH.NLEVGIPALLQDGIK.	88.7	40.8
790.46	1124.67	sp|Q56WF8|SCP48_ARATH.NLEVGIPALLQDGIK.	88.7	40.8
790.46	954.56	sp|Q56WF8|SCP48_ARATH.NLEVGIPALLQDGIK.	88.7	40.8
790.46	673.39	sp|Q56WF8|SCP48_ARATH.NLEVGIPALLQDGIK.	88.7	40.8
790.46	317.22	sp|Q56WF8|SCP48_ARATH.NLEVGIPALLQDGIK.	88.7	40.8
778.35	1097.52	sp|O23402|U84A4_ARATH.EEAESAVAYGGTSER.	87.9	40.1
778.35	939.45	sp|O23402|U84A4_ARATH.EEAESAVAYGGTSER.	87.9	40.1
778.35	840.38	sp|O23402|U84A4_ARATH.EEAESAVAYGGTSER.	87.9	40.1
778.35	769.35	sp|O23402|U84A4_ARATH.EEAESAVAYGGTSER.	87.9	40.1
778.35	606.28	sp|O23402|U84A4_ARATH.EEAESAVAYGGTSER.	87.9	40.1
972.54	802.43	tr|Q9LS50|Q9LS50_ARATH.AVVDVDLNK.	102	51.2
972.54	588.34	tr|Q9LS50|Q9LS50_ARATH.AVVDVDLNK.	102	51.2

972.54	489.27	tr|Q9LS50|Q9LS50_ARATH.AVVDVDLNK.	102	51.2
972.54	374.24	tr|Q9LS50|Q9LS50_ARATH.AVVDVDLNK.	102	51.2
486.77	802.43	tr|Q9LS50|Q9LS50_ARATH.AVVDVDLNK.	66.6	23.5
486.77	703.36	tr|Q9LS50|Q9LS50_ARATH.AVVDVDLNK.	66.6	23.5
486.77	588.34	tr|Q9LS50|Q9LS50_ARATH.AVVDVDLNK.	66.6	23.5
486.77	489.27	tr|Q9LS50|Q9LS50_ARATH.AVVDVDLNK.	66.6	23.5
486.77	374.24	tr|Q9LS50|Q9LS50_ARATH.AVVDVDLNK.	66.6	23.5
526.27	825.37	tr|Q9FM06|Q9FM06_ARATH.LISSEEVM[+16_0]K.	69.5	25.7
526.27	761.37	tr|Q9FM06|Q9FM06_ARATH.LISSEEVM[+16_0]K.	69.5	25.7
526.27	738.33	tr|Q9FM06|Q9FM06_ARATH.LISSEEVM[+16_0]K.	69.5	25.7
526.27	651.30	tr|Q9FM06|Q9FM06_ARATH.LISSEEVM[+16_0]K.	69.5	25.7
526.27	458.26	tr|Q9FM06|Q9FM06_ARATH.LISSEEVM[+16_0]K.	69.5	25.7
518.27	922.46	tr|Q9FM06|Q9FM06_ARATH.LISSEEVMK.	68.9	25.3
518.27	809.37	tr|Q9FM06|Q9FM06_ARATH.LISSEEVMK.	68.9	25.3
518.27	722.34	tr|Q9FM06|Q9FM06_ARATH.LISSEEVMK.	68.9	25.3
518.27	506.26	tr|Q9FM06|Q9FM06_ARATH.LISSEEVMK.	68.9	25.3
518.27	377.22	tr|Q9FM06|Q9FM06_ARATH.LISSEEVMK.	68.9	25.3
824.42	1135.54	tr|F4JTJ2|F4JTJ2_ARATH.VQVSVQSPEGITTM[+16_0]R.	91.2	42.7
824.42	1007.48	tr|F4JTJ2|F4JTJ2_ARATH.VQVSVQSPEGITTM[+16_0]R.	91.2	42.7
824.42	920.45	tr|F4JTJ2|F4JTJ2_ARATH.VQVSVQSPEGITTM[+16_0]R.	91.2	42.7
824.42	856.45	tr|F4JTJ2|F4JTJ2_ARATH.VQVSVQSPEGITTM[+16_0]R.	91.2	42.7
824.42	524.25	tr|F4JTJ2|F4JTJ2_ARATH.VQVSVQSPEGITTM[+16_0]R.	91.2	42.7
870.94	1302.65	tr|F4JTJ2|F4JTJ2_ARATH.QGPGVSLGTGLVC[+57_0]NPER.	94.6	45.4
870.94	1102.53	tr|F4JTJ2|F4JTJ2_ARATH.QGPGVSLGTGLVC[+57_0]NPER.	94.6	45.4
870.94	944.46	tr|F4JTJ2|F4JTJ2_ARATH.QGPGVSLGTGLVC[+57_0]NPER.	94.6	45.4
870.94	675.29	tr|F4JTJ2|F4JTJ2_ARATH.QGPGVSLGTGLVC[+57_0]NPER.	94.6	45.4
870.94	401.21	tr|F4JTJ2|F4JTJ2_ARATH.QGPGVSLGTGLVC[+57_0]NPER.	94.6	45.4
712.42	952.62	tr|F4JTJ2|F4JTJ2_ARATH.QGSAQIVLPLELR.	83.1	36.3
712.42	839.53	tr|F4JTJ2|F4JTJ2_ARATH.QGSAQIVLPLELR.	83.1	36.3
712.42	740.47	tr|F4JTJ2|F4JTJ2_ARATH.QGSAQIVLPLELR.	83.1	36.3
712.42	627.38	tr|F4JTJ2|F4JTJ2_ARATH.QGSAQIVLPLELR.	83.1	36.3
712.42	288.20	tr|F4JTJ2|F4JTJ2_ARATH.QGSAQIVLPLELR.	83.1	36.3
674.34	1134.55	tr|F4JTJ2|F4JTJ2_ARATH.VNDLEGELETTK.	80.3	34.2
674.34	906.44	tr|F4JTJ2|F4JTJ2_ARATH.VNDLEGELETTK.	80.3	34.2
674.34	777.40	tr|F4JTJ2|F4JTJ2_ARATH.VNDLEGELETTK.	80.3	34.2
674.34	591.33	tr|F4JTJ2|F4JTJ2_ARATH.VNDLEGELETTK.	80.3	34.2
674.34	349.21	tr|F4JTJ2|F4JTJ2_ARATH.VNDLEGELETTK.	80.3	34.2
660.32	963.46	tr|F4JTJ2|F4JTJ2_ARATH.ENLEQAIMSER.	79.3	33.4
660.32	635.32	tr|F4JTJ2|F4JTJ2_ARATH.ENLEQAIMSER.	79.3	33.4

660.32	522.23	tr|F4JTJ2|F4JTJ2_ARATH.ENLEQAIMSER.	79.3	33.4
660.32	391.19	tr|F4JTJ2|F4JTJ2_ARATH.ENLEQAIMSER.	79.3	33.4
660.32	175.12	tr|F4JTJ2|F4JTJ2_ARATH.ENLEQAIMSER.	79.3	33.4
668.31	850.41	tr|F4JTJ2|F4JTJ2_ARATH.ENLEQAIM[+16_0]SER.	79.8	33.8
668.31	722.35	tr|F4JTJ2|F4JTJ2_ARATH.ENLEQAIM[+16_0]SER.	79.8	33.8
668.31	651.31	tr|F4JTJ2|F4JTJ2_ARATH.ENLEQAIM[+16_0]SER.	79.8	33.8
668.31	538.23	tr|F4JTJ2|F4JTJ2_ARATH.ENLEQAIM[+16_0]SER.	79.8	33.8
668.31	391.19	tr|F4JTJ2|F4JTJ2_ARATH.ENLEQAIM[+16_0]SER.	79.8	33.8
493.79	760.39	tr|F4JTJ2|F4JTJ2_ARATH.LLENTVAAR.	67.1	23.9
493.79	631.35	tr|F4JTJ2|F4JTJ2_ARATH.LLENTVAAR.	67.1	23.9
493.79	517.31	tr|F4JTJ2|F4JTJ2_ARATH.LLENTVAAR.	67.1	23.9
493.79	416.26	tr|F4JTJ2|F4JTJ2_ARATH.LLENTVAAR.	67.1	23.9
493.79	317.19	tr|F4JTJ2|F4JTJ2_ARATH.LLENTVAAR.	67.1	23.9
702.88	962.54	sp|Q94B59|PP372_ARATH.LTNNGVLGSNFIR.	82.4	35.8
702.88	905.52	sp|Q94B59|PP372_ARATH.LTNNGVLGSNFIR.	82.4	35.8
702.88	806.45	sp|Q94B59|PP372_ARATH.LTNNGVLGSNFIR.	82.4	35.8
702.88	693.37	sp|Q94B59|PP372_ARATH.LTNNGVLGSNFIR.	82.4	35.8
702.88	435.27	sp|Q94B59|PP372_ARATH.LTNNGVLGSNFIR.	82.4	35.8
489.26	878.44	sp|Q94B59|PP372_ARATH.VFGIDAAER.	66.8	23.6
489.26	731.37	sp|Q94B59|PP372_ARATH.VFGIDAAER.	66.8	23.6
489.26	561.26	sp|Q94B59|PP372_ARATH.VFGIDAAER.	66.8	23.6
489.26	446.24	sp|Q94B59|PP372_ARATH.VFGIDAAER.	66.8	23.6
489.26	304.16	sp|Q94B59|PP372_ARATH.VFGIDAAER.	66.8	23.6
744.38	1102.56	sp|Q94B59|PP372_ARATH.VTNAESTLPVEAEK.	85.4	38.2
744.38	973.52	sp|Q94B59|PP372_ARATH.VTNAESTLPVEAEK.	85.4	38.2
744.38	886.49	sp|Q94B59|PP372_ARATH.VTNAESTLPVEAEK.	85.4	38.2
744.38	785.44	sp|Q94B59|PP372_ARATH.VTNAESTLPVEAEK.	85.4	38.2
744.38	672.36	sp|Q94B59|PP372_ARATH.VTNAESTLPVEAEK.	85.4	38.2
635.79	1068.48	sp|Q94B59|PP372_ARATH.TTEFDASAC[+57_0]LR.	77.5	32
635.79	792.37	sp|Q94B59|PP372_ARATH.TTEFDASAC[+57_0]LR.	77.5	32
635.79	677.34	sp|Q94B59|PP372_ARATH.TTEFDASAC[+57_0]LR.	77.5	32
635.79	606.30	sp|Q94B59|PP372_ARATH.TTEFDASAC[+57_0]LR.	77.5	32
635.79	519.27	sp|Q94B59|PP372_ARATH.TTEFDASAC[+57_0]LR.	77.5	32
541.30	867.46	sp|O81770|MGDG1_ARATH.TLASLSFNTK.	70.6	26.6
541.30	796.42	sp|O81770|MGDG1_ARATH.TLASLSFNTK.	70.6	26.6
541.30	709.39	sp|O81770|MGDG1_ARATH.TLASLSFNTK.	70.6	26.6
541.30	596.30	sp|O81770|MGDG1_ARATH.TLASLSFNTK.	70.6	26.6
541.30	509.27	sp|O81770|MGDG1_ARATH.TLASLSFNTK.	70.6	26.6
490.26	795.39	sp|O81770|MGDG1_ARATH.ALADALYDK.	66.9	23.7
490.26	724.35	sp|O81770|MGDG1_ARATH.ALADALYDK.	66.9	23.7
490.26	609.32	sp|O81770|MGDG1_ARATH.ALADALYDK.	66.9	23.7

490.26	538.29	sp|O81770|MGDG1_ARATH.ALADALYDK.	66.9	23.7
490.26	425.20	sp|O81770|MGDG1_ARATH.ALADALYDK.	66.9	23.7
601.81	819.44	sp|O81770|MGDG1_ARATH.AGPGTIAEAM[+16_0]IR.	75	30
601.81	706.36	sp|O81770|MGDG1_ARATH.AGPGTIAEAM[+16_0]IR.	75	30
601.81	642.36	sp|O81770|MGDG1_ARATH.AGPGTIAEAM[+16_0]IR.	75	30
601.81	635.32	sp|O81770|MGDG1_ARATH.AGPGTIAEAM[+16_0]IR.	75	30
601.81	442.28	sp|O81770|MGDG1_ARATH.AGPGTIAEAM[+16_0]IR.	75	30
593.82	961.51	sp|O81770|MGDG1_ARATH.AGPGTIAEAMIR.	74.4	29.6
593.82	803.44	sp|O81770|MGDG1_ARATH.AGPGTIAEAMIR.	74.4	29.6
593.82	690.36	sp|O81770|MGDG1_ARATH.AGPGTIAEAMIR.	74.4	29.6
593.82	619.32	sp|O81770|MGDG1_ARATH.AGPGTIAEAMIR.	74.4	29.6
593.82	490.28	sp|O81770|MGDG1_ARATH.AGPGTIAEAMIR.	74.4	29.6
595.81	978.47	sp|O81770|MGDG1_ARATH.IVADWFGPASK.	74.6	29.7
595.81	907.43	sp|O81770|MGDG1_ARATH.IVADWFGPASK.	74.6	29.7
595.81	792.40	sp|O81770|MGDG1_ARATH.IVADWFGPASK.	74.6	29.7
595.81	606.32	sp|O81770|MGDG1_ARATH.IVADWFGPASK.	74.6	29.7
595.81	459.26	sp|O81770|MGDG1_ARATH.IVADWFGPASK.	74.6	29.7
533.77	882.41	sp|Q94BT0|SPSA1_ARATH.ALGSM[	70	26.2
533.77	818.42	sp|Q94BT0|SPSA1_ARATH.ALGSM[	70	26.2
533.77	591.32	sp|Q94BT0|SPSA1_ARATH.ALGSM[	70	26.2
533.77	494.27	sp|Q94BT0|SPSA1_ARATH.ALGSM[	70	26.2
533.77	338.18	sp|Q94BT0|SPSA1_ARATH.ALGSM[	70	26.2
525.77	866.42	sp|Q94BT0|SPSA1_ARATH.ALGSMPGVYR.	69.4	25.7
525.77	809.40	sp|Q94BT0|SPSA1_ARATH.ALGSMPGVYR.	69.4	25.7
525.77	722.37	sp|Q94BT0|SPSA1_ARATH.ALGSMPGVYR.	69.4	25.7
525.77	591.32	sp|Q94BT0|SPSA1_ARATH.ALGSMPGVYR.	69.4	25.7
525.77	338.18	sp|Q94BT0|SPSA1_ARATH.ALGSMPGVYR.	69.4	25.7
661.86	1039.53	sp|Q9FJZ9|PER72_ARATH.GLLSSDEILFTK.	79.4	33.5
661.86	952.50	sp|Q9FJZ9|PER72_ARATH.GLLSSDEILFTK.	79.4	33.5
661.86	750.44	sp|Q9FJZ9|PER72_ARATH.GLLSSDEILFTK.	79.4	33.5
661.86	508.31	sp|Q9FJZ9|PER72_ARATH.GLLSSDEILFTK.	79.4	33.5
661.86	395.23	sp|Q9FJZ9|PER72_ARATH.GLLSSDEILFTK.	79.4	33.5
771.88	1200.59	tr|Q9FIE8|Q9FIE8_ARATH.NEVVVADNYFTGSK.	87.4	39.7
771.88	1101.52	tr|Q9FIE8|Q9FIE8_ARATH.NEVVVADNYFTGSK.	87.4	39.7
771.88	1002.45	tr|Q9FIE8|Q9FIE8_ARATH.NEVVVADNYFTGSK.	87.4	39.7
771.88	931.42	tr|Q9FIE8|Q9FIE8_ARATH.NEVVVADNYFTGSK.	87.4	39.7
771.88	392.21	tr|Q9FIE8|Q9FIE8_ARATH.NEVVVADNYFTGSK.	87.4	39.7
548.32	867.53	tr|Q93ZX9|Q93ZX9_ARATH.VEALPLGPATK.	71.1	27
548.32	683.41	tr|Q93ZX9|Q93ZX9_ARATH.VEALPLGPATK.	71.1	27
548.32	586.36	tr|Q93ZX9|Q93ZX9_ARATH.VEALPLGPATK.	71.1	27
548.32	473.27	tr|Q93ZX9|Q93ZX9_ARATH.VEALPLGPATK.	71.1	27

548.32	416.25	tr|Q93ZX9|Q93ZX9_ARATH.VEALPLGPATK.	71.1	27

VII. References

Addona, T.A., Abbatiello, S.E., Schilling, B., Skates, S.J., Mani, D.R., Bunk, D.M., Spiegelman, C.H., Zimmerman, L.J., Ham, A.J.L., Keshishian, H., *et al.* (2009). Multi-site assessment of the precision and reproducibility of multiple reaction monitoring-based measurements of proteins in plasma (vol 27, pg 633, 2009). *Nature Biotechnology 27*, 864-864.

Aebersold, R., and Mann, M. (2003). Mass spectrometry-based proteomics. *Nature 422*, 198-207.

Arsova, B., Zauber, H., and Schulze, W.X. (2012). Precision, proteome coverage, and dynamic range of *Arabidopsis* proteome profiling using N-15 metabolic labeling and label-free approaches. *Molecular and Cellular Proteomics 11*, 619-628.

Barsan, C., Zouine, M., Maza, E., Bian, W.P., Egea, I., Rossignol, M., Bouyssie, D., Pichereaux, C., Purgatto, E., Bouzayen, M., *et al.* (2012). Proteomic analysis of chloroplast-to-chromoplast transition in tomato reveals metabolic shifts coupled with disrupted thylakoid biogenesis machinery and elevated energy-production components. *Plant Physiology 160*, 708-725.

Bell, A.W., Deutsch, E.W., Au, C.E., Kearney, R.E., Beavis, R., Sechi, S., Nilsson, T., Bergeron, J.J.M., and Grp, H.T.S.W. (2009). A HUPO test sample study reveals common problems in mass spectrometry-based proteomics. *Nature Methods 6*, 423-U440.

Chen, R.Q., Binder, B.M., Garrett, W.M., Tucker, M.L., Chang, C.R., and Cooper, B. (2011). Proteomic responses in *Arabidopsis thaliana* seedlings treated with ethylene. *Molecular Biosystems 7*, 2637-2650.

Choudhary, C., and Mann, M. (2010). Decoding signalling networks by mass spectrometry-based proteomics. *Nature Reviews Molecular Cellular Biology 11*, 427-439.

Duncan, M.W., Aebersold, R., and Caprioli, R.M. (2010). The pros and cons of peptide-centric proteomics. *Nature Biotechnology 28*, 659-664.

Ebhardt, H.A., Sabido, E., Huttenhain, R., Collins, B., and Aebersold, R. (2012). Range of protein detection by selected/multiple reaction monitoring mass spectrometry in an unfractionated human cell culture lysate. *Proteomics 12*, 1185-1193.

Fusaro, V.A., Mani, D.R., Mesirov, J.P., and Carr, S.A. (2009). Prediction of high-responding peptides for targeted protein assays by mass spectrometry. *Nature Biotechnology 27*, 190-198.

Grewal, R.N., El Aribi, H., Harrison, A.G., Siu, K.W.M., and Hopkinson, A.C. (2004). Fragmentation of protonated tripeptides: The proline effect revisited. *Journal of Physical Chemistry B 108*, 4899-4908.

Lange, V., Picotti, P., Domon, B., and Aebersold, R. (2008). Selected reaction monitoring for quantitative proteomics: a tutorial. *Molecular Systems Biology 4*, 222.

Lewis, D.R., Ramirez, M.V., Miller, N.D., Vallabhaneni, P., Ray, W.K., Helm, R.F., Winkel, B.S.J., and Muday, G.K. (2011). Auxin and ethylene induce flavonol accumulation through distinct transcriptional networks. *Plant Physiology 156*, 144-164.

Lewis, D.R., Olex, A. L., Fetrow, J. S., and Muday, G.K. (2013). A kinetic analysis of auxin-mediated changes in transcript abundance in *Arabidopsis* reveals new mediators of root growth and development. *Submitted.*

MacLean, B., Tomazela, D.M., Shulman, N., Chambers, M., Finney, G.L., Frewen, B., Kern, R., Tabb, D.L., Liebler, D.C., and MacCoss, M.J. (2010). Skyline: an open source document editor for creating and analyzing targeted proteomics experiments. *Bioinformatics 26*, 966-968.

Michalski, A., Cox, J., and Mann, M. (2011a). More than 100,000 detectable peptide species elute in single shotgun proteomics runs but the majority is inaccessible to data-dependent LC-MS/MS. *Journal of Proteome Research 10*, 1785-1793.

Michalski, A., Damoc, E., Hauschild, J.P., Lange, O., Wieghaus, A., Makarov, A., Nagaraj, N., Cox, J., Mann, M., and Horning, S. (2011b). Mass Spectrometry-based Proteomics Using Q Exactive, a high-performance benchtop auadrupole orbitrap mass spectrometer. *Molecular and Cellular Proteomics 10*.

Mortstedt, H., Karedal, M.H., Jonsson, B.A.G., and Lindh, C.H. (2013). Screening method using selected reaction monitoring for targeted proteomics studies of nasal lavage fluid. *Journal of Proteome Research 12*, 234-247.

Onisko, B., Dynin, I., Requena, J.R., Silva, C.J., Erickson, M., and Carter, J.M. (2007). Mass spectrometric detection of attomole amounts of the prion protein by nanoLC/MS/MS. *Journal of the American Society for Mass Spectrometry 18*, 1070-1079.

Picotti, P., and Aebersold, R. (2012). Selected reaction monitoring-based proteomics: workflows, potential, pitfalls and future directions. *Nature Methods 9*, 555-566.

Picotti, P., Bodenmiller, B., Mueller, L.N., Domon, B., and Aebersold, R. (2009). Full dynamic range proteome analysis of *S. cerevisiae* by targeted proteomics. *Cell 138*, 795-806.

Picotti, P., Rinner, O., Stallmach, R., Dautel, F., Farrah, T., Domon, B., Wenschuh, H., and Aebersold, R. (2010). High-throughput generation of selected reaction-monitoring assays for proteins and proteomes. *Nature Methods 7*, 43-U45.

Schafer, A., von Toerne, C., Becker, S., Sarioglu, H., Neschen, S., Kahle, M., Hauck, S.M., and Ueffing, M. (2012). Two-dimensional peptide separation improving sensitivity of selected reaction monitoring-based quantitative proteomics in mouse liver tissue: comparing off-gel electrophoresis and strong cation exchange chromatography. *Analytical Chemistry 84*, 8853-8862.

Schwartz, B.L., and Bursey, M.M. (1992). Some proline substituent effects in the tandem mass-spectrum of protonated pentaalanine. *Biological Mass Spectrometry 21*, 92-96.

Slade, W.O., Ray, W.K., Williams, P.M., Winkel, B.S., and Helm, R.F. (2012). Effects of exogenous auxin and ethylene on the *Arabidopsis* root proteome. *Phytochemistry 84*, 18-23.

Stahl-Zeng, J., Lange, V., Ossola, R., Eckhardt, K., Krek, W., Aebersold, R., and Domon, B. (2007). High sensitivity detection of plasma proteins by multiple reaction monitoring of N-glycosites. *Molecular and Cellular Proteomics 6*, 1809-1817.

Vaudel, M., Sickmann, A., and Martens, L. (2010). Peptide and protein quantification: a map of the minefield. *Proteomics 10*, 650-670.

Wilkins, M.R., Gasteiger, E., Bairoch, A., Sanchez, J.C., Williams, K.L., Appel, R.D., and Hochstrasser, D.F. (1999). Protein identification and analysis tools in the ExPASy server. *Methods in Molecular Biology 112*, 531-552.

Yates, J.R., Gilchrist, A., Howell, K.E., and Bergeron, J.J.M. (2005). Proteomics of organelles and large cellular structures. *Nature Reviews Molecular and Cellular Biology 6*, 702-714.

Zhu, M.M., Dai, S.J., Zhu, N., Booy, A., Simons, B., Yi, S., and Chen, S.X. (2012). Methyl jasmonate responsive proteins in *Brassica napus* guard cells revealed by iTRAQ-based quantitative proteomics. *Journal of Proteome Research 11*, 3728-3742.

Chapter 4

Effects of exogenous auxin on the *Arabidopsis* root proteome as observed using UPLC-Data Independent Acquisition mass spectrometry

William O. Slade[A], Sherry B. Hildreth[A], W. Keith Ray[B], Brenda S.J. Winkel[A], and Richard F. Helm[B]

Departments of Biological Sciences[A], Biochemistry[B]. Virginia Tech, Blacksburg, VA 24061, United States

Contributions

William O. Slade
Designed experiments, performed experiments, analyzed data, and wrote first draft of the manuscript.

W. Keith Ray
Provided technical support.

Richard F. Helm
Conceived experimental idea, designed experiments, analyzed data, and helped write the manuscript.

Sherry B. Hildreth
Provided analytical guidance and technical support.

Brenda S.J. Winkel
Conceived experimental idea, designed experiments, analyzed data, and helped write the manuscript.

I. Abstract

Auxin regulates critical aspects of root development and physiology. The lack of knowledge of how the auxin response is mediated at the protein level represents a major gap in the understanding of plant biology. This study evaluates the effects of treatment with exogenous auxin on the *Arabidopsis* root proteome. Root protein extracts were isolated, converted to peptides, fractionated using strong-cation exchange (SCX) and analyzed using ultra-performance liquid chromatography and data independent acquisition-based mass spectrometry (UPLC-HDMS^{e}). Of the proteins identified, we observed that 30, 25, and 18 were significantly different at 8, 12, and 24 h of exposure, relative to a time-matched control. Interestingly, although the proteins identified at each time point represent similar biological processes, we did not observe consistent regulation of the same protein over multiple time points, in contrast to what is observed in transcript analyses. Thus, while auxin appears to coordinately regulate many physiological events in roots, it does so through regulation of distinct proteins in a time-dependent manner.

II. Introduction

Auxin regulates many critical aspects of root development and physiology, including the response to gravity and light (Buer and Muday, 2005), the orientation and extent of cell division (Overvoorde et al., 2010), and the initiation of lateral roots (Casimiro et al., 2001). These processes are controlled by the establishment and maintenance of distinct intracellular pools of auxin (Overvoorde et al., 2010) generated by cellular- and tissue-specific gradients of the hormone. The maintenance of these specific auxin gradients leads to transcriptional regulation of genes and ultimately manipulation of root physiology. For example, perturbation of the auxin gradient in roots drastically alters the patterning of the root tip (Benjamins and Scheres, 2008).

Proteomic technologies permit interrogation of these processes at the protein level. After exposure to auxin for 2 h, Zhang et al. (2013) observed changes in the phosphorylation status of 20 proteins, including SORTING NEXIN 1 (SNX1), with mutational analysis of serine 16 of SNX1 demonstrating its involvement in lateral root formation. Using a global approach, Deng et al. (2012) uncovered changes in the abundance of 16 proteins after IAA exposure in rye coleoptiles. Given that proteins are often the ultimate effectors of biological function, proteomics technologies can be used to elucidate how auxin affects root biology.

An exciting new approach to the study of complex proteomes is Data-Independent Acquisition (DIA). Traditionally, researchers have used Data-Dependent Acquisition (DDA) methods for the study of complex proteomes. DDA methods select molecular ions of intact peptides for fragmentation based on intensity thresholds. Although DDA is popular due to it's ease of use and high-throughput, it is limited by the dynamic range of complex protein samples (Arsova et al., 2012) and the stochastic nature of molecular ion sampling in DDA (Michalski et al., 2011). In contrast to DDA, DIA fragments many molecular ions simultaneously. The resulting fragment ions are expected to have the same mobility profiles as their parent ions, permitting data processing protocols to align parents ions to their corresponding fragments (Shliaha et al., 2013). Recently, Waters launched the Synapt G2-S, a hybrid quandrupole-TOF instrument that can utilize ion-mobility information to aid in DIA data processing. Researchers have used this set-up to achieve increased accuracy of quantitation (Baker et al., 2010; Valentine et al., 2006) and increased dynamic range (Valentine et al., 2006) over DDA-based methods.

Herein we describe the effects of exogenous auxin on the *Arabidopsis thaliana* root proteome as observed using ultra-performance liquid chromatography high-definition mass spectrometry (UPLC-HDMS^E) (Bond et al., 2013; Shliaha et al., 2013). *Arabidopsis* seedlings were exposed to indole-3-acetic acid (IAA) for 8, 12, or 24 h. Roots were harvested and proteome profiles were analyzed using UPLC-HDMS^E. Although proteins with similar functions in cellular processes were identified as affected by auxin at each time point, there was little overlap between the proteins affected. This is in contrast to analyses at the transcript level (Lewis et al., Submitted), which showed coordinated regulation of the same genes over multiple time points. At least for proteins

observable using UPLC-HDMS^E, the biological effects of auxin appears to be more complex.

III. Results

To characterize the response of the plant root proteome to auxin, *Arabidopsis* Columbia seedlings were grown for 5-6 d following germination on agar plates and transferred to medium containing auxin or no added hormone for 8 h, 12h, or 24 (Figure 4-S1). Roots were excised into liquid nitrogen and protein lysates prepared by a modified phenol-methanol method were digested using an in-solution trypsin digestion protocol.

The mass spectrometer used in this study can perform DIA analyses in two modes, so-called MS^E and HDMS^E. In MS^E mode, the instrument cycles between low-energy scans and high-energy scans, which first record intact precusor masses and then apply a ramp of collision energy to generate fragment ions (Shliaha et al. 2013). HDMS^E mode includes separation of ions using ion-mobility, which can lead to increased accuracy of quantitaiton and a higher dynamic range for peptide detection (Baker et al., 2010, Geromanos, et al., 2012). To determine if ion mobility mode (HDMS^E) is superior to MS^E in terms of protein/peptide identifications, we analyzed unfractionated lysates at a constant loading level of 1 μg and varied the length of the chromatographic separation and the rate of solvent flow. Previously, Shliaha et al. (2013) reported that HDMS^E was superior to MS^E in terms of peptide and protein identification. We observed that regardless of the space of chromatographic separation or rate of solvent flow, HDMS^E yields at least 50% more protein identifications than MS^E for our unfractionated protein lysate from *Arabidopsis* roots (Table 4-S1). Hence all subsequent work was performed in HDMS^E mode.

To assess the technical variation of our LC-MS set up, we analyzed unfractionated protein lysates using duplicate injections. As technical replicates showed excellent reproducibility (Figure 4-S2), we focused our analyses on biological replicates. To account for intrinsic biological variation, three biological replicates were used. In order to increase our coverage of the *Arabidopsis* root proteome, we fractionated peptides using strong-cation exchange (SCX) chromatography and then analyzed the resulting fractions using UPLC-HDMS^E.

In order to identify and quantify proteins that exhibited changes in abundance after auxin treatment, we utilized Scaffold (v3.4.9). Initially, proteins identifications were assigned using Protein Lynx Global Server 3.0 (PLGS). PLGS over estimates protein and peptide assignments and lacks a reliable interface for inter- and intra-treatment comparisons. Hence, Scaffold was used for protein assignments and for statistical analyses. Only proteins meeting stringent criteria (99% protein minimum, 95% peptide minimum, and two peptides per protein) were considered for this analysis. Additionally, protein false-discovery rate was kept to ≤ 2% per time point and peptide false discovery rate (FDR) was kept to ≤ 1.5% (Table 4-S2). We identified between 362 to 416 proteins at each time point, and observed overlap between combined biological replicates per time point in the range of 97-99% (Figure 4-S3). At the peptide level, we identified between 1328 to 1488

peptides at each time point, and observed overlap between combined biological replicates per time point in the range of 72-86% (Figure 4-S4).

In order to uncover proteins differentially accumulating at each time point, we used spectral counting in Scaffold and applied a t-test ($p \leq 0.05$). At 8 h, IAA treatment resulted in the change in abundance of 25 proteins, with 22 increased and three decreased (Table 4-1). Treatment with IAA for 12 h resulted in the change in abundance of 30 proteins, with 17 increased and 13 decreased (Table 4-2). Finally, treatment with IAA for 24 h resulted in the change in abundance of 18 proteins, with 13 increased and five decreased (Table 4-3). To our surprise, only three proteins overlap in regulation after 8 and 12 h of IAA treatment (Figure 4-1). No individual proteins were altered in abundance across the entire time-course treatment or between 8 h or 12 h and 24 h.

IV. Discussion

Auxin regulates many aspects of plant biology. Treatment with exogenous auxin ablates root elongation (Ishikawa and Evans, 1997), induces lateral root formation, and globally affects gene transcription (Nemhauser et al., 2004; Stepanova et al., 2007). At the transcriptional level, treatment with exogenous auxin stimulates a rapid increase in the *GH3*, *SAUR*, and *AUX/IAA* families (Chapman and Estelle, 2009) and precipitates global transcriptional changes that peak from 2 to 8 h and return to baseline around 12 to 24 h (Lewis et al., 2013). These changes correlate at the physiological level with a rapid ablation of root elongation and a slower (around 8 h) induction of lateral root formation (Lewis et al., 2013). In order to better understand the auxin response at the protein level, we exposed *Arabidopsis* seedlings to 1 μm IAA (Lewis et al., 2013) for 8, 12, or 24 h and analyzed root proteome profiles using UPLC-HDMS^E. The results indicate that auxin signaling over our time course occurs through the regulation of proteins representing many similar biological functions. However, there was nosubstantial regulation of the same proteins over different time points. Thus, while auxin coordinately regulates gene expression and physiology over our time course in *Arabidopsis* roots, it appears to do so more by regulating proteins of similar biological functions as opposed to regulating the same proteins that can be quantified using UPLC-HDMS^E over the time course evaluated.

Treatment with IAA increased the abundance of several proteins involved in glucose metabolism. After 8 h of treatment, the abundance of plastidic glyceraldehydge-3-phosphate dehydrogenase, fructose bisphosphate aldolase, and phosphoglycerate mutase all increased. Additionally, after 12 h of treatment IAA increased the abundance of RuBisCO large and small subunits (LSU and SSU). In light-grown roots, the peak of auxin-induced changes in gene expression occurs 2 to 8 h after treatment (Lewis et al., 2013). At the physiological level, auxin induces statistically significant lateral root formation beginning at 8 h, and accumulation of the DR5:GFP protein is maximal at 12 h (Lewis et al., 2013). Perhaps an IAA-induced upregulation of glycolysis via changes in protein abundance provides energy for changes at the gene and physiological levels, peaking around approximately 8 h. This increased glycolytic activity could result in increased mitochondrial activity and thus increased CO_2 production, which could in turn

be scavenged by RuBisCO LSU, a role that has been proposed before (Schwender et al., 2004; Slade et al., 2012). Previously, we reported that treatment with IAA increased the abundance of RuBisCO LSU after 24 h of treatment (Slade et al. 2012). Here, our data also suggests an increase in abundance after 24 h (Figure 4-S5) although it does not meet our p-value filter (0.14). Nonetheless, future studies targeting RuBisCO LSU and its role in auxin-mediated processes are warranted.

The cell wall is a dynamic structure that is continuously modified in a temporal and spatial manner in order to respond to environmental stimuli, including auxin (Cosgrove, 2005; Sanchez-Rodriguez et al., 2010). Here, we observe an increase in the abundance of root hair defective 1 (RHD1), an UDP-glucose-4-epimerase, after 8 and 12 h exposure to auxin. The galactosylation of xyloglucan and arabinogalactan II in a cell-type dependent manner requires RHD1, with mutants at the *RHD1* locus exhibiting abnormal root hair development and root morphology (Rosti et al., 2007; Schiefelbein and Somerville, 1990; Seifert et al., 2002). Higher RHD1 levels could lead to higher RHD1 activity, and could indicate that increased channeling of UDP-D-galactose into cell wall polymers is required for the root response to auxin. Interestingly, we previously reported that rhamnose biosynthesis 1 (RHM1), a putative synthase that converts UDP-D-glucose to UDP-L-rhamnose, is decreased in abundance in light-grown roots after 24 h exposure to auxin (Slade et al., 2012). Thus, opposing regulation of RHD1 and RHM1 protein levels by auxin could affect the incorporation of specific sugar moieties into the cell wall.

Table 4-1. Identities of proteins that change in abundance after treatment with IAA for 8 h.

Proteins differentially accumulating at 8 hours			
Uniprot	**Protein**	**Fold change**	**P-value**
Q9M9K1	Probable 2,3-bisphosphoglycerate-independent phosphoglycerate mutase 2	Present in IAA Only	0.00006
Q8LBW1	Putative lectin	3	0.00049
Q41931	1-aminocyclopropane-1-carboxylate oxidase 2	0.25	0.005
Q39258	V-type proton ATPase subunit E1	3	0.0054
Q9C9C5	60S ribosomal protein L6-3	5	0.0063
Q9C5I5	Putative nuclear DNA-binding protein G2p	2.3	0.0064
Q9C7W7	UDP-glucose 4-epimerase 4 (RHD1)	1.8	0.019
O23629	Histone H2B.6	3	0.019
P56778	Photosystem II CP43 chlorophyll apoprotein	1.5	0.022
Q94B39	H+-transporting ATP synthase-like protein	1.7	0.022
Q0WM29	Methymalonate-semialdehyde dehydrogenase [acylating], mitochondrial	Present in IAA only	0.027
F4IL99	Peptidyl-prolyl cis-trans isomerase CYP19-1	Present in IAA only	0.027
Q9LF98	Fructose-bisphosphate aldolase	2.2	0.031
O23157	Protein maternal effect embryo arrest 59	1.9	0.033
P25857	Glyceraldehyde-3-phosphate dehydrogenase GAPB, plastidic	1.5	0.035
Q9STX5	Endoplasmin homolog	0.7	0.036
Q42589	Non-specific lipid-transfer protein 1	Present in IAA only	0.036
Q07473	Chlorophyll a-b binding protein CP29.1, plastidic	1.9	0.036
P25873	50S ribosomal protein L15, chloroplastic	0.5	0.037
Q9ZUC1	Quinone oxidoreductase-like protein At1g23740, plastidic	2.3	0.037
Q9ZVS4	Aspartyl protease-like protein	1.7	0.038
Q9M5K3	Dihydrolipoyl dehydrogenase 1, mitochondrial	1.3	0.038
P53492	Actin-7	1.7	0.039
Q1JPL7	Pectinesterase/pectinesterase inhibitor 18	1.3	0.045
Q9FVT2	Probable elongation factor 1 gamma 1	Present in IAA only	0.048

Table 4-2. Identities of proteins that change in abundance after treatment with IAA for 12 h

Proteins differentially accumulating at 12 hours			
Uniprot	**Protein**	**Fold Change**	**P-value**
F4JLP5	dihydrolipoyl dehydrogenase	0.4	0.0013
Q9ZUX4	Uncharacterized protein At2G27730, mitochondrial	Present in Control only	0.0069
Q9SDS7	V-type proton ATPase subunit C	2	0.0085
Q38946	Glutamate dehydrogenase 2	Present in IAA only	0.0089
O23708	Proteasome subunit alpha type 2-A	Present in IAA only	0.0089
F4K7T6	1-deoxy-D-xyulose 5-phosphate reductoisomerase	Present in IAA only	0.0089
P10795	Ribulose bisphosphate carboxylase small chain 1A, chloroplastic	2.3	0.0091
O03042	Ribulose bisphosphate carboxylase large chain	Present in IAA only	0.012
Q9SUQ9	Putative major latex protein	Present in IAA only	0.017
Q9CAX6	40S ribosomal protein S14-2	2.3	0.017
Q8GUM2	Heat shock 70 kDa protein 9, mitochondrial	1.7	0.018
Q42564	L-ascorbate peroxidase 3, peroxisomal	Present in Control only	0.018
Q9SRG3	Protein disulfide isomerase-like 1-2	Present in IAA only	0.019
P25697	Phosphoribulokinase, chloroplastic	0.5	0.02
Q9C7W7	UDP-glucose 4-epimerase 4 (RHD1)	1.5	0.022
O64517	Metacaspase-4	Present in IAA only	0.024
Q8W585	ATP-dependent zinc metalloprotease FTSH8, chloroplastic	0.3	0.026
Q9FMV1	Gamma carbonic anhydrase-like 1, mitochondrial	0.5	0.03
P56792	50 S ribosomal protein L14, chloroplastic	0.6	0.031
Q93YR3	FAM10 family protein	0.4	0.034
P59271	Ubiquitin-40 S ribosomal protein s27a-1	1.8	0.035
Q9ZV24	Outer envelope pore protein 16-1, chloroplastic	1.1	0.037
Q9SMT7	4-coumarate-CoA ligase-like 10	1.4	0.042
Q41931	1-aminocyclopropane-1-carboxylase oxidase 2	1.6	0.043
A8MQR4	60S acidic ribosomal protein P0-2	0.3	0.043
Q94JQ4	Endoribonuclease L-PSP family protein	Present in IAA Only	0.044
Q9SGA6	40 S ribosomal protein S19-1	0.48	0.045
Q9LW57	Probable plastid-lipid-associated protein 6, chloroplastic	0.6	0.045

Table 4-3. Identities of proteins that change in abundance after treatment with IAA for 24 h.

Proteins differentially accumulating at 24 hours			
Uniprot	**Protein**	**Fold change**	**P-value**
P0DKC3/P0DKC4	Phosphoglycerate phosphatase 1A/1B, chloroplastic	Present in IAA only	0.000016
Q9XF91	Photosystem II 22 kDa protein, chloroplastic	4.3	0.0004
Q9STF2	Protein plastid transcriptionally active 16	3.3	0.0044
Q9XF89	Chlorophyll a-b binding protein CP26, chloroplastic	5.1	0.0063
Q0WWW3/Q93VR3	GDP-mannose 3',5'-epimerase	Present in IAA only	0.0081
Q9SMW7	BTF3b-like factor	Present in IAA only	0.012
Q8W4S4	Vacuolar proton ATPase a3	2.4	0.012
Q9M158	Rhodanese-like domain-containing protein 4, chloroplastic	3.2	0.018
Q94BN4	Putative methionine synthase	2.8	0.019
P47999	Cysteine synthase, plastidic	2.5	0.021
Q9ZNZ7	Ferredoxin-dependent glutamate synthase 1, plastidic/mitochondrial	0.5	0.031
A8MS83	60S ribosomal protein L23a-2	1.2	0.033
O23144	Proton pump-interactor 1	Present in Control only	0.037
Q0WL56	Elongation factor 1-alpha 3	2.5	0.039
Q42522	Glutamate-1-semialdehyde 2,1-aminomutase 2, plastidic	0.5	0.042
P16181	40S ribosomal protein S11-1	0.6	0.044
Q9SCY0	Phophoglucomutase, plastidic	1.8	0.046
Q9SZD6	Elongation factor Ts	0.5	0.049

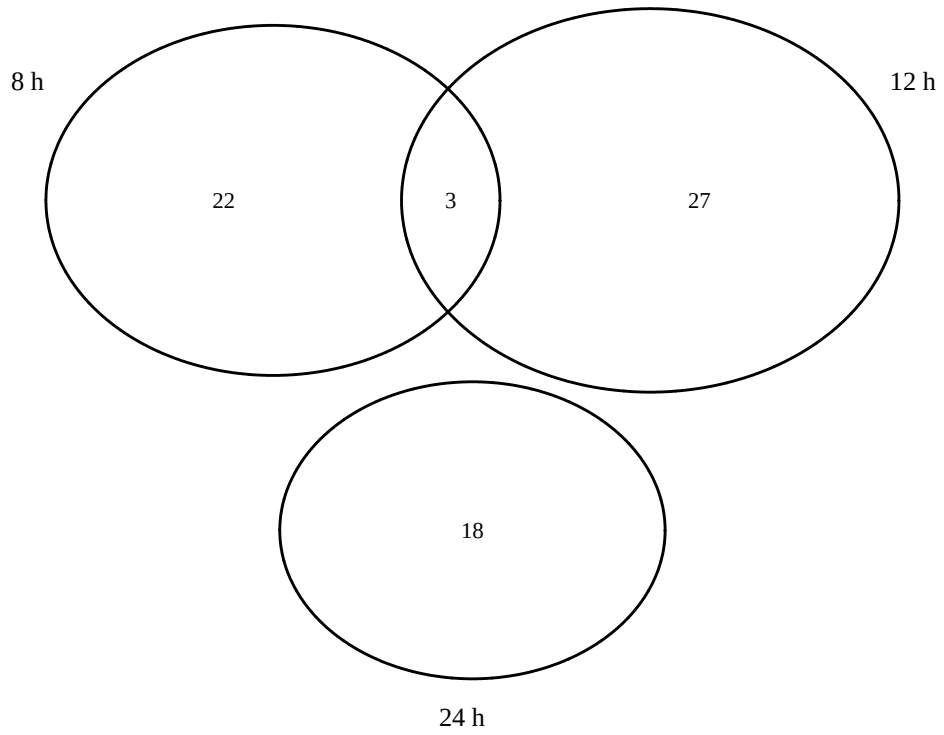

Figure 4-1. Three-way Venn diagram. Shows the overlap among differentially-accumulating proteins after IAA treatment at the three time points.

The cytoskeleton facilitates a cell's response to environmental stimuli by controlling cell proliferation, cell expansion, and cell differentiation (Wasteneys and Galway, 2003). Previously, we hypothesized that the cytoskeleton is regulated by auxin and reported that treatment with IAA for 24 h in light-grown roots decreases the abundance of TUA2/4, a structural constituent of the cytoskeleton (Slade et al., 2012). In this study, treatment with IAA for 8 h increased the abundance of ACT7, a gene previously shown to be responsive to auxin and required for cell proliferation and callous formation. Thus, a plausible hypothesis is that auxin regulates specific proteins involved in the formation and maintenance of the cytoskeleton in a temporally controlled manner, which has been proposed previously (Meagher et al., 2011).

We observed that treatment with IAA for 8, 12, or 24 h affects proteins of similar biological processes but generally not the same protein at more than one time point. In contrast to these results, analyses of changes in gene transcription in light-grown roots over a similar time-course reveals that auxin affects the abundance of many transcripts over several time points (Lewis, 2013). However, we also observe that treatment with IAA affects changes in the root metabolite pool distinctly at individual time points without overlap (Hildreth et al. unpublished results). One possibility is that changes at the transcript level must be sustained for a longer period of time than protein or metabolite changes to precipitate a biological effect. Additionally, global protein and

metabolite analyses currently only reflect snapshots of steady-state levels, which do not reflect protein and metabolite flux that perhaps occur much faster or more dynamically than changes in transcript levels.

Our dataset displays little overlap with analyses at the transcript level or with our previous protein dataset obtained by a 2D-gel approach (Table 4-S3, Figure 4-S6) (Lewis, 2013; Slade et al., 2012). An observable proteome is dependent upon the methodology used (Alvarez et al., 2009) and different analytical strategies often yield complementary proteomes (Alvarez et al., 2013). Additionally, transcript abundance correlates poorly with protein abundance in *Arabidopsis* roots (Petricka et al., 2012). Thus, our dataset represents a complementary proteome that can serve the community as a resource for understanding how auxin elicits changes in biology through modulating protein abundances.

Analyses of T-DNA insertion lines (Alonso, 2003) for genes encoding the proteins identified here can serve as a proof-of-concept for our approach. We selected 54 T-DNA lines representing 32 auxin-responsive genes and characterized the presence of a homozygous T-DNA insertion using PCR. Thirty-one lines were confirmed to be homozygous for the T-DNA insertion. One gene (AT1G11580) encodes PME18, a putative pectinesterase involved in the formation and maintenance of cell walls. Indeed, Lewis et al. (2013) observed a consistent increase in the transcript level of *pme18* in response to exogenous auxin over a 24 h time-course, while we observed an increase in PME18 protein abundance after 8 h of treatment with auxin (Figure 4-S7). At the physiological level, preliminary analyses of one of our T-DNA lines homozygous for insertion (*pme18-1)* displayed reduced lateral root formation. Additionally, induction of lateral root formation by application of exogenous auxin was normal. These results suggest our approach can find physiological relevant players in the auxin response.

To summarize, the present study examines how treatment with exogenous IAA for 8, 12, or 24 h affects the levels of proteins in *Arabidopsis* roots observable by UPLC-HDMS$^{E.}$ Across the time course, IAA affected the abundance of proteins involved in many biological processes, including glycolysis, the maintenance and formation of cell walls, and cytoskeleton dynamics. In contrast to what occurs at the transcript level, treatment with IAA generally did not affect the same proteins at different time points, although this distinct regulation mirrors what is observed at the metabolite level. Current efforts are aimed at exploring how the proteins observed in this study connect with previously identified genes and metabolites to regulate the auxin response.

V. Experimental

i. Plant material

Plant material was prepared according to Slade et al. (2012). Briefly, seeds of the Columbia (Col-0) ecotype of *Arabidopsis* were obtained from Lehle Seeds (Round Rock, Texas). Plants were grown on 1X Musharige and Skoog medium from Caisson labs (North Logan, Utah) pH 5.7, 0.8% (w/v) agar, and supplemented with 1% (w/v) sucrose. After cold treatment for 48-72 h at 4°C, seeds were moved to a growth chamber and

grown under 100 μmol m^{-2} s^{-2} cool-white light (24 h lightning). The growth chamber was maintained at 22°C and 60% relative humidity. All assays were conducted 5 d after germination, which was typically 6-7 d after the cold treatment.

ii. Hormone treatments

Hormone-transfer assays were conducted as described by Lewis et al. (2011). Plants were germinated on nylon mesh (03-100/32; Sefar Filtration, Depew, NY) pressed tightly against control medium, with approximately 200 seedlings per plate. At 5 d post-germination, the filter was transferred to a control plate or medium supplemented with 1 μM IAA. After 8, 12, or 24h, seedlings were collected and immediately frozen in liquid N_2. A razor blade was then used to carefully excise the roots at the root-shoot junction. Samples were stored at -80°C until protein extraction.

iii. Protein extraction

Each biological replicate (~150 mg) of root tissue was ground to a fine powder and mixed with three volumes of SDS extraction buffer (100 mM Tris-HCl, pH 8.0, 2% SDS (v/v), 1% β-mercaptoethanol (v/v), 5 mM EGTA, 10 mM EDTA), heated for 10 min at 65°C, and then centrifuged at 6710 *g* for 20 min. The supernatant was mixed with 1 volume of ice-cold Tris-buffered phenol, pH 7.5, and centrifuged at 6710 *g* for 6 min to separate the aqueous and phenol phases. The aqueous phase was removed leaving the interface intact, and the phenol phase was extracted twice with ice-cold 50 mM Tris-HCl, pH 8.0, then mixed with 5 volumes of ice-cold 0.1 M $(NH_4)OAc$ in MeOH, once with EtOH, and then resuspended in resuspension buffer (7 M Urea, 2 M thiourea, 4% CHAPS (w/v). After centrifugation, protein concentration was determined using the 2D-Quant Kit (GE Healthcare; Piscataway, NJ) using BSA as a standard. This extraction method yielded 0.4-0.6 mg protein per biological replicate.

iv. In-solution digestion

Disulfide bonds were reduced using 5 mM tris-carboxyethylphosphine at room temperature for 30 min and then alkylated using 50 mM iodoacetamide at room temperature in the dark for 40 min. Samples were diluted with 50 mM ammonium bicarbonate so that the urea concentration was 1.6 M, and then trypsin (Promega, Madison, WI) was added at a 50:1 ratio of protein:trypsin and incubated at 37°C for 16 h. Reactions were quenched by the addition of TFA to a final concentration of 1% (v/v).

v. C18-RP SPE and Ion-exchange chromatography

Samples were evaporated to near dryness using a vacuum centrifuge and then resuspended in 1 mL 95% water, 5 ACN, 0.1% TFA by sonication for 20 min. After centrifugation, the pH was adjusted to ≤ 3 if necessary using 5% TFA. C18RP-SPE was performed using Sep-Pak 1cc C18 cartridges (Waters, Milford, MA). Cartridges were washed using 2 mL of MeOH and equilibrated with 4 mL 0.1% TFA. Samples were loaded using gravity flow and then the original tubes were rinsed with 1 mL 95% water, 5% ACN, 0.1% TFA and the rinse also loaded. Cartridges were then washed with 3 mL 95% water, 5% ACN, 0.1% TFA. Peptides were eluted using 2 mL 60% ACN, 0.1% TFA.

ACN was removed using a vacuum centrifuge and samples were diluted to 4 mL using 10 mM KH_2PO_4, pH 3.0, 25% CH_3OH. Strata-X-C 33u cartridges (Phenomenex, Torrance, CA) were washed 1 mL MeOH and then equilibrated with 3 mL 10 mM KH_2PO_4, pH 3.0, 25% CH_3OH. After centrifugation of the samples, the pH was checked and adjusted to ≤ 3 using H_3P0_4 if necessary. Samples were loaded using gravity flow and then the original tubes were rinsed with 1 mL 10 mM KH_2PO_4, pH 3.0, 25% CH_3OH and that rinse was added to the cartridge. Cartridges were washed with 3 mL 10 mM KH_2PO_4, pH 3.0, 25% CH_3CH. Peptides were eluted in six steps using increasing concentrations of KCl in 10 mM KH_2PO_4, pH 3.0, 25% CH_3OH: 25 mM, 50 mM, 75 mM, 150 mM, 350 mM, and 1 M. ACN was removed using a vacuum centrifuge and samples were desalted using C18-RP SPE as described above. ACN was removed using a vacuum centrifuge and samples were then freeze-dried and stored at -80°C until further use.

vi. LC-MS configuration

Peptides were separated using an Acquity UPLC system (Waters; Milford, MA). The mobile phases were 0.1% formic acid (aqueous) and acetonitrile with 0.1% formic acid (organic). The samples were injected in 10 μL volume at an approximate concentration of 0.1 mg/ml. The separation was performed on a C18 CSH130 1.7μ 1.0 x 150 mm column (Waters; Milford, MA) at 50 μL/min flow rate using a 120 min gradient from 3-40% organic. After separation, the column was washed with 90% organic for 5 min and re-equilibrated with 5% organic for 15 min. The column temperature was maintained at 40°C. To incorporate lock-mass correction, one-hundred fmol/μL [Glu1]-fibrinopeptide B was infused at 10 μL/min in 30 sec intervals.

Mass spectrometric analysis of peptides was performed on a Synapt G2-S HDMS mass spectrometer (Waters, Manchester, UK) in $HDMS^E$ mode using settings suggested by the manufacturer. The Synapt G2-S was operated at a scan speed of 1.2s and in resolution mode (Supplemental Figure 4-8). For fragmentation in $HDMS^E$ mode, the collision energy was linearly ramped in the transfer region of the TriWave from 20-50 V (Supplemental Figure 4-9) across the duration of the high-energy scan.

vii. Data Analysis

Data processing was performed in PLGS 3.0, with the data lock mass corrected post acquisition. Noise reduction thresholds for low-energy scan ion, high-energy scan ion, and peptide intensity were fixed at 150, 10, and 750 counts, respectively. Protein identifications were obtained utilizing Mascot Daemon v. 2.2.2 (Matrix Science, Inc., Boston, MA), which automatically submitted peak lists as .pkl files to a local Mascot Server v. 2.2.2 (Matrix Science, Inc., Boston, MA) search engine utilizing the *Arabidopsis* protein database (NCBInr 20100131) appended with its reverse decoy. Charge state deconvolution and de-isotoping were not performed. Searches used trypsin specificity, the possibility of 1 missed cleavage, a peptide tolerance of 20 ppm, a MS/MS tolerance of 0.01 Da (Supplemental Table T4), with static modification of carbamidomethylation at cysteine and variable modification of oxidation at methionine.

Scaffold (v3.4.9) was used to validate MS/MS based peptide and protein identifications and quantify the data based on spectral counting. Peptide identifications were accepted if

they could be established at greater than 95.0% probably according to the Peptide Prophet algorithm (Keller et al., 2002). Protein identifications were accepted if they could be established at greater than 99.0% probability and contained at least 2 identified peptides. Protein probabilities were assigned by the Protein Prophet algorithm (Nesvizhskii et al., 2003). Proteins that contained similar peptides and could not be differentiated based on MS/MS analysis alone were grouped to satisfy the principles of parsimony.

VI. Supplemental

Table 4-S1. Analysis of MS^E versus $HDMS^E$ using intensity mode at a constant loading level, different gradient lengths, and different flow rates.

Loading (µg)	Gradient_Length (min)	Flow_rate (µl/min)	MS^E Protein IDs	$HDMS^E$ Protein IDs
1	100	50	393	866
1	160	50	400	872
1	200	50	254	792
1	100	20	278	632
1	160	20	345	624
1	200	20	116	785

Table 4-S2. Number of proteins and peptides identified and corresponding false discovery (FDR) rates.

TimePoint)	Proteins)	Protein_FDR)	Spectra)	Pep4de_FDR)
8"	416"	2%"	5335"	1.50%"
12"	362"	2%"	4874"	1.40%"
24"	392"	1.30%"	4636"	0.80%"

Table 4-S3. Evaluation of the effect of MS/MS tolerance (Da) parameters on data quality for the merged control samples at the 8 h time point.

MS/MS Tol. (Da)	Proteins	Protein FDR	Spectra	Peptide FDR
0.01	277	1.8%	1094	1.9%
0.05	298	4.2%	1113	3.1%
0.1	316	4.6%	1165	3.3%

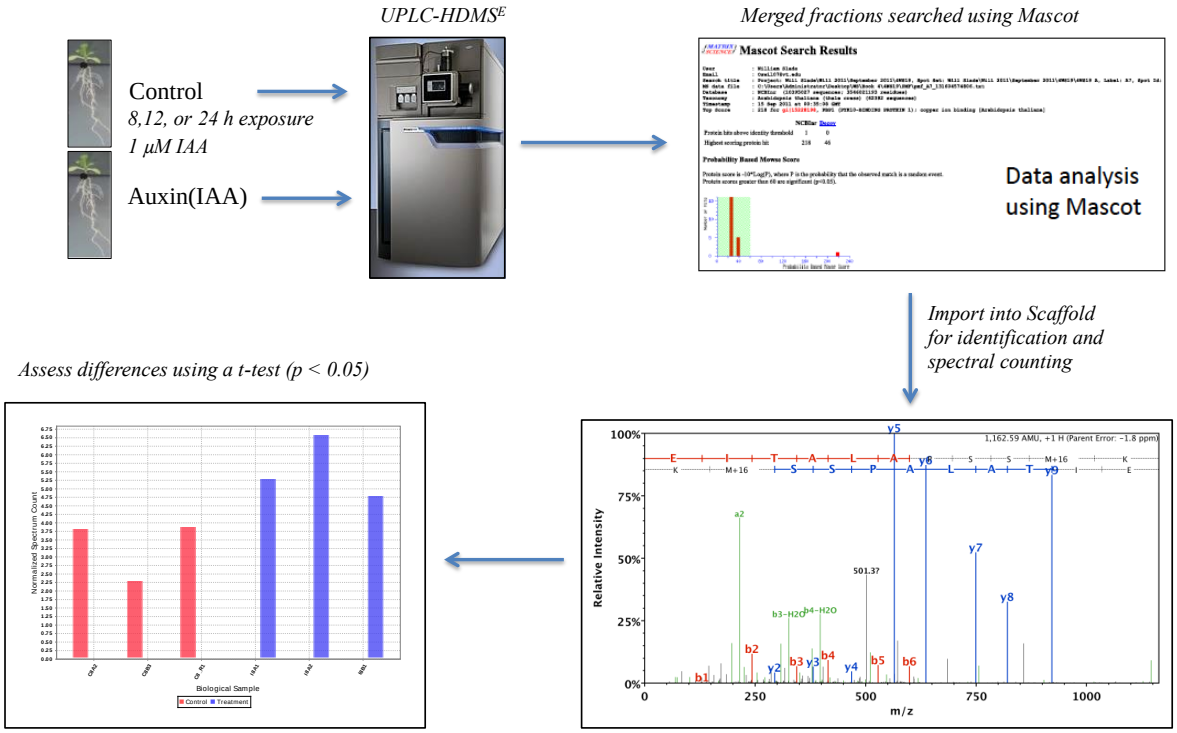

Figure 4-S1. Experimental schematic.

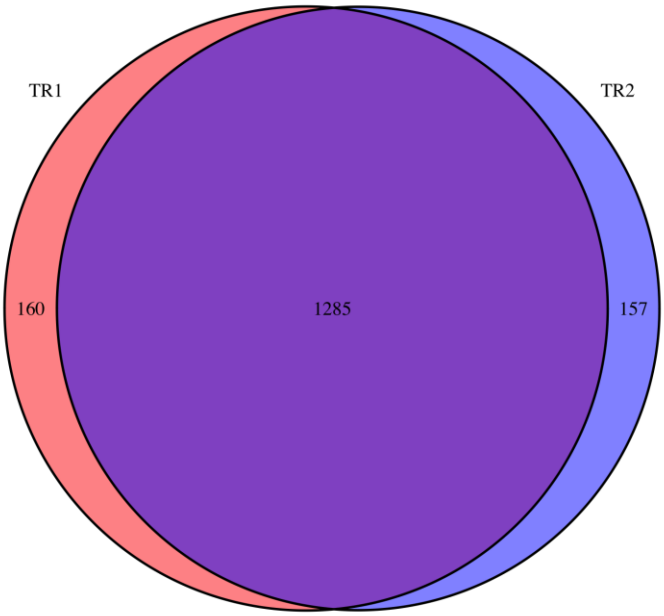

Figure 4-S2. Comparison of the reproducibility of unfractionated technical replicates at the level of protein identifications.

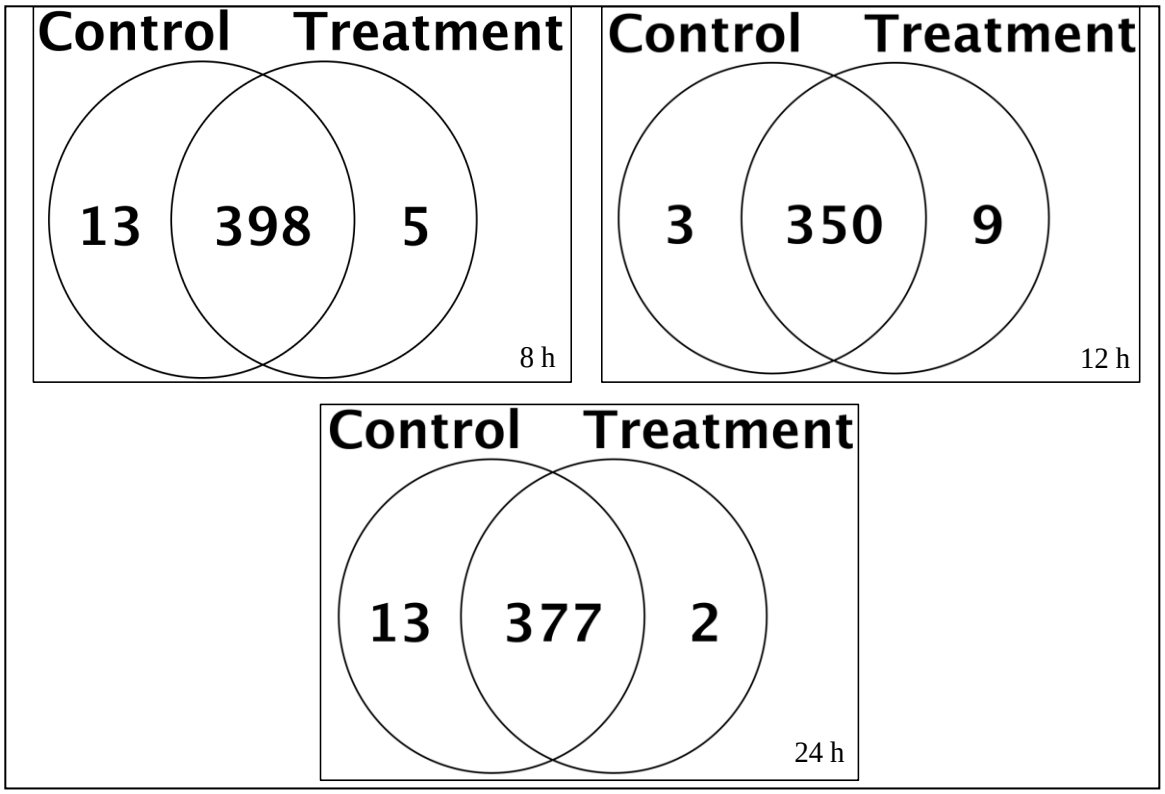

Figure 4-S3. Venn diagram comparing the proteins identified at each time point and the overlap between combined Control (no IAA) and Treatment (+ IAA) biological replicates.

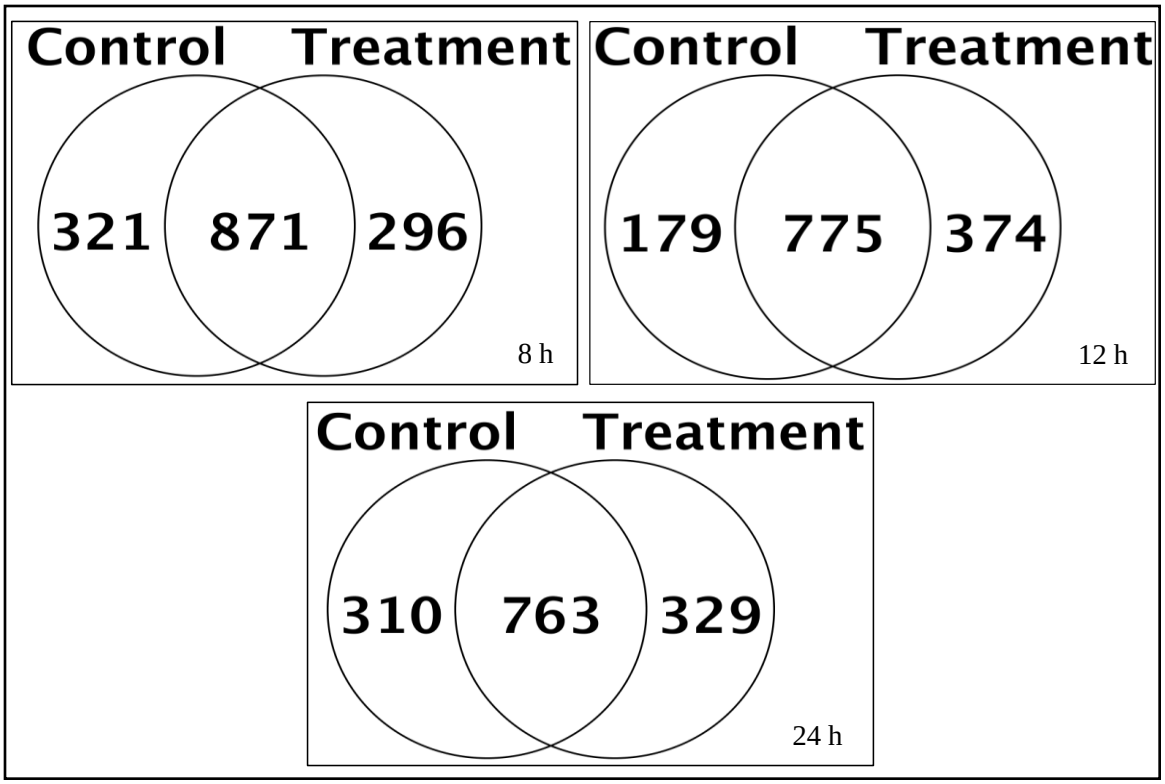

Figure 4-S4. Venn diagram comparing the peptides identified at each time point and the overlap between combined Control (no IAA) and Treatment (+ IAA) biological replicates.

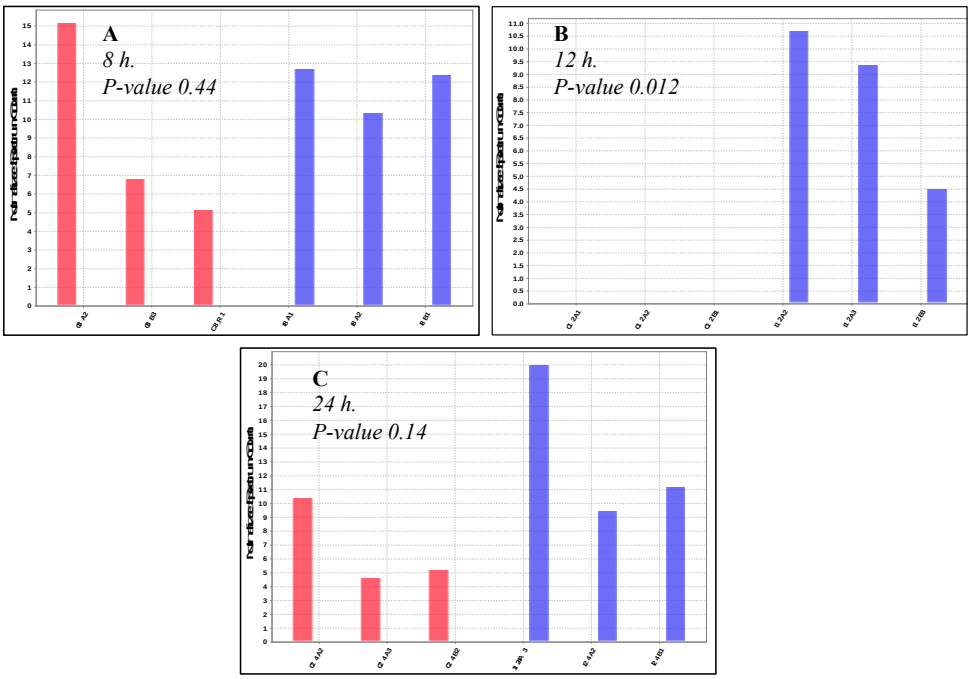

Figure 4-S5. Comparison of RuBiSCo LSU proteins levels across the time-course, with control values in red and treatment values in blue.

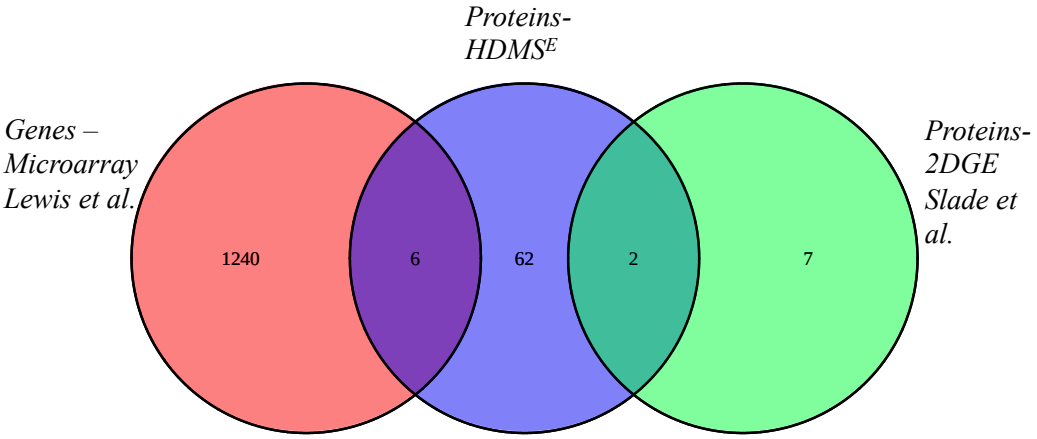

Figure 4-S6. Three-way Venn diagram demonstrating the overlap among our dataset, a comparable microarray dataset, and our previously published protein dataset.

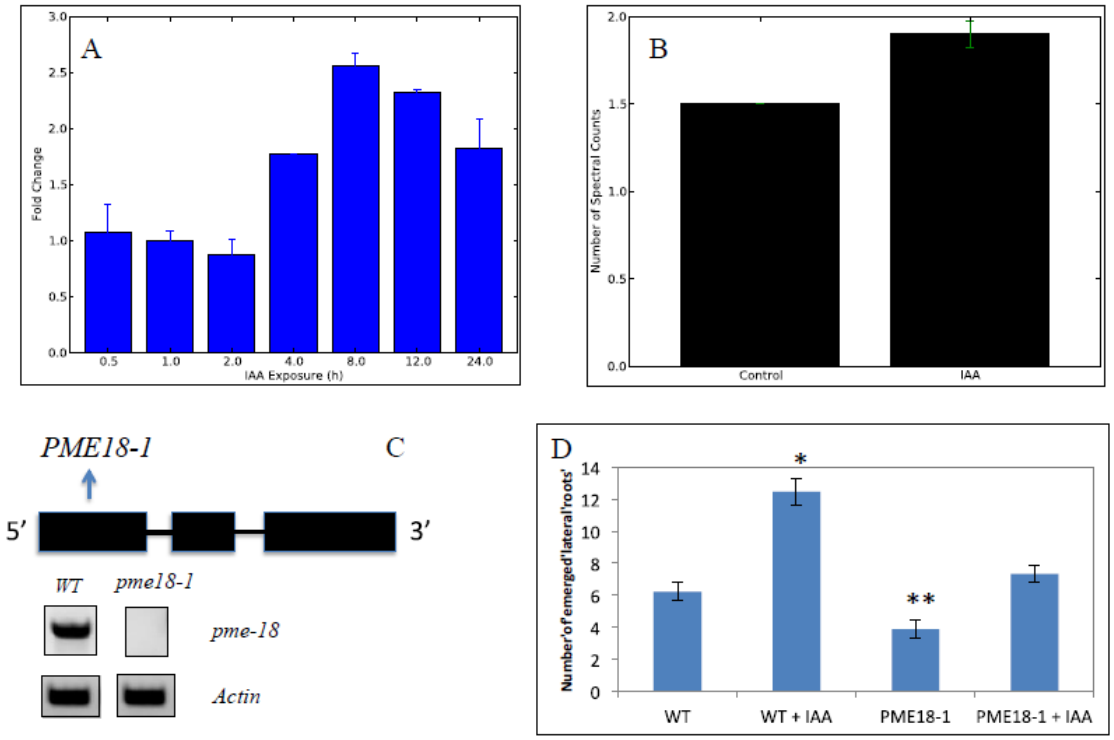

Figure 4-S7. *pme18* mediates lateral root formation. Exogenous auxin increases the transcript level of *pme18* relative to a time-matched control over a 24 h time-course (A) and increases the protein abundance of PME18 after 8 h (B). A homozygous T-DNA insertion was characterized and named *pme18* (C). *pme18* exhibits less lateral root formation and a normal response to exogenous auxin (D). Statistics were performed using a t-test in excel compared to the WT distribution. * $p < 0.03$, ** $p < 0.05$.

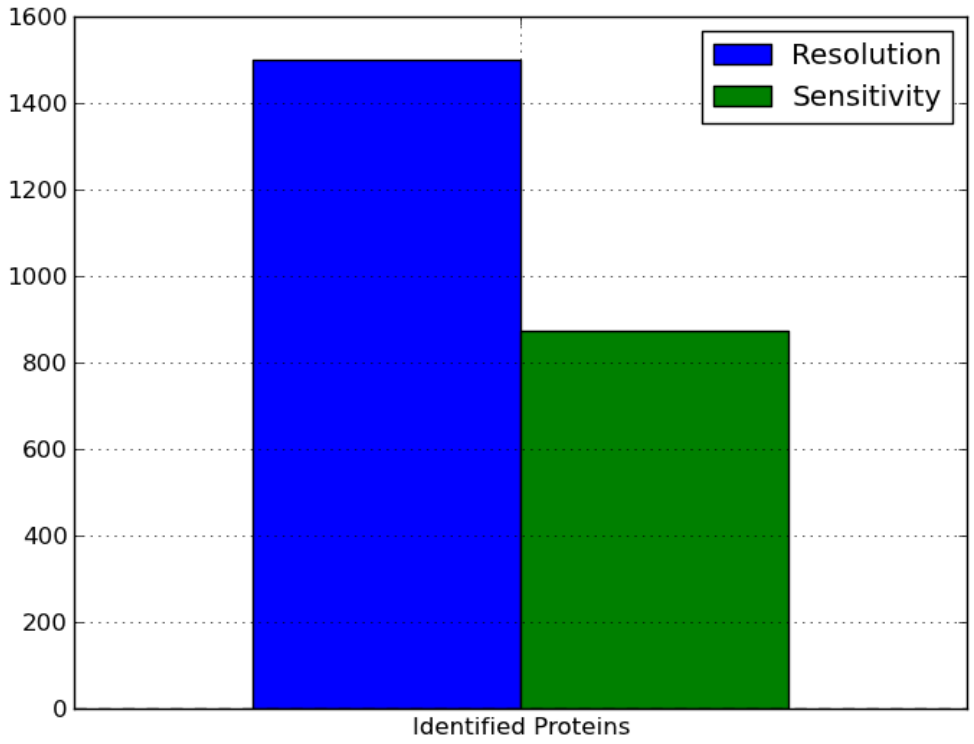

Figure 4-S8. Comparison of identified proteins in an unfractionated lysate using UPLC-HDMS^{E} in sensitivity or resolution mode.

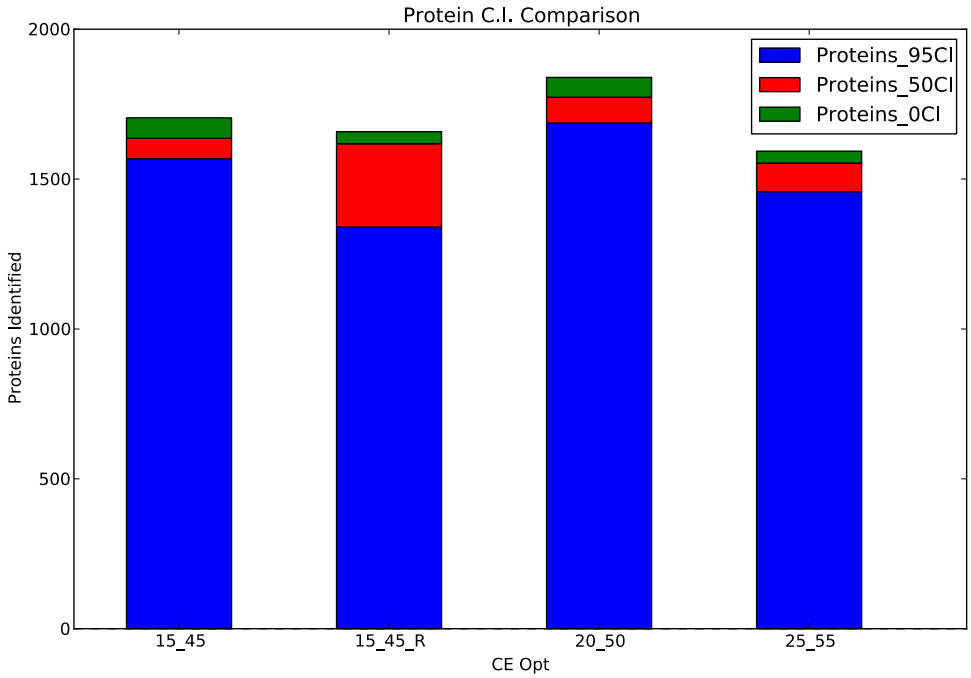

Figure 4-S9. Comparison of identified proteins using different collision energy ramps in HDMS^E mode. Protein hits are grouped according to their confidence interval association, as determined by PLGS 3.0

VII. References

Alonso, J. M., 2003. Genome-wide insertional mutagenesis of *Arabidopsis thaliana* (vol 301, pg 653, 2003). *Science* 301, 1849-1849.

Alvarez, S., Berla, B. M., Sheffield, J., Cahoon, R. E., Jez, J. M., Hicks, L. M., 2009. Comprehensive analysis of the *Brassica juncea* root proteome in response to cadmium exposure by complementary proteomic approaches. *Proteomics* 9, 2419-2431.

Alvarez, S., Choudhury, S. R., Hicks, L. M., Pandey, S., 2013. Quantitative proteomics-based analysis supports a significant role of GTG proteins in regulation of ABA response in *Arabidopsis* roots. *Journal of Proteome Research* 12, 1487-1501.

Arsova, B., Zauber, H., Schulze, W. X., 2012. Precision, proteome coverage, and dynamic range of *Arabidopsis* proteome profiling using N-15 metabolic labeling and label-free approaches. *Molecular and Cellular Proteomics* 11, 619-628l

Baker, E. S., Livesay, E. A., Orton, D. J., Moore, R. J., Danielson, W. F., 3rd, Prior, D. C., Ibrahim, Y. M., LaMarche, B. L., Mayampurath, A. M., Schepmoes, A. A., Hopkins, D. F., Tang, K., Smith, R. D., Belov, M. E., 2010. An LC-IMS-MS platform providing increased dynamic range for high-throughput proteomic studies. *Journal of Proteome Research* 9, 997-1006.

Benjamins, R., Scheres, B., 2008. Auxin: the looping star in plant development. *Annual Review of Plant Biology* 59, 443-465.

Bond, N. J., Shliaha, P. V., Lilley, K. S., Gatto, L., 2013. Improving qualitative and quantitative performance for MSE-based label-free proteomics. *Journal of Proteome Research* 12, 2340-2353.

Buer, C. S., Muday, G. K., 2005. The *transparent testa4* mutation prevents flavonoid synthesis and alters auxin transport and the response of *Arabidopsis* roots to gravity and light (vol 16, pg 1191, 2004). *Plant Cell* 17, 2614-2614.

Casimiro, I., Marchant, A., Bhalerao, R. P., Beeckman, T., Dhooge, S., Swarup, R., Graham, N., Inze, D., Sandberg, G., Casero, P. J., Bennett, M., 2001. Auxin transport promotes *Arabidopsis* lateral root initiation. *Plant Cell* 13, 843-852.

Chapman, E. J., Estelle, M., 2009. Mechanism of auxin-regulated gene expression in plants. *Annual Review of Genetics* 43, 265-285.

Cosgrove, D. J., 2005. Growth of the plant cell wall. *Nature Reviews Molecular Cellular Biology* 6, 850-861.

Deng, Z., Xu, S., Chalkley, R. J., Oses-Prieto, J. A., Burlingame, A. L., Wang, Z. Y., Kutschera, U., 2012. Rapid auxin-mediated changes in the proteome of the epidermal cells in rye coleoptiles: implications for the initiation of growth. *Plant Biology* 14, 420-427.

Ishikawa, H., Evans, M. L., 1997. Novel software for analysis of root gravitropism: Comparative response patterns of *Arabidopsis* wild-type and axr1 seedlings. *Plant Cell Environment* 20, 919-928.

Keller, A., Nesvizhskii, A. I., Kolker, E., Aebersold, R., 2002. Empirical statistical model to estimate the accuracy of peptide identifications made by MS/MS and database search. *Analytical Chemistry* 74, 5383-5392.

Lewis, D. R., Fetrow,J., Muday, G., 2013. A kinetic analysis of auxin-mediated changes in transcript abundance in *Arabidopsis* reveals new mediators of root growth and development. *Submitted*.

Lewis, D. R., Ramirez, M. V., Miller, N. D., Vallabhaneni, P., Ray, W. K., Helm, R. F., Winkel, B. S. J., Muday, G. K., 2011. Auxin and ethylene induce flavonol accumulation through distinct transcriptional networks. *Plant Physiology* 156, 144-164.

Meagher, R. B., Kandasamy, M. K., King, L., 2011. Actin functions in the cytoplasmic and nuclear compartments. *Advances in Plant Biology* 2, 3-32.

Michalski, A., Cox, J., Mann, M., 2011. More than 100,000 detectable peptide species elute in single shotgun proteomics runs but the majority is inaccessible to Data-Dependent LC-MS/MS. *Journal of Proteome Research* 10, 1785-1793.

Nemhauser, J. L., Mockler, T. C., Chory, J., 2004. Interdependency of brassinosteroid and auxin signaling in *Arabidopsis*. *Plos Biology* 2, 1460-1471.

Nesvizhskii, A. I., Keller, A., Kolker, E., Aebersold, R., 2003. A statistical model for identifying proteins by tandem mass spectrometry. *Analytical Chemistry* 75, 4646-4658.

Overvoorde, P., Fukaki, H., Beeckman, T., 2010. Auxin control of root development. *Cold Spring Harber Perspectives in Biology* 2.

Petricka, J. J., Schauer, M. A., Megraw, M., Breakfield, N. W., Thompson, J. W., Georgiev, S., Soderblom, E. J., Ohler, U., Moseley, M. A., Grossniklaus, U., Benfey, P. N., 2012. The protein expression landscape of the *Arabidopsis* root. *Proceedings of the National Academy of Sciences* 18, 6811-6818.

Rosti, J., Barton, C. J., Albrecht, S., Dupree, P., Pauly, M., Findlay, K., Roberts, K., Seifert, G. J., 2007. UDP-glucose 4-epimerase isoforms UGE2 and UGE4 cooperate in providing UDP-galactose for cell wall biosynthesis and growth of *Arabidopsis thaliana*. *Plant Cell* 19, 1565-1579.

Sanchez-Rodriguez, C., Rubio-Somoza, I., Sibout, R., Persson, S., 2010. Phytohormones and the cell wall in *Arabidopsis* during seedling growth. *Trends in Plant Science* 15, 291-301.

Schiefelbein, J. W., Somerville, C., 1990. Genetic control of root hair development in *Arabidopsis thaliana*. *Plant Cell* 2, 235-243.

Schwender, J., Goffman, F., Ohlrogge, J. B., Shachar-Hill, Y., 2004. Rubisco without the Calvin cycle improves the carbon efficiency of developing green seeds. *Nature* 432, 779-782.

Seifert, G. J., Barber, C., Wells, B., Dolan, L., Roberts, K., 2002. Galactose biosynthesis in *Arabidopsis*: genetic evidence for substrate channeling from UDP-D-galactose into cell wall polymers. *Current biology : CB* 12, 1840-1845.

Shliaha, P. V., Bond, N. J., Gatto, L., Lilley, K. S., 2013. Effects of traveling wave ion mobility separation on data independent acquisition in proteomics studies. *Journal of Proteome Research.* 12, 2323-2339.

Slade, W. O., Ray, W. K., Williams, P. M., Winkel, B. S., Helm, R. F., 2012. Effects of exogenous auxin and ethylene on the *Arabidopsis* root proteome. *Phytochemistry* 84, 18-23.

Stepanova, A. N., Yun, J., Likhacheva, A. V., Alonso, J. M., 2007. Multilevel interactions between ethylene and auxin in *Arabidopsis* roots. *Plant Cell* 19, 2169-2185.

Valentine, S. J., Plasencia, M. D., Liu, X., Krishnan, M., Naylor, S., Udseth, H. R., Smith, R. D., Clemmer, D. E., 2006. Toward plasma proteome profiling with ion mobility-mass spectrometry. *Journal of Proteome Research* 5, 2977-2984.

Wasteneys, G. O., Galway, M. E., 2003. Remodelling the cytoskeleton for growth and form: An overview with some new views. *Annual Review of Plant Biology* 54, 691-722.

Zhang, H., Zhou, H., Berke, L., Heck, A. J., Mohammed, S., Scheres, B., Menke, F. L., 2013. Quantitative phosphoproteomics after auxin-stimulated lateral root induction identifies a SNX1 phosphorylation site required for growth. *Molecular and Cellular Proteomics.* 12.5, 1158-1169.

Chapter 5

Conclusions

I. Context

Mass spectrometry-based proteomics is a tool to explore how proteins control and regulate important molecular and physiological processes. This body of work assesses the technical feasibility of several major proteomics technologies applied to *Arabidopsis thaliana*, including 2D-GE, DiGE, iTRAQ, label-free peptide quantification, selected-reaction monitoring (SRM) for targeted proteomics, and data-independent acquisition (MS^e). In addition to assessing the capabilities of these technologies, we applied them to the context of uncovering new insights into the flavonoid biosynthetic pathway and the auxin and ethylene signaling pathways.

II. Summary

The optimization of a workflow for analyzing *Arabidopsis* root protein lysate using 2D-GE is described in Chapter 2 and Appendix A. We used this workflow to ask how the *Arabidopsis* root proteome responded to the treatment of two phytohormones, auxin and ethylene, over a period of 24 h. We observed that although auxin and ethylene affected the abundance of several proteins (24/500 and 7/500, respectively) there was no overlap among the two sets of proteins that the two hormones regulate. This is in contrast to analyses at the gene and physiological level, which suggest these two hormones regulate similar genes. Additionally, we used this workflow for the experiments described in Appendix A to assess how perturbation of the flavonoid biosynthetic pathway affects the seedling, root and flower proteome, and observed no effect, at least among the ~500 for the most abundant proteins detectable by 2D-GE.

In Appendix B we assessed the efficacy of HILIC-iTRAQ for global proteomics in *Arabidopsis* roots. HILIC-iTRAQ is positioned as an improvement to conventional label-free workflows. Additionally, in Chapter 4 we assessed the efficacy of UPLC-$HDMS^E$ for global proteomics in Arabidopsis. We used these methods to assess how the *Arabidopsis* root proteome responded to auxin treatment over a period of 8, 12, and 24 h. We observed that HILIC-iTRAQ on a MALDI TOF/TOF was not a robust platform for proteomics in *Arabidopsis* roots. In contrast, UPLC-$HDMS^E$ using a Synapt G2-S is a robust platform for peptide quantification in *Arabidopsis*. Finally, in Chapter 3 we assessed the efficacy of selected-reaction monitoring (SRM) for peptide quantification in *Arabidopsis* roots. We observed that SRM is a robust technology that requires fractionation and is suitable for peptide-level quantification.

III. Outlook

Proteomics is facing a revolution. The evolution of molecular biology into a quantitative, systems-level science has catapulted proteomics into the realm of big data and big science. As an example, a single $HDMS^E$ run contained 10GB of data, while an entire experiment contained 4 TB that required the computational processing power of a graphical processing unit. Advances in transcriptomics have made systems-level analyses of gene expression a reality for most researchers, while analyses of protein abundances have remained technically difficult and experimentally expensive. The

proteomics community has worked diligently to catalyze technical and computational improvements to make the comprehensive characterization of complex proteomes potentially feasible. Although these improvements have made things like sub-ppm mass accuracy of peptides routine, the comprehensive characterization of any proteome is not yet possible. I posit that the current focus on global proteomics is stagnating the field of proteomics, and a paradigm shift is necessary for the field to advance. For a paradigm shift to occur, the field of proteomics must embrace hypothesis-driven research and challenge their premises about systems-level proteomics.

Proteomics has traditionally embraced hypothesis-independent research questions. The underlying premise is that systems-level coverage of protein abundances is applicable to most questions of biological significance, which is a hard stance to challenge. What is challengeable, though, is the premise that proteomics affords enough systems-level information about protein abundances to warrant an approach in the absence of a hypothesis, or what is called discovery proteomics. For example, there are, at least, 30,000 proteins and over 1,000,000 peptides in the *Arabidopsis* proteome. The most extensive coverage to date has only characterized ~5000 proteins and 20,000 peptides (Baerenfaller et al., 2008). If we consider multiple isoforms per protein and imperfect digestion conditions, which are both a reality, then these numbers are pushed to at least 60,000 proteins and tens of millions of peptides. Even in what is considered the ideal proteomics system, yeast, protein coverage only reaches ~70% (de Godoy et al., 2008). The dynamic range of complex proteome samples (Corthals et al., 2000), coupled with the stochastic nature of gene expression (Elowitz et al., 2002) in a cell and peptide sampling in a mass spectrometer (Michalski et al., 2011) makes comprehensive coverage currently impossible. Thus, systems-level conclusions that are made using data that does not approach systems-level coverage will likely be flawed. Additionally, if the community continues to focus on what is likely an impossible goal, the true power of proteomics will be lost: the ability to ask specific, hypothesis-driven questions about a specific group of proteins and the ability to characterize those proteins with extremely high precision.

IV. Future Directions

The success of proteomics depends on the community's response to hypothesis-dependent research. Fortunately, many groups have already accepted this paradigm shift. For example, Zhao et al. (2013) used hypothesis-driven, targeted proteomics to assess the temporal activation of the innate immune response in response to double-stranded RNA activiation and observed dynamic regulation of the NF-KB-IKBα negative feedback loop. In plants, Zhang et al. (2013) asked a specific question about how auxin-induced lateral root formation affects the pool of phosphorylated proteins and observed a novel phosphorylation site on Sorting Nexin 1 (SNX1), which was shown to be required for lateral root formation. In summary, these studies indicate the power of hypothesis-dependent experiments using proteomics. If the community can embrace this paradigm shift, proteomics just might return to the forefront of understanding how cells and organisms adapt to their environments at the molecular level.

In order to study how exogenous auxin affects the *Arabidopsis* root proteome, a serial enrichment strategy for post-translational modifications could be developed and applied to the analysis of root tips. In roots, auxin affects changes in transcript and metabolite abundance primarily in root tips, with other regions relatively unaffected (Zhao et al 2010). Analysis of root tips would presumably be a simpler tissue source than whole roots and perhaps more informative of how auxin regulates root development and physiology.

V. References

Baerenfaller, K., Grossmann, J., Grobei, M. A., Hull, R., Hirsch-Hoffmann, M., Yalovsky, S., Zimmermann, P., Grossniklaus, U., Gruissem, W., Baginsky, S., 2008. Genome-scale proteomics reveals *Arabidopsis thaliana* gene models and proteome dynamics. *Science* 320, 938-941.

Corthals, G. L., Wasinger, V. C., Hochstrasser, D. F., Sanchez, J. C., 2000. The dynamic range of protein expression: A challenge for proteomic research. *Electrophoresis* 21, 1104-1115.

de Godoy, L. M. F., Olsen, J. V., Cox, J., Nielsen, M. L., Hubner, N. C., Frohlich, F., Walther, T. C., Mann, M., 2008. Comprehensive mass-spectrometry-based proteome quantification of haploid versus diploid yeast. *Nature* 455, 1251-U1260.

Elowitz, M. B., Levine, A. J., Siggia, E. D., Swain, P. S., 2002. Stochastic gene expression in a single cell. *Science* 297, 1183-1186.

Michalski, A., Cox, J., Mann, M., 2011. More than 100,000 detectable peptide species elute in single shotgun proteomics runs but the majority is inaccessible to data-dependent LC-MS/MS. *Journal of Proteome Research* 10, 1785-1793.

Zhang, H., Zhou, H., Berke, L., Heck, A. J., Mohammed, S., Scheres, B., Menke, F. L., 2013. Quantitative phosphoproteomics after auxin-stimulated lateral root induction identifies a SNX1 phosphorylation site required for growth. *Molecular and Cellular Proteomics* 12, 1158-1169.

Zhao, Y. 2010. Auxin biosynthesis and its role in plant development. *Annual Review of Plant Biology.* 61, 49-64.

Zhao, Y., Tian, B., Edeh, C. B., Brasier, A. R., 2013. Quantitation of the dynamic profiles of the innate immune response using multiplex selected reaction monitoring-mass spectrometry. *Molecular and Cellular Proteomics* 12, 1513-1529.

Appendix A

Effects of perturbing the flavonoid biosynthetic pathway on the *Arabidopsis* seedling, root, and flower proteomes

William O. Slade[A], Patricia M. Williams[C], W. Keith Ray[B], Richard F. Helm[B], Brenda S.J. Winkel[C]

Departments of Biological Sciences[A], Biochemistry[B], and Animal and Poultry Sciences[C]. Virginia Tech, Blacksburg, VA 24061-0406, United States

Contributions

William O. Slade
Designed the experiments, performed the experiments, analyzed the data, and wrote the manuscript.

Patricia M. Williams
Proved analytical and technical support.

W. Keith Ray
Provided technical support.

Richard F. Helm
Provided analytical and technical support, helped write the manuscript.

Brenda S.J. Winkel
Helped write the manuscript.

I. Abstract

The flavonoid biosynthetic pathway affects many important cellular and physiological processes. The lack of knowledge regarding how these underlying processes are mediated by the regulation of a plant's proteome represents a major gap in understanding plant biology, including that mediated by the flavonoid biosynthetic pathway. This chapter presents the first analysis of how perturbing the flavonoid pathway affects the seedling, flower, and root proteome of the model plant, *Arabidopsis thaliana*. Tissue-specific protein extracts were analyzed using two-dimensional gel-electrophoresis (2D-GE) and Difference in-Gel Electrophoresis (DiGE). Of the hundreds of matched spots across each experiment, none were observed as different using a student's t-test. This report demonstrates that although the flavonoid pathway affects many important processes in seedlings, roots, and flowers, these effects do not occur by modulating the levels of the most abundant proteins in these tissues.

II. Introduction

In plants, the flavonoid biosynthetic pathway affects many integral and disparate cellular processes, including the response to herbivory, pollen germination, UV-B protection, auxin transport, and root development (Winkel-Shirley, 2001). These processes are regulated in part by the effect of flavonoids on specific genes, proteins, and metabolites. For example, Buer et al. (2006) observed that ethylene regulates root gravitropism in *Arabidopsis* through the increase in abundance of specific flavonoid metabolites. Additionally, changes in the levels of UV-absorbing flavonoids are part of the plant's response to UV-B (Li et al., 1993).

Systems biology permits interrogation of the effects of the flavonoid pathway at the gene, metabolite, and protein levels. Previous efforts have focused on global analyses of metabolites in response to perturbation of the flavonoid pathway. Kusano et al. (2011) observed that plants carrying mutations in key flavonoid genes exhibit substantial metabolic reprogramming, especially in the context of the ability to respond to UV-B irradiation. Additionally, several studies have implicated flavonoid genes and metabolites as effectors of auxin and ethylene signaling and function (Lewis et al., 2011; Muday et al., 2012). Given that proteins are often the ultimate determinants of biological function, proteomic studies investigating the effects of mutations in specific flavonoid genes on the *Arabidopsis* proteome may help to further delineate the physiological functions of this pathway.

This chapter describes the first analysis of the effects of a flavonoid gene mutation on the *Arabidopsis* shoot, root, and flower proteomes. First, we confirmed the absence of the flavonoid enzyme, chalcone synthase (CHS) in a putative *tt4* null mutant (Bowerman et al. 2012) using selected reaction monitoring (SRM). Next, *tt4* and Columbia wild-type plants were grown in parallel, either in soil or on agar and tissue-specific proteome profiles were analyzed using 2D-GE and DiGE. Although several hundred spots were matched and analyzed across experiments, we observed no significant differences in protein abundance between *tt4* and wild type plants. This is in contrast to studies at the

gene and metabolite level, which indicates perturbing the flavonoid pathway affects many disparate pathways, including the auxin and ethylene signaling pathway and the response to light and gravity (Buer and Muday, 2004). Thus, while the flavonoid pathway regulates diverse cellular processes in seedlings, roots, and flowers, it does not appear to do so through the action of the most abundant proteins observed by 2D-GE and DiGE.

III. Results

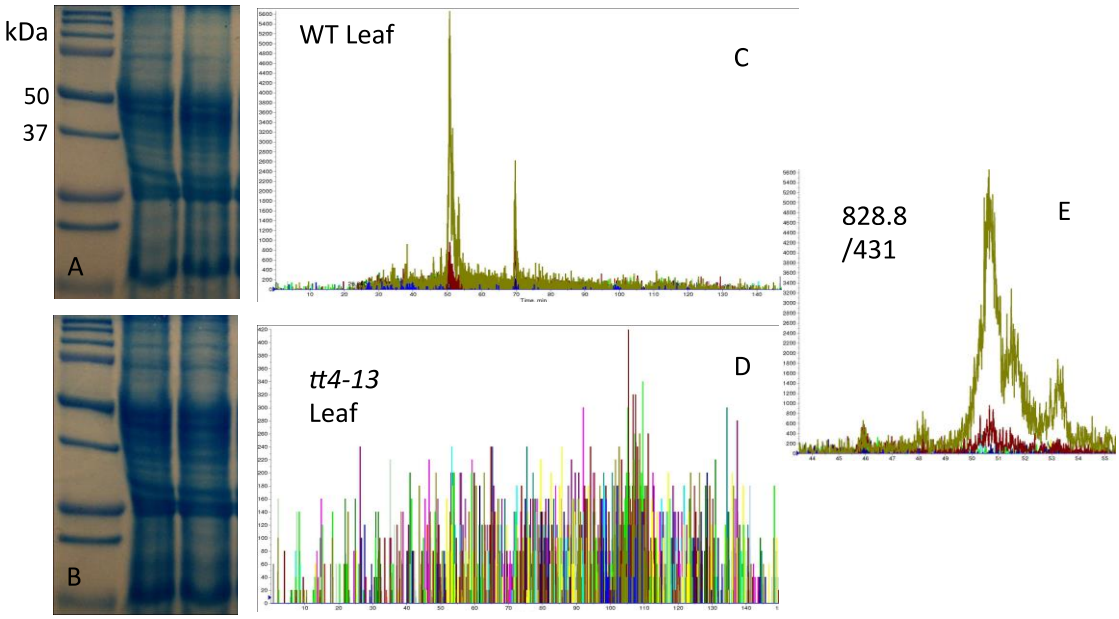

Figure A-1. SRM analysis of CHS in WT and *tt4-13*. Proteins were extracted from WT (A) or *tt4-13* (B) leaves. SRM analysis of the 50-37 gel region for CHS displays a robust response in WT(C,E) and no response in *tt4-13* (D).

Polymerase chain reaction (PCR) confirmation of homozygous alleles and UPLC analysis of metabolite levels indicates that T-DNA insertion in *tt4-13* (SALK_020583) ablates transcription of the CHS gene and downstream production of flavonoid metabolites (Bowerman et al., 2012). To further characterize this mutant, a selected-reaction monitoring assay was developed that targeted peptides upstream of the T-DNA insertion. The results demonstrated that the T-DNA insertion reduced accumulation of the CHS protein to undetectable levels (Figure A-1). Although previous analyses indicated that the *tt4-13* mutation abolishes flavonoid accumulation (Bowerman et al., 2012; Endo et al., 2012) the T-DNA insertion is located in the second exon and should still allow production of a truncated CHS protein. The current results suggest that the mutation may result in destabilization of the CHS protein and that *tt4-13* is a bona-fide null, also at the protein level.

To determine the effects of the CHS mutation on the *Arabidopsis* seedling proteome, we compared the root proteome profiles of wild-type (Col-0) and *tt4-13* plants using 2D-GE technology. Gel images were first analyzed by automated matching and then manually validated. The results indicated that under the experimental and detection system

employed the null CHS mutation did not affect the *Arabidopsis* seedlings proteome (Figure A-2).

To determine if the CHS gene loss affected the *Arabidopsis* proteome in a tissue-specific manner, we next compared the root and flower proteome profiles of wild-type (Col-0) and *tt4* plants using 2D-GE. Our results again indicated that root and flower bud proteomes were unaffected (Figure A-3 and A-4).

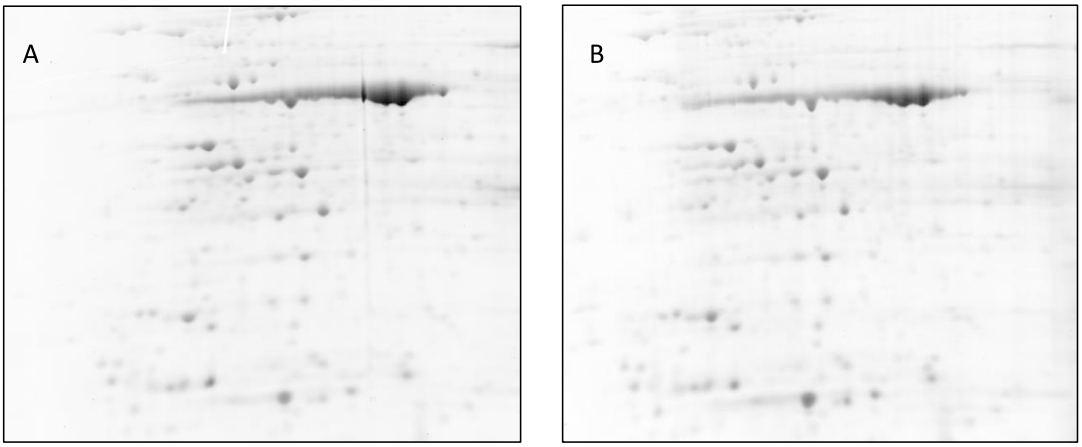

Figure A-2. 2D-GE analysis of WT and *tt4-13* in seedlings. 500 spots represnting proteins were matched and analyzed between WT (A) and *tt4-13* (B) seedling protomes. A student's t-test ($p < 0.05$) indicates no differences.

IV. Discussion

In order to better understand how the flavonoid pathway affects the abundance of other plant proteins, we used a proteomics approach to evaluate the potential effects of a mutation in the first enzyme in the central pathway on the *Arabidopsis* root proteome. To our surprise we observed that disrupting the flavonoid pathway did not affect the *Arabidopsis* seedling proteome, at least for the most abundant proteins in *Arabidopsis* seedlings. Our study suggests that while the flavonoid pathway affects many physiological and molecular processes in *Arabidopsis* seedlings, these processes are not reflected in changes in the abundance of the proteins detectable by 2D-GE.

Previous work has demonstrated that perturbing the flavonoid pathway affects the regulation of certain metabolites and proteins. First, Kusano et al. (2011) observed that plants carrying mutations in key flavonoid genes substantially reprogram their metabolic pathways, especially in regard to their ability to respond to UV-B irradiation. In addition to the metabolic changes observed by Kusano et al. (2011), Pelletier et al. (1999) observed that mutations in key flavonoid enzymes caused higher accumulation of specific flavonoid enzymes and end-products. These results suggest that the flavonoid proteins not only catalyze an enzymatic reaction but also function to regulate specific metabolites and proteins.

Although we observed that the *Arabidopsis* seedling proteome appeared to be unaffected in a null CHS mutant, we hypothesized that tissue-specific changes would be detectable. Flavonoids affect many physiological and molecular processes observable in *Arabidopsis* roots and flower buds. In roots, a null CHS mutation not only impairs root gravitropism (Buer and Muday, 2005), but also disrupts auxin- and ethylene-mediated root processes. In flowers, flavonoids are not only responsible for pigmentation but other key roles such as signaling between plants and microbes and UV protection (Winkel-Shirley, 2001). Surprisingly, we observed that disrupting the flavonoid pathway also did not affect the most abundant proteins in *Arabidopsis* roots or flowers. Our results suggest that while the flavonoid pathway is instrumental in many molecular and physiological processes in *Arabidopsis*, those processes are not reflected in changes in the levels of abundant proteins observed by 2D-GE and DiGE.

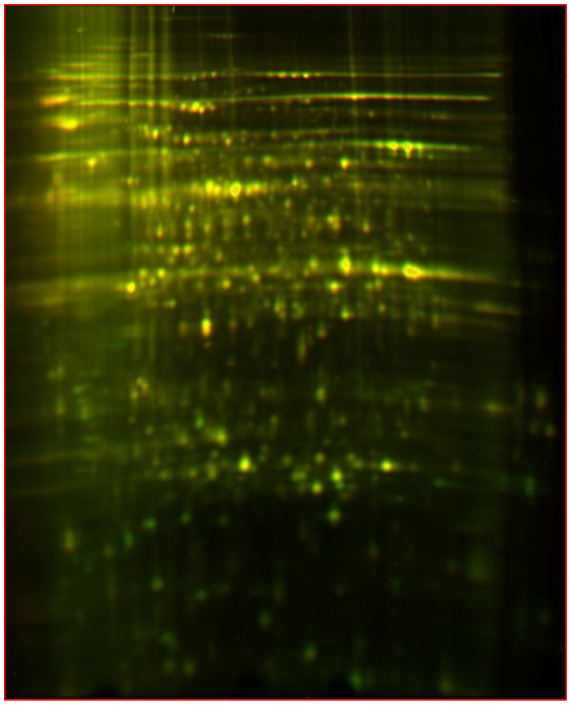

Figure A-3. DiGE analysis of WT and *tt4-13* in roots. 1200 spots representing root proteins were matched and analyzed between WT (A) and *tt4-13* (B) seedlings proteomes. A student's t-test ($p < 0.05$) indicates no differences

Interrogation of changes in protein abundance is limited by the chosen technology (Alvarez et al., 2009). Proteins observed by 2D-GE and DIGE, in particular, are likely to represent highly expressed or constitutive proteins, rather than low abundance transcription factors or transient signaling pathway proteins (Gygi et al., 2000). Despite these limitations, DiGE has proven to be a useful assessment of proteome status across multiple organisms and experimental questions (Chevalier, 2010; Rabilloud et al., 2010). For example, Tang et al (2008) used DiGE to demonstrate that the brassinosteroid (BR) signaling pathway is activated by substrate binding of brassinosteroid-signaling kinases to the BRL1 receptor kinase.

In the future, researchers should utilize improved proteome technologies, such as ultra-high-performance liquid chromatography (UPLC) coupled to high mass-accuracy mass spectrometry in order to study how mutations in key flavonoid genes affect the *Arabidopsis* proteome. These results will inform researchers not only on how the flavonoid pathway affects plant biology but also on how the manipulation of the flavnoid can intersect with, and improve, human health.

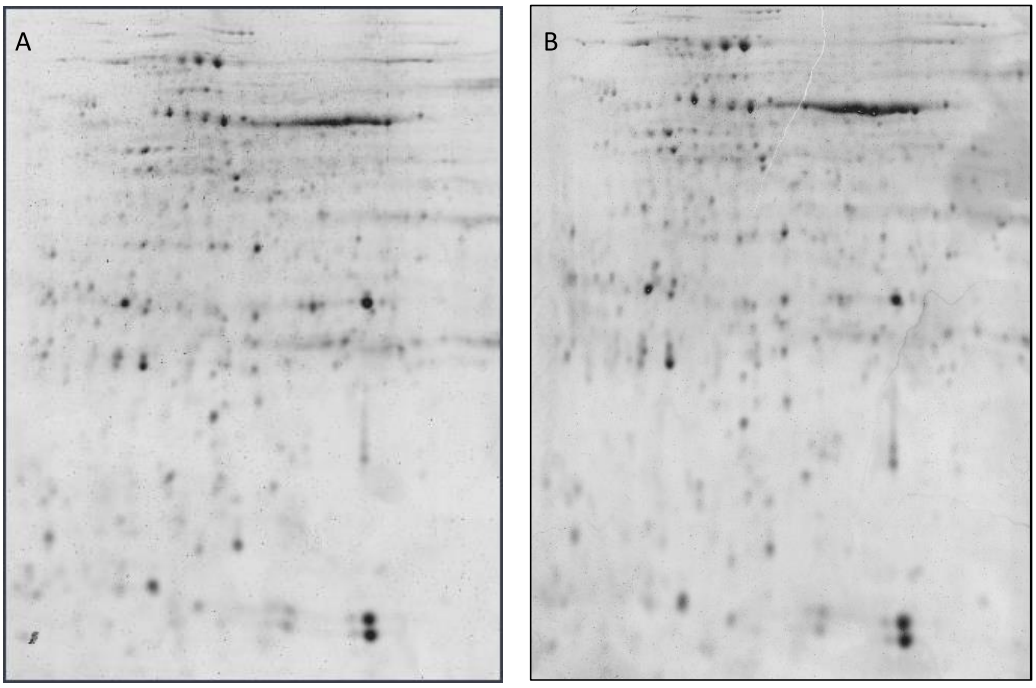

Figure A-4. 2D-GE analysis in WT and *tt4-13* in flowers. 400 spots representing flower proteins were matched and analyzed between WT (A) and *tt4-13* (B) seedling proteomes. A studetn's t-test ($p < 0.05$) indicates no differences.

V. Experimental

i. Plant Material

Plant material was prepared according to Slade et al. (2012). Briefly, seeds of the Columbia (Col-0) ecotype of *Arabidopsis* were obtained from Lehle Seeds (Round Rock, Texas). The T-DNA insertion line, *tt4-13,* in ecotype Col-0 was obtained from the Arabidopsis Biological Resource Center (ABRC, Columbus, OH) and characterized as described previously (Bowerman et al., 2012). Plants were grown on 1X Murashige and Skoog medium from Caisson labs (North Logan, Utah), pH 5.7, 0.8% (w/v) agar, supplemented with 1% (w/v) sucrose. After cold treatment for 48-72 h at 4°C, seeds were moved to a growth chamber and grown under 100 μmol m^{-2} s^{-2} cool-white light (24h lighting). The growth chamber was maintained at 22°C and 60% relative humidity . All assays were conducted 5 d after germination, which was typically 6-7 d after the cold treatment.

ii. Protein extraction

Proteins were extracted according to the phenol-MeOH method (Hurkman and Tanaka, 1986) with modifications as follows. For each biological replicate, plant tissue (0.3 g), were mixed with three volumes of SDS extraction buffer (100 mM Tris-HCl, pH 8.0, 2% SDS (v/v), 1% β-mercaptoethanol (v/v), 5 mM EGTA, 10 mM EDTA), heated for 10 min at 65°C, and then centrifuged at 6710*g* for 10 min to separate aqueous and phenol phases. The aqueous phase was removed leaving the interface intact, and the phenol phase was extracted twice with ice-cold 50 mM Tris-HCL, pH 8.0 then mixed with 5 volumes of ice-cold 0.1 M (NH_4)OAc in MeOH and left at -20°C overnight. After centrifugation at 6710*g* for 10 min, the protein pellet was washed three times with ice-cold 0.1 M (NH_4)OAc in MeOH, once with ice-cold EtOH, and once with ice-cold 70% EtOH, and then resuspended in rehydration buffer [7 M urea, 2 M thiourea, 4% CHAPS (w/v), 0.5% IPG buffer (v/v)]. After centrifugation at 6710*g* for 10 min protein concentration was determined using the 2D-Quant Kit (GE Healthcare; Piscataway, NJ) using BSA as a standard.

iii. DiGE Labeling

Protein samples were labeled according to the manufacter's protocol for minimal labeling. Protein concentrations were adjusted to 3 μg/μL by adding rehydration buffer. Cy-Dyes (1 μL of 400 pmol/μl in dimethyl formamide) were added to 50 μg protein aliquots and incubated on ice in the dark for 30 min. For each replicate reaction, one sample was labeled with Cy3, the other with Cy5, and the internal standard with Cy2. The internal standard was prepared by mixing a 25 μg aliquot from every biological replicate. The reactions were terminated by adding 1.5 μL of 10 mM lysine and incubating for 10 min. Experimental scheme 1 (Supplemental Figure 1) analyzed wild-type Col-0 vs. *tt4-13* across one biological replicate.

iv. Isoeletric focusing

Samples were diluted to a final volume of 350 μl and applied to wells in isoeletric focusing (IEF) trays (17 cm; Bio-Rad, Hercules, CA) in IEF cell units (Bio-Rad, Hercules, CA). The pH 3-11 nonlinear immobilized pH gradient (IPG) strips were

applied to the wells followed by an overlay of mineral oil (Bio-Rad; Hercules, CA). IEF was carried out at 20°C with a maximum 50 μA/strip and the following setting: active rehydration for 12 h at 50V, then 500 and 1000 V each for 1 h, gradient increase to 8000 V in 3 h, and remaining at 8000 V until reaching 50,000 V-h. After IEF, the strips were equilibrated in three successive steps on an orbital shaker: (1) 15 min in buffer 1 [4% SDS (w/v) 0.37 M, Tris-Cl, pH 8.8, 20% glycerol (v/v)], (2) 15 min in 2% DTT (w/v) in buffer 1, (3) 15 min in 2.5% iodoacetamide (w/v) in buffer 1.

v. SDS-PAGE electrophoresis

Strips were transferred onto pre-cast 12% gels containing 0.375 M Tris-Cl, pH 8.8 and 0.1% SDS (w/v) (Jule; Milford, CT, USA) and coated with 0.5% agarose (w/v) containing bromophenol blue. Plates were then transferred to a Protean plus Dodeca Cell (Bio-Rad; Hercules, CA) tank containing 0.0125 M Tris, 0.096 M glycine, and 0.05% SDS (w/v) at 20°C. Electrophoresis was carried out for approximately 16 h or until the dye front migrated within 1 cm of the gel's edge. Glass plates were rinsed with ultrapure water and EtOH before images were acquired using the Typhoon Trio (GE Healthcare; Piscataway, NJ, USA).

vi. Image analysis

Images were analyzed using PDQuest v7.3.1 (Bio-Rad; Hercules, CA). Following automated spot detection and matching, replicate groups were manually assigned. The group consensus tool was then used to manually examine each spot considered in the analysis. Only spots that could be reliably detected on all gels were considered further. A student's t-test was then performed to evaluate which spots showed a difference in accumulation between the two samples ($p < 0.05$).

vii. Selected-Reaction Monitoring

FASTA-formatted sequences were downloaded from UniProt and digested *in silico* using Peptide Cutter. Peptides were queried for SRM robustness using ESP Predictor and for SRM uniqueness using TAIR PatMatch (Supplemental Figure 2). The MS platform used was a 4000 QTRAP hybrid triple quadrupole/linear ion mass spectrometer equipped with a Nanospray II ion source coupled to an online nano liquid chromatography system (Tempo, Eksigient) with an autosampler (AS2, Eksigient). The unit was calibrated with 50 fmol/μl Glu-Fib and PPGs according to the manufacturer's instruction. The following MS settings were used: Quad Resolution: Unit; Curtain gas: 10V; ion source: 2800V; gas source one (GS1): 35. Mobile phases were as follows: (A) 0.1% formic acid in ddH_2O and (B) CH_3CN. Analytical columns consisted of fritted capillaries (PST-LC75-eFRIT, Phoenix ST) packed to a length of 15 cm with Magic C18AQ Resin (3 μm, 200Å, Michrom Bioresources) resuspended in chloroform using a pressure bomb.

viii. In-gel tryptic digestion

Gel slices were washed once with ultrapure H_2O followed by washes with CH_3CN-H_2O (1:1,v/v), 50 mM NH_4CO_3, pH 8.0 until the slices were no longer colored. Following dehydration with CH_3CN, cores were rehydrated in 10 mM DTT for 20 min at 55°C. Gel pieces were cooled to room temperature and then incubated in 10 mM iodoacetamide for

20 min at RT in the dark. After one wash in ultrapure H_2O and two washes CH_3CN-H_2O (1:1,v/v), 50 mM NH_4CO_3, pH 8.0, the gel pieces were dehydrated with CH_3CN. Samples were dried in a vacuum centrifuge and then stored at -80°C until further use. Samples were rehydrated in 10 ng/nl trypsin (Promega, Madison, WI) at 4°C for 90 min and then incubated at 37°C for 16 h. Peptides were extracted twice using CH_3CN/H_2O/formic acid (50/40/10), lyophilized, and stored at -80°C until use.

VI. Supplementary Material

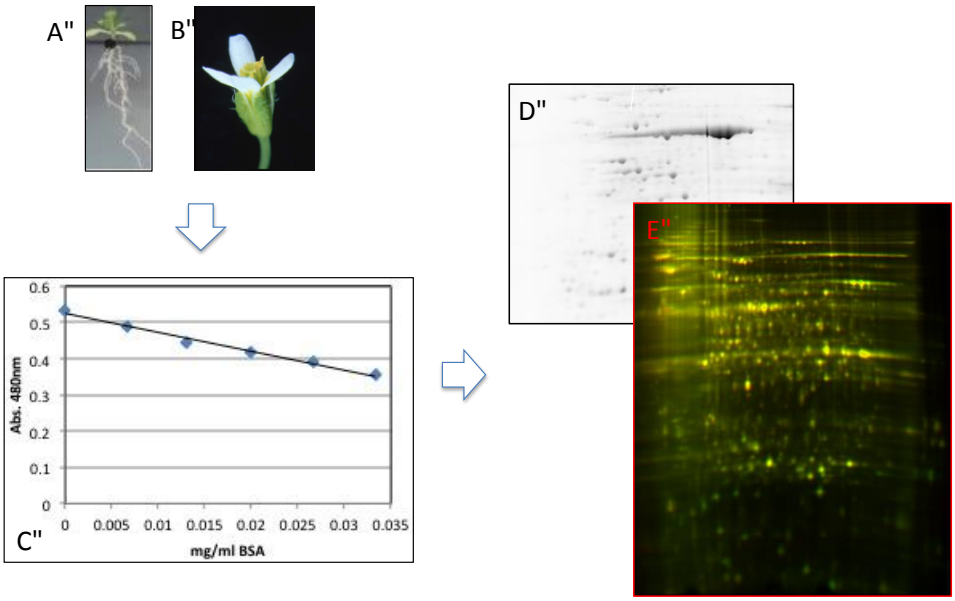

Figure A-S1. Experimental Scheme. Proteins were extracted from *Arabidopsis* seedlings (A), roots (A), or flowers (B) and quantified with the 2D-Quant Kit (C). Proteins were separated and analyzed using 2D-GE (D) or DiGE (E).

```
>sp|P13114|CHSY_ARATH Chalcone synthase OS=Arabidopsis thaliana GN=CHS
PE=1 SV=1
MVMAGASSLDEIRQAQRADGPAGILAIGTANPENHVLQAEYPDYYFRITNSEHMTDLKEK
FKRMCDKSTIRKRHMHLTEEFLKENPHMCAYMAPSLDTRQDIVVVEVPKLGKEAAVKAIKEWGQPKSKITH
VVFCTTSGVDMPGADYQLTKLLGLRPSVKRLMMYQQGCFAGGTVLRIAKDLAENNRGARVLVVCSEITAVT
FRGPSDTHLDSLVGQALFSDGAAALIVGSDPDTSVGEKPIFEMVSAAQTILPDSDGAIDGHLREVGLTFHL
LKDVPGLISKNIVKSLDEAFKPLGISDWNSLFWIAHPGGPAILDQVEIKLGLKEEKMRATRHVLSEYGNMS
SACVLFILDEMRRKSAKDGVATTGEGLEWGVLFGFGPGLTVETVVLHSVPL
!
```

Pep5de'	Parent'Ion'(monoisotopic)''	Daughter'Ion'(monoisotopic)'' '	Collision'Energy'	Declustering'Poten5al'
HMHLTEEFLK"	428.740"	766.3"	35"	76"
HMHLTEEFLK" "	428.740" "	665.5"	38"	74"
HMHLTEEFLK" "	428.740" "	878.4"	28"	76"
ADGPAGILAIGTANPENHVLQ AEYPDYYFR"	1088.742"	1193.3"	40"	88"
ADGPAGILAIGTANPENHVLQ AEYPDYYFR" "	1088.742" "	1285.3"	38"	86"
ADGPAGILAIGTANPENHVLQ AEYPDYYFR" "	1088.742" "	1341.4"	36"	84"
ITHVVFCTTSGVDMPGADYQL TK'"	828.836"	933.1"	28"	68"
ITHVVFCTTSGVDMPGADYQL TK'" "	828.836" "	496.9"	26"	70"
ITHVVFCTTSGVDMPGADYQL TK'" "	828.836" "	352.1"	24"	72"

Figure A-S2. The primary amino acid sequence of CHS (top) with the unique peptides (proteotypic) highlighted in yellow. The data for SRM detection is shown in the Table (bottom).

VII. References

Alvarez, S., Berla, B.M., Sheffield, J., Cahoon, R.E., Jez, J.M., and Hicks, L.M. (2009). Comprefahensive analysis of the *Brassica juncea* root proteome in response to cadmium exposure by complementary proteomic approaches. *Proteomics 9*, 2419-2431.

Bowerman, P.A., Ramirez, M.V., Price, M.B., Helm, R.F., and Winkel, B.S. (2012). Analysis of T-DNA alleles of flavonoid biosynthesis genes in *Arabidopsis* ecotype Columbia. *BMC Research Notes 5*, 485.

Buer, C.S. and Muday, G.K. (2004). The *transparent testa4* mutation prevents flavonoid synthesis and alters auxin transport and the response of *Arabidopsis* roots to gravity and light. *Plant Cell 16*, 1191-1205.

Buer, C.S., Sukumar, P., and Muday, G.K. (2006). Ethylene modulates flavonoid accumulation and gravitropic responses in roots of *Arabidopsis*. *Plant Physiology 140*, 1384-1396.

Chevalier, F. (2010). Highlights on the capacities of "Gel-based" proteomics. *Proteome Science 8*.

Endo, A., Tatematsu, K., Hanada, K., Duermeyer, L., Okamoto, M., Yonekura-Sakakibara, K., Saito, K., Toyoda, T., Kawakami, N., Kamiya, Y., *et al.* (2012). Tissue-specific transcriptome analysis reveals cell wall metabolism, flavonol biosynthesis and defense responses are activated in the endosperm of germinating *Arabidopsis thaliana* seeds. *Plant Cell Physiology 53*, 16-27.

Gygi, S.P., Corthals, G.L., Zhang, Y., Rochon, Y., and Aebersold, R. (2000). Evaluation of two-dimensional gel electrophoresis-based proteome analysis technology. *Proceeding of the National Academy of Sciences 97*, 9390-9395.

Hurkman, W.J., and Tanaka, C.K. (1986). Solubilization of plant membrane-proteins for analysis by two-dimensional gel-electrophoresis. *Plant Physiology 81*, 802-806.

Kusano, M., Tohge, T., Fukushima, A., Kobayashi, M., Hayashi, N., Otsuki, H., Kondou, Y., Goto, H., Kawashima, M., Matsuda, F., *et al.* (2011). Metabolomics reveals comprehensive reprogramming involving two independent metabolic responses of Arabidopsis to UV-B light. *Plant Journal 67*, 354-369.

Lewis, D.R., Ramirez, M.V., Miller, N.D., Vallabhaneni, P., Ray, W.K., Helm, R.F., Winkel, B.S., and Muday, G.K. (2011). Auxin and ethylene induce flavonol accumulation through distinct transcriptional networks. *Plant Physiology 156*, 144-164.

Li, J., Ou-Lee, T.M., Raba, R., Amundson, R.G., and Last, R.L. (1993). *Arabidopsis* flavonoid mutants are hypersensitive to UV-B irradiation. *Plant Cell 5*, 171-179.

Muday, G.K., Rahman, A., and Binder, B.M. (2012). Auxin and ethylene: collaborators or competitors? *Trends in Plant Science 17*. 181-195

Pelletier, M.K., Burbulis, I.E., and Winkel-Shirley, B. (1999). Disruption of specific flavonoid genes enhances the accumulation of flavonoid enzymes and end-products in *Arabidopsis* seedlings. *Plant Molecular Biology 40*, 45-54.

Rabilloud, T., Chevallet, M., Luche, S., and Lelong, C. (2010). Two-dimensional gel electrophoresis in proteomics: Past, present and future. *Journal of Proteomics 73*, 2064-2077.

Slade, W.O., Ray, W.K., Williams, P.M., Winkel, B.S., and Helm, R.F. (2012). Effects of exogenous auxin and ethylene on the *Arabidopsis* root proteome. *Phytochemistry 84*, 18-23.

Tang, W.Q., Kim, T.W., Oses-Prieto, J.A., Sun, Y., Deng, Z.P., Zhu, S.W., Wang, R.J., Burlingame, A.L., and Wang, Z.Y. (2008). BSKs mediate signal transduction from the receptor kinase BRI1 in *Arabidopsis*. *Science 321*, 557-560.

Winkel-Shirley, B. (2001). Flavonoid biosynthesis. A colorful model for genetics, biochemistry, cell biology, and biotechnology. *Plant Physiology 126*, 485-493.

Appendix B

Evaluation of isobaric tagged for relative and absolute quantification (iTRAQ) using hydrophilic interaction chromatography (HILIC) on a MALDI TOF/TOF platform for relative quantification of peptides in *Arabidopsis thaliana*

William O. Slade[A], *W. Keith Ray*[B], *Brenda S.J. Winkel*[A], *Richard F. Helm*[B]

Departments of Biological Sciences[A] *and Biochemistry*[B], *Virginia Tech, Blacksburg, VA 24061-0406, United States*

Contributions

William O. Slade
Designed the experiments, performed the experiments, analyzed the data, and wrote the manuscript.

W. Keith Ray
Provided technical support.

Brenda S.J. Winkel
Helped write the manuscript.

Richard F. Helm
Provided analytical guidance and helped write the manuscript.

I. Abstract

Plant proteomics requires specialized analytical solutions for mass spectral analyses. Traditionally, plant researchers have used strong-cation exchange chromatograpy (SCX) coupled with reverse phase (RP) using ESI-MS for peptide quantification. However, there are numerous limitations to SCX-RP using ESI-MS, such as the non-orthogonal separation of peptides. Isobaric tagged for relative and absolute quantification (iTRAQ) coupled with HILIC using MALDI TOF/TOF has been proposed as superior to SCX-RP using ESI-MS (Yang et al., 2007). Here, we assess the efficacy of iTRAQ-HILIC using MALDI TOF/TOF for relative quantification of peptides in *Arabidopsis thaliana*.

II. Introduction

Proteomics in plants requires specialized analytical solutions. Most plants, including *Arabidopsis* displays a wide dynamic range of protein concentrations (10^5) (Arsova et al., 2012), exceeding the capabilities of most modern mass spectrometers. Additionally, digestion with trypsin, which allows for more in-depth study of proteins, could yield more than 1,000,000 peptides, most of which are inaccessible to current LC-MS/MS methods (Michalski et al., 2011), due to the dynamic range of peptide concentrations and the stochastic nature of peptide sampling by mass spectrometers (Bell et al., 2009). Current approaches rely upon extensive fractionation using strong-cation exchange (SCX) chromatography coupled with reverse-phase (RP) chromatography (Aebersold and Mann, 2003). This 2D-LC system is coupled in tandem with a mass spectrometer using electrospray ionization (ESI-MS). ESI-MS methods typically quantitate peptides based on MS1 information, a reliable and proven technique.

The traditional ESI-MS protocol using SCX-RP has limitations. First, SCX and RP separate peptides based on similar physiochemical properties, suggesting the resolution of separation is not optimal. Additionally, label-free approaches do not permit multiplexing, which can induce technical variability among biological replicates. Although quantitation based on MS1 information is a sound technique, complex samples generate proteome backgrounds that often display low signal-to-noise ratios (Evans et al., 2012), thus complicating the differentiation of peptides.

Isobaric tagged for relative and absolute quantification (iTRAQ) labeling of peptides in conjunction with hydrophilic interaction chromatography (HILIC) aims to solve the issues of ESI-MS using a SCX-RP approach to chromatography. First, HILIC separates peptides orthogonally to RP. Compared to SCX, HILIC provides higher-resolution separation of peptides. Additionally, iTRAQ reagents label peptides via their N-terminus and at the E side chains of lysines through stable N-hydroxysuccinimide (NHS) ester chemistry. Up to 8 different iTRAQ tags can be processed in parallel, theoretically circumventing the technical variation induced by label-free approaches that require extensive fractionation. In contrast to MS1 approaches that quantitate peptides at the MS1 level, iTRAQ quantitates peptides at the MS2 level, effectively linking quantitation to identification, and theoretically yielding higher signal to noise ratios. Given these

theoretical advantages of iTRAQ coupled to HILIC over conventional SCX-RP, we were surprised to find few reports of its efficacy in the literature.

Herein, we assess the utility of iTRAQ using HILIC for relative peptide quantification. *Arabidopsis* root protein lysates were fractionated using HILIC and analyzed using MALDI TOF/TOF. Out of 90 HILIC fractions, 40 were selected for further offline separation into 384 fractions each using C18-RP. We observed the confident identification of 33 proteins from *Arabidopsis* roots. This compares poorly to other discovery proteomics schemes, where the identification of 100s if not 1000s of proteins is routine. Thus, we conclude that HILIC-iTRAQ using a MALDI TOF/TOF is not a robust platform for discovery proteomics in *Arabidopsis.*

III. Results

To assess the efficacy of iTRAQ-HILIC in *Arabidopsis*, we used an extensive fractionation scheme. Protein lysates were fractionated based on hydrophilicity using HILIC intro 60 fractions. Of those 60 fractions, 40 were selected for further fractionation based on hydrophobicity using C18-RP. Per HILIC fraction, C18-RP separated peptides into 384 more fractions. Analysis of each fraction by MALDI TOF/TOF resulted in the identification of 33 proteins of high confidence (see Data Analysis section) (Table B-1).

IV. Discussion

Our results suggest that iTRAQ-HILIC using MALDI TOF/TOF is not a robust platform for peptide quantification in *Arabidopsis*. We showed that only 33 proteins were identifiable using an extensive HILIC-C18RP fractionation scheme. These results compare poorly to other studies where less-extensive fractionation schemes are used to routinely identify 1000s of proteins. For example, Lan et al. (2011) identified 4,454 proteins in *Arabidopsis* roots with a false discovery rate (FDR) of less than 1.1% using nanoLC coupled with an LTQ-Orbitrap.

In contrast to our results, Sardar et al. (2013) and Hou et al. (2013) used iTRAQ labeling on a nanoLC-MALDI-TOF/TOF platform to identify 1653 and 641 proteins from *Leishmania* and gastric cancer cell lines, respectively. Although these results demonstrate what is possible, there are differences when using *Arabidopsis* for proteome studies that much be considered. First, the complexity of post-translational modifications (PTMs) complicates global proteome analyses. Emerging evidence suggests that PTM patterns increase in complexity from unicellular to multicellular eukaryotes (Garcia et al., 2007). This, coupled with the existence of over 300 PTMs (Jensen, 2004; Kwon et al., 2006) means any single peptide in a complex organism could be modified several times, meaning lower amounts available for analysis by mass spectrometry. Thus, the difference in complexity of PTM processing in *Arabidopsis* compared to simpler systems could explain our results.

Identified Proteins	Accession Number	Molecular Weight
Peroxidase	gi|1402908	39 kDa
Unknown protein	gi|13899069	16 kDa
Unknown protein	gi|24417262	44 kDa
40S ribosomal protein S9 (RPS9B)	gi|15242241	23 kDa
Fructose-bisphosphate aldolase	gi|15231715	39 kDa
Ribosomal Protein S13A	gi|18411224	17 kDa
Heat Shock Protein 81-2	gi|15241115	80 kDa
ribosomal protein S5	gi|1522811	23 kDa
Actin (Act3)	gi|11276980	47 kDa
Acetoacetyl-CoA Thiolase 2	gi|30695411	41 kDa
mitochondrial F1 ATP synthase beta subunit	gi|17939849	63 kDa
Maternal Effect Embryo Arrest 58	gi|15236376	53 kDa
Embryo sac development arrest 9	gi|15235282	63 kDa
Glyceraldehyde-3-phosphate-dehydrogenase C2	gi|145323882	34 kDa
40S Ribosomal protein S25	gi|15226590	12 kDa
60S ribosomal protein L7	gi|145328234	22 kDa
Annexin Arabidopsis 2	gi|15238320	36 kDa
Rotamase Cyp 1	gi|15234781	18 kDa
Vacuolar ATP Synthase Subunit A	gi|15219234	69 kDa
NADH-ubiquinone oxidoreductase-related	gi|18423437	19 kDa
ATP synthase subunit alpha, mitochondrial	gi|14916970	55 kDa
chaperonin, putative	gi|15229866	60 kDa
At1g35160/T32G9_30	gi|14532442	30 kDa
LOS2; copper ion binding / phosphopyruvate hydratase	gi|15227987	48 kDa
At1g76180 [Arabidopsis thaliana]	gi|13265523	21 kDa
succinyl-CoA ligase (GDP-forming) beta-chain, mitochondrial, putative	gi|15225353	45 kDa
PKT3 (PEROXISOMAL 3-KETOACYL-COA THIOLASE 3)	gi|15225798	49 kDa
CDC48 (CELL DIVISION CYCLE 48)	gi|15232776	89 kDa
caffeoyl-CoA 3-O-methyltransferase, putative	gi|15235213	29 kDa
PIP2B (PLASMA MEMBRANE INTRINSIC PROTEIN 2)	gi|15228095	30 kDa
ATMS1; 5-methyltetrahydropteroyltriglutamate-homocysteine S-methyltransferase	gi|15238686	84 kDa
AHA2; ATPase/ hydrogen-exporting ATPase	gi|15234666	104 kDa
fructose-bisphosphate aldolase, putative	gi|15226185	42 kDa

Table B-1. *Arabidopsis* proteins identified with high confidence using iTRAQ-HILIC on a MALDI TOF/TOF.

Additionally, proteomics workflows used in systems such as yeast or human cell lines might not be applicable to more complex systems such as *Arabidopsis*. Most analyses have shown that approximately 1 μg of either simple or complex mixtures are reasonable amounts for on-column loading prior to analysis by mass spectrometry (Shliaha et al., 2013). By estimating losses due to sample fractionation/preparation 100 μg is the traditional starting amount of protein for LC-MS analyses. Although this has proven to be adequate for analysis of the full dynamic range of proteins in yeast and human cell lines, emerging evidence suggests that starting with more micrograms of protein (~400-2000 μg) results in better proteome coverage when coupled with extensive fractionation schemes.

In summary, we assessed the efficacy of iTRAQ-HILIC using MALDI TOF/TOF to relatively quantify peptides in *Arabidopsis*. Using an extensive fractionation scheme that employed iTRAQ-HILIC and C18RP, we were only able to identify 33 proteins using a MALDI TOF/TOF. Current efforts are aimed at uncovering how improvements in mass spectrometry technology affect coverage of the *Arabidopsis* proteome.

V. Experimental

i. Plant Material

Plant material was prepared according to Slade et al. (2012) Briefly, seeds of the Columbia (Col-0) ecotype of *Arabidopsis* were obtained from Lehle Seeds (Round Rock, Texas, USA). Plants were grown on 1X Musharige and Skoog medium from Caisson labs (North Logan, Utah, USA) pH 5.7, 0.8% (w/v) agar, and supplemented with 1% (w/v) sucrose. After cold treatment for 48-72 h at 4°C, seeds were moved to a growth chamber and grown under 100 μmol $m^{-2}s^{-2}$ cool-white light (24 h lighting). The growth chamber was maintained at 22°C and 60% relative humidity. All assays were conducted 5 d after germination, which was typically 6-7 d after the cold treatment.

ii. Protein Extraction

Proteins were extracted according to the phenol-MeOH method (Hurkman and Tanaka, 1986) with the following modifications. For each biological replicate, plant tissue (0.3 g), was mixed with 3 volumes of SDS extraction buffer (100 mM Tris-HCL, pH 8.0, 2% SDS (v/v), 1% β-mercaptoethanol (v/v), 5 mM EGTA, 10 mM EDTA) heated for 10 min at 65°C, and then centrifuged at 6710g for 6 min to separate aqueous and phenol phases. The aqueous phase was removed leaving the interface intact, and the phenol phase was extracted twice with ice-cold 50 mM Tris-HCL, pH 8.0 then mixed with 5 volumes of ice-cold 0.1 M (NH_4)OAc in MeOH and left at -20°C. After centrifugation at 6710*g* for 10min, the protein pellet was washed three times with ice-cold 0.1 M (NH_4)OAc in MeOH, once with ice-cold EtOH, and once with ice-cold 70% EtOH and then resuspended in rehydration buffer (7 M Urea, 2 M thiourea, 4% CHAPS (w/v), 0.5% IPG buffer (v/v). After centrifugation, protein concentration was determined using the 2D-Quant Kit (GE Healthcare; Piscataway, NJ) using BSA as a standard.

iii. In-solution digestion

In-solution digestions were performed using 100 μg per biological replicate. First, disulfide bonds were reduced using 5 mM tris-carboxyethylphosphine for 30 min at room temperature. Peptides were then alkylated using 40 mM iodoacetamide for 40 min at room temperature in the dark. Samples were diluted to 1.6 M urea using 50 mM triethylammonium bicarbonate and incubated with 2 μg trypsin (50:1 protein:protease ratio) for 16 h at 37°C.

iv. Peptide labeling using iTRAQ reagents

Peptides were labeled with iTRAQ reagents according to manufacturer's instructions. Briefly, an iTRAQ sample vial, resuspended in 70 μl isoproponal, was added to each sample vial and incubated for 2 h. Next, all samples were pooled and processed further in

parallel. The pooled samples were evaporated to 30 μl using a vacuum centrifuge and stored at -80°C until use.

v. Solid-phase extraction

Samples were next desalted using C18 Sep-Pak 1cc Cartridges (Waters, Cambridge, MA) according to the manufacturer's instructions. Briefly, samples resuspended in 95% H_2O, 5% CH_3CN, 0.1% CF_3CO_2H by sonication for 15 min. The pH of the samples was checked and adjusted to ≤ 3 using 5% CF_3CO_2H. Cartridges were equilibrated first with 10 column volumes of MeOH and then 10 column volumes of 95% H_20, 5% CH_3CN, 0.1% CF_3CO_2H. After application of the sample, cartridges were washed with 20 column volumes of 95% H_2O, 5% CH_3CN, 0.1% CF_3CO_2H. Peptides were eluted from the cartridge using 5 column volumes of 40% H_2O, 60% CH_3CN, 0.1% CF_3CO_2H. Peptides were evaporated to ~30 μl using a vacuum centrifuge and stored at -80°C until further use.

vi. Hydrophilic-interaction Chromatography

Samples were resuspended in 1 mL of 10% H_2O, 90% CH_3CN, 0.1% CF_3CO_2H by sonication for 15 min. Samples were then centrifuged at 6710*g* for 10 min. A manual injection valve was then used to load 500 μL onto a 4.6mm x 25cm TSKgel Amide-80 column (TOSOH Biosciences). A 120 min gradient was then applied to elute the peptides based on their hydrophilicity. The gradient started at 10% H_2O, 90% CH_3CN, 0.1% CF_3CO_2H and ramped to 40% H_2O, 60% CH_3CN, 0.1% CF_3CO_2H over 60 min at a flow rate of 750 μl/min. As peptides eluted, 1 mL fractions were collected. The gradient was then ramped to 90% H_2O, 10% CH_3CN, 0.1% CF_3CO_2H in 10 min, then to 10% H_2O, 90% CH_3CN, 0.1% CF_3CO_2H in 5 min to equilibrate for 45 min. A total of 96 fractions were collected.

vii. Nano liquid chromatography

Peptides were resuspended in 20 μl of 95% H_20, 5% CH_3CN, 0.1% CF_3CO_2H by sonication for 15 min. A refrigerated nanoLC autosampler was used to load 10 μl onto a C18 cartridge, which was then washed with 200 μl of 95% H_2O, 5% CH_3CN, 0.1% CF_3CO_2H before switching the cartridge in-line with a C18 nanoLC column. A 90 min gradient was then applied to elute peptides based on their hydrophobicity. The gradient started at 95% H_20, 5% CH_3CN, 0.1% CF_3CO_2H and ramped to 10% H_2O, 90% CH_3CN, 0.1% CF_3CO_2H over 60 min at a flow rate of 750 nl/min. As peptides eluted, 1μl fractions were mixed 1:2 with freshly prepared alpha-cyano-4-hydroxycinnamic acid onto a freshly polished MALDI target plate for a total of 384 fractions.

viii. MALDI TOF/TOF

The instrument was calibrated using the AnaSpec peptide mass spec standards kit according to the manufacturer's instructions. The Maldi TOF/TOF was operated in MS Reflector positive mode using the following acquisition parameters: mass range (da): 1000 to 4000, focus mass (da): 2200, shot/sub-spectrum: 25, total shots/spectrum: 750, average laser intensity: 5000. A job-wide interpretation method acquired fragmentation information for the top 12 peaks per spot using the following parameters: minimum s/n: 50, precursor exclusion: 160, adduct tolerance (m/z): 0.1, strongest precursors first.

x. Data Processing

The 4000 series explorer was used to build a peak list using MALDI data. The following settings were used: MS/MS peak filter mass range: 60, peak density: 5 peaks per 200 Da, minimum s/n: 5, minimum area: 1000, maximum peaks per precursor: 20.

Mascot Daemon v 2.2.2 (Matrix Science, Inc., Boston, MA) was used to automatically submit peak lists to a local Mascot Server v 2.2.2 (Matrix Science, Inc., Boston, MA) search engine utilizing the *Arabidopsis* protein database (NCBInr 20100131) appended with its reverse decoy. Searches of MS/MS data used trypsin specificity with the possibility of one missed cleavage, a peptide mass tolerance of ± 150 ppm, a peptide fragment mass tolerance of ± 0.6 Da, and the possibility of carbidomethylation at cysteine, oxidation at methionine and tryptophan.

Mascot results were submitted as .dat files to Scaffold using the Mascot and X! Tandem search engines. The following parameters were used: Fragment tolerance: 0.40 Da (Monoisotopic), parent tolerance: 400 ppm (Monoisotopic), enzyme: trypsin, missed cleavages: 2. Protein identifications were assessed using the following parameters: peptide threshold: 50% minimum, protein thresholds: 99%, minimum peptides: 2.

VI. References

Aebersold, R., Mann, M., 2003. Mass spectrometry-based proteomics. *Nature* 422, 198-207.

Arsova, B., Zauber, H., Schulze, W. X., 2012. Precision, proteome coverage, and dynamic range of *Arabidopsis* proteome profiling using N-15 metabolic labeling and label-free approaches. *Molecular and Cellular Proteomics* 11, 619-628.

Bell, A. W., Deutsch, E. W., Au, C. E., Kearney, R. E., Beavis, R., Sechi, S., Nilsson, T., Bergeron, J. J. M., Grp, H. T. S. W., 2009. A HUPO test sample study reveals common problems in mass spectrometry-based proteomics (vol 6, pg 423, 2009). *Nature Methods* 6, 546-546.

Evans, C., Noirel, J., Ow, S. Y., Salim, M., Pereira-Medrano, A. G., Couto, N., Pandhal, J., Smith, D., Pham, T. K., Karunakaran, E., Zou, X., Biggs, C. A., Wright, P. C., 2012. An insight into iTRAQ: where do we stand now? *Analytical and Bioanalytical Chemistry* 404, 1011-1027.

Garcia, B. A., Hake, S. B., Diaz, R. L., Kauer, M., Morris, S. A., Recht, J., Shabanowitz, J., Mishra, N., Strahl, B. D., Allis, C. D., Hunt, D. F., 2007. Organismal differences in post-translational modifications in histones H3 and H4. *Journal of Biological Chemistry* 282, 7641-7655.

Hou, Q., Tan, H. T., Lim, K. H., Lim, T. K., Khoo, A., Tan, I. B. H., Yeoh, K. G., Chung, M. C. M., 2013. Identification and functional validation of caldesmon as a potential gastric cancer metastasis-associated protein. *Journal of Proteome Research* 12, 980-990.

Hurkman, W. J., Tanaka, C. K., 1986. Solubilization of plant membrane-proteins for analysis by two-dimensional gel-electrophoresis. *Plant Physiology* 81, 802-806.

Jensen, O. N., 2004. Modification-specific proteomics: characterization of post-translational modifications by mass spectrometry. *Current Opinion in Chemical Biology* 8, 33-41.

Kwon, S. J., Choi, E. Y., Choi, Y. J., Ahn, J. H., Park, O. K., 2006. Proteomics studies of post-translational modifications in plants. *Journal of Experimental Botany* 57, 1547-1551.

Lan, P., Li, W. F., Wen, T. N., Shiau, J. Y., Wu, Y. C., Lin, W. D., Schmidt, W., 2011. iTRAQ protein profile analysis of *Arabidopsis* roots reveals new aspects critical for iron homeostasis. *Plant Physiology* 155, 821-834.

Michalski, A., Cox, J., Mann, M., 2011. More than 100,000 detectable peptide species elute in single shotgun proteomics runs but the majority is inaccessible to data-dependent LC-MS/MS. *Journal of Proteome Research* 10, 1785-1793.

Sardar, A. H., Kumar, S., Kumar, A., Purkait, B., Das, S., Sen, A., Kumar, M., Sinha, K. K., Singh, D., Equbal, A., Ali, V., Das, P., 2013. Proteome changes associated with *Leishmania donovani* promastigote adaptation to oxidative and nitrosative stresses. *Journal of Proteomic*s 81, 185-199.

Shliaha, P. V., Bond, N. J., Gatto, L., Lilley, K. S., 2013. Effects of traveling wave ion mobility separation on data independent acquisition in proteomics studies. *Journal of Proteome Research.* 12, 2323-2339.

Slade, W. O., Ray, W. K., Williams, P. M., Winkel, B. S., Helm, R. F., 2012. Effects of exogenous auxin and ethylene on the *Arabidopsis* root proteome. *Phytochemistry* 84, 18-23.

Yang, Y., Zhang, S., Howe, K., Wilson, D.B., Moser, F., Irwin, D., Thannhauser, T.W. 2007. A comparison of nLC-ESI-MS/MS and nLC-MALDI-MS/MS for GeLC-based protein identification and iTRAQ-based shotgun quantitative proteomics. *Journal of Biomolecular Techniques* 18, 226-237.

Appendix C

Supplementary Information

William O. Slade[A]*, Brenda S.J. Winkel*[A]*, and Richard F. Helm*[B]*

Deptartments of Biological Sciences[A] *and Biochemistry*[B]*, Virginia Tech, Blacksburg, VA*

For access to the supplemental information provided here, please contact Richard F. Helm (helmrf@vt.edu)

Table of contents

Appendix C: Supplemental Information

I. Chapter 3

i. Skyline file containing all data for unfractionated and gel-based schemes; "Chapter3_AllMRM.zip", 70 MB

II. Chapter 4

i. Scaffold files (.sf3) for 8, 12, and 24 h time points; "8.sf3", 61 MB; "12.sf3", 44 MB; "24.sf3", 38 MB.